PHOTO-RESPIROMETRIC METHODS TO EVALUATE MICROALGAE-BACTERIA DYNAMICS

Applications to photobioreactors monitoring and modelling

Simone Rossi

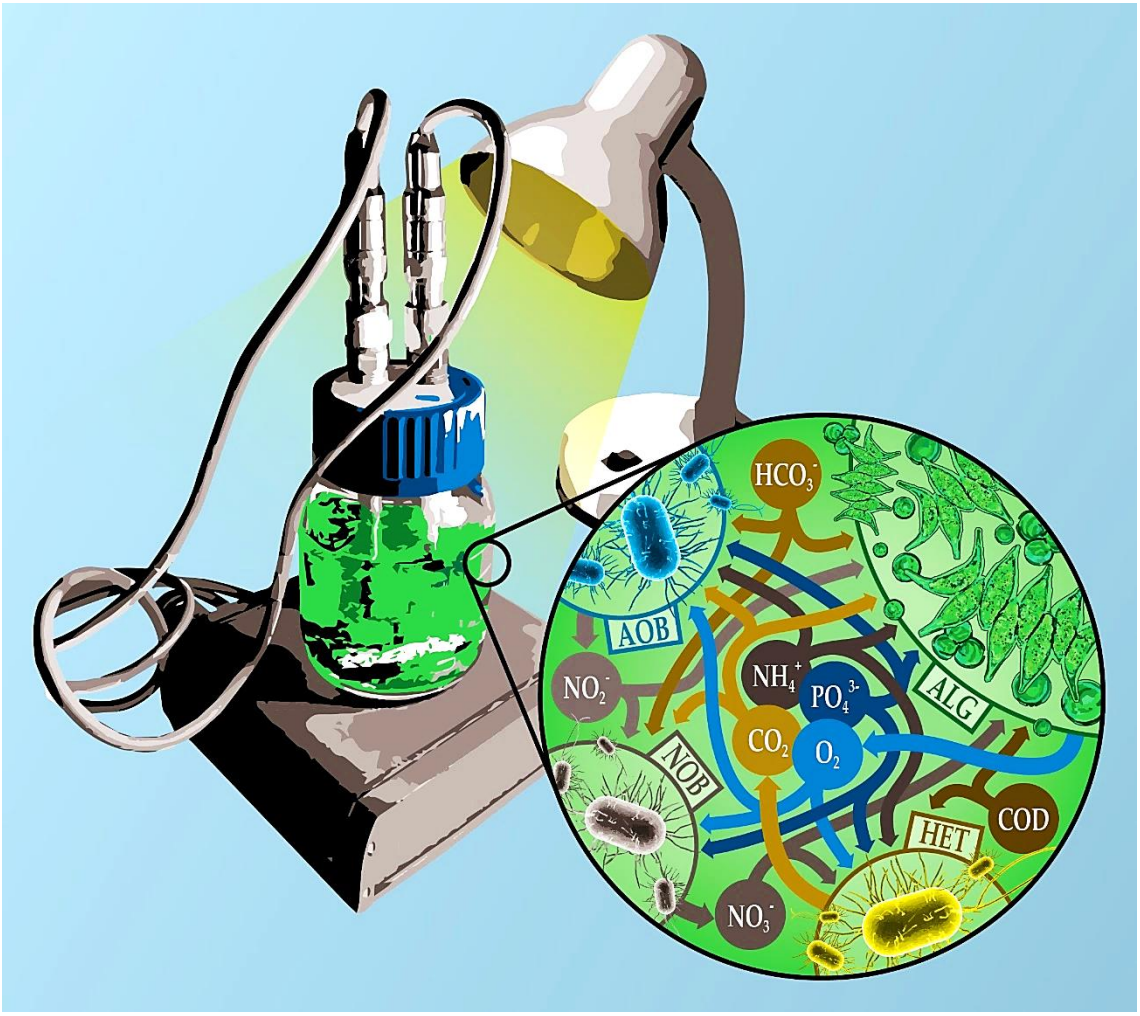

POLITECNICO
MILANO 1863

Simone Rossi

Photo-respirometric methods to evaluate microalgae-bacteria dynamics

Applications to photobioreactors monitoring and modelling

Ph.D. Thesis

POLITECNICO DI MILANO, 2020 (XXXII CYCLE)

DICA - Department of Civil and Environmental Engineering

Doctoral program in Environmental and Infrastructure Engineering

Supervisor: Prof. Elena Ficara

Tutor: Prof. Roberto Canziani

Chair of the doctoral program: Prof. Riccardo Barzaghi

A Francesca,

Alla mia famiglia

ACKNOWLEDGEMENTS

This thesis represented a great personal challenge, and many people contributed to this achievement. I want to express my gratitude to all of them.

First of all, I want to thank my supervisor, Prof. Elena Ficara, for the patience and for her extra-ordinary humanity and empathy. I am grateful to her for believing in me and for transmitting me her enthusiasm, pragmatism and indefinite amount of knowledge. Thank you very much!

I am grateful to Jean-Philippe Steyer and Enrica Uggetti, for reviewing this work and for the useful comments received. I also want to thank Prof. Roberto Canziani and all the other professors, researcher, laboratory and administrative staff members of the Department of Civil and Environmental Engineering (DICA), Politecnico di Milano, for their for their suggestions and availability.

I am grateful to algae people in Milano, for always being kind and collaborative, and for allowing me to conduct this work: Davide S, Micol B, Andrea P (Politecnico di Milano), Prof. Valeria Mezzanotte, Francesca M, Riccardo F, Marco M (University of Milano-Bicocca), Josuè GC (Universidad Politecnica de Valencia. To the students involved in photo-respirometry and modelling: Bruno B, Beatriz C, Marianna B, Margherita B, Alessandro M, Erica M and Arianna B. I am especially grateful to other people involved in my lie in Milano. Very special thanks goes to Arianna C, for sharing happyness/difficulties of the Ph.D. life and for valuable suggestions and help. I am extremely grateful to Nadia M, for her irreplaceable help, availability and kindness in laboratory and for the cheerful break times. Special thanks also goes to Tommaso C, for the nice times spent in Milano and for the (fruitful?) mathematical discussions. Aronne T is kindly acknowledged for providing the photo-respirometer and the technical assistance. Thanks to other colleagues at DICA: Giacomo B, Caterina L, Cuijie F, Andrea T,

the colleagues from my ex- (Roberto DC, Giovanni D, Camilla T and Sara P) and from my present office (Anna S, Sara G, Federica C and Hitomi M), and all the other funny people enlighting my days at DICA.

I want to thank Prof. Joan Garcìa and all the people of the GEMMA group, UPC BarcelonaTech, especially: Jaume P, Ruben DM, Marco H, Estel R, Marta F and Manuel B, for their kind availability and for the pleasant technical/non-technical discussions. Thanks to my flatmes Alice and Lorenz, for empathy and paranoic discussions and for calm exclamations during Skype calls, respectively.

A special chapter of my life is represented by my Florence, where I met the most important people of my life. First, I want to thank Prof. Claudio Lubello and professors and researchers from the Department of Civil and Evironmental Engineering (DICEA), University of Florence, for their rigorous teachings and research opportunities provided. A very important thank is for Tommaso L, the first scientist menthor and friend I had, for introducing me to Anammox bacteria and the world of bioprocess engineering, for transmitting me his enthusiasm in the applied research and for teaching me much more than you think! Many thanks to to Prof. Giulio Munz and to Francesco S for having introduced me to the world of respirometry and sulphur-oxidizing bacteria and to Alberto M, for having introduced me to the challenges of the real engineering world.

Huge thanks to all the historic IAT colleagues at the University of Florence. Special thanks to Claudia N, for having shared with me unforgettable moments and for always being present to handle happy and difficult situations, to Tullio C and to Davide R, for the endless laughs during the endless days and nights spent together, to Francesco B, for the nice discussions on Ph.D. and engineering life and for always maintaining the same spirit when we met at the university. Without knowing you all, on that first day of lessons, handling that engineering degree could have been a real trouble.

Huge thanks goes to my FACAꟻ friends, for the pleasant discussions, the (uncountable) hilariously crazy moments and the (few) serious moments, and for having accompanied me in many epic adventures: to, Cisco, Emtwozed, Bianco, Blunt, Giova, Zillo, Bernach, Cagno, Oliver, Giannei, Ferro, Zeta and Sho-Kaze (also for the graphical design of the front page). Thank you all brothers!

I want to thank Anna and Paolo, for their hospitality, for always believing in me and Francesca and for encouraging and sustaining us in difficult situations.

I want to express my immense gratitude to my loving family: Carlo, Rosellina ed nonna Elvira. Your presence was fundamental in my personal and professional life, and everything you made for me was aimed at obtaining my best. Thank you for your constant and endless support and for always being available to face with me every kind of challenge and necessity. What I learned from you is something that you cannot learn in a Ph.D. course, and is definitely more durable and important. This work is dedicated to you and to my father, Fernando: I know that today you would be proud of me.

Finally, thanks to Francesca, the most smart and beautiful bioprocess modellist I could work with, and the girl I am lucky I can share my life with. Thank you for every day you spent with me, and for each other day we will spend together. Thank you for accompanying me in this journey, from the very first days when we were two disoriented engineering students, until today that I am earning a Ph.D. degree and I have a woman in front of me. You thaught me how (and why) to believe in myself and in my dreams, to always find something to smile for, to give priorities in the office and at home. And thousands other things you made for me and can't be described with simple words. Feeling loved and supported by you was the most important reason I never gave up. Today I'm glad I followed this path, but without you on my side, anything of this would have been possible. I love you!

Simone

SUMMARY

Nutrient removal from wastewater is crucial to preserve the equilibria of natural ecosystems by increasing anthropic pressures. On the other hand, the scarcity of natural resources is pushing agriculture and water industries to move from a linear to a circular approach in the management of nutrient resources. Within this context, the bioremediation of municipal/industrial wastewater in microalgae-based biorefineries are particularly interesting, due to the possibility of achieving important goals while treating gas, liquid and solid waste streams: i) reducing the energy requirement for the aerobic treatment of wastewaters by exploiting the photosynthetic oxygenation by microalgae, ii) recovering either wastewater nutrients (mainly N and P) and bioproducts (bioplastics, biofertilizers) or energy as biomethane from the digestion of algal biomass, and iii) capturing greenhouse gases such as CO_2 and other gaseous contaminants (H_2S, SO_x, NO_x) from polluted gas streams. Due to these reasons, the use of microalgae-bacteria consortia in wastewater treatment recently gained interest in the scientific community. However, a lack a knowledge of the complex interaction among phototrophic, autotrophic and heterotrophic microorganisms in these systems practically hinders the application of the process at full scale (chapter 1). Respirometry-based techniques have been historically applied to characterize conventional nutrient removal biotechnologies (mainly activated sludge) and the dependence of microalgal photosynthesis on light, temperature, nutrient concentrations and other parameters (photo-respirometry). Currently, only a few studies attempted to further characterize the complicated processes occurring in microalgae-bacteria systems by using photo-respirometry. In this work, the most important studies exploiting respirometric and photo-respirometric methods were reviewed (chapter 2), providing an extensive overview of experimental devices, protocols and potential applications of respirometry-based techniques which

allowed defining the gaps and steps required toward effective and harmonized test procedures, experimental setup and operational conditions.

The main findings of the literature review process were used to define design an appropriate respirometric apparatus and three standardized protocols, which revealed useful for monitoring and modelling the evolution of microalgae-bacteria systems: the *monitoring*, *model calibration* and *inhibition* protocols (chapter 4).

The *monitoring protocol* allowed to distinguish between the algal and nitrifying oxygen consumption rates in algae-bacteria consortia sampled from six cultivation systems fed with different types of wastewaters (chapter 3), constituting a rich dataset to which future studies should be compared (chapter 5). The *model calibration protocol* was defined to characterize the optimal cultivation conditions in a pilot-scale microalgae-bacteria system. The application of the protocol allowed to successfully identify optimal irradiance, pH, DO and temperature, in correspondence of which the photosynthesis and the respiratory activities were highest, and to identify minimum and maximum thresholds, for which the metabolic activities are stopped, with direct applications to microalgae-bacteria modelling (Chapter 5). In the *inhibition protocol*, the application of the standardized procedure allowed to successfully identify the FA inhibition parameter (EC_{50}) for both green algae and cyanobacteria. Testing the activity reduction on both monocultures and mixed algae-bacteria cultures is an innovative approach compared to available literature works, were the inhibition is generally assessed on pure cultures.

On the overall, this thesis demonstrated that photo-respirometry is a suitable and promising technique to gain insights into oxygen dynamics in microalgae-bacteria systems. The definition of standardized protocols allowed to perform the experiments under comparable conditions and to minimize the experimental

error. The standardization efforts were also aimed at identifying a set of guidelines for future photo-respirometric studies, in order to facilitate the spreading of this technique. Indeed, adopting the described set of protocols could be a very simple and effective tool for monitoring outdoor and/or indoor microalgae-bacteria photobioreactors treating industrial and municipal wastewaters and for the calibration of mathematical models describing their evolution. The application of the described methodology as routine monitoring procedure is expected to provide additional accuracy and reliability to algae-bacteria growth models, making them an even more reliable tool for the analysis and optimization of these bioprocesses.

TABLE OF CONTENTS

ACKNOWLEDGEMENTS ..... **i**

SUMMARY ..... **v**

TABLE OF CONTENTS **1**

LIST OF PUBLICATIONS **5**

LIST OF FIGURES **7**

LIST OF TABLES **11**

LIST OF ACRONYMS AND ABBREVIATIONS **13**

1. INTRODUCTION **21**

1.1. Algal-based wastewater treatment: advantages and challenges **21**

1.2. Aims and outline of the thesis **35**

2. PHOTO-RESPIROMETRY TO SHED LIGHT ON MICROALGAE-BACTERIA CONSORTIA: A REVIEW **41**

2.1. Conventional respirometric methods **41**

2.1.1. Respirometric devices **42**

2.1.2. Typical applications in the field of wastewater treatment **45**

2.1.3. Conventional respirometric protocols **46**

2.2. Photo-respirometric methods applied to axenic cultures of phototrophic organisms **51**

2.2.1. Photo-respirometric devices and protocols **52**

2.2.1.1. Effects of environmental conditions **56**

2.2.1.1.1. Light intensity and quality **57**

2.2.1.1.2. Availability of inorganic carbon, nitrogen and phosphorus **62**

2.2.1.1.3. Temperature **65**

2.2.1.1.4. pH **67**

2.2.1.1.5. Dissolved oxygen **69**

2.2.1.1.6. Salinity **69**

2.2.1.2. Effects of inhibitory compounds **71**

2.2.2. Combination with fluorescence and other measurements 73
2.3. Photo-respirometric methods applied to microalgae-bacteria consortia 76
2.3.1. In-reactor photo-respirometry 77
2.3.2. External photo-respirometry 80
2.3.2.1. Physical separation of algae and bacteria 81
2.3.2.2. Selective inhibitors to discriminate populations 81
2.3.3. Mathematical modelling 84
2.3.4. Advantages, challenges and potential applications 85
3. MATERIALS AND METHODS 93
3.1. Photo-respirometric devices 93
3.1.1. Basic instrumentation 93
3.1.2. Fully-equipped photo-respirometer 94
3.2. Cultivation systems tested 97
3.3. Cultivation systems treating digestates from municipal and agro-industrial wastewaters 98
3.3.1. Pilot-scale HRAP treating municipal digestate 98
3.3.2. Pilot-scale bubble-column treating municipal digestate 100
3.3.3. Pilot-scale bubble-column treating agricultural digestate 102
3.3.4. Lab-scale PBRs treating agricultural digestate 103
3.4. Cultivation systems treating other industrial wastewaters 105
3.4.1. Demonstrative-scale semi-closed PBRs treating agricultural runoff 105
3.4.2. Lab-scale PBRs treating acquaculture and piggery wastewaters 107
3.5. Cultivation of microalgae and cyanobacteria monocultures 110
3.5.1. Cultivation of green microalgae monocultures 110
3.5.2. Cultivation of cyanobacteria monocultures 111
3.6. Analytical methods 112
4. DEFINITION AND STANDARDIZATION OF TEST PROTOCOLS 115
4.1. Standardization of test procedures and conditions 115

4.1.1. Sample characteristics and pre-treatments 115
4.1.2. Optical properties, light penetration and solid concentrations 118
4.1.3. Nutrient concentrations 119
4.1.4. Test conditions and interferences of environmental control systems 120
4.1.5. Evaluation of algal and bacterial contributions on oxygen dynamics 122
4.1.5.1. Alternation and duration of light/dark phases and acclimation of the sample 122
4.1.5.2. Evaluation of bacterial activity during photo-respirometric assays 123
4.2. Photo-respirometric protocols and numerical methods 125
4.2.1. Photo-respirometric protocols 125
4.2.1.1. Monitoring protocol 125
4.2.1.2. Model calibration protocol 129
4.2.1.3. Inhibition protocol 134
4.2.2. Numerical methods 136
4.2.2.1. Data processing and OPR calculation 136
4.2.2.2. Photosynthesis, respiration and inhibition models 138
4.2.2.1. Statistical methods 142
5. RESULTS AND DISCUSSION 147
5.1. Monitoring protocol 147
5.1.1. Pilot-scale HRAP treating municipal digestate 147
5.1.2. Pilot-scale bubble-column treating municipal digestate 156
5.1.3. Pilot-scale bubble-column treating agricultural digestate 159
5.1.4. Lab-scale PBRs treating agricultural digestate 161
5.1.5. Demonstrative-scale semi-closed PBRs treating agricultural runoff 163
5.1.6. Lab-scale PBRs treating aquaculture and piggery wastewaters 167
5.1.7. Results and discussion 171
5.2. Model calibration protocol 179
5.2.1. Selection of photosynthesis models 179

5.2.1.1. Irradiance models 179

5.2.1.2. Temperature models 180

5.2.1.3. pH models 180

5.2.1.4. Dissolved oxygen models 181

5.2.2. Selection of respiration models 181

5.2.2.1. Irradiance models 181

5.2.2.2. Temperature models 182

5.2.2.3. pH models 182

5.2.2.4. Dissolved oxygen models 183

5.2.3. Data fitting considering all parameters 183

5.3. Inhibition protocol 192

5.3.1. Selection of free ammonia inhibition models 192

5.3.1. Effects of free ammonia on axenic microalgae and cyanobacteria 194

5.3.2. Effects of free ammonia on mixed algae-bacteria consortia 196

5.3.3. Free ammonia inhibition scenarios in microalgae-based wastewater treatment 198

6. CONCLUSIONS AND PERSPECTIVES 211

6.1. Conclusions 211

6.2. Further research required 216

BIBLIOGRAPHY 221

LIST OF PUBLICATIONS

Part of the work reported in this thesis is based on the following papers:

- S. Rossi, E. Sforza, M. Pastore, M. Bellucci, F. Casagli, F. Marazzi, E. Ficara. Photo-respirometry to shed light on microalgae-bacteria consortia—a review. *Reviews in Environmental Science and Bio/Technology*, 19(1), 43-72. https://doi.org/10.1007/s11157-020-09524-2

- S. Rossi, M. Bellucci, F. Marazzi, V. Mezzanotte, E. Ficara (2018) Activity assessment of microalgal-bacterial consortia based on respirometric tests. *Water Science and Technology*, 78(1), 207-215. https://doi.org/10.2166/wst.2018.078

- S. Rossi, F. Casagli, M. Mantovani, V. Mezzanotte, E. Ficara. Selection of photosynthesis and respiration models for evaluating the effect of environmental conditions on microalgae-bacteria suspensions. *Bioresource technology*, 305, 122995. https://doi.org/10.1016/j.biortech.2020.122995

- S. Rossi, R. Díez-Montero, E. Rueda, F. Castillo Cascino, K. Parati, J. García, E. Ficara. Free ammonia inhibition in microalgae and cyanobacteria grown in wastewaters: photo-respirometric evaluation and modelling. *Bioresource Technology*, 305, 123046. https://doi.org/10.1016/j.biortech.2020.123046

- V. Andreotti, A. Solimeno, S. Rossi, E. Ficara, F. Marazzi, V. Mezzanotte, J. García. Bioremediation of aquaculture wastewater with the microalgae Tetraselmis suecica: semi-continuous experiments, simulation and respirometric tests. *Journal of cleaner production* (Submitted)

During the execution of the research project, the following papers related to the subjects discussed in this thesis, were also published or submitted:

- F. Marazzi, M. Bellucci, S. Rossi, R. Fornaroli, E. Ficara, V. Mezzanotte (2019) Outdoor pilot trial integrating a sidestream microalgae process for the treatment of centrate under non optimal climate conditions. *Algal Research*, 39, 101430

- F. Casagli, A. Pizzera, S. Rossi, J.P. Steyer, O. Bernard, E. Ficara. Application of the ALBA (ALgae - BActeria) model to a pilot scale raceway for agricultural digestate treatment. (In preparation)

LIST OF FIGURES

Figure 1.1. Possible configurations for the integration of microalgae-bacteria consortia in existing municipal wastewater treatment plants (A: Secondary treatment; B: Tertiary treatment; C: Treatment of anaerobic digestate). 24

Figure 1.2.Possible interactions among phototrophic organisms, nitrifying bacteria and heterotrophic bacteria. Green lines are synergic interactions, red lines are competitive interactions (A: simplified scheme of synergic interactions, B: Interactions between phototrophs and heterotrophic bacteria; C:interactions between phototrophs and nitrifying bacteria). 33

Figure 2.1. Typical respirometric tests performed to evaluate the exogenous OUR of heterotrophic and nitrifying sludge maintained under endogenous conditions (24 h under aeration). A: activity of activated sludge (2.9 g TSS L^{-1}) after the addition of acetate (50 mg L^{-1}) and ATU (10 mg L^{-1}); B: activity of nitrifying sludge (2.5 g TSS L^{-1}) after the addition of ammonium (15 mg N L^{-1}) and nitrite (10 mg N L^{-1}). 50

Figure 2.2. Wastewater fractions identifiable from respirometric assays (A: identifiable COD fractions, B: identifiable TKN fractions). 47

Figure 2.3. Effects of pH on ionization equilibria for the main dissolved macronutrients (A: carbonates, B: ammonia, C: phosphates). 68

Figure 2.4. Possible effects of different bacterial and photosynthesis inhibitors on the microalgae-bacteria consortium. 83

Figure 3.1. Layout of the basic photo-respirometric device. 94

Figure 3.2. Fully-equipped photo-respirometer used in this study. 95

Figure 3.3. Experimental setup: fully-equipped photo-respirometer and thermo-incubator. Legend: 1) Mixing and signal communication unit, 2) Glass bottles, 3) DO, temperature and pH probes, 4) Acid/base dosage pumps, 5) Air/gas pumps, 6) Normally closed electro-valves, 7) Gas cylinder (CO_2/O_2/N_2), 8) Acid/base solutions, 9) Industrial grade PC, 10) Heating/cooling fans, 11) Air temperature probe, 12) Fluorescent tubes, 13) Additional LED lamps. 96

Figure 3.4. Pilot-scale HRAP located at the Bresso-Niguarda WWTP. 99

Figure 3.5. Bubble-column (left) and HRAP (right) pilot plants at the Bresso-Niguarda WWTP. 101

Figure 3.6. Pilot-scale bubble-column treating agricultural wastewaters. 103

Figure 3.7. Demonstrative-scale hybrid PBRs for the treatment of agricultural runoff wastewaters (Arias, 2018). 106

Figure 3.8. Lab-scale column PBRs used to grow monocultures of T.Suecica for aquaculture wastewater treatment *(Andreotti 2019)*. 107

Figure 4.1. Schematization of different pre-treatment options for conducting photo-respirometric tests on microalgae-bacteria suspensions. 117

Figure 4.2. Typical result of a photo-respirometric test following the "monitoring protocol". L/D phases are reported together with the addition of substrates and inhibitors. 129

Figure 4.3. Typical result of a photo-respirometric test following the "model calibration protocol". L/D phases are reported together with the addition of substrates or inhibitors. 131

Figure 4.4. Typical result of a photo-respirometric test following the "inhibition protocol". L/D phases are reported together with the addition of substrates or inhibitors. 136

Figure 5.1. Temperature and irradiance during the HRAP monitoring campaigns and their 5-points moving average (A: 2017 monitoring campaign, B: 2018 monitoring campaign). 149

Figure 5.2. Microalgae and bacteria activities measured during monitoring tests: comparison between specific OPR by microalgal photosynthesis (sOPR), microalgal respiration ($sOPR_{RESP}$) and nitrification ($sOPR_{NIT}$) during the two monitoring campaigns (A: 2017 monitoring campaign, B: 2018 monitoring campaign) 150

Figure 5.3. Microalgae and bacteria activities measured during monitoring tests: A,C)) Comparison between microalgae OPR rates calculated by photo-respirometric tests (OPR (RESP)), rate of variation of the optical density at 680 nm (rOD_{680}) and its 3-points moving average (rOD_{680},Mov_Avg) (A: 2017 monitoring campaign, C: 2018 monitoring campaign); B, D) Comparison between nitrification rates calculated by photo-respirometric tests (OUR_{NIT} (RESP)), monitoring data (OUR_{NIT} (NO_X)) and its 3-points moving average OUR_{NIT} (NO_X,Mov_Avg) (B: 2017 monitoring campaign, D: 2018 monitoring campaign). 154

Figure 5.4. Results of the FISH analysis: microalgae (dark red) and AOB colonies (light red) observed in samples collected from the HRAP using a fluorescent microscope 155

Figure 5.5. Temperature and irradiance during the HRAP monitoring campaigns and their 5-points moving average (A: 2017 monitoring campaign, B: 2018 monitoring campaign). 158

Figure 5.6. Microalgae and bacteria activities measured during monitoring tests performed on the pilot-scale bubble-column: comparison between specific OPR by microalgal photosynthesis (sOPR), microalgal respiration ($sOPR_{RESP}$) and nitrification ($sOPR_{NIT}$). 158

Figure 5.7. Microalgae and bacteria activities measured during monitoring tests performed on the pilot-scale bubble-column: comparison between specific OPR by microalgal photosynthesis (sOPR), microalgal respiration ($sOPR_{RESP}$) and nitrification ($sOPR_{NIT}$) during two series of tests (A: autumn 2016, B: winter 2017). 161

Figure 5.8. Microalgae and bacteria activities measured during monitoring tests performed on lab-scale PBRs: comparison between specific OPR by microalgal photosynthesis (sOPR), microalgal respiration ($sOPR_{RESP}$) and nitrification ($sOPR_{NIT}$) during two series of tests. 162

Figure 5.9. Temperature, irradiance and their 5-days moving average during the monitoring campaign of the demonstrative-scale PBRs. 165

Figure 5.10. Microalgae and bacteria activities measured during monitoring tests performed on the demonstrative-scale semi-closed PBRs: comparison between specific OPR by microalgal photosynthesis (sOPR), microalgal respiration ($sOPR_{RESP}$) and nitrification ($sOPR_{NIT}$) (A: Semi-closed PBR 1, B: Semi-closed PBR 2, C: Semi-closed PBR 3). 166

Figure 5.11. Microalgae and bacteria activities measured during monitoring tests performed on the lab-scale PBRs treating aquaculture wastewater: comparison between specific OPR by microalgal photosynthesis (sOPR), microalgal respiration ($sOPR_{RESP}$) and nitrification ($sOPR_{NIT}$). 168

Figure 5.12. Microalgae and bacteria activities measured during monitoring tests: comparison between specific OPR by microalgal photosynthesis (sOPR), microalgal respiration ($sOPR_{RESP}$) and nitrification ($sOPR_{NIT}$) in a microalgae-bacteria consoritum (A) and in a microalgae-bacteria consortium contaminated with filamentous green algae (B). 169

Figure 5.13. Correlation between sOPR measured in photo-respirometic tests and TSS. 174

Figure 5.14. Correlation between specific nitrfication rates ($sOPR_{NIT}$) and specific photosynthesis rates (sOPR) in tests performed on systems treating municipal and piggery wastewaters. 174

Figure 5.15. Results of the principal component analysis applied to the pilot-scale HRAP and bubble-column treating digestates (I_4d: average irradiance on the four days preceeding the test, T_4d: average irradiance on the four days preceeding the test). 178

Figure 5.16. Fit of different photosynthesis models to normalized sOPR data: irradiance (A), temperature (B), pH (C) and DO (D) (error bars indicate standard deviations for three sOPR determination, shaded areas indicate 95% confidence intervals for fitting functions). 184

Figure 5.17. Fit of different respiration models to normalized sOUR data: irradiance (A), temperature (B), pH (C) and DO (D) (error bars indicate standard deviations for three sOUR determination, shaded areas indicate 95% confidence intervals for fitting functions). 185

Figure 5.18. Effects of free ammonia inhibition on microalgae and cyanobacteria: reduction of f_{NH3}, non-competitive inhibition model fit and estimated model parameters (A: Microalgae, B: Cyanobacteria, samples abbreviations: M_1 = *Chlorella vulgaris*, M_2 = *Scenedesmus quadricauda*, M_3 = *Chlorella sorokiniana*, M_4 = *Scenedesmus obliquus*, MB = Sample from the HRAP; C_1 = *Synechocystis*, C_2 = *Synechococcus*, C_3 = *Leptolyngbya*, CB_1 = Sample from the semi-closed PBR_1, CB_2 = Sample from the semi-closed PBR_2, CB_3 = Sample from the semi-closed PBR_3. Shaded areas and error bars represent 95% confidence intervals). 197

Figure 5.19. Typical daily variations of water temperature and irradiance for different seasons (A = water temperature in the HRAP, B = water temperature in semi-closed PBRs, C = irradiance data for the HRAP, dataset: January 2017 - November 2019). 201

Figure 5.20. Simulated evolution of the inhibition function (f_{NH3}) under typical daily variations for different seasons, pH values and TAN concentrations. Inhibition functions are calculated considering microalgae (A - D) and cyanobacteria (E - H) as dominant species in mixed phototrophs-bacteria consortia. 205

Figure 5.21. Simulated evolution of switch functions in the HRAP at 60 mg N-TAN L-1 for different seasons and pH values (A = summer, low pH, B = autumn, low pH, C = summer, high pH, D = autumn, high pH). 206

Figure 5.22. Simulated evolution of different switch functions to to describe the combined effects of environmental parameters and free ammonia: product of all the switch functions (black) and minimum of each switch function (magenta) (A = summer, low pH, B = autumn, low pH, C = summer, high pH, D = autumn, high pH). 207

LIST OF TABLES

Table 1.1. Main challenges for the application of microalgae-based wastewater treatment at full-scale. 28

Table 2.1. Main advantages and disadvantages of microalgae-bacteria-based wastewater treatment. 55

Table 2.2. Main cultivation conditions, biomass characteristics and test conditions in microalgae-bacteria photo-respirometry. 79

Table 2.3. Microalgal-bacterial photo-respirometric protocols and main test outputs. 89

Table 3.1. Characterization of the LFAD used as influent faor the Bresso-Niguarda HRAP (Milan, Italy) over three monitoring campaigns. Values are expressed as mean ± standard deviation. 100

Table 3.2. Characterization of Bresso-Niguarda HRAP effluent used to feed the bubble-column PBR. Values are expressed as mean ± standard deviation. 102

Table 3.3. Characterization of the digestate used as influent to the pilot-scale bubble-column located in Casaletto di Sopra (CR). Values are expressed as mean ± standard deviation. 103

Table 3.4. Characterization of the digestate used as influent to the laboratory-scale bubble-columns located at the A. Rozzi laboratory (DICA - Politecnico di Milano, Cremona, Italy). Values are expressed as mean ± standard deviation. 104

Table 3.5. Characterization of aquaculture wastewaters used as influent to the laboratory-scale bubble-columns located at the A. Rozzi laboratory (DICA - Politecnico di Milano, Cremona, Italy). 108

Table 3.6. Characterization of pre-treated piggery wastewaters used as influent to the laboratory-scale bubble-columns located at the A. Rozzi laboratory (DICA - Politecnico di Milano, Cremona, Italy). Values are expressed as mean ± standard deviation. 110

Table 4.1. Models describing the dependance of photosynthetic rates on local irradiance, temperature, pH and dissolved oxygen. 140

Table 4.2. Models describing the dependance of respiratory rates on local irradiance, temperature, pH and dissolved oxygen. 141

Table 5.1. Environmental conditions and operating parameters in the HRAP in correspondence of the photo-respirometric tests. Values are expressed as mean ± standard deviation. 148

Table 5.2. Environmental conditions and operating parameters in the pilot-scale bubble-column in correspondence of the photo-respirometric tests. Values are expressed as mean ± standard deviation. 160

Table 5.3. Environmental conditions and operating parameters in the demonstrative-scale semi-closed PBRs in correspondence of the photo-respirometric tests. Values are expressed as mean ± standard deviation. 165

Table 5.4 Summary of the results obtained following the photo-respirometric monitoring protocol and comparison with literature results. Values are expressed as mean ± standard deviation (minimum, maximum). 175

Table 5.5. Normalized photosynthesis and respiration rates in tests performed on systems treating municipal and piggery wastewaters with green microalgae as dominant phototrophic organisms. Values are expressed as mean ± standard deviation (minimum, maximum). 177

Table 5.6. Estimated parameters and information criteria for the described photosynthesis models (data in square brackets indicate 95% confidence intervals for the estimated value). ... 186

Table 5.7. Estimated parameters and information criteria for the described respiration models (data in square brackets indicate 95% confidence intervals for the estimated value). ... 187

Table 5.8. Estimated parameter values for selected models considering the interactions among all environmental parameters (data in square brackets indicate 95% confidence intervals for the estimated value). 190

Table 5.9. Free ammonia inhibition tests performed and conditions applied. Temperature and irradiance data are reported as mean ± standard deviation. 193

Table 5.10. Selection criteria and estimated parameters for selected free ammonia inhibition models. 95% confidence intervals on estimated parameters are reported in square brackets. Averaged data are reported as mean ± standard deviation. 195

LIST OF ACRONYMS AND ABBREVIATIONS

AIC_C	Akaike's information criterion corrected for small samples
ALG	Algal biomass [M L^{-3}]
ANOVA	Analysis of variance
AOB	Ammonia-oxidizing bacteria
AGR	Algal growth rate [T^{-1}]
ARR	Volumetric ammonia removal rate [M L^{-3} T^{-1}]
ARWW	Agricultural runoff wastewater
ASM	Activated sludge model
AS	Activated sludge
ASP	Activated sludge process
ATP	Adenosin-triphosphate
ATU	Allylthiourea [M L^{-3}]
AW	Atomic weigth [N M^{-1}]
AWW	Aquaculture wastewater
BG11	Blue-geen medium no. 11
BOD	Biochemical oxygen demand [M L^{-3}]
CC	Microsccope cell counts
COD	Chemical oxygen demand [M L^{-3}]
COEL	*Coelastrum* sp.
CHL	Chlorophyll [M L^{-3}]
CHLAM	*Chlamydomonas* sp.
CHLO	*Chlorella* sp.
CHP	Combined heat and power unit
COC	*Synechococcus* sp.
CPM	Cardinal pH model
CPMI	Cardinal pH model with inflection
CR	Closed respirometer
CSTR	Completely mixed stirred tank reactor
CTMI	Cardinal temperature model with inflection
CUV	Cuvette respirometer
CV	Coefficient of variation [%]

CYS	*Synechocystis* sp.
DNR	Volumetric denitrification rate [M L^{-3} T^{-1}]
DO	Dissolved oxygen [M L^{-3}]
DO_{SAT}	Dissolved oxygen saturation [M L^{-3}]
EC_{50}	Effective concentration causing 50% inhibition [M L^{-3}]
ETR	Electron transpoert rate [N L^{-2} T^{-1}]
EUGL	*Euglena* sp.
FA	Free (or unionized) ammonia [M L^{-3}]
FCB	Filamentous cyanobacteria
FISH	Fluoresence in-situ hybridization
FLUO	Fluorescent lamps
FPBR	Flat-plate photobioreactor
FPWW	Food processing wastewater
HAL	Halogen lamps
HET	Heterotrophic bacteria
HRAP	High rate algal pond
HRT	Hydraulic retention time
IA	Inhibitor addition in respirometric tests
INC	Incandescence lamps
IRR	In-reactor respirometry
IS	Inhibitor solution
k_La	Volumetric mass transfer coefficient [T^{-1}]
L/D	Light/dark
LED	Light emitting diode
LEP	*Leptolyngbya* sp.
LFAD	Liquid fraction of anaerobic digestate
LFADM	Liquid fraction of anaerobic digestate from municipal wastewater
LFADP	Liquid fraction of anaerobic digestate from piggery wastewater
LPBR	Lab-scale photobioreactor
MA	Microalgae
MB	Microalgae-bacteria consortium
MBBM	Modified Bold's basal medium
MBBR	Moving bed biofilm reactor
MBR	Membrane bioreacctor
MIX	Mixed algal and bacterial species

MM	Mineral medium
MW	Molecular weight [N M^{-1}]
MWW	Municipal wastewater
NADPH	Reduced form of nicotinamide adenine dinucleotide phosphate
NL	Natural lights
NIT	Nitrifying bacteria
NOB	Nitrite-oxidizing bacteria
NO_X	Oxidized nitrogen compounds (sum of NO_2^- and NO_3^-) [M L^{-3}]
NR	Volumetric nitrification rate [M L^{-3} T^{-1}]
OD_{680}	Optical density at the wavelength of 680 nm [N]
OEC	Oxygen evolving complex
OPR	Gross volumetric oxygen production rate by microalgae [M L^{-3} T^{-1}]
OPR_{NET}	Net oxygen production rate by microalgae [M L^{-3} T^{-1}]
OR	Open respirometer
OTR	Volumetric oxygen transfer rate [M L^{-3} T^{-1}]
OUR	Volumetric oxygen uptake rate [M L^{-3} T^{-1}]
OUR_{AOB}	Oxygen uptake rate of ammonia-ozidizing bacteria [M L^{-3} T^{-1}]
OUR_{HET}	Oxygen uptake rate of hetereotrophic bacteria [M L^{-3} T^{-1}]
OUR_{NOB}	Oxygen uptake rate of nitrite-oxidizing bacteria [M L^{-3} T^{-1}]
OUR_{OO}	Oxygen uptake rate of other aerobic organisms [M L^{-3} T^{-1}]
OUR_{RESP}	Respiratory oxygen uptake rate of microalgae [M L^{-3} T^{-1}]
PAM	Pulse-amplitude modulated fluorometry
PAR	Photosynthetically active radiation
PBR	Photobioreactor
P-I	Photosynthesis-irradiance
PG	Bacterial growth on plates
PQ	Photosynthetic quotient [N]
PRT	Photo-respirometric test
PS	Photosynthesis
PSBR	Photo-sequencing batch reactor
PSI	Photosystem I
PSII	Photosystem II
PWW	Piggery wastewater
Q_{IN}	Influent flowrate [L^3 T^{-1}]

Q_{OUT}	Effluent flowrate [L^3 T^{-1}]
rbCOD	Readily biodegradable COD [M L^{-3}]
RPM	Revolutions per minute [N T^{-1}]
RQ	Respiratory quotient [N]
Rubisco	Ribulose-1,5-bisphosphate carboxylase/oxygenase enxyme
rOD_{680}	Rate of variation of the opticaal density at 680 nm [T^{-1}]
r_{NIT}	Rate of nitrification [M L^{-3} T^{-1}]
r_X	Rate of Variation of the generic X compound [M L^{-3} T^{-1}]
S/V	Surface/volume ratio [L^{-1}]
SA	Substrate addition in respirometric protocols
sARR	Specific ammonia removal rate [M L^{-3} T^{-1}]
sbCOD	Slowly biodegradable COD [M L^{-3}]
SBR	Sequencing bacth reactor
SCEN	*Scenedesmus* sp.
sNRR	Specific nitrite removal rate [M M^{-1} T^{-1}]
sOPR	Specific gross oxygen production rate by microalgae [M M^{-1} T^{-1}]
$sOPR_{NET}$	Specific net oxygen production rate by microalgae [M M^{-1} T^{-1}]
sOUR	Specific oxygen uptake rate [M M^{-1} T^{-1}]
$sOUR_{AOB}$	Specific oxygen uptake rate of ammonia-ozidizing bacteria [M M^{-1} T^{-1}]
$sOUR_{HET}$	Specific oxygen uptake rate of hetereotrophic bacteria [M M^{-1} T^{-1}]
$sOUR_{NOB}$	Specific oxygen uptake rate of nitrite-oxidizing bacteria [M M^{-1} T^{-1}]
$sOUR_{RESP}$	Specific respiratory oxygen uptake rate of microalgae [M M^{-1} T^{-1}]
sPY	Specific photosynthetic yield [N]
SS	Substrate solution
SSE	Sum of squared error
SST	Sum of squared total
STIG	*Stigeoclonium* sp.
SW	Synthetic wastewater
TAN	Total ammonia nitriogen [M L^{-3}]
TETR	*Tetraselmis* sp.
TKN	Total Kjeldahl nitrogen [M L^{-3}]
TRIB	*Tribonema* sp.
TSS	Total suspended solids [M L^{-3}]
UPC	Universitat Politècnica de Catalunya · BarcelonaTech
V	Reactor's volume [L^3]

VFA	Volatile fatty acids [M L^{-3}]
VSS	Volatile suspended solids [M L^{-3}]
WILD	Wild microalgal strains isolated from natural environments
WWTP	Wastewater treatment plant

CHAPTER 1

INTRODUCTION

1. INTRODUCTION

1.1. Algal-based wastewater treatment: advantages and challenges

Due to the uncontrolled growth of the world population, combined with severe anthropic alterations of biogeochemical nutrient and water cycles, several nations are recently experiencing problems connected with the scarcity of water and natural resources [1]. In addition, the accelerated economic development experienced in the last decades by developing countries greatly contributed to increase the global demand of freshwater and energy, in order to satisfy requests from both human and industrial activities. As a consequence, the production rate of municipal and industrial wastewaters has also remarkably increased in the last decades [1]. Wastewater treatment is crucial to preserve the quality of receiving water bodies and to avoid the uncontrolled release of nutrients in the environment, possibly resulting in the formation of algal blooms and dissolved oxygen (DO) depletion in lakes and rivers, with relevant consequences on the human health and local economies [2]. However, thanks to important scientific and technological advances in the wastewater treatment sector, high water quality standards can be achieved by conventional biological treatment processes, such as the activated sludge or anaerobic digestion processes. These are mature processes that can rely on exhaustive descriptions in the scientific literature, standardized methodologies and robust mathematical modelling, making it possible to reach high organic matter and/or nutrient removal efficiencies and to process large volumes of wastewaters [3]–[5]. However, conventional processes have severe limitations: i) high operational costs and energy requirements for the aeration of mixed liquor and sludge dewatering [6], [7] and ii) high environmental impacts for direct and indirect greenhouse gases (CO_2, CH_4 and N_2O) emissions [8]. These aspects highlight how the conventional

solutions for wastewater bioremediation still need substantial improvements to be considered economically and environmentally sustainable.

The rapid depletion of natural resources experienced in the last century (mainly phosphorus and other rare earth elements) made it necessary to rethink the planning of resource extraction and the management of nutrient biogeochemical cycles in a circular and more sustainable way [9], [10]. Within this context, wastewater are increasingly considered as a valuable and renewable resource, due to its nutrient contents and the availability of valorization alternatives to recover these compounds, allowing to increase the economic and environmental sustainability of the sanitation process [11]–[15]. The concept of wastewater biorefineries has been recently introduced as a mean to simultaneously produce valuable products from wastewater and to safely remove/recover the nutrients/pollutants contained in it, while lowering the overall energy consumption [13], [16]. Wastewater biorefineries can be implemented by using combinations of different treatment units, so to enhance nutrient removal performances and to increase the resilience and stability of the plant, also aimed at improving the overall economic profitability of the process [15], [17], [18].

Recent studies have underlined that a further improvement to wastewater biorefineries can be achieved by integrating phototrophic organisms which can grow in consortia with wastewater-associated bacteria (hereafter referred to as or microalgae-bacteria consortia). Exploiting these consortia can lead to significant advantages in terms of process efficiency and sustainability [19], [20], while guaranteeing a good effluent quality [21]–[23]. The synergic exchange of metabolites (CO_2 and O_2) between algae and bacteria (photo-oxygenation) is probably the most significant feature of this bioprocess, allowing to cut the costs due to aeration in conventional wastewater processes and also to lower the emissions of greenhouse gases due to energy saving and to carbon dioxide negative emissions in algae culturing [24]–[28]. Sludge disposal and energy

supply costs can be also reduced with the algae/bacteria-based treatment. This is achieved for example by recovering nutrients (biofertilizers/biostimulants) or other bioproducts (bioplastics), and by directly producing biogas/biomethane from the anaerobic digestion of the algal-bacterial biomass [29]–[32].

During the past two decades, phototrophs have been successfully exploited in municipal wastewater bioremediation [33], [34]. The use of industrial wastewaters to grow microalgae-bacteria consortia was also reported in several literature reviews. Agro-industrial [35]–[37], textile [38], pharmaceutical wastewaters [39], landfill leachate [40] and anaerobic digestion effluents [29], [41] are only some of the possible liquid streams supporting the growth of algae in association with bacteria. Successful applications of phototrophs to remove undesired compounds from gaseous streams, such as SO_x and NO_x from flue-gases and CO_2 from biogas were also recently reported [42]–[44], suggesting interesting potentialities for the integration of microalgae cultivation units in existing biogas plants. The integration of microalgae-bacteria processes can be implemented in different positions of the treatment scheme of existing WWTPs provided with anaerobic digestion of the excess sludge [33], [45] (Figure 1.1):

A. In the main stream, replacing secondary treatments (activated sludge) for COD, N and P removal;

B. In the main stream, replacing tertiary treatments for the removal of pathogens, metals and contaminants of emerging concern;

C. In the side stream, for the removal of reduced N and P compounds from the liquid fraction of digested wastewaters.

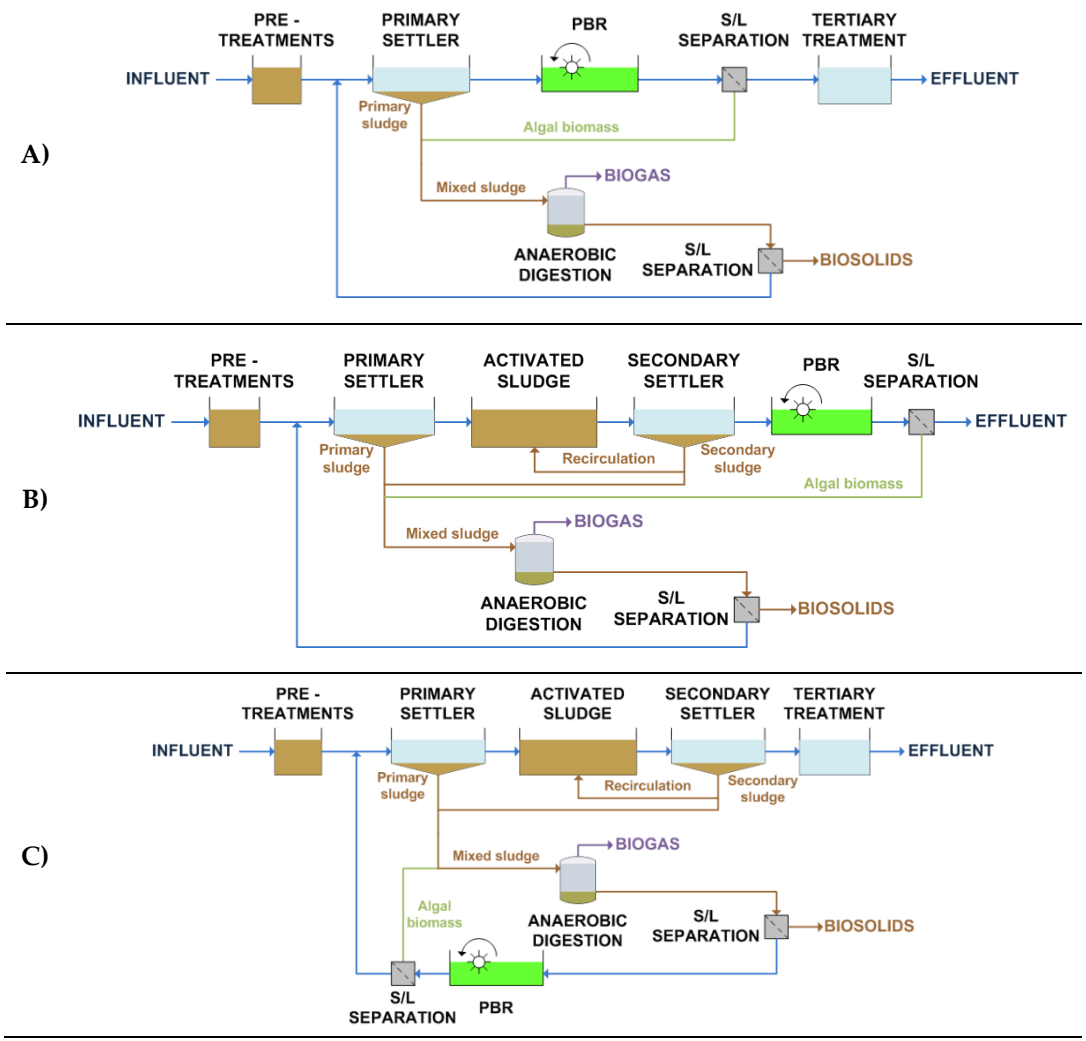

Figure 1.1. Possible configurations for the integration of microalgae-bacteria consortia in existing municipal wastewater treatment plants (A: Secondary treatment; B: Tertiary treatment; C: Treatment of anaerobic digestate).

Among these configurations, [33] reported that, with respect to the optimal wastewater composition, the most suitable condition is the configuration A, where the ratios between nutrients are similar to the typical composition of microalgal biomass. On the contrary, in other configurations it is possible that nitrogen and phosphorus are present at inhibitory concentrations, or that carbon is limiting for algal growth. However, it should be also considered that the two configurations in the mainstream (i.e. configurations A and B) must guarantee very stable performances, as the effluent from the algal-bacterial unit is released with no further treatments aimed at removing nutrients. As further discussed below, the stability of the algal-bacterial system is highly dependent of the atmospheric conditions and it is possible that, under suboptimal conditions, the discharged effluent may not be adequately treated to meet effluent standards set by law.

Therefore, configuration C seems to be the most suitable option to reduce the nitrogen and phosphorus loads under suboptimal climatic conditions, while maintaining the system stability and reducing the overall energy requirements of the WWTP [32], [46].

As highlighted, the biotechnological potential of wastewater bioremediation using microalgae/cyanobacteria is very high, thanks to the environmental and energetic sustainability of the process. However, important bottlenecks still need to be solved before applying algae-bacteria systems at full-scale. These challenges are linked to both the process stability and the optimization of particularly important aspects of algal-bacterial cultivation, as extensively reported in the last years [33], [47]–[49]. Some of the reported challenges were described for pure microalgae cultivation systems but can be applicable to algae-bacteria systems in the same way. Among these aspects, the most relevant for a full-scale application of the process are related to: i) the type of reactor used (HRAPs or closed PBRs),

ii) the environmental conditions, iii) the self-shading effect that is in turn related to i) and ii), iv) the downstream processing of algal biomass, and v) the large land use of these systems (Table 1.1).

The choice of the reactor type has impacts on the process stability, on the biomass productivity and eventually on the economics of the system. Using HRAPs results in operational costs that are even lower than conventional systems. In these reactors, however, other problems may occur, such as the contamination of the culture and the high evaporation losses due to the large specific surface of the HRAP. On the contrary, closed PBRs are generally characterized by higher capital and operational costs. However, a higher photosynthetic efficiency may be reached in closed PBRs, due to the improved capturing of the light energy. The contamination from undesirable algae species or from other microorganisms and the loss of water through evaporation are less likely to occur in these reactors, since the biomass is physically separated from the environment.

On the other hand, the photosynthetically produced oxygen and all other gaseous metabolites are held in the reactor with possible inhibitory effects on the biomass, thus requiring a degassing unit.

Environmental conditions in the cultivation reactor can strongly affect nutrient removal and biomass growth rates. The most important environmental parameters are light, temperature, pH and DO. Limitations to microbial growth due to weather conditions can be a relevant problem, especially in those regions where the average local temperature and irradiance are very different from optimal growth parameters. Indeed, under suboptimal conditions growth can be inhibited, with consequences on the photo-oxygenation capability and on the stability of the system. In particularly severe weather conditions, artificial lights and heating systems can be employed to guarantee a constant productivity over the year. However, this results in increased operational costs and the real

applicability should be carefully evaluated. Regarding temperature, this parameter regulates the thermodynamics and kinetics of all chemical-physical processes, such as the solubility of all gaseous compounds (e.g. NH_3, CO_2), and has a strong direct effect on metabolic activities of algae/bacteria [50], [51].

pH is another important environmental factor that regulates all chemical equilibria in solution and therefore the availability of nutrients for the biomass (ammonium/ammonia, phosphates, carbonates). pH can affect both algal and bacterial metabolic activities, similarly to what happens to temperature [52], [53] and can be responsible for a reduction of nutrient concentrations due to stripping of unionized-ammonia and phosphates/metals precipitation at high pH. The DO concentration is another key aspect that can potentially inhibit the growth and photosynthetic efficiency of microalgae/cyanobacteria [54], [55]. [53] has shown that respiratory activities are affected by the DO concentration, with limitation of respiratory rates at low DO and inhibition at very high DO concentrations, making degassing units necessary for closed PBRs as previously underlined.

The self-shading effect is the phenomenon in which the increase in algal biomass concentration is responsible for a decreased light availability in the reactor. This effect can be only partially reduced, e.g. by increasing the mixing rate in the culture in order to let algal cells move towards the illuminated parts of the reactor [48].

Several harvesting methods to recover the algal biomass are available, however the final separation of the biomass from the treated water is a limiting factor. Indeed, due to the small size of algal cells, low-cost technologies (natural settling, filtration) cannot be applied. Although quite efficient, other commonly adopted biomass separation methods (floatation, centrifugation and electro-dewatering) are characterized by high energy requirements and therefore by high operational costs.

Table 1.1. Main challenges for the application of microalgae-based wastewater treatment at full-scale.

COMPARTMENT	PROBLEM	DESCRIPTION	CONSEQUENCES
Wastewater	Turbidity / color	High turbidity/TSS concentrations	Reduction of light availability, reduction in photosynthetic oxygen production
		Colored wastewater	Reduction of light availability, alteration of sunlight spectrum
	Content of nutrients and other compounds	Low alkalinity/inorganic carbon content	Carbon limitation for nitriying bacteria and phototrophic biomass; high fluctuations in pH
		Excessive organic carbon content	Possible inhibition of phototrophic growth, possible mixotrophic algal growth and limited growth for heterotrophic bacteria
		Excessive NH_4^+ concentration	Possible inhibition of microalgae growth, generation of unionized ammonia high pH with possible inhibition of microalgae and nitrifying bacteria
		Unbalanced C/N/P ratio	Excessive N and P concentrations can result in inhibited algal growth, low inorganic C concentrations can result in limited algal growth
		Presence of heavy metals	Possible inhibition of photosynthesis
		Presence of emerging contaminants	Possible growth inhibition for algal and bacterial biomass
Site	Environmental conditions	Suboptimal conditions	Excessively low or high irradiance and temperature values result in inhibited algal growth, the variation of light and temperature along the day result in extremely varying pH and DO concentration, possibly affecting algal and bacterial growth rates
		Differentail seasonal efficiency	According to the location of the algal-bacterial PBR and the tolerance of microorganisms to extremely cold conditions can result in a decresed removal efficiency, for a significant period of the year
Process	Process knowledge	Undefined algal species involved	Scarce informations to predict the shift of predominant algal species at different environmental/operational conditions
		Undefined bacterial species involved	Great diversity of bacteria living in symbiosis with phototrophs, different dominant species for different wastewaters
		Unknown algae-bacteria interactions and optimal growth conditions	Scarce information about the interactions (both competititve and synergic behaviours reported), difficult determination of optimal growth conditions, no robust microalgae-bacteria models available
		Stability of the process and overall WWTP stability	Microalgae-based processes should be sufficiently stable to ensure effluent quality, the collapse of a main stream culture can result in a failure of the entire WWTP
	Low removal rates	Limited algal growth	Low S/V ratios and poor mixing conditions can result in a low light availability due to self-shading,
	Biomass harvesting costs	Unknown/unsufficient auto-flocculation properties	Microscopic size of microalgae does not allow for separation by settling, the formation of algal-bacterial flocs and granules is not well understood, use of flocculants or other energy-expensive solid/liquid separation can be required
	Biogas production	Low methane yield	The presence of cell walls makes the digestion process inefficient unless expensive pretreatments are carried out
PBR	Scaling-up	No established scale-up methodology	Incerasing the reactor size can result in limited light availability, poor excess DO removal capabilities and CO_2 losses
	Large footprint	High S/V ratio needed	PBRs require large land surfaces to obtain high photosynthetic efficicency
	High costs	High installation/operational costs	The high energy consumption in closed PBRs translates in high specific energy consumption, if the system is operated at high HRT
	Nutrient losses	Ammonia loss through stripping	Open reactors (especially HRAPs) are characterized by high ammonia stripping if the pH is not controlled
		Phosphates losses through precipitiation	Phosphates in the suspension may precipitate if the pH is not controlled
Legislation/market	Unsuitable biomass use for direct/indirect valorization	Difficulty in reaching the feed and chemicals industry	Regulatory problems occurs in the use of algal-bacterial biomass as animal feed or to produce high-value chemicals
		Excessive heavy metals in the biomass	Heavy metals absorbed or metabolized by microalgae can be excessive for direct land application

Flocculation is one of the most used techniques to enhance solid/liquid separation, which can be achieved using chemicals, assisted by other organisms (bio-flocculation) or directly performed by phototrophs (auto-flocculation). In these cases, operational costs are generally lower but other problems may occur, such as the contamination of the biomass with chemical flocculants or the insufficient knowledge of bio-/auto-flocculation properties.

The large surface requirement of algal cultivation systems is a well-known critical aspect. Indeed, the surface requirements for algal photobioreactors are especially relevant for outdoor HRAPs, in which the water depth is limited to 0.2 - 0.3 m, in order to allow for light penetration. These reactors are generally characterized by a high surface/volume ratio, thus resulting in a large area requirement to maximize the photosynthetic efficiency.

Regarding other aspects, that are directly connected with the cultivation of phototrophs-bacteria consortia, the following ones should be considered, as discussed below: i) the scarce knowledge of algae-bacteria interactions, ii) the characteristics of influent wastewaters, and iii) the biomass valorisation alternatives.

The biological complexity of algae-bacteria consortia is quite high, due to the simultaneous presence of synergy and competition mechanisms as shown in Figure 1.2. Synergic interactions can occur between phototrophs and heterotrophic bacteria, thanks to the photosynthetic O_2 production and bacterial CO_2 production. However, other interactions are mainly based on a competition for common resources: (inorganic N, P and C compounds), often resulting in limited growth for some populations. Other authors [21], [56], [57] also underlined that both algae and bacteria can release complex substances, interacting with the other microbial populations present in the consortium. These

metabolites may include both compounds with bactericidal effects released by algae and compounds with algaecide effects released by bacteria.

A wide range of algal and bacterial species were identified in mixed consortia fed with municipal/industrial wastewaters and are reported in literature, eventually correlated with the composition of the wastewater and with operational and/or environmental conditions applied [49], [58], [59]. Generally, a low microbial diversity is found among algal species residing in algae-bacteria reactors, with a few species mainly belonging to green algae and cyanobacteria commonly present (*Chlamydomonas* sp., *Scenedesmus* sp., *Chlorella* sp., *Oscillatoria* sp., *Nitzschia* sp., *Euglena* sp., *Navicula* sp.and *Stigeoclonium* sp.) and a single strain dominating over other algae [33], [45]. Among these algal species, *Chlorella* sp. or *Scenedesmus* sp. frequently dominate the consortium.

Regarding the diversity of bacterial species in algae-bacteria units, only a few information is available in literature [33]. However, it has been observed that the bacterial community developing in the system is highly dependent on environmental conditions and wastewater characteristics [60], [61]. As mentioned, activated sludge bacteria are normally present, although many other bacteria can be found at lower concentrations [62].

A systematic identification of bacterial species growing in outdoor PBRs is however difficult to be obtained because of the continuous perturbations applied to the system (wastewater composition and weather conditions), thus resulting in frequent modifications of the bacterial population [60]. This contributes to provide uncertainty in modelling the evolution of the consortium and may constitute a relevant problem for the identification of bacterial kinetic or stoichiometric parameters. Even if the variability of phototrophic species is low compared to bacteria, the phototrophic metabolism is quite effective in modifying the conditions inside the PBR (i.e., pH and DO). In addition, the

concentration of phototrophs is generally higher than bacterial biomass and a shift in the phototrophic population can strongly affect the entire consortium, also resulting in unavoidable under/overestimations of removal efficiencies and biomass productivities. This lack of knowledge has crucial consequences on the interpretation of algae-bacteria dynamics and particularly on the prediction of the system efficiency/stability with mathematical models.

Bottlenecks related to the wastewater characteristics are typical of any biological process. As for the algal-bacterial consortia, the relevant ones are: i) the optical properties of the influent wastewater, ii) the balance among nutrient concentrations (i.e. the C/N/P ratio) and iii) the presence of toxic/inhibitory compounds.

Poor optical properties of the wastewater (e.g. the presence of high turbidity and/or high TSS concentrations) can negatively affect the growth of phototrophic microorganisms in algae-bacteria consortia, due to a low light availability. Indeed, the absence or malfunctioning of wastewater solid/liquid separation systems can be a failure cause for algal-bacterial PBRs. Another typical drawback is the presence of a background colour, which is commonly found in industrial waste streams [63], [64]: landfill leachate [65], dairy [66] or tannery and textile wastewaters [67], brewery/distillery [68] and pulp and paper industry effluents [69].

As reported in previous findings [22], [57], [70], among others, wastewaters from different sources are characterized by extremely different contents in terms of nitrogen, phosphorus and organic/inorganic organic carbon concentrations. According to the composition of wastewaters and to the relative proportions of these compounds, inappropriate C/N/P ratios can be found in industrial wastewaters, causing limited growth for algae or bacteria. Not only the average C/N/P ratio should be known before designing the algal-bacterial unit, but also

the absolute concentrations of mentioned nutrients must be measured, as too high or too low concentrations can also cause limited/inhibited growth. For example, excessive TAN (total ammonium nitrogen) concentrations can cause inhibition for both algae and bacteria [71], [72]. In addition, the presence of high concentrations of ammonium (NH_4^+), combined with high pH values (above 8.5 - 9) can cause the generation of unionized-ammonia (or free ammonia, NH_3), which is a strong inhibitor of the photosynthetic process [21], [73], [74]. Although some phototrophic species can grow heterotrophically on aromatic hydrocarbons and other complex organic compounds, high concentrations of these compounds can result in inhibited growth for algae [21]. The presence of organic carbon in the influent wastewater can also activate mixotrophic algal growth, for which synergic/competition interactions with heterotrophic bacteria are not well understood yet [75].

Specific compounds can also have adverse effects on algal photosystems, such as heavy metals, pharmaceuticals and personal care products, among others [21], [39]. Although these compounds are generally available in very low concentrations in municipal wastewaters [76], the presence of heavy metals could be relevant in industrial wastewaters, possibly resulting in the inhibition of the photosynthetic process [77]. For the reasons described above, the composition of wastewater (over a statistically significant period) and the availability of local waste streams should be determined before designing the bioremediation system.

In order to reduce adverse effects, the characteristics of the wastewaters can be optimized, for example by: i) pre-treating the wastewater to improve its optical properties, e.g. by using activated carbon or bio-char to remove the colour, [64], ii) blending the wastewater with other waste streams, to obtain a C/N/P ratio close to the optimal [78], or iii) diluting the wastewater (to reduce the concentrations of inhibitory compounds, [79].

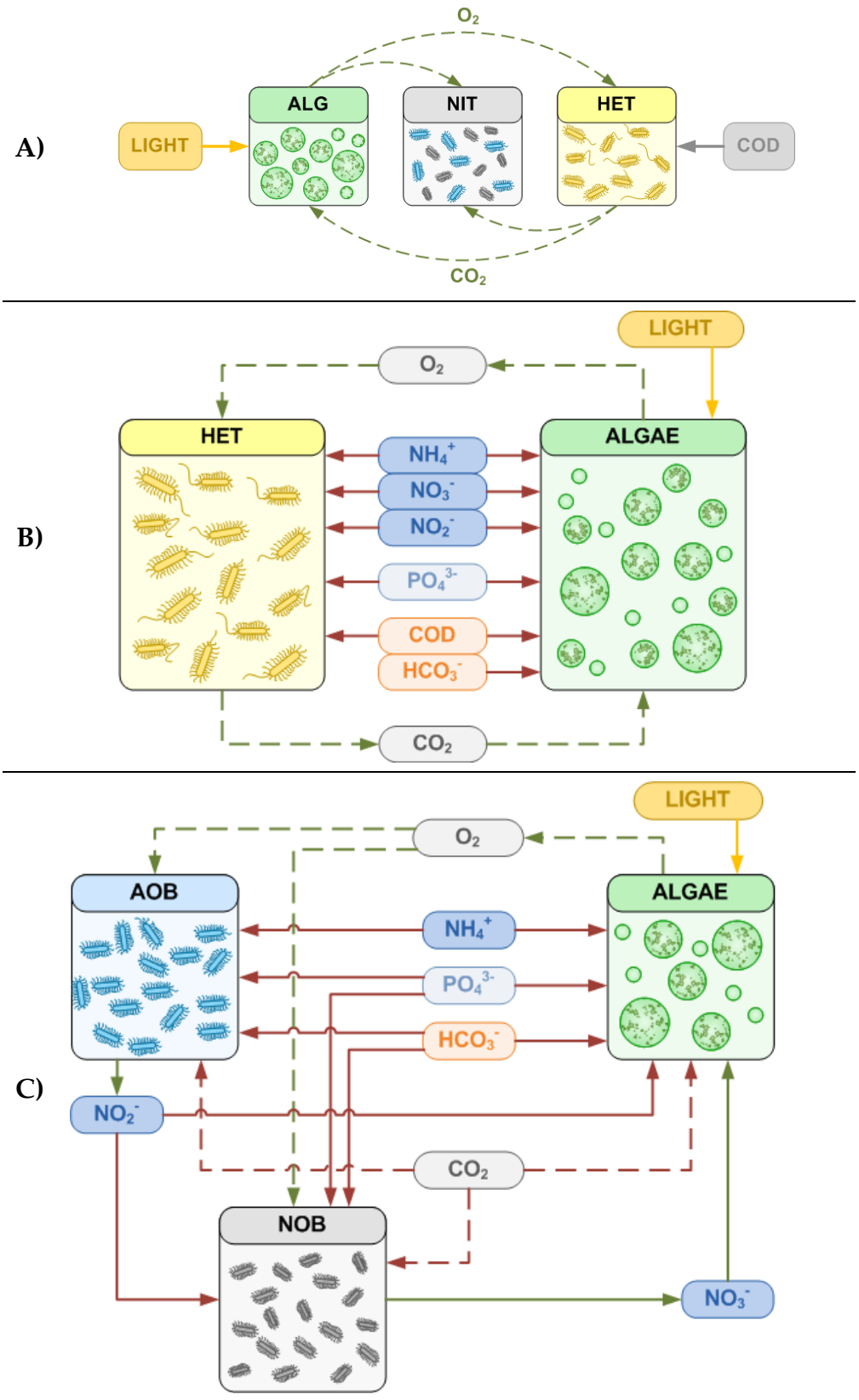

Figure 1.2. Possible interactions among phototrophic organisms, nitrifying bacteria and heterotrophic bacteria. Green lines are synergic interactions, red lines are competitive interactions (A: simplified scheme of synergic interactions, B: Interactions between phototrophs and heterotrophic bacteria; C:interactions between phototrophs and nitrifying bacteria).

As mentioned, a key point of algae/bacteria-based processes is the valorisation of the algal-bacterial biomass as different products: animal feed, bioenergy (biofuels) and bioproducts (bioplastics/biofertilizers). Due to the high content in lipids, carbohydrates and proteins, microalgae represent an excellent feed for the aquaculture industry [80] and can be also added as feed supplement to other animals. Microalgae can be exploited either as a direct food source for animals or indirectly, by using the phototrophic biomass to grow rotifers or crustaceans that are subsequently fed to aquaculture organisms. However, some concerns were raised about the use of algal-bacterial biomass as animal feed, mainly due to the public unacceptance of introducing wastewater-grown biomass in the food chain. With respect to this point, further research is needed to define toxicity and microbiological quality assays for the harvested biomass, as recently suggested [59].

The use of microalgae as soil conditioners or biofertilizers is also an attractive feature, due to the possibility of recycling nutrients (mainly nitrogen) instead of making use of environmentally unsustainable chemical fertilizers. Bioactive compounds from microalgae are thought to promote the growth of higher plants and to reduce plant diseases [81], [82]. However, the use of algal-bacterial biomass to produce biofertilizers is subordinated to respecting local regulations for the introduction of nutrients, recalcitrant organic compounds and heavy metals in the soil.

Finally, with respect to the use of algal-bacterial biomass for biogas production, the main challenges are related to the necessity of operating pre-treatments to the biomass to facilitate the anaerobic digestion of algae cells by methanogenic bacteria. Indeed, the anaerobic degradation of microalgae/cyanobacteria is hindered by the presence of a cell wall characterized by a very low biodegradability, which makes the digestion process inefficient and force to

apply expensive mechanical, chemical, biological or thermal pre-treatments, to obtain acceptable biogas yields [29], [30].

1.2. Aims and outline of the thesis

As discussed in paragraph 1.1, several disadvantages exist in the context of algal-bacterial wastewater treatment hindering the scale-up to full-scale systems. In particular, the poor knowledge of the process, in terms of interactions between algae and bacteria, was recognized as one of the relevant drawbacks, causing large uncertainties in process modelling and preventing the successful exploitation of the numerous environmental and economic advantages of algal-bacterial bioremediation. The main consequences of this lack of knowledge are that algae-bacteria systems suffer from unstable operation making it difficult to obtain the desired removal efficiencies during long-term operation.

For the same reasons, it is quite difficult to describe algal and bacterial growth through mathematical models, which would in turn allow to predict the system's efficiency and to retrieve other important information about the metabolic state of the consortium. This translates in a general diffidence by wastewater stakeholders towards the application of the described biotechnology.

The aim of this thesis is therefore to provide a set of standardized protocols in which photo-respirometric methods, based on dissolved oxygen measurements, are exploited to retrieve relevant information on the algae-bacteria system. By performing such experiments, mathematical models describing the growth of algae and bacteria can be more easily calibrated, resulting in a better understanding and prediction of the system behaviour.

In this thesis work, three different protocols were defined, and validated, on different algae-bacteria systems at lab-, pilot- and demonstrative-scales:

1. A "**monitoring**" protocol, aimed at evaluating the evolution of phototrophic organisms and nitrifying bacteria in algae-bacteria systems. This protocol was applied to monitor several algae-bacteria reactors, fed with different types of wastewaters: synthetic, aquaculture and piggery wastewaters, agricultural runoff and anaerobic digestates from municipal and piggery wastewaters;

2. A "**model calibration**" protocol, aimed at evaluating useful parameters to describe the growth of phototrophs in algae-bacteria systems and to calibrate algae-bacteria growth models. This protocol was applied to determine optimal environmental conditions (irradiance, temperature, pH and DO) for phototrophic organisms grown in a pilot-scale HRAP for anaerobic digestate treatment.

3. An "**inhibition**" protocol, aimed at evaluating the effects of inhibitory compounds on phototrophic organisms. This protocol was applied to retrieve EC_{50} concentrations and to describe the inhibition of photosynthesis due to unionized ammonia in different phototrophic species (microalgae and cyanobacteria), sampled from both phototrophs' monocultures and mixed microalgae-bacteria cultures.

In the following chapters, the review of the relevant literature, material and methods and main results are described as follow.

In **Chapter 2**, a review on (photo-) respirometric methods applied to the characterization of different microorganisms is reported. Conventional respirometric and photo-respirometric methods are reviewed, with a focus on the characterization of activated sludge bacteria and microalgae/cyanobacteria monocultures, respectively. Finally, photo-respirometric methods applied to algae-bacteria consortia are reviewed, focusing on potential applications of the technique and on the most important challenges faced in this research line.

Applications to reactors monitoring and mathematical model calibration are also discussed.

Chapter 3 describes all the experimental devices used in this work (namely, the photo-respirometric devices and the cultivation systems from which the biomass samples were taken) and the analytical methods applied.

In **Chapter 4**, the three mentioned photo-respirometric protocols are described in detail, together with a series of indications aimed at improving the repeatability of such experiments, through the definition of standard methodologies and the evaluation of common mistakes to be avoided during photo-respirometry assays.

Chapter 5 reports the results obtained during this work, namely the outputs of photo-respirometric tests for "*monitoring*", "*model calibration*" and "*inhibition*" protocols, in all the systems to which the protocols have been applied.

Finally, in **Chapter 6**, a set of guidelines for executing photo-respirometric tests on algae-bacteria consortia are given, together with an analysis of further research needs, as emerged from the review of literature works and the experimental activities described in the present work.

CHAPTER 2

PHOTO-RESPIROMETRY TO SHED LIGHT ON MICROALGAE-BACTERIA CONSORTIA: A REVIEW

2. PHOTO-RESPIROMETRY TO SHED LIGHT ON MICROALGAE-BACTERIA CONSORTIA: A REVIEW

2.1. Conventional respirometric methods

Respiration is the catabolic process generating adenosin-triphosphate (ATP), from the chemical energy contained in an electron donor into ATP molecules. During the anabolic phase, this energy is used to synthetize new components for cell growth and maintenance. In activated sludge processes (ASP), electron donors can be organic or inorganic compounds, while the electron acceptor is an inorganic compound (O_2 or, less frequently, other molecules such as NO_3^-, NO_2^- or other S and Fe oxidized forms). Estimating microbial respiration by calculating the electron acceptor's consumption rate gives an indication of the metabolic state of microorganisms. Moreover, energy generation results in CO_2 variation, so that respirometry may also include the monitoring of CO_2 production rates [83], [84]. In principle, electron donors' consumption rates could also return the same information, but this measurement is not universally considered respirometry, as other processes not directly linked to energy generation might be present (e.g. internal storage and/or direct electron donor's uptake processes).

Respirometry allows for a fast and simple assessment of bacterial kinetics. Indeed, the duration of respirometric assays may range from ten minutes to some hours and can be carried out by using conventional laboratory equipment. Furthermore, respirometry is a repeatable and very flexible technique, since experiments can be performed by varying almost every operational/environmental parameter [85]–[89]. The method is also quite effective to perform kinetic/stoichiometric parameter estimation in wastewater treatment modelling, often coupled titrimetry and biomolecular techniques (such as Fluorescence In Situ Hybridization, FISH). While molecular tools allow

gathering additional community characteristics, they generally imply long time response [90], [91]. On the contrary, titrimetric methods are easily integrated with respirometry, having similar instrumentations and timing. The output of a titrimetric test is the titrant (acidic/alkaline solution) volume required to maintain a determined pH setpoint. According to the stoichiometry of biochemical pH-affecting reactions, the volume of added titrant is proportional to the microbial growth/respiration rate [92]–[94]. The design of respirometric and titrimetric experiments in wastewater processes has been discussed in detail, especially as for the parameters included into the Activated Sludge Models (ASM) [3], [95]–[97].

2.1.1. Respirometric devices

Respirometry is typically performed in dedicated reactors (respirometers), under controlled conditions. Common equipments constituting a respirometer are: a glass/plastic reaction vessel, a liquor mixing system and a system for thermal regulation. Temperature and dissolved oxygen (DO) probes must be present in the gas or liquid phase, having appropriate response times to avoid erroneous estimations. When the test is meant to last for more than few minutes, a device for the reaeration of the bacterial suspension is also necessary to maintain aerobic conditions. For lab-scale respirometers, this is achieved using an air compressor connected to a fine bubble diffuser. In the titrimetric configuration, a pH-meter and a dosing system for acid/base and/or CO_2 gas are also required. Finally, a data logger is needed to store DO, temperature, pH and titration data. Other common auxiliary devices may include pumps for substrates dosing and additional tanks for storing substrates or acid/base solutions. N_2 or other inert gases may be also required to deoxygenate water and to determine the oxygen mass-transfer coefficient (k_La) without modifying the salinity of the water as it

happens using Na_2SO_3 [98]. In terms of respirometric devices, no standardized setup actually exists; however, almost all respirometric devices can be classified into eight main classes, according to two main characteristics [84], [99]: i) the phase in which the oxygen concentration is measured, i.e. in the liquid (L) or in the gas (G) phase, and ii) the presence or absence of a flow in the liquid or gas phase (F for flowing gas/liquid, S for static gas/liquid). To each respirometric configuration, a mathematical model explaining both physical and biochemical processes can be coupled to estimate the respiration rates, considering the oxygen transfer rates (OTR) and the influent and effluent gas/liquid oxygen loads, when relevant. Oxygen mass balances allow for the assessment of O_2 consumption over time, known as Oxygen Uptake Rate (OUR), representing the main output of the bioassay. The OUR typically depends on the rates of organic matter oxidation and nitrification processes over time [100], [101]. After evaluating the k_La, the OTR can be evaluated and the bacterial OUR inferred, according to Equations 2.1 and 2.2:

$$\frac{d(DO)}{dt} = OTR - OUR \quad 2.1$$

$$OTR = k_L a^* (DO_{SAT} - DO) \quad 2.2$$

Where DO_{SAT} is the DO concentration corresponding to the saturation level at the test temperature [98].

A common alternative to evaluating the OUR in biological systems is to apply a mass balance to the biological treatment tank, based on the characterization of the chemical species involved in the bioprocess to be monitored. In this case, the mass balance allows to define a rate of variation for each compound X present in the bioreactor at the instant i:

$$\frac{\Delta X(t_i)}{\Delta t} = \frac{\overline{Q_{IN}}(t_i) * \overline{X_{IN}}(t_i)}{\overline{V}(t_i)} - \frac{\overline{Q_{OUT}}(t_i) * \overline{X_{OUT}}(t_i)}{\overline{V}(t_i)} - \frac{\overline{X_{OUT}}(t_i)}{\overline{V}(t_i)} * \frac{\Delta V(t_i)}{\Delta t} + r_X(t_i) \quad 2.3$$

Where: $\Delta X(t_i)=\left(X(t_i)-X(t_{i-1})\right)$ is the variation of the compound X between two consecutive time points [mg L^{-1}], $\Delta t=(t_i-t_{i-1})$ is the time step [d], $\overline{Q_{IN}}(t_i)=\text{average}\left(Q_{IN}(t_i),Q_{IN}(t_{i-1})\right)$ and $\overline{Q_{OUT}}(t_i)=\text{average}\left(Q_{OUT}(t_i),Q_{OUT}(t_{i-1})\right)$ are the influent and effluent flowrates, respectively [L d^{-1}], $\overline{X_{IN}}(t_i)=\text{average}\left(X_{IN}(t_i),X_{IN}(t_{i-1})\right)$ and $\overline{X_{OUT}}(t_i)=\text{average}\left(X_{OUT}(t_i),X_{OUT}(t_{i-1})\right)$ are the average concentrations of the compound X in the influent and effluent, respectively [mg L^{-1}], $\overline{V}(t_i))=\text{average}\left(V(t_i),V(t_{i-1})\right)$ is the average volume between two consecutive time points [L], $\Delta V(t_i)=\left(V(t_i)-V(t_{i-1})\right)$ is the variation of volume between two consecutive time points [L], and $r_X(t_i)$ is the rate of variation of the compound X at the time t_i [mg L^{-1} d^{-1}].

As an example, the OUR due to nitrification can be evaluated by calculating the rate of variation of the oxidized compounds NO_2^- (r_{NO2} [mg N L^{-1} d^{-1}]) and NO_3^- (r_{NO3} [mg N L^{-1} d^{-1}]), from which the activity rates of AOB and NOB are computed:

$$r_{AOB}(t_i)=r_{NO2}(t_i) \quad 2.4$$

$$r_{NOB}(t_i)=r_{NO2}(t_i)+r_{NO3}(t_i) \quad 2.5$$

The overall OUR due to nitrification is then expressed by taking into account the stoichiometric amount of O_2 needed to oxidize NH_4^+ to NO_2^- (3.25 g O_2 g N^{-1}) and NO_2^- to NO_3^- (1.08 g O_2 g N^{-1}) [5]:

$$OUR_{NIT}(t_i)=r_{AOB}(t_i)*3.25+r_{NOB}(t_i)*1.08 \quad 2.6$$

The main advantage of using respirometric methods is that, contrary to the method just explained, the measurement of OUR can be performed in a very rapid way, as detailed in the following sections.

2.1.2. Typical applications in the field of wastewater treatment

Respirometry has been successfully exploited for bioremediation applications, which ultimately relate to: i) the estimation of kinetic/stoichiometric and inhibition parameters in conventional ASPs and ii) the monitoring/optimization of biological wastewater treatment sections. Indeed, relevant parameters for both nitrifying and heterotrophic bacteria can be estimated by modeling respirometric tests. Wastewater characterization can be also targeted, being normally required to apply ASMs. Biochemical Oxygen Demand (BOD) is largely applied to this purpose, though requiring from 5 to 20 days, while faster alternatives are available [84], [102]–[104], also in combination with titrimetry [93]. In the ASP, pH-affecting reactions occur due to the consumption/production of strong or weak acidic/alkaline compounds (e.g. consumption of NH_4^+ and production of NO_2^-, consumption of organic acids and production of CO_2 [92] and the calculation of titrimetric rates may significantly improve the robustness of estimated parameters [95], [105]. Titrimetry is especially useful in case of nitrification kinetics, being responsible of a direct H^+ production [95], [106], [107].

Finally, respirometric methods allows assessing the active fraction of the autotrophic and heterotrophic bacteria in activated sludge [108]–[110] and characterizing short-term inhibition in presence of specific chemicals/wastewaters [111], [112]. Respirometry/titrimetry can be applied to monitor and to control bioprocess performances using automated devices [99], [113]. Respirometry-based control loops can rely on the assessment of biomass activity assessment [114], [115] or on the detection of inhibition phenomena [116]. Bioprocess control techniques based on oxygen measurements are particularly suitable for sequencing batch reactors (SBR), where control logics play a crucial role [117]. Other respirometric control strategies, proposed in the framework of

benchmark simulation models, improved the process efficiency and stability, also guaranteeing a cost reduction [118], [119].

2.1.3. Conventional respirometric protocols

Three main typical applications of respirometry are currently adopted in the field of biological wastewater treatment: i) the characterization of wastewaters, in terms of organics and nitrogen fractions, including the active biomass concentration; ii) the estimation of kinetic/stoichiometric parameters describing bacterial growth and substrate assimilation, and iii) the estimation of inhibition coefficients for toxic wastewaters/compounds. These applications are briefly reviewed in the following paragraphs. It is useful to stress here that, by selecting appropriate experimental designs and mathematical models, more than one of the mentioned parameters can be assessed from a single respirometric assay.

Wastewater characterization

The characterization of influent wastewaters is crucial in wastewater treatment operation and modelling. As for modelling, influent concentrations in terms of each relevant component should be defined for dynamic simulations. Figure 2.1 reports an overview of identifiable wastewater characteristics. The total COD is divided into particulate/soluble, as well as into biodegradable/unbiodegradable components. Respirometric tests can be easily designed to derive biodegradable fractions, i.e. the soluble biodegradable or readily biodegradable COD (rbCOD, composed of low molecular weight compounds such as glucose, acetate, ethanol, volatile fatty acids, etc.), and the slowly biodegradable COD (sbCOD, composed by complex colloidal/particulate compounds with a high molecular weight, needing to be hydrolyzed prior to assimilation).

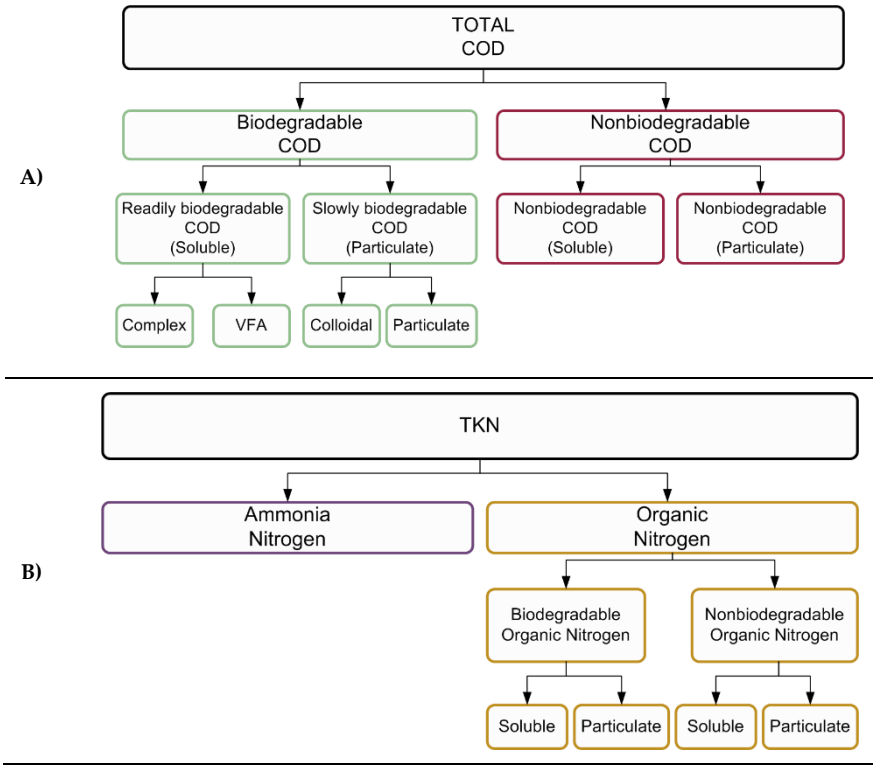

Figure 2.1. Wastewater fractions identifiable from respirometric assays (A: identifiable COD fractions, B: identifiable TKN fractions).

The guidelines for good modelling practice for ASMs provide useful recommendations to assess COD- and N-fractionation, using respirometry [120]. rbCOD and sbCOD can be determined by adding the wastewater to an activated sludge sample under endogenous conditions. Nitrification inhibitors (generally allylthiourea, ATU) are dosed to avoid overestimations due to the NH_4^+ oxidation, although this step is not strictly required if both oxidation kinetics are modelled [121], [122]. The OUR is then monitored until the respiration rate returns to the endogenous level. In this context, expertise in respirograms interpretation might be required, due to the difficult definition of the actual areas of the respirograms identifying rbCOD and sbCOD [84]. As for influent nitrogen, respirometric fractionation can be also performed, obtaining NH_4^+ and organic N concentrations [84]. Ammoniacal N can be assessed from batch tests with nitrifying sludge: the initial NH_4^+ concentration can be estimated, provided that

the yield coefficients and NH_4^+ requirements for heterotrophic growth are calculated. Organic N (both readily hydrolysable and slowly hydrolysable organic N) can be also estimated, by interpreting the respiration rate as a function of organic N ammonification. Finally, the amount of active biomass in wastewaters or activated sludge samples can be identified from correctly designed respirometric tests. This can be done, again, by observing OUR dynamics in the sample and comparing with the values obtained after a significant period of growth [108], [110]. Although nitrifiers concentration is theoretically identifiable from the described procedure, this assay is normally performed to identify heterotrophic growth, as initial concentrations and net growth rates for nitrifiers are lower. The determination of autotrophic biomass concentrations is generally limited to the case of industrial wastewaters characterized by high N-loads.

Biomass characterization

In the last decades, the estimation of kinetic/stoichiometric parameters from respirometric/titrimetric data has been widely adopted, to improve the prediction accuracy of ASMs. Vanrolleghem et al. and Petersen et al. reported exhaustive overviews [96], [123], confirming that respirometry is an excellent tool to this scope. Some identifiable parameters in this framework are the yield and decay coefficients, maximum specific growth rates and half-saturation constants for both heterotrophic and autotrophic biomasses. The heterotrophic yield can be evaluated by dosing wastewater or readily biodegradable substrates to a sludge sample kept under endogenous conditions. The respiration rate is monitored until endogenous conditions are reached again, to evaluate the exogenous O_2 requirement (Figure 2.2). By comparing it to the COD consumption, the yield coefficient is then calculated. A similar procedure in which NH_4^+ or NO_2^- are added, allows estimating nitrifying yields [124]. Decay coefficients are generally

identified in batch tests in which the sludge is kept under aerated endogenous conditions and the respiration rate is fitted to a decreasing exponential curve, with the apparent decay coefficient being represented by the slope of logarithmic respiration rates over time [110]. In this case, knowing other parameters (e.g. the inert particulate fraction of the biomass) may be required to correctly interpret the test [96].

Maximum specific growth rates and half-saturation constants are generally characterized together, as they are strictly correlated in Monod-type models. These parameters can be evaluated for heterotrophic biomass, by measuring the respiration rate after consecutive substrate additions. An OUR value is then associated to each substrate concentration, allowing to fit the Monod model. Similar tests can be performed on nitrifiers, upon addition of variable concentrations of NH_4^+ or NO_2^- [124]–[126]. Several experimental procedures were proposed for the direct determination of the mentioned parameters; the reader is referred to Ruiz et al. and to Spanjers and Vanrolleghem for a more detailed description [84], [127].

Inhibition assays

The assessment of toxic/inhibitory effects on the ASP is also of great interest. Insel et al. and Cokgor et al. [111], [128] presented an overlook of respirometric methods to assess the inhibition on activated sludge bacteria and from these reviews, respirometry emerged as a suitable and consolidated method for inhibition assays. The selection of a proper inhibition model is of crucial importance, and respiration data can be used for identifying and calibrating the most appropriate one [129], [130]. Respirometric tests to assess inhibition or toxicity phenomena basically consist in the measurement of the respiration rate

under well-defined reference conditions (control) and the repetition of the test, in order to evaluate the OUR reduction after the addition of increasing amounts of toxicants [84]. As the contact time is also a key parameter influencing the inhibition process, additional care is required when planning the experiment and comparing results. Indeed, in the described protocol, the contact time increases after each toxicant addition, unless the biomass sample is not renewed for each inhibitory concentration tested [84], [131], [132].

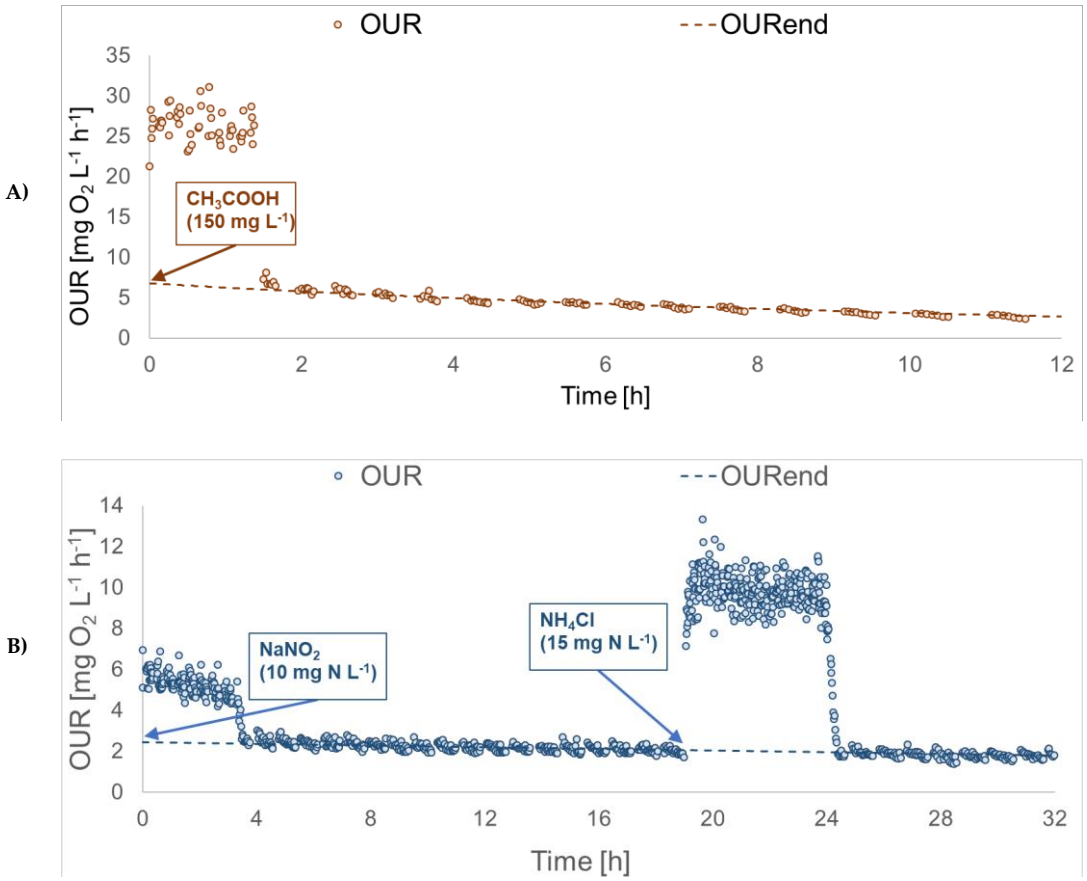

Figure 2.2. Typical respirometric tests performed to evaluate the exogenous OUR of heterotrophic and nitrifying sludge maintained under endogenous conditions (24 h under aeration). A: activity of activated sludge (2.9 g TSS L^{-1}) after the addition of acetate (50 mg L^{-1}) and ATU (10 mg L^{-1}), 20.3 ± 0.3 °C; B: activity of nitrifying sludge (2.5 g TSS L^{-1}) after the addition of ammonium (15 mg N L^{-1}) and nitrite (10 mg N L^{-1}), 21.9 ± 0.1 °C.

2.2. Photo-respirometric methods applied to axenic cultures of phototrophic organisms

In phototrophic organisms, the measurement of oxygen evolution over time can be exploited to quantify algal photosynthetic rates, since oxygen is generated as a by-product of photosynthetic reactions, and for evaluating the oxygen request associated to algal respiration. Indeed, the net oxygen production rate (OPR_{NET}) results from the combination of photosynthesis and respiration processes. Accordingly, the gross oxygen production rate (OPR) is the sum of the net photosynthesis (OPR_{NET}) and the respiration rate (OUR_{RESP}, which has a negative value), or the difference between OPR_{NET} and OPR_{RESP} (which is obviously negative), according to Equation 2.7:

$$OPR=OPR_{NET}+OUR_{RESP}=OPR_{NET}-OPR_{RESP} \quad 2.7$$

The gross OPR gives then an indication of the overall photosynthetic oxygen production and of phototrophic growth [133], [134]. According to this scheme, photo-respirometric methods were intensively used to evaluate the effects environmental parameters and to derive optimal growth conditions for phototrophs. As an example, photosynthesis versus irradiance (P-I) curves are obtained by calculating the OPR at different light intensities, as to evaluate radiation levels causing light-limited growth, photosaturation and photoinhibition phenomena. Moreover, OPR is strongly reduced in the presence of growth inhibiting compounds, so that the photo-respirometric tool may be exploited to study inhibitory effects of toxic chemicals/wastewaters. When studying photo-autotrophic reactions, the OPR assessment is often coupled with the measurement of CO_2 consumption rates or the assimilation of ^{14}C in algal biomass, for studying more in depth the photosynthetic and respiratory processes, with the latter occurring under both light conditions (light respiration) and in the absence of light (dark respiration). The photosynthetic quotient (PQ),

defined as the moles of O_2 released per mole of CO_2 assimilated during photosynthesis, and the analogous respiratory quotient (RQ), representing the moles of CO_2 released per mole of O_2 uptaken during respiration, are also commonly used, providing further information about the biomass activity and carbon utilization rates [135]–[137]. Also in the case of algal activity assays, titrimetry can be coupled to photo-respirometric methods, since photosynthetic reactions are responsible of pronounced increases in pH values [138], [139]. Another useful technique often coupled to photo-respirometric measurements is the fluorescence method [140]. In this section, an overview of these aspects is given, together with a description of the most common photo-respirometric procedures/devices adopted to retrieve information about axenic phototrophic cultures.

2.2.1. Photo-respirometric devices and protocols

The application of respirometric assays to measure photosynthesis and organelles metabolism in photosynthetic cells was successfully applied since over 30 years [141]. Many works based on a photo-respirometric approach aimed at evaluating the behavior of microalgae cultivations under different conditions. During the execution of a microalgal photo-respirometric test, environmental conditions should be carefully controlled, as they can affect measurements and the output of the test. In the same way, these parameters can be controlled and varied during the test, in order to assess their influence on the phototrophic metabolism.

Respirometric devices are often coupled with cultivation reactors, working under similar conditions, so to better represent the cultivation system. In this view, the respirometric device is a complementary measuring method, allowing to better interpret growth data of full-scale systems. For these reasons, the use of a photo-

respirometer is generally preferred than performing the study directly in the cultivation reactor. Photo-respirometers used to assess microalgae OPR and OUR have some common feature with conventional respirometers. Some additional elements, however, are required to characterize photosynthetic processes. A fundamental component in algal photo-respirometry is the light source, allowing to reach desired irradiance levels in the vessel. Light sources found in literature can space from LED lights to fluorescent/incandescent lamps, with consequent differences in emission spectra inside the PAR region (400 - 700 nm). However, in some case the geometry of lightning systems, emission spectra, the light quality (duty cycle, flashing frequency, duration of light/dark (L/D) cycles, etc.) and intensity are not well characterized, making difficult to replicate the conditions applied, or to properly model the light distribution/availability. In order to obtain irradiance levels comparable to those obtained under full solar radiation, it is often necessary to adjust the number of lamps or their distance from the photo-respirometer, therefore requiring additional flexibility for the laboratory setup. The reaction vessel is another element to be chosen carefully, according to the optical property of the material, thus allowing for a correct light penetration at the tested biomass concentration and light intensity. Glass, polycarbonate and acrylic polymers are among the most used materials, as their light transmittance is comparably high. As for the respirometer's geometry and configuration, many possible combinations exist. Experimental layouts may range from small-size cuvettes (1-10 mL), often equipped with integrated light sources, receivers or other devices (absorbance and/or fluorescence measurements), to simple glass flasks exposed to lights. In most cases, however, the photo-respirometer vessel is a small-size equipment with a volume not exceeding 1 L, and algal photo-respirometry is performed in a designated photo-respirometer, external to the cultivation unit.

Basic sensors required to perform algal photo-respirometry and titrimetry are not particularly different from those used in conventional respirometry: pH, DO and temperature probes, on/off signals from peristaltic pumps/electrovalves and flow rates (in the presence of a gas/liquid flow) are indeed the main instruments required. In some cases, dissolved CO_2 or CO_2 probes in the gas phase are substituted to or integrated with classic DO sensors, to better follow the autotrophic metabolisms. In general terms, coupling the two probes (O_2 and CO_2) would be an ideal chaaracteristic of microalgal photo-respirometers, allowing for online estimation of the PQ and RQ and defining operational parameters to avoid photorespiration and inorganic carbon limitation. However, this setup is not commonly used in literature, also due to the higher costs of CO_2 probes. Regarding the control of the main environmental parameters (i.e., light, temperature, DO and pH), the most used devices in photo-respirometry and the differences with conventional respirometry are described in Table 2.1. Other important differences are present when comparing the protocols used in conventional and photo-respirometry. In general terms, the photo-respirometric experiment is a batch test during which different phases succeed, each one being characterized by the presence/absence of light. The succession of L/D phases may be repeated over time (also allowing to determine replicated values and their statistical significance) or the photo-respirometric test can be performed as batch tests in which the lightning condition is constant (i.e., only the light or dark phase characterizes the test). In this case, however, it is not possible to evaluate the gross OPR and this condition should be therefore avoided.

Table 2.1. Main advantages and disadvantages of environmental controls systems in respirometric and photo-respirometric assays.

PARAMETER	DEVICE	DESCRIPTION	ADVANTAGES	DISADVANTAGES
Light	External light source, internal light meter	Radiometric detection of the light intensity, control of external lightning elements	Accurate control of light intensity; possibility of varying the light quality (optical filters); any light source can be used	Irregular radiation field; effective light intensity is reduced through the respirometer's surface (additional PAR measurements); temperature increase
	Internal light source, external light meter	Detection of light intensity through radiometric measurement, control of internal lightning elements	Accurate control of the light intensity; uniform radiation field; low light dispersion (lower radiation exposure for operators)	Higher temperature increase (direct contact with lightning elements); necessity of impermeable barriers for light elements; impossibility of using optical filters
Temperature	Heating/cooling fans	Measurement of air temperature, temperature control with heat exchangers and fans	Absence of interferences with light penetration; gradual temperature variation (low thermal excursion)	Longer response times (delayed heat exchange and temperature control); temperature setpoint relative to the air temperature, rather than to the algal suspension
	Water-jacket reactor	Measurement of temperature, circulation of heating/cooling water through an external jacket	Very fast and efficient heat exchange; simple configuration; temperature setpoint relative to the algal suspension	Interference with the lightning system (light diffraction due to multiple physical barriers, reduction of light availability)
	Direct insertion of heating/cooling elements	Measurement and control of the suspension temperature with submerged heat exchangers	Efficient heat exchange; simple configuration; the setpoint is relative to the algal suspension	Presence of shaded zones (reduction in effective light penetration); higher temperature gradients in the suspension
	Direct heating/cooling of the suspension	Measurement of temperature, direct heating/cooling of the suspension	Accurate temperature control; simple operation	Higher temperature gradients (higher thermal stress (variations in calculated OPRs)
DO	Air sparging	Measurement of DO concentration, injection of compressed air	Efficient re-oxygenation of the suspension; simple configuration; Additional CO_2 source	Impossible to decrease DO below DO_{SAT}; interferences in heterotrophic algal growth (CO_2 injection); air filtration to avoid contamination; N_2 fixation may occur (e.g. cyanobacteria)
	Pure O_2 sparging	Measurement of DO concentration, injection of pure O_2	Very efficient and fast re-oxygenation	No additional C-source provided; dissolved CO_2 stripping
	Other gases sparging	Measurement of DO concentration, injection of N_2 or other inert gases	Efficient/fast de-oxygenation; possibility of using gas mixtures (e.g. air + CO_2)	Dissolved CO_2 stripping, N_2 fixation may occur (e.g. cyanobacteria)
	Dilution with DO-adjusted medium	Measurement of DO concentration, diluting of the biomass with DO-adjusted media	Simple operation; no interferences with other control devices	Only applicable to closed systems or with limited gas-transfer; variations of DO concentration during the test cannot be achieved; possible CO_2 limitation in the DO-adjusted medium
pH	Acid/base solutions	Measurement of pH value, dosage of concentrated acid/base solutions	Very accurate regulation of pH; simplicity in calculating titration data; possibility of providing additional nutrient sources	CO_2 stripping; high pH-gradients at the injection point (high stirring required); volume increase (higher light penetration, variations in OPRs)
	CO_2 sparging	Measurement of pH value, sparging with pure or diluted CO_2 gas	Accurate regulation of pH, possibility of providing additional C-source	Interferences with DO dynamics (DO stripping), difficulty in calculating titration data

In some case, a pre-treatment of the biomass (sample dilution/concentration or sample washing), is required for obtaining the same initial biomass concentration and optical properties of the suspension, or to remove any dissolved residual component from the sample. The biomass concentration in the algal sample can be expressed as total or volatile suspended solids (VSS or TSS, respectively), optical measurements (light absorbance or turbidity) or by evaluating the chlorophyll content in algal cells. The sample dilution simply consists in adding an appropriate volume of synthetic medium to the sample, while the sample concentration consists in the separation of the biomass via centrifugation or filtration, followed by the recovery of concentrated biomass and its resuspension into fresh medium. The concentration procedure is often associated to the washing procedure: the concentration is repeated more than one time, and every time the concentrated biomass is washed with the new medium. Finally, an important aspect, which is normally not accounted for in photo-respirometric studies, is the acclimation of the sample to the test light and temperature conditions, as these aspects may strongly influence the biomass response.

2.2.1.1. Effects of environmental conditions

As highlighted, several environmental and operational conditions may result in metabolic unbalances and stress for the microalgal culture, thus affecting microalgal growth [142]. As an example, nutrient starvation may significantly reduce the photosynthetic activity after a significant period of depletion, altering the optimal irradiance value, but also inducing strong photoinhibition processes [143]. Recently, photo-respirometric approaches were aimed at indirectly investigating the phototrophic metabolism, as a function of such environmental conditions [144]. Similar approaches were also aimed at specifically investigating the effects of light intensity and nutrient availability onto the mixotrophic metabolism of microalgae/cyanobacteria, with potential applications to

microalgal-bacterial wastewater treatament [75], [145], [146]. In order to evaluate stressing conditions for phototrophs, many photo-respirometric approaches were reported, mostly focused on the light intensity and quality, the availability of dissolved components (DO, nutrients), the values of physical/chemical parameters (pH, temperature, salinity).

2.2.1.1.1. Light intensity and quality

The light availability and quality are certainly among the most important variables in activity bioassays, as they drive photosaturation and photoinhibition processes, also influencing the photoacclimation of cells. A deep comprehension of the effects of light intensity on oxygen yield was extensively investigated in recent studies [147], [148]. The net OPR, studied under repeated L/D cycles, was strongly affected by the light intensity, which also affected the maintenance rate of cells (including mitochondrial respiration). In this sense, intermittent L/D protocols may be helpful to explore different metabolic aspects, such as the effects of nutrient starvation [143], photorespiration [149] or photo-acclimation [150].

However, it was shown that equivalent light regimes, in terms of duty cycles and incident light irradiance, can provide quite different photosynthetic activities, depending on the shape of the function describing the time-dependent light intensity, therefore the choice of proper light regimes in photo-respirometry should be carefully evaluated with dedicated experiments [134], [147]. Due to the nature of photosynthetic cultures, the biomass concentration is also seminal to describe the effective light penetration, and therefore the light perceived by algal cells. Indeed, in a dense culture, self-shading effects strongly affect the exposure of cells to light. The light intensity and quality, and the time fraction in which the

algae are effectively exposed to light during L/D cycles (duty cycle), drive photosynthetic reactions. When cells are exposed to light, several processes impacting oxygen dynamics occur.

The first process, photosynthesis, is responsible for O_2 release and for the generation of ATP and NADPH, required for the subsequent CO_2 fixation into new biomass cells. Light respiration processes, implying a simultaneous oxygen consumption in the light, can also occur through O_2-reducing processes: the Mehler reaction, the photorespiration and mitochondrial respiration [151], [152]. These processes are directly influenced by the DO and CO_2 concentrations, and are favored by high O_2/CO_2 ratios [153]. The mitochondrial respiration, associated to maintenance and biomass buildup processes, takes place with the generation of ATP and the oxidation of NADPH, to which the oxygen consumption is finally associated. Another important process occurring in the light is the photorespiration, in which O_2 is consumed in place of CO_2, by means of Ribulose-1,5-bisphosphate carboxylase/oxygenase (Rubisco) activity, requiring high amounts of energy as ATP and NADPH [153].

The effects of light intensity on the photosynthetic activity are completely described through P-I curves [154], [155], in which different regions can be discerned: an initial light-limited region at low light intensities, where the photosynthetic rates linearly increase with the increasing irradiance, a light-saturated region where photosynthetic rates are almost constant and independent on the external irradiance, and finally a photo-inhibition region, in which photosynthetic rates decreases with increasing irradiance levels. By monitoring the oxygen evolution over time, photo-respirometric assays are pivotal tools for understanding metabolic mechanisms occurring in algal cultures, as well as the photosynthetic efficiency as a function of light quality (emission spectra, flashing frequency and duty cycle), intensity (photo-saturation and light attenuation) and history (light amount and quality received prior to the

bioassay). This approach was widely used in the 70's to construct P-I curves for marine and benthic algal species, with the final aim of quantifying dark respiration and photoinhibition contributions on the gross OPR [156]. More recently, the effects of light intensity were evaluated with photo-respirometry and modelled in combination with the variation of other important parameters, such as: biomass concentration [157], temperature, pH and DO [143], [158]. In-situ OPR microsensor measurements recently confirmed that respiration processes could be responsible of gross OPR increases, up to 35-40% in *Chlorella sorokiniana* [153]. However, these activity assessments were done immediately upon transfer to darkness and it was shown that the enhanced post-illumination respiration effect may also increase the oxygen production up to about 50-140%, as reported by [159]. Instead, the dark respiration rate seems to represent about 10-20% of the gross OPR under optimal condition [136]. In coastal lagoons, the assessment of photosynthetic OPR in phytoplankton have been often used to correlate the photosynthetic performances with the depth and quality of the water column. The OPR was found to be dependent on the depth, illuminance and transparency of the water, as well as the composition of the phototrophic community. Indeed, some species are adapted to live in defined depth of the water column, while other species can be severely photoinhibited or even photodamaged [160].

The photo-respirometric methodology was recently adopted by Tamburic et al. [161] to identify the wavelengths at which *Nannochloropsis* species utilized light more efficiently, by calculating oxygen evolution rates for different wavelengths across the entire visible spectrum and obtaining the maximum OPR for blue lights. In a similar study performed by Luimstra et al. [162] on *Synechocystis* species and *Chlorella sorokiniana*, it was shown that the specific growth rates of cyanobacteria were similar under orange and red lights, but much lower under blue lights. For the green alga, similar OPRs were obtained under blue and red

lights, while the oxygen production was lower under orange lights. Jeon et al. [163] tested the photosynthetic activity of *Haematococcus pluvialis* under various intensities of simulated sunlight, green, and red lights, by assessing the net OPR. They also confirmed that the light absorption strongly depended on wavelengths applied, being maximum under red lights. Consistent results obtained by Kim et al. [164] also suggested that the growth rates obtained at different wavelengths were comparable for *Nannochloropsis Gaditana*, while the photosynthetic efficiency and lipid production were higher under red lights, also suggesting that the light quality control could be exploited to obtain lipids accumulation. A similar study [165] was performed on *Chlorella vulgaris*, including a comparison between different kinetic models describing light- and wavelength-dependent growth.

Photo-respirometric tools were also used during previous experiments, [135] and [166], in which the effects of light adaptation were investigated. In this work, P-I curves were exploited to assess the capability of different microalgae strains to adapt to light intensity. Prior to the analysis, algal cultures were exposed to high and low light intensities for two days. Results showed that the light energy conversion efficiency and the maximum chlorophyll-specific photosynthetic rates were higher in the cultures exposed to low lights. Shuler et al. [167] measured the OPR of a *Chlorella pyrenoidosa* culture, as a function of the light gradient in the suspension due to the culture thickness. Results obtained at different light intensities clearly indicated that the rate of oxygen evolution and the light intensity were logarithmically correlated, while the rate of oxygen evolution per unit of suspension volume was linearly correlated with the reciprocal of the culture thickness.

With respect to the effect of duty cycles on the OPRs it should be stressed that in microalgal cultures the light attenuation due to algal density, together with the presence of turbulent flow regimes due to mixing, expose microalgae to very fast

L/D cycles, reflecting in high fluctuations of the light energy supply. This also results in different average OPRs, as previously reported [168]. Here, the authors used flashing LED lights at high frequencies and calculated the specific OPR of a high-density *Chlorella kessleri* culture. They demonstrated that the mutual shading effect can be overcome by maintaining high-frequency flashing lights, and this is particularly effective for dense cultures. Similar photo-respirometric experiments, [148] and [169], showed the influence of different duty cycles and flashing frequencies on the absorbed light energy and OPR in *Chlamydomonas reinhardtii* and *Scenedesmus Almeriensis*. The net OPR increased at increasing duty cycles and flashing frequencies, and the oxygen yield was also higher at increasing flashing frequencies, while at lower duty cycles the yield was reduced due to increased maintenance respiration. At higher duty cycles, instead, photon absorption rate exceeded the maximal photon utilization rate and, as a result, the surplus light energy was dissipated, leading to a reduction in net OPR [148]. On the contrary, it was shown that in *Chlorella* species cultures grown in lab-scale tubular PBRs with varied turbulence regimes to obtain different L/D cycles, the linear positive correlation between productivity and increased turbulent regimes is mainly due to the improved exchange rates of nutrients and metabolites, rather than to the fluctuating light regime [170].

As reported, one of the final aims of typical photo-respirometric protocols for determining the effect of light intensity is to build P-I curves. In general terms, P-I experiments are performed by measuring the sum of photosynthetic and respiratory rates, measured during light and dark phases, respectively. After an OPR measurements is performed, the irradiance level is varied stepwise and the OPR is calculated again, until the last investigated radiation level is reached [166]. As previously mentioned, effects of light quality (in terms of emission spectra and duty cycles) can be also assessed thanks to respirometry. Although in this case complete protocols are not always reported in literature, similar procedures

to the ones used in P-I experiments can be applied. Minor variations in these protocols involve the presence or absence of an intermediate dark phase between each light phase, or the execution of single batch tests (with biomass renovation) for every value of the parameter to be tested.

2.2.1.1.2. Availability of inorganic carbon, nitrogen and phosphorus

Among the other variables to be considered when conducting photo-respirometric tests, nutrient availability obviously represents a crucial aspect. The availability of inorganic carbon has been extensively debated and addressed and appeared to be the most important variable to be controlled, as CO_2 represents the major nutrient for phototrophic algal metabolism [147], [139].

Carbon availability is seminal to avoid data misinterpretation, which is not always straightforward, due to the complex equilibrium of inorganic carbon species in the liquid phase. The relationships of inorganic carbon species with pH values may result in difficult interpretations of photo-respirometric data, when carrying out photo-respirometric assays to determine the effects of the only carbon source on microalgal growth. Indeed, CO_2 has a very low solubility in water, and when dissolved, pH-dependent chemical equilibria with bicarbonate and carbonate species occur. The photosynthetic consumption of dissolved CO_2 or HCO_3^- also results in a pH increase in the system, as protons are consumed during the process. The increase of pH also causes a shift of the carbonate equilibrium towards the carbonate species, thus causing carbon limitation and obviously affecting the photosynthetic activity. Decostere et al. [139] pointed out that acid dosage should be used to maintain a constant pH, allowing to evaluate the only effects due to other parameters, such as nutrient concentrations. In a subsequent study [171], authors drawn the attention on the interpretation of

titrimetric data, and the relationship with the inorganic carbon speciation. Several processes impacting pH must be in fact accounted for, when analyzing titrimetric outputs: CO_2 and HCO_3^- consumption rates due to algal growth, atmospheric CO_2 mass transfer and CO_2 production due to algal dark respiration.

Although other nutrients (N and P) play an important role in microalgal phototrophic growth, this aspect has been poorly investigated using photo-respirometric approaches [172], as most literature studies focusing on the dependence of algal growth on nutrient availability are normally performed with growth experiments. In the research work performed by Tang et al. [144], the effects of both C- and N-sources were evaluated by applying photo-respirometric methods on both green algae (*Chlorella vulgaris*) and cyanobacteria (*Microcystis aeruginosa*). During tests performed to assess the effects of carbon availability, different HCO_3^- concentrations were tested (100-800 mg $NaHCO_3$ L^{-1}), and the pH was corrected after the addition of inorganic C. In this case, the specific OPR allowed evaluating different growth rates obtained using NO_3^- or NH_4^+ as nitrogen-source, confirming that considerably higher growth rates are obtained using ammonium rather than nitrate. In all tests, bicarbonate was dosed at the beginning of the test (acting as pH-buffer and ensuring no limitation), and the pH was maintained at 7 with the aim of proposing a standardized procedure for conducting photo-respirometric tests. Continuous photo-respirometric-titrimetric tests performed in a gas-tight PBR by Eriksen et al. [137] allowed identifying NH_4^+ as the preferred N-source, compared to nitrite and nitrate compounds for both *Chlorella* sp. and *Chlamydomonas reinhardtii*.

Apart from determining the photosynthetic activity at different nutrient concentrations, in some case photo-respirometric tools have been applied to characterize microalgal cultivations maintained under N- and P-depleted conditions for biodiesel production. The effect of nitrogen starvation has been

discussed by Quiao et al. [173], in which the gross OPR measured in *Isochrysis Zhangjiangensis* was strongly reduced (72 %) after only 2 days of N-deprivation and the cells were almost inactive after 20 days. A similar result (about 50 % OPR inhibition after 3 days) was reported for a green alga belonging to the *Scenedesmaceae* family [174]. In both cases, the strong reduction of photosynthetic OPR could be associated to the conversion of carbohydrates to triacylglycerols at the cellular level. It was also reported that the dry weight concentration did not decrease due to the starvation and that the carbon fixation could be carried out, regardless of nutrient deficiency. Zhang et al. [175] also reported consistent results, showing that the reduction in the gross OPR in nitrogen-depleted cells also resulted in a decreased respiration rate, which was correlated to the reduced intracellular nitrogen quota.

Regarding inorganic phosphorus, only a few photo-respirometric approaches are available in literature, attempting to evaluate the effects on photosynthesis and lipids accumulation in axenic microalgae cultivations. For example, Hu et al. [176] used a photo-respirometric approach to evaluate the effect of nutrient deficiency on *Nannochloropsis* sp. El-Sheek et al. [177] compared the effects of 6 days P-starvation on *Chlorella Kessleri* cells, reporting decreased photosynthetic activities, dark respiration rates and chlorophill contents, combined with an increase in the algal dry wegth, which was explained by an increase in cell biovolumes and the accumulation of storage compounds. Similarly, Thedorou et al. [178] hypotized that P-limitation activated alternative respiratory pathways in the green alga *Selenastrum Minutuum*, resulting in decreased respiratory and photosynthetic activities (up to 5- and 3-fold, respectively) when compared to a nutrient-sufficient control.

2.2.1.1.3. Temperature

Temperature influences almost all biochemical parameters and reactions rates, including: the rate of photosynthesis and chlorophyll fluorescence parameters [179], the affinity of Rubisco for CO_2 and therefore the regulation of respiratory and photorespiratory processes [180]. In addition, temperature also plays a crucial role in boosting the photoinhibition process and in speciation of ionic compounds (e.g. ionization of free ammonia), influencing different aspects of microalgae activity.

Microalgae optimum growth temperature is highly species-specific, and most microalgae and cyanobacteria can tolerate temperatures up to 15 °C lower than their optimal temperature, while the tolerance to temperatures higher than the optimal is generally much lower [181]. Decostere et al. [182] assessed the effect of temperature on microalgal growth rates. In their experiment with *Chlorella vulgaris* pure cultures, initial nutrient concentration was non-limiting and a heat-jacketed vessel was used, allowing for precise temperature control (15 and 26°C). Results reported that the microalgal OPRs were similar at the two temperatures investigated, and it was concluded that no significant influence of temperature could be evaluated, contrarily to what expected [183]. Manhaeghe et al. [184] used instead a similar modelling approach, showing a marked influence of temperature on the photosynthetic growth rate of axenic *Chlorella vulgaris*, based on photo-respirometric/titrimetric tests. Ippoliti et al. [53] also tested a wide range of temperatures (15 to 45 °C) on a lab-scale culture of *Isochrysis galbana* species, obtaining consistent results and being able to fit experimental data with the cardinal model developed for describing temperature-dependant microbial growth [185]. The authors identified optimal temperatures leading to maximum photosynthetic and respiration rates (about 35 °C and 30-35 °C, respectively). A more detailed study on the effect of temperature on dark respiration rates can be

found in [186]. Here, the authors showed that the dark respiration of *Chlamidomonas Reinhardtii* and *Arthrospira Platensis* increases up to 4- to 10- times, respectively, for temperatures ranging from 20 °C to 35 °C, and the increased respiration rate could be modelled according to an Arrhenius-type exponential law. Costche et al. and Barceló-Villalobos et al., [181] and [187], adopted a similar experimental design to assess the temperature effect on *Scenedesmus almeriensis*. By varying the temperature and measuring the photosynthetic OPR, optimal values of 30 and 35 °C were obtained, respectively, also obtaining consistent results with those reported by Cabello et al., [143] for *Scenedesmus Obtusiusculus* under nitrogen-replete conditions. In the same study it was shown that nitrogen starvation induced a shift in the optimal temperature of almost 10°C. Wieland et al. [188] calculated the areal OPRs of a cyanobacterial mat by using oxygen microsensors, obtaining an exponential increase of photosynthetic production with temperature in the interval tested (10 to 25 °C).

The dark respiration rates seemed to be less affected by temperature variations than OPRs, showing maximum values close to 15-20 °C. Bechèt et al., [189] and [190], also adopted a photo-respirometric methodology to determine the effects of temperature (4 - 42 °C) on the productivities of *Dunaliella salina* and *Chlorella vulgaris*. Results allowed calibrating a mathematical model in which the dark respiration exponentially increases with temperature. Minimum, maximum and optimal temperatures supporting microalgal growth could be calculated as well. It should be stressed that in these works regarding the effects of temperature (and, more in general in papers regarding the effect of environmental parameters on photosynthesis), the biomass was generally not subject to an acclimation period to the tested temperature, therefore these effects should be always regarded as short-term effects [181]. In reviewed studies determining the effects of temperature on algal photosynthesis, the photo-respirometric protocols are normally constituted by repeated batch tests, among which the temperature is

varied, with the OPR measurement repeated at each temperature condition. The duration of L/D phase is generally limited to few minutes, before the light regime is varied. It was suggested to renew the biomass after maximum 1 h after the beginning of each test, in order to avoid the instauration of long-term effects, such as acclimation and changes in the chemical composition of the biomass [189].

2.2.1.1.4. pH

The pH value is another key-factor to be controlled during microalgae growth, as extensively reported in literature. pH determines the balance among dissolved inorganic species and, in conjunction with the mass transfer capacity and operation mode, the availability of inorganic carbon and other nutrients. Besides its effects on chemical speciation, pH also has a direct influence on the algal activity, being the optimal pH values for phototrophic growth in the range 7-8. The characterization of pH-dependent OPRs was recently evaluated [182]. However, in these experiments, the effect was associated to carbon availability, rather than to the pH value. Experiments specifically conducted to assess the dependence of OPR on microalgal cultures were instead proposed by other researchers [53], [181], [187]. [53] found that the maximum OPRs and respiration rate could be found at pH values close to 7.5 for *Isochrisis galbana*, while Costache et al. [181] showed that the optimal pH for *Scenedesmus almeriensis* ranged from 7.0 to 9.0, with no large variations being measured between these values. Similar results, obtained in a similar range of pH-values (6.5 to 8.5), were reported by Tang et al. [144], for both green algae and cyanobacteria. Reported photo-respirometric protocols used to assess the effect of pH on phototrophic activity consisted in batch tests performed with nutrient availability, under constant light/dark regime and temperature. Results from another study [143] showed similar pH optima, but they also demonstrated that optima are strongly reduced

(to about 5.5 pH values) after 4 days nitrogen deprivation, suggesting that nutrient availability should be included as additional parameter in the design of experiments for assessing optimal growth conditions. In addition, as pH has a direct effect on each ionization equilibrium in the system (Figure 2.3), the choice of non-limiting nutrient concentrations should be carefully evaluated after the calculation of theoretical speciation at the investigated pH value. This is particularly true for NH_4^+/ NH_3 and carbonate equilibria, due to the possibility of NH_3 and/or CO_2 stripping at high pH and temperatures.

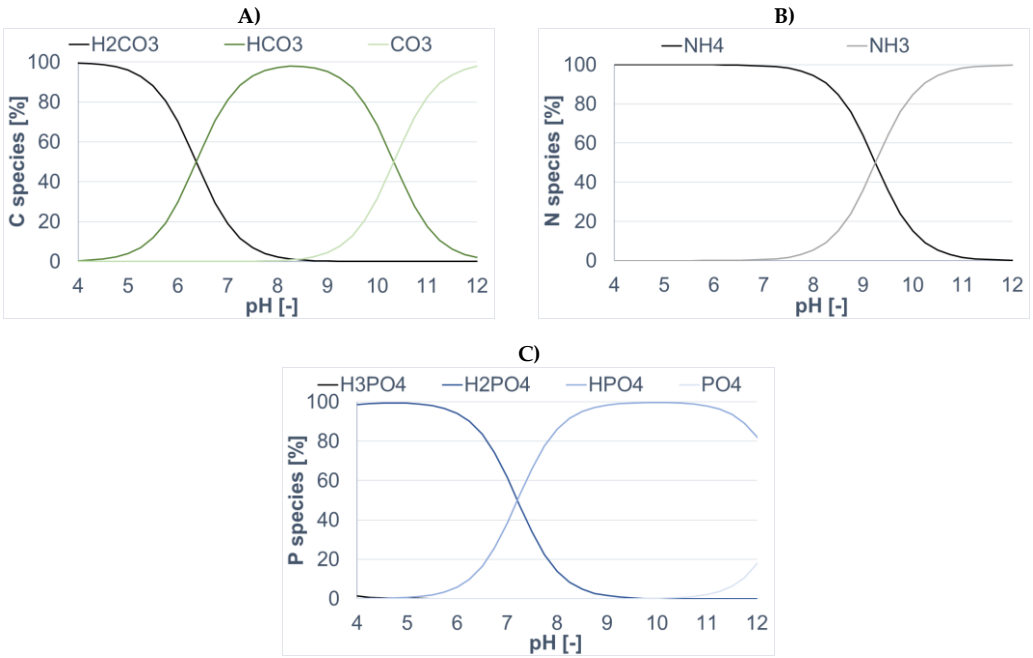

Figure 2.3. Effects of pH on ionization equilibria for the main dissolved macronutrients (A: carbonates, B: ammonia, C: phosphates).

2.2.1.1.5. Dissolved oxygen

DO accumulation is one of the major problems in the design and operation of closed PBRs [191]. Indeed, the photosynthetic activity can provide high quantities of O_2, reducing the photosynthetic OPR due to its inhibitory effects, and thus favoring the photorespiration of cultures [192], [193]. [158] demonstrated that the extraction of excess oxygen from PBRs could improve the assimilation of carbon and the photosynthetic activity, thus increasing the overall productivity. Results derived from photo-respirometric tests showed that if the DO is kept under the saturation level, the photosynthetic OPR is almost unaffected by the DO concentration, while an exponential reduction can be observed for DO saturations higher than 225-250% [181], [187].

In the work of Ippoliti et al. [53] it was also shown that the respiratory OUR is reduced by DO availability for DO concentrations lower than saturation. Regarding experimental procedures to measure the activity reduction due to DO concentrations, photo-respirometric tests can be represented by a continuous test, directly performed in the cultivation reactor or a series of repeated batch tests performed in photo-respirometers. General considerations reported for the photo-respirometric assessment of light, temperature and pH effects still hold for determining DO effects on phototrophic activity.

2.2.1.1.6. Salinity

Although the presence of dissolved salts in the cultivation medium is essential for the growth of phototrophs, high salinities can induce increased respiratory activities, physiological alterations and eventually the death of cells [194]. In addition to direct effects on the metabolism, salinity can also influence microalgal growth indirectly, being responsible for a decreased oxygen solubility and for a

modification of the diffusive boundary layer, therefore influencing all diffusive processes. The phototrophic responses to salinity levels is especially useful in the bioremediation of saline wastewaters (food processing, leather treatment, oil industries, among the others), using halotolerant microalgae [195], or to evaluate the effects of increased salinity in open ponds, due to water evaporation. The tolerance to salts should be also considered in photo-respirometric tests, as it can be necessary to dilute/concentrate the algal suspension with synthetic media, thus modifying the salinity.

Few respirometric studies attemped evaluating the photosynthetic response to increasing salt levels. For example, Martínez-Roldán et al. [196] assessed the effect of salinity (NaCl) on both the net photosynthesis and respiration of *Nannochloropsis* sp., coupled to fluorescence measurements. Vonshak et al. [197] compared the response of different *Spirulina Platensis* isolates, showing that the increasing salinity caused both a reduction in the net OPR and an increased photoinhibition. Similar results were confirmed by Lu and coworkers [198], using the same methodology coupled to fluorescence measurements. In the study, cyanobacteria were acclimate for 12 h at different salinities, and it was concluded that salt stress significantly inhibited the electron transport processes as a consequence of adaptation mechanisms.

The effects of rapid salinity increases on *Chlorella vulgaris* and *Dunaliella maritima* were also investigated by Alyabyev et al. [199] by coupling photo-respirometry and micro-calorimetry. With respect to the respiration and photosynthesis rates, different behaviors for the two species were found. The halotolerant *Dunaliella salina*, showed increased OUR_{RESP} and OPR at increasing NaCl concentrations, while in *Chlorella vulgaris* OPR reductions were recorded. The increased energy dissipation rate at higher salinities was therefore associated to adaptation processes. Short-term effects of salinity, temperature and irradiance were investigated by [188], who used oxygen microsensors to investigate the OPR at

different lengths inside a cyanobacterial hypersaline mat. Because of adaptation mechanisms, the shape of the P-I curve varied with salinity, showing lower maxima at salinities higher than the one measured in situ. An effect could be also observed for salinities lower than the value measured in situ, although the reduction was lower. It was shown that the respiratory activities were less affected by salinity than the OPR. Also in the case of photo-respirometric methods to assess the effects of salinity, complete experimental protocols (duration and succession of L/D phases, presence and description of pre-treatments, renewal of the biomass sample, etc.) are often not reported or incomplete. The duration of L/D phases is frequently missing, while the reported timings are normally comprised in few minutes of L/D exposures, or they last until a constant rate is measured. In almost all cases, procedures to estimate phototrophic activities included an acclimation period in the dark, whose duration ranged widely (from 5 min to 12 h). OPRs and respiratory OURs are generally assessed in separate batch experiments, although it is also possible to determine these rates, during the same test, in consecutive L/D phases.

2.2.1.2. Effects of inhibitory compounds

Photo-respirometric tests were used as fast assays for *in vivo* toxicity evaluations. Effects of toxic and/or inhibitory compounds on photosynthetic efficiency are often the result of complex interactions on algal metabolism. Photo-respirometry demonstrated to be a versatile tool to study short term effects on phototrophs. This is particularly relevant when exploiting phototrophs in the treatment of waste streams, which are naturally variable in composition and chemical species, often containing toxic/recalcitrant compounds. Based on quick toxicity detection methods, a stricter control of the operating variables in real plants may indeeed avoid the collapse of the entire biological section.

Many different compounds present in wastewater were found to affect algal growth: ammonia [200]–[202], sulphide [203], ethanol [204], heavy metals [144], herbicides [205], [206], nitrite [207], bicarbonate [208], hydrogen peroxide [209] and antibiotics [210].

Among those inhibitors, some deserve particular attention. In particular, free ammonia has been identified as an important short-term and species-specific inhibitor of the photosynthetic process, with some species being particularly resistant to elevated concentrations of ammonia and other being much more sensitive [72], [74], [201]. The two main mechanisms of action of the photosynthesis inhibition are: i) ammonia causes damages to the oxygen evolving complex (OEC) of the photosystem II, acting as an uncoupler of the Mn cluster of the OEC and displacing a water ligand [211], [212]; ii) ammonia diffuses through membranes and accumulates, acting as an uncoupler and disrupting the ΔpH component of the thylakoid proton gradient [201], [213], [214]. Besides these effects, the activity of photosystem I and the dark respiration rates are also negatively affected by FA and ammonia toxicity also seems to be amplified at elevated light intensities, although the mechanisms are not fully understood [74]. Quantifying the inhibition of photosynthetic activities is of particular interest in algae-based wastewater treatment processes [215]–[217]. Indeed, the equilibrium reaction between FA and ammoniacal nitrogen (NH_4^+) shifts toward FA under the following conditions: i) high pH values associated to photosynthetic processes, ii) high temperatures due to atmospheric conditions and iii) high total ammoniacal nitrogen (TAN = NH_3 + NH_4^+) concentrations [71], [72]. The inhibition of photosynthesis due to the presence is normally evaluated by coupling photo-respirometry with the measurement of nutrient uptake [73], [215], [218], [219], or pulse-amplitude modulation (PAM) [74], [211], [214], [220].

Due to the remarkable sensitivity of photosynthetic activity to inhibitory compounds, phototrophic organisms were proposed for their applications as

biosensors [205], [221]. Whole-cell based biosensors exploit the unicellular nature of phototrophic organisms, to give a real time response on environmental conditions, thus helping the estimation of toxic effects. Accordingly, above-mentioned photo-respirometric assays often utilized microalgae to establish environmental effects of pesticide, herbicides or other chemicals. In particular, *Raphidocelis subcapitata* (formerly known as *Selenastrum capricornutum* or *Pseudokirchneriella subcapitata*) is a model organism of freshwater algae commonly used in standard toxicity tests [222] and also very popular among the microorganisms used for photo-respirometric tests [209], [210], [221]. However, in many other works, diatoms and cyanobacteria are also used [209].

Generally, these bioassays are based on the observation of dose-dependent effects of toxic compounds on the microorganisms' photosynthetic capability. While few examples of field works are available in literature [200], most of the papers focuses on the lab scale, with the final aim to provide methods that can be applied in industrial relevant applications.

2.2.2. Combination with fluorescence and other measurements

Photo-respirometric tests have been often coupled with fluorescence measurements. In the past decades, several authors tried comparing the oxigen evolution method and fluorescence in ecological field, in order to study the carbon cycle at oceanographic level. A growing worldwide interest for efficiently monitoring the primary phytoplankton production is indeed reported [223].

Fluorescence techniques substituted the traditional for assessing aquatic photosynthesis (^{14}C method), as the pulse-amplitude modulated (PAM) fluorimetry can be used to estimate the primary productivity. Several works have compared the results from fluorescence methods and photo-respirometric

methods. The use of chlorophyll fluorescence to monitor photosynthetic performances is widespread and commonly accepted as a reliable procedure to study the acclimation of photosystems to environmental conditions, especially in the case of light acclimation. Fluorescence parameters can be indeed used to evaluate changes in photosystem II (PSII) photochemistry and linear electron flux [224]. In photosynthesis, oxygen production happens at the water-splitting complex of the reaction center of the PSII, so confirming that the two techniques are potentially complementary for physiological studies. In the PAM technique, dark-acclimated cells are excited with a red non-actinic light, not inducing photosynthesis but ensuring that the detected fluorescence is only derived from light-harvesting antenna pigments. The initial fluorescence (often called F_0) is then used as a normalization factor for subsequent fluorescence intensity measurements, under different light pulses. Different combinations of L/D pulses have been proposed, and based on these protocols, fluorescence data can be used to estimate chemical and non-photochemical quenching, to evaluate electron transport rates (ETR) and to derive the overall efficiency of photosystems [224]. The most common parameter monitored is the F_V/F_M, a ratio representing the quantum efficiency of PSII.

The PAM was also applied in cultivation systems, to monitor and control the physiological state of large-scale cultures. As an example, Qiao et al. [173] proposed a simple method to determine the optimum harvest time of starved microalgae cultivations for lipid production. Based on the measurement of F_V/F_M, a range for the F_V/F_M value around the lipid saturation point could be defined as control strategy. In a previous study, the authors focused on the utilization of organic carbon, during the heterotrophic cultivation of *Chlorella sorokiniana*, in order to optimize the lipids productivity of this strain [225]. However, the concept of photo-respirometry applied to cultivation systems, is more comprehensive, not only focusing on photosynthetic oxygen evolution, but being

oriented to the description of metabolism at the macroscale, thus based on mass and energy balances. On the contrary, fluorimetric methods allow for the assessment of the photosynthetic efficiency and electron transport chain, but do not directly measure photosynthetic rates [226]. Moreover, there is the need to resolve simultaneous fluxes of the gaseous substrates and products of photosynthesis, CO_2, and O_2, as the net O_2 evolution and CO_2 uptake reflect the combination of pathways producing and competing for energy (ATP) and reductant (NADPH) [151]. Lefebvre et al. [140] have extensively compared fluorescence and photo-respirometric assays in different conditions, observing that many discrepancies remain.

Comparison between respirometry and fluorimetry was evaluated by evidencing the effect of seasonality on P-I curves. Within each season, characterized by a different average irradiance, photoperiod and temperature, the relationships between OPR and ETR were found linearly correlated. Thus, if cells are acclimated to particular light conditions, there is apparently a common response of the photosynthetic apparatus and the flux to carbon fixation. On the other hand, other authors observed that O_2 evolution in microalgae was not (or only partially) linearly correlated with fluorescence measurements [227]. The relationship between OPR and ETR is usually linear at low to medium irradiances, but the relationship does not hold at high irradiances. This was explained by Lefebvre et al. [140], based on seasonal acclimation phenomena: when cells are acclimated to different seasonal temperature and light regimes, the correspondence between ETR and OPR can significantly change. The temperature is actually a key variable, as reported in Morris and Kromkamp [228], showing that the linear correlation between the two parameters may change depending on the temperature range in *Cylindrotheca closterium*. Possibly, different time scales of the energy capture and transfer at the photosystem level may be differently influenced by temperature, if compared to the overall effect

of temperature on growth rates, accounting for all phenomena affecting oxygen production/consumption. Indeed, as reported before, the gross OPR is the sum of production and respiration rates, and the latter can be only ascertained with photo-respirometric protocols.

2.3. Photo-respirometric methods applied to microalgae-bacteria consortia

Many respirometric studies on axenic microalgae and activated sludge are available in literature, while only fewer applications have been proposed for microalgae-bacteria consortia. Respirometric protocols defined for axenic microalgae cultivations and activated sludge can be in some case modified and transposed to microalgae-bacteria consortia, allowing to monitor the evolution of the process over time. In addition, fundamental information about the optimal environmental conditions and effects due to inhibitory compounds may be easily assessed. From this perspective, photo-respirometric protocols carried out on non-axenic cultures may also help to better understand those phenomena occurring in such complex environments and communities. In the studies reviewed, different microalgae-bacteria suspensions were tested. The suspensions were withdrawn from lab-scale cultivation PBRs (with volumes ranging from 250 mL to 15 L) to pilot- and full-scale HRAPs (with volumes ranging from 70 L up to about 500 m3) (Table 2.2). These systems were fed with synthetic media/wastewaters or with real wastewaters from different sources (anaerobic digestates, agricultural and food processing wastewaters). The most common class of algae was *Chlorophyceae* (mainly *Chlorella* and *Scenedesmus* genus) or mixed/wild algal strains.

In some cases, the DO mass balance is applied to the entire cultivation bioreactor ("in-reactor" photo-respirometry), therefore a respirometric device is not needed.

In most cases, however, the bioassay is performed in conventional respirometers, on samples withdrawn from the cultivation reactor (later on referred to as "external" photo-respirometry). The photo-respirometer configuration can range from cuvettes (0.2-10 mL) to open/closed respirometers (25-250 mL). Table 2.2 summarizes the main cultivation conditions, biomass characteristics and photo-respirometric test conditions found in published studies.

Although studies on microalgae-bacteria systems are available, the understanding of some interactions involved in microalgae-bacteria consortia is still incomplete. In this sense, photo-respirometric tests can help shedding light in interpreting O_2 trends in algal ponds, allowing to single out specific contributions to the overall balance. As shown in equation (4), O2 dynamics is indeed influenced by several processes:

$$\frac{d(DO)}{dt} = OTR + OPR + \sum_i OPR_i = OTR + OPR - \sum_i OUR_i \quad (i = RESP, AOB, NOB, HET, OO) \quad 2.8$$

Where oxygen uptake terms are those relative to: algal respiration (OUR_{ALG}), nitritation and nitratation activities (OUR_{AOB}, OUR_{NOB}), heterotrophic activity (OUR_{HET}) and the aerobic activity of other organisms normally present in wastewater treatment systems (other aerobic bacteria, fungi, larvae and bacteria grazers, such as nematodes, rotifers or protozoans) (OUR_{OO}). The estimation of oxygen consuming processes can be quite difficult in the presence of mixed communities. Indeed, several aspects complicate the estimation of the terms included in the DO balances. Common approaches are discussed below.

2.3.1. In-reactor photo-respirometry

The availability of in-reactor and on-line DO measurements in High Rate Algal Ponds (HRAP) and other PBRs inherently allows to apply the respirometry

technique by considering the overall reactor as a large respirometric vessel and by exploiting the natural alternation of L/D cycles that takes place in outdoor reactors. Although this sounds a simple and straightforward, retrieving OPR and OUR data requires more complex data processing and a precise knowledge of both all those conditions that are inherently variable (T, pH, I, etc.) in outdoor reactors and of those concomitant processes that affect the DO dynamics in large reactors (i.e. the DO liquid/gas transfer). The estimation of the potential of photosynthetic oxygenation in High Rate Algal Ponds (HRAP) and other PBRs has been the object of several studies in the past [229]. The methodology eventually allows to model most relevant contributions due to mass transfer and to environmental conditions [193], [230]. As an example, this methodology proved to be suitable to monitor the evolution of the photosynthetic activity in HRAPs [231], [232].

Again, the impossibility of determining different biological contributions to oxygen uptake is a general drawback of this kind of respirometric procedure. As discussed, this leads to obtaining only an aggregated information about the overall respiration of the consortium.

As for the conventional photo-respirometry, a complementary approach involves the use of stoichiometric relationships and further cultivation data. For example, oxygen production by microalgae and nitrifying activities could be estimated by coupling DO dynamics with measurements of the nitrogen compounds [28], [233]–[235].

Table 2.2. Main cultivation conditions, biomass characteristics and test conditions in microalgae-bacteria photo-respirometry.

REFERENCE	BIOMASS			CULTIVATION			PHOTO-RESPIROMETRY	
	DOMINANT PHOTOTROPHS	BACTERIA INVOLVED	BIOMASS ESTIMATE	PBR	INFLUENT	I [$\mu E\ m^{-2}\ s^{-1}$]	RESPIROMETER	T [°C], pH [-], I [$\mu E\ m^{-2}\ s^{-1}$]
[236]	SCEN (P)	Generic	TSS, VSS	PBR 1.1 m^2, HRAP 0.15 - 0.3 m^3	(UR)	INC	IRR	T: 25, pH: 6.7-8
[24]	EUGL sp. (P)	Generic	CHL, CC	HRAP	SW (Corg, HCO_3, NH_4)	100 – 2400 (FLUO)	IRR	T: 25
[229]	N.r. (P)	Generic	N.r.	HRAP 500 m^3	MWW	NL	IRR	I: NL
[237]	WILD (granular) (P/M)	AS	TSS	PSBR 1.4 L	SW (Corg, NH_4)	NL	CR 100 mL	T: 25
[27]	CHLO (P/H)	HET	TSS, CHL, OD	LPBR 0.2 L	MM (Corg, NH_4)	150 FLUO	CR 250 mL	I. 150 (FLUO)
[238]	WILD (P)	Generic	TSS,VSS, CHL, OD	HRAP 2.2 m^2	MWW	NL	IRR	I: NL
[239]	CHLO (P/M)	AS	TSS, CC	LPBR	SW (Corg, HCO_3, NH_4)	100	CR 100 mL	T: 25, pH: 8, I: 10-130 (LED)
[240]	MIX (P)	AS	TSS, VSS	FPBR 4 L	MM (Corg, HCO_3, NH_4)	766.5	CUV 10 mL	I: 300 (LED)
[241]	CHLO (P)	NIT	TSS, VSS	LPBR 0.25 L	MM, SW (Corg, HCO_3, NH^4)	150 LED	CR 70 mL	I: 0-1250 (LED)
[242]	CHLO, SCEN (P)	NIT	TSS, OD	PBR 2 - 85 L, HRAP 800 L	LFADM (Corg, NH^4)	NL	OR 0.25 L	I: 40.8-59.2
[232]	WILD (COEL) (P)	HET	TSS	HRAP 9.6 m^3	LFADM (Corg, NH^4)	NL	IRR	I: 261-719
[243]	N.r.	Generic	CHL	HRAP 50 m^3	MWW	NL	CUV	I: 0-2000 (HAL)
[244]	N.r. (P)	N.r.	TSS	MBBR 0.75 m^3	MWW	NL	OR 5 L	n.r.
[231]	SCEN (P)	Generic	VSS	HRAP 2.5-5.3 m^3	FPWW (Corg)	NL	IRR	I: NL
[75]	CHLO (M)	AS	TSS, CC	LPBR 0.25 L	MM, SW, MWW (Corg, CO_3, NH^4)	N.r.	CR 25 mL	T:25, pH: 8, I: 45 (FLUO)
[245]	N.r. (P)	NIT	TSS, VSS, CHL	PBR 1.5 L	MWW (HCO_3, NH_4)	67.5	CR 140 mL	pH: 7, I: 67.5
[246]	WILD (P)	NIT	TSS, CHL	PSBR 2 L	LFADP (Corg, NH_4)	200-400	IRR	T: 21, I: 74-105
[234]	CHLO	AS	TSS, CHL	PSBR 9.2 L	MM, SW (Corg, NH_4)	92-183 (LED)	IRR	T: 26, I: 92-183 (LED)
[247]	CHLO, WILD (P)	NIT	COD	CSTR 14 L	SW (HCO_3, NH_4, NO_3)	(FLUO)	CR 50 mL	T:25, pH: 7.5
[248]	CHLO (P)	NIT	TSS, COD, PG	MBR 7.2 L	SW (HCO_3, NO_3)	80 (FLUO)	IRR	I: 80 (FLUO)
[249]	WILD (P/M)	AS	TSS, VSS, CHL, PG	PSBR 2 L	SW (Corg, HCO_3, NH_4)	45-225 (LED)	CR (100 mL)	T: 25°C, I: 135
[250]	WILD (P/M)	AS	TSS, CHL	PSBR 12.6 L	MWW (Corg, NH_4)	500 (LED)	CR (300 mL)	T: 25, I: 250-2000 (LED)
[251]	WILD (P/M)	AS	TSS, CHL	PSBR 12.6 L	MWW (Corg, NH_4)	250-2000 (LED)	IRR	250-3000 (LED)

Abbreviations: P: Photo-autotrophic, M: Mixotrophic, H: Heterotrophic, CHL Chlorophill, CC Cell counts, OD Optical density, PG: Plates growth, INC: Incandescent lamps, FLUO: Fluorescent lamps, NL: Natural light, LED: Light-emitting diodes, IRR: In-reactor respirometry, CR: closed respirometer, OR: open respirometer, CUV: cuvette respirometer

2.3.2. External photo-respirometry

Performing photo-respirometric tests in dedicated reactors allows the standardization of testing conditions and their controlled variation during the test. Indeed, the technique is often preferred to assess the effect of specific parameters such as the light intensity, or nutrient concentrations. The suspensions are generally withdrawn from the cultivation system and diluted with synthetic media prior to the activity test [79], [144], [250]. The measurement of DO is sometime coupled to other cultivation data or to stoichiometry assumptions to estimate the bacterial activity [252]. For example, Vargas et al. [245] developed a protocol for the activity assessment of a microalgae-nitrifying bacteria consortium, during the lab-scale bioremediation of ammonia-concentrated synthetic wastewaters. The experimental procedure consisted in the alternation of two L/D cycles, separated by the addition of a concentrated substrate solution. Microalgae and nitrifying activities were calculated through the linear regression of DO data versus time, assuming bacterial yield factors from literature and stoichiometric growth for microalgae.

Other possible ways to distinguish the main contributions to oxygen production/consumption rate in algae-bacteria photo-respirometry are listed below, namely: i) performing a physical separation of algae and bacteria and ii) making use of selective photosynthesis and/or bacterial inhibitors. Those alternatives are hereafter discussed.

2.3.2.1. Physical separation of algae and bacteria

The determination of both bacterial and microalgal activities would be relatively easy after a physical separation the two populations. This was achieved for example by gravity separation [247], membrane separation [244], [248] or using attached/immobilized microalgae [27]. To the aim of separating suspended cultures of microalgae and bacteria, centrifugation on discontinuous density gradients is also an attractive option, as no adverse inhibitory effects on photosynthesis have been reported [253], [254]. Sutherland et al. [238] also proposed to calculate bacterial oxygen consumption in the dark after filtering the algae/bacteria suspensions (GF/F filters). Although this allows to get rid of microalgal OPR, the bacterial OUR is underestimated since it does not account for bacteria attached to microalgal cells.

2.3.2.2. Selective inhibitors to discriminate populations

Several organic and inorganic compounds are known to inhibit the bacterial or algal metabolism and can be considered for their use in photo-respirometric tests. For example, the use of disinfectants for inhibiting bacteria or antibiotics, herbicides and pesticides for inhibiting phototrophs have been proposed [206], [210]. Nevertheless, these substances have many drawbacks such as they lack selectivity for a single population, or they require a relevant contact time to be effective (Figure 4). In general terms, selective inhibitors used during photo-respirometric tests should have some desirable characteristics: 1) the selectivity for a specific group of microorganisms, 2) the effectiveness at the temporal scale of the test, 3) the absence of other physical and/or physiological effects (e.g. flocculation, cell disruption or toxicity), and 4) the absence of acclimation processes (due to the inhibitor's biodegradability or the generation of protecting

enzymes/proteins). Although not necessary, the reversibility of the inhibitory effect is also a desirable feature, allowing to perform non-destructive tests. For the reasons described before, the use of selective inhibitors is, up to now, only practically applicable to nitrifying bacteria. Indeed, the combined use of nitrifying inhibitors was successfully exploited for estimating OUR_{AOB} and OUR_{NOB} in activated sludge samples. For example, the activity of AOB can be prevented using ATU [125], [255], while sodium chlorate is highly selective towards NOB [256], [257].

ATU was particularly exploited to isolate the oxygen consumption by nitrifiers from the overall OUR of the consortium, allowing to study the effects of light intensity/quality and aeration rates on algae-bacteria systems [250], [256]. The protocols described in the following paragraphs are all based on this principle [242], [258], [259]. The procedure reported in [242] allowed to compare the activities of lab- and pilot-scale PBRs and to monitor microalgae and nitrifiers evolution in a system treating municipal anaerobic effluents from sludge dewatering.

In this case, selective inhibitors for nitrifying bacteria were dosed between L/D cycles, allowing to calculate the bacterial activity as difference among two consecutive phases. Respirometric results were then supported by the analyses of inorganic N-compounds. It was also advised on the fact that the OUR due to heterotrophic activity is eventually embedded with the dark respiration rate of microalgae, therefore the protocol should be carefully applied if high concentrations of heterotrophic bacteria are expected to grow in the system. In the work of Rada-Ariza [240], photo-respirometric tools were applied for estimating kinetic parameters in a flat-panel PBR treating synthetic wastewater. The respirometric procedure consisted in the de-oxygenation of the suspension, followed by the addition of the synthetic medium and nitrification inhibitors, under light conditions. The volume of the photo-respirometer (10 mL) was then

recirculated into an external reactor before a new determination started. DO evolution was measured alternating L/D phases until the end of the test. The application of photo-respirometry led to the estimation of important kinetic parameters and finally to the expansion of a mathematical growth model accounting for storage processes.

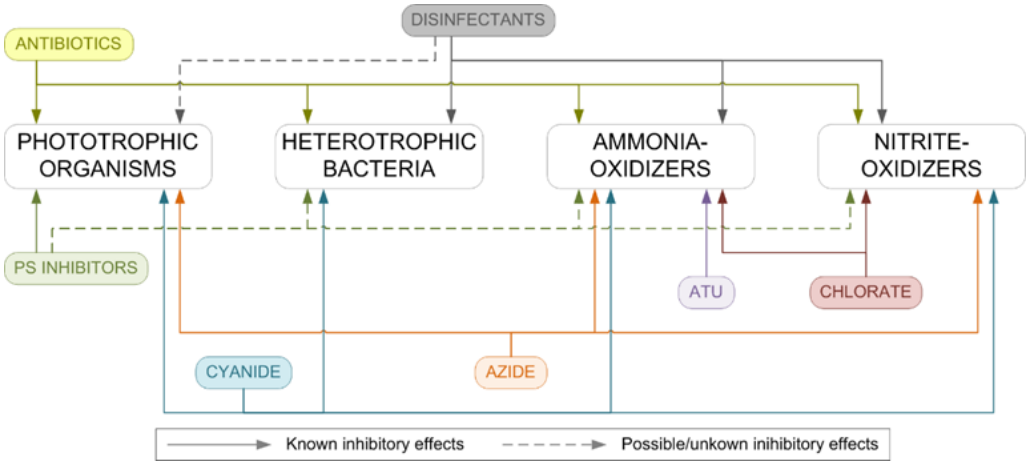

Figure 2.4. Possible effects of different bacterial and photosynthesis inhibitors on the microalgae-bacteria consortium.

The availability of an inhibitor for the sole heterotrophic bacteria would enable discriminating between bacterial and algal respiration processes as well as to distinguish algae from bacteria heterotrophic oxygen consumption. Up to now no such a substance has been yet identified. Indeed, while algae mixotrophic behaviour could be addressed in axenic cultures [145], [260], [261], only a few studies recently attempted to characterize wastewater-grown consortia [146]. Indeed, this remain a challenging topic deserving further insights.

2.3.3. Mathematical modelling

The exploitation of mathematical models can be of great support in the field of respirometry since it allows for a knowledge-based description of the numerous biological and physical-chemical processes affecting the DO dynamics as well as of the complex interactions among microorganism occurring during photo-respirometry. This promising approach is still in its infancy since modelling of algae-bacteria consortia is an on-going research topic [262].

Coupling a mathematical model to photo-respirometric tests enables to estimate different kinetic and stoichiometric parameters of the consortium, thus making the model more effective in describing the system [263], [264]. Once a calibrated model is available, key-mechanisms and interactions among algae and bacteria can be better discerned by analysing its theoretical outputs. This is carried out, in practice, by applying respirometric protocols under different conditions (e.g., light intensity, nutrient concentrations or hydraulic/biomass retention times). The variation of such conditions implies the activation of different metabolisms of algae and bacteria, which are modelled to allow for the identification of uncertain parameters.

On the other hand, photo-respirometry is a valuable tool to be coupled to the modelling of algae-bacteria systems allowing for retrieving informative data for model parameter identification. For example, Zambrano et al. [265] presented a mathematical growth model and performed dedicate photo-respirometric tests to calibrate the most sensitive parameters (maximum growth rate of bacteria and algae, yield coefficients of nitrogen, affinity constant for CO_2). Rada-Ariza [240] constructed a model accounting for the main processes occurring in the algal-bacterial PBR. The model was calibrated based on photo-respirometric assays, allowing to estimate algal/bacterial growth parameters and to evaluate the relevance of nitrogen storage by phototrophs. By coupling mathematical

modelling and photo-respirometry, various relevant aspects could be better addressed such as: the synergic or competitive interactions among phototrophs, nitrifying bacteria, and heterotrophic bacteria that are responsible for the shaping of the final algae-bacteria consortia which is still to be fully understood [237], [247], [252], [266], the potential influence of photo-inhibition of nitrifying bacteria at high light intensities [241], [267]; the complex interactions between algae/bacteria heterotrophic behaviour when treating wastewater [146], [239], [268].

2.3.4. Advantages, challenges and potential applications

Based on the literature analysis, a series of indications emerged and are here briefly discussed. As highlighted, several advantages can be associated to the applicaton of respirometric tools to activated sludge, phototrophic organisms and algal-bacterial systems. For microalgae-bacteria reactors, the main advantage of using photo-respirometric methods is represented by the possibility of evaluating in a fast, economic and reliable way, the photo-oxygenation potential given by the presence of phototrophs, together with the actual oxygen request by bacterial communities. More in general, a deeper understanding of symbiotic and competition mechanisms in microalgae-bacteria consortia can be theoretically achieved by coupling photo-respirometric tests with mathematical modelling. Indeed, one of the final aims of respirometry is the calibration of mathematical models, as for ASM, and the possibility of assessing crucial parameters (e.g. yield factors, specific growth rates and affinity constants for both microalgae and bacteria), resulting in improved model performances. Respirometric protocols defined for axenic microalgae cultivations and activated sludge can be in some case modified and transposed to microalgae-bacteria consortia, allowing to monitor the evolution of the process over time, but also to provide fundamental

information about the optimal environmental conditions or to evaluate the effects due to inhibitory compounds. This allows calibrating models accounting for pH-, temperature- and light-limited growth, in addition to gathering information about nutrient limitation. In the same way, the activity reduction due to the presence of inhibitory/toxic compounds can be assessed using photo-respirometric methods, allowing to define specific acceptance criteria for wastewaters or tolerable loads for pilot- and full-scale plants operations. From this perspective, photo-respirometric protocols carried out on axenic species may also help to better understand those phenomena occurring in such complex environments and communities.

In the execution of photo-respirometric tests, many variables should be accounted for, to obtain clear and informative results. In general terms, the use of an external respirometer is highly recommended when performing photo-respirometric tests, as it allows to vary and control almost every parameters of interest in a fast and repeatable way. Contrarily, in applying "in-reactor" photo-respirometry the following aspects should be considered: i) the impossibility of maintaining strictly controlled environmental conditions (temperature, irradiance, DO, pH, etc.); ii) the necessity to take liquid/gas exchange into consideration. In general, "in-reactor" data refer to sub-optimal conditions since nutrients/light availability and environmental conditions cannot be carefully controlled.

Literature data also pointed out the lack of standardized protocols, resulting in a wide range of conditions applied. Indeed, photo-respirometric protocol are generally based on the alternation of L/D cycles. However, a large diversity in protocols were applied. The bioassays normally include a single light or dark phase, although more articulated protocols were proposed. In general, the total duration of the test is generally contained in 1 - 3 hours and each phase has a typical duration of 10 - 30 minutes. Regarding the test conditions, a certain

variability can be also found among different studies. Important parameters having direct effects on the photosynthesis and respiration rates (i.e. the light intensity and the nutrient/biomass concentrations) are sometime missing or extremely different among the studies. The light intensity is one of the major variables affecting the photosynthetic productivity, so that its control is seminal to have a complete picture of the consortium. Moreover, a large variability was observed in the methods used to assess the biomass concentration. The most common method is the measurement of TSS and/or VSS, which includes microalgae and bacteria, but also any other particulate substance. Chlorophyll concentration and microscope cell count are other common techniques applicable to the quantify the algal biomass, which do not give information about the bacterial presence/abundance. Other methods such as the measurement of optical density or particulate COD were only seldom applied. As a result, the specific OPR, algal respiration rate, and bacterial respiration rates are often expressed using different units (Table 2.3), thus making the comparison of specific OPR and OUR among different studies quite difficult.

According to these findings, it is recommended to always report relevant data to facilitate the comparison with the existing literature. To this aim, the information listed below should be always provided, when describing photo-respirometric tests.

- A comprehensive description of the biomass cultivation system:

- Environmental/operational conditions applied (temperature, light and nutrients availability)

- Expected composition of the microbial community (generic microalgae-bacteria consortium, dominant algal and bacterial strains)

- Assessment of microalgae and bacteria concentrations (TSS/VSS, COD, turbidity, OD, cell counts, chlorophyll content)

- The photo-respirometric testing procedure:

- Suspension characteristics (microalgae and bacteria initial concentrations)

- Operational conditions (nutrient sources, setpoints and control systems for temperature, pH, DO, light intensity and quality)

- Test procedure (suspension preparation, test protocol, duration of L/D phases)

- Test outputs and data processing (OPR and OUR computation, parameters estimation)

In the following sections, a set of generalized photo-respirometric test protocols and a series of recommendations for conducting photo-respirometric studies are given, based on the reported literature findings and protocols.

Table 2.3. Microalgal-bacterial photo-respirometric protocols and main test outputs.

REFERENCE	PROTOCOL	ALGAL PHOTOSYNTHESIS	ALGAL RESPIRATION	BACTERIAL RESPIRATION	OTHER PARAMETERS	NOTES
[236]	D-L (L 2h, D 1h)	-	-	-	sPY	DO-stat using Na_2SO_3 solution
[24]	D	-	-	-	CUR/OPR ratio	Bacterial respiration estimated as BOD/HRT
[229]	n.r.	OPR 25 [mg O_2 L^{-1} h^{-1}]	OUR 8 [mg O_2 L^{-1} h^{-1}]	-	-	Algal respiration measured in dark bottles, bacterial and algal respiration aggregated
[237]	n.r.	-	-	sOUR 40-76 [mg O_2 g VSS^{-1} h^{-1}]	sARR, sNRR	Only OUR considered (aerobic granules)
[27]	n.r.	OPR 1.83-3.75 [mg O_2 L^{-1} h^{-1}]	-	sOUR 1.94-240 [mol O_2 kg $cell^{-1}$ h^{-1}]	-	Bacterial OUR assessed separately from microalgae
[238]	L (15')	sOPR 0-12 [mg O_2 mg $(chl\text{-}a)^{-1}$ h^{-1}]	n.r.	OUR ~25% sOPR	P-I parameters	Bacterial respiration is measured on filtered samples
[239]	L-D-L-D-L-D (15')	sOPR 0-0.46 [mg O_2 $g(DW)^{-1}$ min^{-1}]	sOUR 0.18-0.5 [mg O_2 g TSS^{-1} min^{-1}]	-	-	Bacterial and algal respiration aggregated
[240]	D-(N_2)-(SA)-(IA)-L-D	OPR 0.02-0.13 [gO_2 L^{-1} h^{-1}]	-	-	ARR	-
[241]	L (30 min)	-	-	OUR 0.14-0.27 [mg O_2 L^{-1} min^{-1}]	sARR, sNRR	Nitrifiers' photoinhibition
[242]	(SA)-L-D-(IA)-D-L-D (10-15 min)	sOPR 10-44 [mg O_2 g $(TSS)^{-1}$ h^{-1}]	sOUR 2-19 [mg O_2 g $(TSS)^{-1}$ h^{-1}]	sOUR 4.8-7.8 [mg O_2 g TSS^{-1} h^{-1}]	NR	Heterotrophic bacteria and algae respiration are aggregated
[232]	n.r.	OPR 4.82-9.5 [mg O_2 L^{-1} h^{-1}]; 1.75-2.34 [mol O_2 g $(VSS)^{-1}$ min^{-1}]	-	OUR 2-3.9 [mg O_2 L^{-1} h^{-1}]	P-I parameters	Bacterial and algal respiration aggregated
[243]	n.r.	OPR 0-12 [mg C L^{-1} h^{-1}]	OUR 2.49 [mg O_2 L^{-1} h^{-1}]	-	-	Results axpressed as primary productivity, bacterial and algal respiration aggregated
[244]	D (10 min)	-	OUR 0.02-0.24 [mg O_2 L^{-1} s^{-1}]	-	-	Bacterial and algal respiration aggregated
[231]	n.r.	sOPR 0-3.5 [mg O_2 mg $(chl)^{-1}$ h^{-1}]	sOUR 0-0.42 [mg O_2 g $(VSS)^{-1}$ d^{-1}]	-	P-I parameters	Bacterial and algal respiration aggregated
[75]	L-D-L-D-L-D (15 min)	sOPR 0.1-0.65 [mg O_2 g $(TSS)^{-1}$ min^{-1}]	sOUR 0.2-0.65 [mg O_2 g $(TSS)^{-1}$ min^{-1}]	-	$Y_{ALG,N}$, $Y_{ALG,P}$	Bacterial and algal respiration aggregated
[245]	D-L-(SA)-D-L (20-45 min)	sOPR 0-0.03 [mg N_NH_4 g $(VSS)^{-1}$ h^{-1}]	-	sOUR 0-0.12 [mg N_NH_4 g VSS^{-1} h^{-1}]	-	-
[246]	n.r.	OPR 193 [mg O_2 L^{-1} h^{-1}]		OUR 261 [mg O_2 L^{-1} h^{-1}]	-	Bacterial OUR calculated from oxidation rates
[234]	L-D-L-D (L: 20 min, D: 10 min)	sOPR 6.7-22.6 [mg O_2 g $(TSS)^{-1}$ h^{-1}]; 1.8-6.6 [fmol O_2 $cell^{-1}$ h^{-1}]	-	-	NR, DNR	sOPR and sOUR are calculated as difference with control reactors.
[247]	(SA)	sOPR 0.1 [mg O_2 mg COD^{-1} d^{-1}]	-	sOUR 0.5 [mg O_2 mg COD^{-1} d^{-1}]	AGR	Algal and bacterial activities measured on settled samples
[248]	(SA)	sOPR 0.2-0.68 [mg O_2 mg COD^{-1} d^{-1}]	-	-	AGR	-
[249]	D, L (2 h)	sOPR 0.1-0.5 [mg O_2 mg VSS^{-1} h^{-1}]	sOUR 30-80 [mg O_2 g VSS^{-1} h^{-1}]	-	sARR, sNRR	Bacterial and algal respiration aggregated
[250]	L-D (L: 60 min, D: 10 min)	sOPR [mg O_2 g TSS^{-1} h^{-1}]	sOUR [mg O_2 g TSS^{-1} h^{-1}]	-	-	Bacterial and algal respiration aggregated
[251]	(N_2)-IA-L (60 min)	OPR 1320-14000 [mg O_2 L^{-1} h^{-1}]	-	-	-	-

Notes: L: Light phase, D: Dark phase, SA: Substrate addition, IA: Inhibitor addition, N_2: de-oxygenation using N_2, sPY: specific photosynthetic yield, CUR: CO_2 utilization rate, sAUR: specific ammonium utilization rate, sNUR: specific nitrite utilization rate, NR: nitrification rate, DNR:denitrification rate , $Y_{ALG,N}$: Algal yield on N $Y_{ALG,P}$: algal yield on P, AGR: algal growth rate

CHAPTER 3

MATERIALS AND METHODS

3. MATERIALS AND METHODS

In this section, the photo-respirometric devices used and the microalgae-bacteria cultivation systems tested are described in detail (section 3.1 and 3.2 and , respectively).

3.1. Photo-respirometric devices

3.1.1. Basic instrumentation

A simple photo-respirometer was inititally set up (Figure 3.1) to perform photo-respirometric assays (monitoring protocol).

The instrument consisted in: a 250 mL transparent glass flask used as photo-respirometric vessel; a DO probe (Hach-Lange, LDO101) connected to a multi-meter (Hach-Lange, HQ40D); an aeration system, composed by an air pump (KW Zone, M-102) and a porous stone diffuser to bubble unsterilized ambient air.

A lighting system was made of two fluorescent lights (OSRAM Fluora, 30W, providing an incident irradiance of approximately 75 - 100 $\mu E\ m^{-2}\ s^{-1}$) and a magnetic mixing system (VELP Scientifica, Microstirrer) was normally operated at 150 RPM, in order to minimize oxygen mass-transfer during the experiments. Temperature was logged by the DO probe, at the log frequency of 2 data min^{-1}. The glass flask was covered by aluminium foils during the dark phases of photo-respirometric tests.

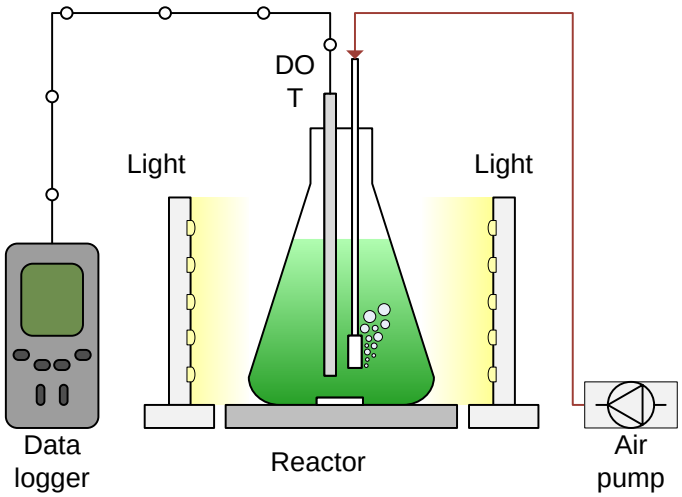

Figure 3.1. Layout of the basic photo-respirometric device.

3.1.2. Fully-equipped photo-respirometer

A fully equipped photo-respirometric/titrimetric unit, provided with different options for DO- and pH-control was then developed (Figure 3.2). The photo-respirometer was designed by IDEA Bioprocess Technologies s.r.l. according to the specifications given by Politecnico di Milano and included: a closed bioreactor (0.5 L glass bottle, DURAN protect, GLS80 headplate) filled with 0.50 - 0.65 L of algal-bacterial suspension, a gas injection system (an air pump and a gas cylinder connected to a set of electro-valves), a signal/communication and mixing (0 - 300 RPM) unit and an acid/base dosage system (two 0 - 12 RPM peristaltic pumps) and an additional peristaltic pump for substrates dosage (manually adjustable in the range 0 - 12 RPM).

The DO-control system was made of a DO probe (Hamilton VisiFerm, DO Arc 120) and a DO-stat system by bubbling pure O_2/N_2 or unsterilized air, while the pH-control system was made of a pH probe (Hamilton Polylite Plus, H Arc 120) and a pH-control system by CO_2 bubbling or acid/base dosage.

Figure 3.2. Fully-equipped photo-respirometer used in this study.

The entire system was controlled with an industrial grade PC running a LabView®-based control software (IDEA Bioprocess Technology s.r.l.). The sampling interval for temperature, pH and DO data was set to 3 s.

In order to also provide an accurate control of light and temperature, during some experiments the photo-respirometric devices were placed into a thermostatic chamber provided with irradiance and air temperature regulation (F.lli Della Marca s.r.l., TS series). In this case, four internal fluorescent elements were present (OSRAM L36W/965 - Deluxe cool daylight), providing an adjustable light intensity up to 200 - 250 $\mu E\ m^{-2}\ s^{-1}$ (Figure 3.3).

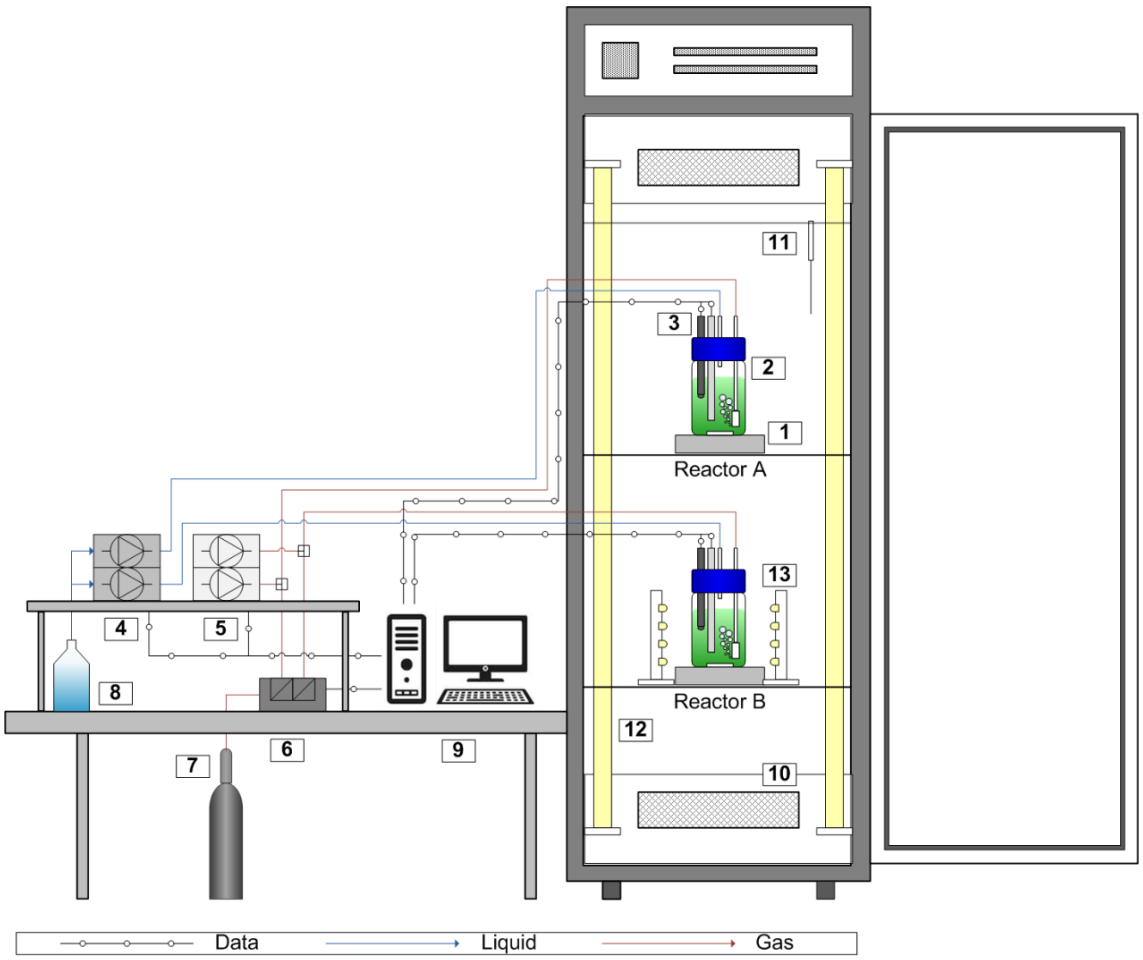

Figure 3.3. Experimental setup: fully-equipped photo-respirometer and thermo-incubator. Legend: 1) Mixing and signal communication unit, 2) Glass bottles, 3) DO, temperature and pH probes, 4) Acid/base dosage pumps, 5) Air/gas pumps, 6) Normally closed electro-valves, 7) Gas cylinder ($CO_2/O_2/N_2$), 8) Acid/base solutions, 9) Industrial grade PC, 10) Heating/cooling fans, 11) Air temperature probe, 12) Fluorescent tubes, 13) Additional LED lamps.

3.2. Cultivation systems tested

In this work, the monitoring, model calibration and inhibition protocols were applied on a series of biomass cultivation systems:

- A pilot-scale HRAP (1.2 m^3) treating municipal digestate located in Milan (Italy);

- A pilot-scale bubble-column (75 L) treating municipal digestate located in Milan (Italy);

- A pilot-scale bubble-column (75 L) agricultural digestate located in Casaletto di Sopra (Italy);

- A set of four lab-scale PBRs (2 L each) agricultural digestate located in Cremona (Italy);

- A set of three demonstrative-scale semi-closed PBRs (11.7 m^3 each) treating agricultural runoff located in Barcelona (Spain);

- A set of two lab-scale PBRs (3.5 L each) treating aquaculture wastewaters located in Cremona (Italy);

- A set of two lab-scale PBRs (3.5 L each) treating piggery wastewaters located in Cremona (Italy);

- A set of four lab-scale PBRs (1 L each) fed with synthetic medium for the cultivation of microalgae monocultures located in Rivolta d'Adda (Italy);

- A set of three lab-scale PBRs (1 L each) fed with synthetic medium for the cultivation of cyanobacteria monocultures located in Barcelona (Spain).

More details on the cultivation systems are reported in the following sections.

3.3. Cultivation systems treating digestates from municipal and agro-industrial wastewaters

Anaerobic digestates from municipal of agro-zootechnical sources were used to grow the algal-bacterial consortia on which photo-respirometry was applied. As detailed below, one HRAP, two bubble-column PBRs and four different lab-scale systems were used.

3.3.1. Pilot-scale HRAP treating municipal digestate

A pilot-scale HRAP installed at the Bresso-Niguarda WWTP (Milan, Italy, 45°31'25.9"N, 9°11'52.3"E) was usecd to grow algae-bacteria biomass. The WWTP, serving about 200,000 inhabitant equivalents, includes: mechanical pre-treatment units, primary settling, secondary treatments (conventional activated sludge with nitrification/denitrification), tertiary treatment by filtration and disinfection by UV radiation. The excess sludge generated during the bioremediation is sent to two mesophilic anaerobic digesters (operating at 35°C, with an HRT of approximately 25 days), generating biogas to feed two CHP units (220 and 320 kW_{EL}, respectively). The digested sludge is then concentrated in a gravity post-thickener and centrifuged (SNF Italia, EM516GK) using cationic polyelectrolytes for enhancing the dewatering performance.

The liquid fraction of anaerobic digestate (LFAD) was used to feed the HRAP without the need for dilution or nutrient supplementation, having the LFAD adequate characteristics, in terms of both nutrient availability and turbidity, as detailed below and in previous works on this stream as nutrient source [46], [269]. The pilot scale HRAP, having a working volume of approximately 1,200 L (surface = 5.8 m^2, water depth = 0.2 m), was installed outdoor in the WWTP (Figure 3.4). During the 2019 monitoring campaign, the HRAP was covered by a polycarbonate roof to protect the pond from rain.

Figure 3.4. Pilot-scale HRAP located at the Bresso-Niguarda WWTP.

The HRAP was operated for three consecutive monitoring campaigns (2017, 2018 and 2019). During these campaigns, the HRAP was operated from spring to autumn, due to the poor irradiance and temperature conditions recorded during winter periods. The influent digestate was fed in continuous, to obtain an average HRT ranging from 8 to 20 days. During the experimentation, no CO_2 was added and pH-control was not implemented.

The LFAD was characterized by high concentrations of ammoniacal nitrogen and moderate concentrations of phosphate and COD. Solids concentrations were highly variable during the monitoring campaigns, however the optical properties remained favourable for algal cultivation (Table 3.1).

Table 3.1. Characterization of the LFAD used as influent for the Bresso-Niguarda HRAP (Milan, Italy) over three monitoring campaigns. Values are expressed as mean ± standard deviation.

PARAMETER	VALUES			UNIT
	2017	2018	2019	
pH	8.1 ± 0.3	7.9 ± 0.3	8.0 ± 0.4	-
Conductivity	1.49 ± 0.27	-	-	[mS cm $^{-1}$]
TSS	81.2 ± 41.5	162 ± 142	114 ± 71	[mg TSS L $^{-1}$]
Turbidity	64.7 ± 46.2	119 ± 118	71.8 ± 9.73	[FAU]
$N\text{-}NH_4^+$	235 ± 81	220 ± 76	224 ± 58	[mg N L^{-1}]
$N\text{-}NO_2^-$	0.1 ± 0.3	1.5 ± 5.9	2.6 ± 7.1	[mg N L^{-1}]
$N\text{-}NO_3^-$	0.2 ± 0.3	0.2 ± 0.8	0.8 ± 4.0	[mg N L^{-1}]
$P\text{-}PO_4^{3-}$	5.5 ± 0.9	4.7 ±0.9	5.0 ± 1.9	[mg P L^{-1}]
Soluble COD	19 ± 53	90 ± 34	143 ± 65	[mg COD L^{-1}]
Total COD	175 ± 84	207 ± 95	410 ± 252	[mg COD L^{-1}]

During the monitroing campaigns, microalgae species were monitored and identified, with *Chlorella* sp and *Scenedesmus* sp. being almost always the two dominant species, although contamination with other species occurred at some time (e.g., *Chlamydomonas* sp. or unidentified diatoms and cyanobacteria).

3.3.2. Pilot-scale bubble-column treating municipal digestate

A bubble-column PBR located in the WWTP described in the previous section 3.3.1 (Bresso-Niguarda WWTP) was used to grow microalgal -bacterial biomass. The pilot-scale column was realized in plexiglass, with a working volume of approximately 75 L and a diameter of 29 cm. Compressed air was sparged at bottom of the column through porous stones (average air flowrate = 0.12 vvm), to provide adequate mixing and CO_2. The bubble-column was covered with a transparent plexiglass cap, to avoid rainwater infiltration and it was manually fed in semi-batch regime, with an average HRT of 10 days.

The bubble-column PBR was operated from May 2019 to November 2019, by feeding the effluent of the Bresso-Niguarda HRAP after solid/liquid separation, obtained by centrifugation (Elecrem tipy 125 L). The particular experimental setup was tested to assess whether the NO_X produced in the HRAP could be

effectively used to grow algal biomass. In this configuration, it was expected that the nitrogen load recirculated to the water line of the WWTP would decrease, while the algal biomass production would increase. A characterization of the HRAP effluent is reported in Table 3.2, while the pilot-scale bubble-column is shown in Figure 3.5. The pilot-scale column was inoculated with the HRAP suspension, being *Chlorella sp*. and *Scenedesmus sp*. the dominant species. However, after approximately two months from the inoculation, a contamination from filamentous cyanobacteria was recorded in the pilot-column.

Figure 3.5. Bubble-column (left) and HRAP (right) pilot plants at the Bresso-Niguarda WWTP.

Table 3.2. Characterization of Bresso-Niguarda HRAP effluent used to feed the bubble-column PBR. Values are expressed as mean ± standard deviation.

PARAMETER	VALUE	UNIT
OD_{680}	0.03 ± 0.03	-
Turbidity	39.7 ± 45.5	[FAU]
pH	7.1 ± 0.7	-
$N\text{-}NH_4^+$	14.4 ± 9.9	[mg N L^{-1}]
$N\text{-}NO_2^-$	19.3 ± 24.6	[mg N L^{-1}]
$N\text{-}NO_3^-$	277 ± 50	[mg N L^{-1}]
N_{TOT}	310 ± 52	[mg N L^{-1}]
$P\text{-}PO_4^{3-}$	2.4 ± 1.7	[mg P L^{-1}]
Soluble COD	129 ± 48	[mg COD L^{-1}]

3.3.3. Pilot-scale bubble-column treating agricultural digestate

An outdoor bubble-column was installed in a piggery farm breeding approximately 20.000 pigs in the province of Cremona (Casaletto di Sopra, Italy). The piggery wastewater was treated in a dedicated WWTP, composed of primary treatment (fine screening and dissolved air floatation), pre-denitrification/nitrification and secondary settling. Piggery wastewater sludge was co-digested with energy crops and other agricultural wastes, in anaerobic digesters operated at an HRT of approximately 30 days and a temperature of 40°C. The LFAD was separated through centrifugation and used to feed the pilot-scale bubble-column. More details about the piggery WWTP and the anaerobic digestate can be found in previous works [46], [235], [270].

The pilot-scale bubble-column consisted of a Plexiglass (Polymethyl-Methacrylate) cylinder with a working volume of approximately 75 L and a diameter of 29 cm (Figure 3.6). The PBR was continuously fed with the LFAD using a peristaltic pump (Rocking Piston Pump 40RNS), while the discharge was realized with an overflow drain. CO_2 was supplied to the culture by bubbling air at the bottom of the column, using an air compressor (Etatron DS, DLX-PH/M). Air bubbling also provided adequate mixing to the suspension. The HRT was set to 20 days due to the high strength of the wastewater (Table 3.3). The MB culture was dominated by *Chlorella* and *Scenedesmus spp*.

Table 3.3. Characterization of the digestate used as influent to the pilot-scale bubble-column located in Casaletto di Sopra (CR). Values are expressed as mean ± standard deviation.

PARAMETER	VALUE	UNIT
OD_{680}	0.16 ± 0.15	-
Turbidity	137 ± 176	[FAU]
TSS	126 ± 119	[mg TSS L^{-1}]
pH	7.9 ± 0.2	-
Conductivity	3.2 ± 0.3	[mS cm^{-1}]
$N\text{-}NH_4^+$	251 ± 86	[mg N L^{-1}]
$N\text{-}NO_3^-$	8.6 ± 2.9	[mg N L^{-1}]
$P\text{-}PO_4^{3-}$	19.8 ± 8.2	[mg P L^{-1}]
Soluble COD	362 ± 153	[mg COD L^{-1}]

Figure 3.6. Pilot-scale bubble-column treating agricultural wastewaters.

3.3.4. Lab-scale PBRs treating agricultural digestate

A lab-scale cultivation system composed of 4 glass cylinders, with a working volume of 2 L each, was setup in the A. Rozzi laboratory of Politecnico di Milano, Cremona (Italy). The four lab-cylinders were operated under the same cultivation conditions (semi-batch feeding), with an average HRT of 20 d. The PBRs were fed

on the same LFAD from agro-wastewaters described in the previous section 3.3.3. The digestate was diluted twice with tap water, due to high nutrient contents and also to provide different conditions from other systems for the validation of the monitoring protocol, resulting in the characterization of the influent digestate is reported in Table 3.4 [242]. Every cylinder was equipped with an aeration system for mixing and CO_2-supply (WAVE Mouse 2). No pH-control was implemented during the cultivation. Lab-cylinders were exposed to artificial fluorescent lights (OSRAM Fluora, 2x30W), providing a PAR of approximately 68 ± 17 mE m^{-2} s^{-1}, with 12h/12h L/D cycles. The average room temperature was approximately 24°C. The microalgae-bacteria consortium was dominated by *Chlorella* and *Scenedesmus spp.*, as confirmed by optical microscopy observations.

Table 3.4. Characterization of the digestate used as influent to the laboratory-scale bubble-columns located at the A. Rozzi laboratory (DICA - Politecnico di Milano, Cremona, Italy). Values are expressed as mean ± standard deviation.

PARAMETER	VALUE	UNIT
OD_{680}	0.09 ± 0.06	-
Turbidity	76 ± 91	[FAU]
TSS	54 ± 62	[mg TSS L^{-1}]
pH	7.8 ± 0.5	-
Conductivity	2.7 ± 0.7	[mS cm^{-1}]
$N\text{-}NH_4^+$	134 ± 47	[mg N L^{-1}]
$N\text{-}NO_3^-$	4.3 ± 1.1	[mg N L^{-1}]
$P\text{-}PO_4^{3-}$	9.1 ± 4.4	[mg P L^{-1}]
Soluble COD	271 ± 216	[mg COD L^{-1}]

3.4. Cultivation systems treating other industrial wastewaters

3.4.1. Demonstrative-scale semi-closed PBRs treating agricultural runoff

Outdoor PBRs treating agricultural runoff were a set of three demonstrative-scale tubular semi-closed PBRs (volume = 11.7 m^3 each), located in the Agròpolis experimental campus of Universitat Politècnica de Catalunya (UPC) (Barcelona, Spain). In brief, each PBR consisted of 2 lateral open tanks connected through 16 transparent tubes (diameter = 125 mm, length = 47 m). Each tank was equipped with a paddle wheel ensuring proper mixing and circulation of the suspension through the tubes and the reduction of excess dissolved oxygen (DO). The three PBRs were connected in series to promote the selection of cyanobacteria and the production and the accumulation of biopolymers, using agricultural runoff as feedstock medium, as schematized in Figure 3.7. Each PBR was operated in continuous with an HRT of 5 d, therefore obtaining an overall HRT of 15 days for the entire system. More detailed information about PBRs design, start-up and operation is available in other works [271], [272].

Nutrient concentrations in the first PBR were adapted to reach the optimum ratio favouring the growth of cyanobacteria over green microalgae, by adding an external source of NO_3 (potassium nitrate inorganic fertilizer, NK13-46, 13% N-NO_3). The culture was mainly dominated by cyanobacteria of the species *Synechococcus* sp. and *Synechocystis* sp. In the second PBR, a feast and famine regime was applied by adding an external inorganic carbon source during 6 h d^{-1}, in order to enhance the cyanobacterial carbon uptake efficiency and the subsequent biopolymers accumulation.

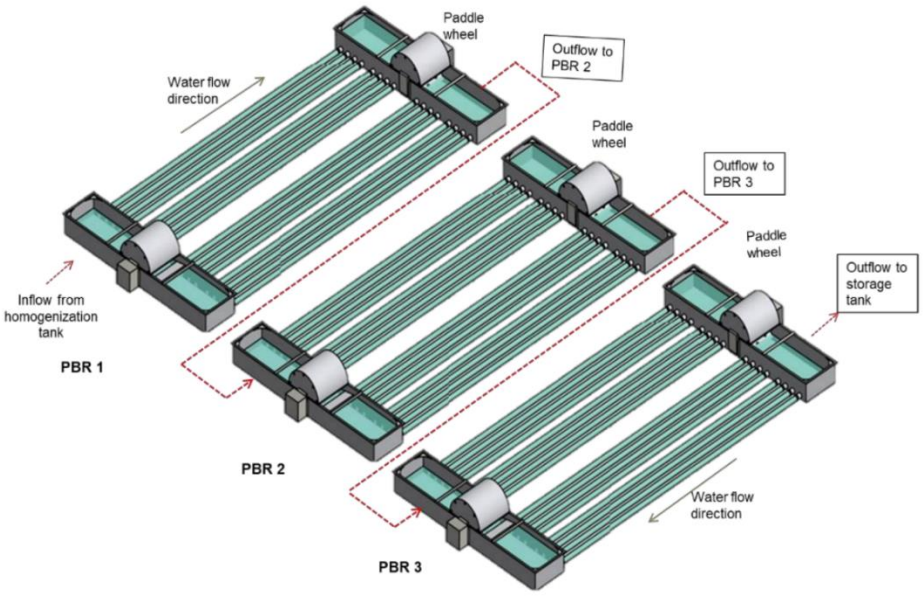

Figure 3.7. Demonstrative-scale hybrid PBRs for the treatment of agricultural runoff wastewaters [272].

In the third PBR, the inorganic carbon was continuously provided to increase the accumulation of biopolymers after the feast and famine phase. CO_2 and sodium bicarbonate ($NaHCO_3$) were used as external inorganic carbon source in both the second and third PBRs. CO_2 was injected by means of diffusers in the lateral open tanks of the PBRs and regulated by a pH-control system. $NaHCO_3$ was added by a daily dose of a concentrated solution of $NaHCO_3$. Detailed information about the operational strategies adopted, wastewater characteristics and biopolymers production can be found elsewhere [273].

The main species dominating the three semi-closed PBRs were identified as cyanobacteria of the species *Synechocystis* sp. and *Synechococcus* sp.

3.4.2. Lab-scale PBRs treating acquaculture and piggery wastewaters

A lab-scale cultivation systems was a set of four column PBRs located at the A. Rozzi laboratory of Politecnico di Milano, Cremona (Italy). The cultivatoin sytem was realized in Plexiglass, with an operational volume of 3.5 L and a diameter of 10 cm for each PBR (Figure 3.8). These PBRs were used to grow: i) the marine green microalga *T. suecica* for the remediation of aquaculture wastewaters and ii) mixed microalgae-bacteria consortia for the remediation of pre-treated piggery wastewaters.

Figure 3.8. Lab-scale column PBRs used to grow monocultures of T.Suecica for aquaculture wastewater treatment [274].

During the first experimentation, the effects of different HRTs on the growth of *T. suecica* were investigated in two runs (namely, HRT = 10 days for Run 1 and HRT = 7 days for Run 2) and photo-respirometric monitoring tests were carried out on the suspensions, as decribed elsewhere [274]. The characteristics of aquaculture wastewaters used in the two experiments are reported in Table 3.5. During this experiment, $NaNO_3$ and K_2HPO_4 were supplemented to the wastewater, in order to avoid nutrient limitation. The initial concentrations of N and P were raised to approximately 20 mg N L^{-1} and 10 mg P L^{-1}, respectively, corresponding to Italian regulations for discharge (Table 3.5). The two reactors were operated in semi-continuous mode and fed with a peristaltic pump (Watson-Marlow Limited, mod. 323), by setting two influent feedings with the duration of 1 hour each, programmed daily at 12:00 am and 12:00 pm. For each feeding, the flowrate was set according to the HRT imposed (4.2 L d^{-1} and 6.0 L d^{-1} for Run 1 and Run 2, respectively). The culture mixig was guaranteed by magnetic mixers (150 RPM) and non-sterilized air injection into the PBRs (air flowrate = 1.8 L min^{-1}). pH and temperature data were acquired by pH probes (Hamilton, Polilyte Plus, PHI Arc 325) with a frequency of 1 datum min^{-1}.

Table 3.5. Characterization of aquaculture wastewaters used as influent to the laboratory-scale bubble-columns located at the A. Rozzi laboratory (DICA - Politecnico di Milano, Cremona, Italy).

PARAMETER	VALUES		UNIT
	HRT 10 d	HRT 7 d	
pH	8.2	8.3	-
Conductivity	52	53	[mS cm^{-1}]
$N\text{-}NH_4^+$	0.4	0.4	[mg N L^{-1}]
$N\text{-}NO_2^-$	0.5	0.7	[mg N L^{-1}]
$N\text{-}NO_3^-$	18.2	19.7	[mg N L^{-1}]
$P\text{-}PO_4^{3-}$	10.8	11.1	[mg P L^{-1}]
Soluble COD	165	155	[mg COD L^{-1}]

The average temperature in the PBRs was 27.5 ± 0.2 °C (no temperature control), and the pH was maintained at 8.2 ± 0.5 by on-demand injection of pure CO_2. The PBRs were illuminated by four fluorescent lamps (OSRAM Fluora, 18W 77), providing a PAR level of 120 μE m^{-2} s^{-2}. L/D cycles were set to 12h/12h. Microscope observation confirmed that the monoculture of *T. suecica* was not contaminated by other algal species.

During the second experimentation using this lab-scale cultivation system, consortia of microalgae-bacteria were grown using piggery wastewaters. The raw wastewaters were taken from the wastewater treatment plant of the previously described piggery farm (section 3.3.3), after a flotation pre-treatment to remove suspended solids, possibly causing a reduction of the light availability. A characterization of the piggery wastewater is reported in Table 3.6. The system was operated in semi-continuous at 10 days HRT, following the same operational modes as the one described for the remediation of aquaculture wastewaters (two feedings per day with the duration of one hour each, and an average flowrate of 4.2 L d^{-1}). The pH was controlled at 8.5 ± 0.9 with the on-demand injection of pure CO_2.

During the experimentation, the two column PBRs were inoculated with samples coming from a pilot-scale HRAP. In particular, a control PBRs was inoculated with the suspended biomass sampled from the Bresso-Niguarda HRAP, while a second reactor was inoculated with the same inoculum, and with biofilm samples grown on the paddlewheel of an HRAP (treating the same wastewater described in Table 3.3), containing filamentous green algae. The control reactor was dominated by green microalgae of the species *Chlorella sp.*, *Scenedesmus sp.* and *Chlamydomonas sp.* The other reactor was instead characterized by the presence of filamentous green algae of the species *Tribonema sp.* and *Stigeoclonium sp.*

Table 3.6. Characterization of pre-treated piggery wastewaters used as influent to the laboratory-scale bubble-columns located at the A. Rozzi laboratory (DICA - Politecnico di Milano, Cremona, Italy). Values are expressed as mean ± standard deviation.

PARAMETER	VALUE	UNIT
OD_{680}	0.17 ± 0.05	-
Turbidity	233 ± 146	[FAU]
pH	8.4 ± 0.3	-
Conductivity	2.7 ± 0.7	[mS cm^{-1}]
$N\text{-}NH_4^+$	122 ± 10	[mg N L^{-1}]
$N\text{-}NO_2^-$	0.9 ± 1.1	[mg N L^{-1}]
$N\text{-}NO_3^-$	2.2 ± 0.2	[mg N L^{-1}]
$P\text{-}PO_4^{3-}$	9.7 ± 3.3	[mg P L^{-1}]
Soluble COD	514 ± 93	[mg COD L^{-1}]

3.5. Cultivation of microalgae and cyanobacteria monocultures

The dominant species of microalgae and cyanobacteria residing in the described pilot- and demonstrative-scale systems (the HRAP located in Bresso-Niguarda and the series of semi-closed PBRs located in the UPC Agropolis facility, respectively) were identified by microscope observations and cultured at the laboratory-scale, as detailed below.

3.5.1. Cultivation of green microalgae monocultures

Four different species of green microalgae were selected after microscope observations in the Bresso-Niguarda HRAP and cultured in the laboratories of the *Instituto Sperimentale Italiano Lazzaro Spallanzani* (Rivolta d'Adda, IT). Two strains of *Chlorella spp.* (*Chlorella vulgaris, SAG211-11j and Chlorella sorokiniana, SAG211-8k*) and one strain of *Scenedesmus* (*Scenedesmus quadricauda, or Desmodesmus armatus, SAG276-4d*) were acquired from the Culture Collection of Algae at the University of Göttingen (SAG, Germany), while one strain of *Scenedesmus spp.* (identified as *Scenedesmus obliquus*) was isolated from an outdoor pond.

All strains were cultured in 500 mL glass Erlenmeyer flasks, using commercially available Modified Bold Basal Medium (MBBM, Sigma-Aldrich), at room temperature (20 - 25 °C) and under controlled irradiance (cool white fluorescent lamps, Philips F58W/33-640 58W, 12 h/12 h L/D cycles). Sterile air (0.2 μm cutoff) was bubbled in the PBRs to provide carbon dioxide and mixing. The cultivation of green microalgae was achieved without pH-control.

3.5.2. Cultivation of cyanobacteria monocultures

Three different species of cyanobacteria were identified and isolated from the semi-closed PBRs fed with agricultural runoff and cultured under controlled conditions: *Synechococcus* sp., *Synechocystis* sp., and *Leptolyngbya* sp. The strains were sampled from the first semi-closed PBR and inoculated in plates prepared with 1% bacteriological agar and commercially available BG11 medium (Sigma-Aldrich, St. Louis, US), by direct streaking or after serial dilutions in saline media, as explained in Rueda et al. (2020).

Once cyanobacteria colonies were obtained, they were transferred into 2 mL of medium contained in 15 mL test tubes and scaled-up (scaling ratio = 1:5), until 1 L cultures were obtained. Finally, they were kept in Erlenmeyer flasks at room temperature (30 ± 2°C), under controlled irradiance (approximately 36.2 μE m^{-2} s^{-1} using 14W cool-white LED lights) under 15 h/9 h L/D cycles. Sterile air (0.2 μm cutoff) was bubbled to provide mixing and CO_2 and to remove accumulated DO. The cultivation was achieved without pH-control. More information about the cultivation of cyanobacteria monocultures can be found elsewhere Rueda et al. (2020).

3.6. Analytical methods

TSS were determined according to Standard Methods [275]. Optical density at 680 nm and turbidity were measured in 1 cm and 5 cm cuvettes respectively, by a spectrophotometer (Hach-Lange, DR 3900). pH and DO were measured by a portable multi-meter (Hach-Lange, HQ40D). Microalgae were counted using an optical microscope (Optika, B 350) at 40x magnification or an epi-fluorescence illuminated microscope (Nikon Eclipse E200). Soluble COD, ammonia, nitrate and nitrite-nitrogen and phosphate-phosphorus were determined using spectrophotometric test kits (Hach-Lange, LCK 314, LCK 303, LCK 339, LCK 342 and LCK 348, respectively) on filtered samples (0.45 μm).

In same cases, ion chromatography (DIONEX ICS 1000, Thermo-scientific, USA) was used to measure nitrate, nitrite and orthophosphate. COD measurements were also carried out using the procedure indicated in the Standard methods (APHA, 2005).

Fluorescence *in situ* hybridisation (FISH) was used to confirm the presence of Ammonia-Oxidizing Bacteria (AOB) in MB suspensions. FISH was carried out on samples collected and stored in ethanol (sample/ethanol ratio 1:1 v/v) at 20°C prior to fixation, which was performed using 4% paraformaldehyde fixative solution as described by Amann et al. [276]. Hybridization was performed with a mix of Cy3 labelled probes and competitors targeting AOB (Nso 1225, NEU, CTE, 6a192, c6a192), according to a protocol described in Bellucci and Curtis [277]. Hybridized MB samples were then visualized under a fluorescent microscope (Zeiss, Axioskop HBO 50) and recorded.

CHAPTER 4

DEFINITION AND STANDARDIZATION OF TEST PROTOCOLS

4. DEFINITION AND STANDARDIZATION OF TEST PROTOCOLS

4.1. Standardization of test procedures and conditions

In this section, the most important aspects regarding the standardization of test protocols are discussed, with a particular focus on those aspects that can strongly impact on the measured photosynthetic and respiratory rates: i) the characteristics of the sample (in terms of pre-treatments, having consequences on its optical properties and nutrient concentrations), ii) the environmental conditions maintained during the test, and iii) the possible alternatives to evaluate the activities of algae and bacteria.

4.1.1. Sample characteristics and pre-treatments

In this work, the samples of algal suspension (approximately 1 L volume) were always collected from the cultivation systems during the morning, between 09:00 AM and 10:00 AM in order to reduce the variability over time, that could impact the resulting sOPR [187], [278]. For the transportation of the samples, they were transferred in white non-refrigerated polypropylene bottles, kept in the dark. The duration of the transportation lasted approximately 30 - 45 minutes. The choice of the sampling point can have important consequences, especially in reactors where the mixing conditions are not adequate or in very long PBRs, such as in thin layer reactors [187]. When sampling from the Bresso-Nigurda HRAP and from the semi-closed systems at the Agropolis campus, the samples were always collected downstream to the paddlewheels, where the mixing rate was the highest [279].

Prior to the execution of photo-respirometric tests, it was necessary to pre-treat samples, in order to assess the photosynthetic and respiratory activities under constant and standardized conditions. Indeed, as previously mentioneed, a high variability can be found, in microalgae-bacteria consortia, as a consequence of: i) the daily and seasonal variation of environmental conditions in outdoor PBRs, and ii) the large variability of the influent wastewater characteristics. This variability has further consequences on the variation of other important parameters (i.e., the pH value and DO concentrations).

With respect to the pre-treatment of the sample, several options exist, as schematized in Figure 4.1: the dilution of the sample or the solid/liquid separation followed by resuspension of the biomass into a specific mineral medium (MM). The OD_{680} was measured before each test and adjusted to a fixed interval (from 0.2 to 0.6, as explained in section 4.1.2), in order to obtain comparable light penetrations during each test. When only dilution was applied as a pre-treatment to modify the initial concentration of nutrients in microalgae and cyanobacteria monocultures (section 4.2.1.3), cultivation media were used for resuspension (MBBM and BG11 for microalgae and cyanobacteria, respectively). In this case, the dilution factors applied (approximately 1:10 - 1:20) could guarantee the nutrient availability, without imposing an additional mechanical stress to the biomass. When it was not possible to simply dilute the suspension, solid/liquid separation was applied, after which the algal paste was respuspended into a synthetic MM or in the effluent of the plant. For those systems in which the algae-bacteria consortium grew in suspension (such as for the culture in the Bresso-Niguarda HRAP, section 3.3.1), the samples were first screened with a mesh (300 μm cut-off), in order to remove detached biofilms, insect larvae and inert particles.

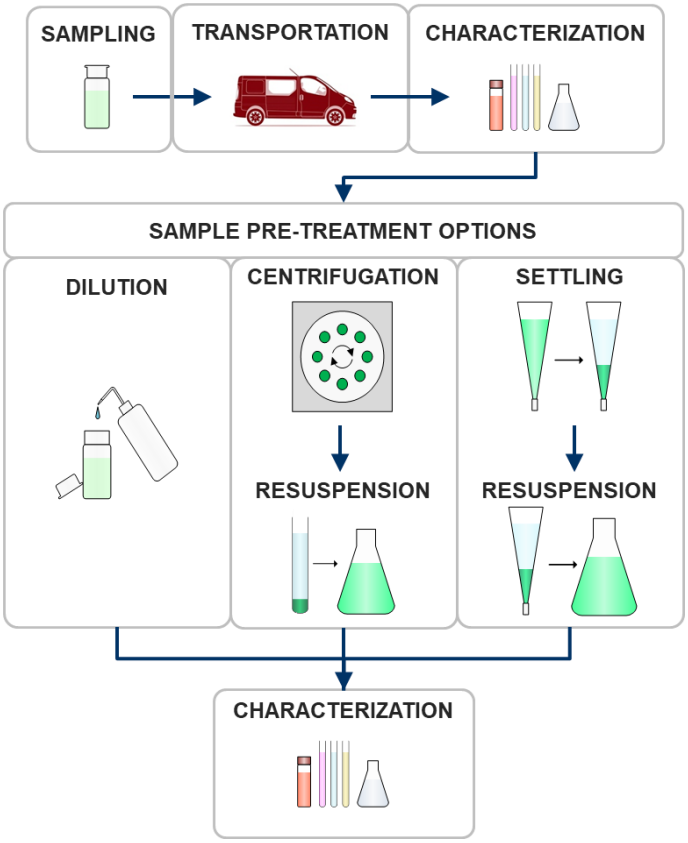

Figure 4.1. Schematization of different pre-treatment options for conducting photo-respirometric tests on microalgae-bacteria suspensions.

The solid/liquid separation could be achieved by centrifugation of the sample, or by gravity settling. Both methods were quite effective in obtaining a standardized initial condition, in terms of optical density and of light availability. Regarding the centrifugation pretreatment, a nutrient-free MM was used to resuspend the algal biomass after centrifugation at 5000 RPM for 10 minutes. The composition of the MM was specifically designed to mimic the ionic composition present in the cultivation system, thus avoiding excessive osmotic shocks. To this aim, the concentrations of metals (Na, Ca, Mg, K, Co, Mn, Fe, Ni, Al, Cu and Zn) in the cultivation system were determined in three independent samples, and the MM was prepared accordingly. Regarding natural settling, this option was suitable when dealing with floccular biomass for which the settling process was very fast. The strategy was applied to the cyanobacteria-bacteria consortia developed in

the semi-closed PBRs, containing filamentous cyanobacteria flocs, which made difficult to determine the OD_{680}. In this case, the TSS concentrations were used to evaluate the amount of biomass to be diluted in the effluent of each PBR and the dilution with the effluent of the plant was preferred to dilution with synthetic media, since the ionic composition of semi-closed PBRs suspensions could not be characterized.

4.1.2. Optical properties, light penetration and solid concentrations

The optical properties of samples, resulting from the presence of solids/turbidity in the suspensions, are of crucial importance because they can strongly affect the penetration of light in the photo-respirometric vessel. Indeed, the combination of a different PAR intensity and light absorbance (or solids concentration) of the suspension has obvious consequences on the photosynthetic OPRs and respiratory OURs for phototrophs. Therefore, in order to conduct PRTs under optimal (i.e. non-limiting and non-inhibiting) conditions of light availability, while avoiding a too fast DO accumulation in the vessel, a standardized range of value was evluated, as described below.

In order to allow for a reasonable ligth availability in the photo-respirometer (i.e., avoiding light limitation and photo-inhibition), a light distribution model based on the application of the Beer-Lambert's law was preliminarily applied (data not shown), allowing to estimate the effective light availability. According to the results obtained, the light intensity during photo-respirometric tests was maintained in the range 40 - 120 $\mu E\ m^{-2}\ s^{-1}$, and the initial OD_{680} was maintained in the range 0.2 - 0.6, corresponding to approximately 0.18 - 0.53 g TSS L^{-1}. Results from preliminary evaluations also showed that a high variability in the oxygen production and consumption rates was obtained when performing the activity

tests outside of the proposed range of biomass concentrations. On the contrary, the measured variability was almost constant inside the proposed range, thus the tests were carried out under these conditions. PAR measurements were carried out at different heights of the respirometer and in different directions, in order to evaluate the effective light distribution and to keep into account additional contributions given by reflected/diffuse radiation. When possible, the light source was selected by choosing a light spectrum that is compatible with the photobiological processes of algae and superior plants (e.g. OSRAM Fluora or similar fluorescent lamps), and also as close as possible to the light conditions applied in the cultivation reactor (i.e. to sunlight).

Due to the fact that different solutions are injected in the respirometric reactor during the test, dilution occurs and should be accounted for, if the volume increase is significant. In this work, the sum of injected volumes (i.e. nutrient solutions, acid/base titrants and inhibitors solutions) caused an increase in volume always lower than 4.0 - 8.5%, therefore, dilution correction factors were not considered during calculations.

4.1.3. Nutrient concentrations

As previously mentioned, during photo-respirometric tests, the nutrient concentrations were kept at a level to which both growth limitation and substrate inhibition could be excluded (i.e. by maintaining nutrient concentrations above the affinity constant, but well below concentrations causing a substantial inhibition). To this aim, the solid/liquid separation, followed by the resuspension into a nutrient-free MM and the addition of concentrated solutions was considered the best option, as previously described. Indeed, by adopting this methodology, the concentrations of nutrients could be brought to the initial

desired level, similar for all photo-respirometric tests thus operating under standardized initial conditions. For providing the desired concentrations of substrates and inhibitors, the following concentrated solutions were dosed:

- SS_1: Ammonium chloride (11.5 g NH_4Cl L^{-1}), supplied in the proportion of 10 μL L^{-1} to obtain a final concentration of 30 mg N L^{-1} in the photo-respirometer;

- SS_2: Sodium bicarbonate (52.4 g $NaHCO_3$ L^{-1}), supplied in the proportion of 20 μL L^{-1} to obtain a final concentration of 150 mg C L^{-1} in the photo-respirometer;

- SS_3: Potassium monohydrogen phosphate (25.5 g K_2HPO_4 L^{-1}), supplied in the proportion of 2 μL L^{-1} to obtain a final concentration of 10 mg P L^{-1} in the photo-respirometer.

During the execution of the inhibition protocol on microalgae-bacteria suspensions, the nutrient solutions were the same described here, with the only difference that in this case the concentration of the NH_4Cl solution was halved in order to reduce the initial FA concentration, while still guaranteeing nitrogen availability. Nutrients were not added during PRTs performed on microalgae/cyanobacteria monocultures, as the nutrient availability was guaranteed by the resuspension in the MM (see section 4.1.1).

4.1.4. Test conditions and interferences of environmental control systems

When possible, during photo-respirometric tests the environmental parameters were kept as close as possible to reference conditions by using the control systems for irradiance, temperature, pH and DO. The conditions defined as reference values and the available options for their control are briefly discussed below.

Since the test conditions generally differed from the outdoor PBRs conditions, an acclimation phase to test conditions was also included, as better detailed in section 4.1.5.1.

Regarding the control of light, external illumination devices were used to maintain the desired light availability. As mentioned, during the execution of monitoring tests, the light intensity was set to 40 - 120 $\mu E\ m^{-2}\ s^{-1}$ as this iradiance level did not limit nor inhibit the algal-bacterial biomass.

Regarding temperature, during photo-respirometric assays performed with the fully-equipped photo-respirometer placed in the thermo-incubator (see paragraph 3.1.2), 20 °C were maintained through the control of air temperature in the chamber, in order to avoid the instauration of a thermal stress in the biomass. When using the basic instrumentation (see paragraph 3.1.1), the maximum temperature variation was on average ± 2.5 °C, although slightly higher temperatures were also obtained in some case. In these cases, OPR values were corrected by using the temperature switch described in section 5.2.

The pH was controlled using concentrated acid/base solutions (HCl or NaOH, 0.1 - 0.5 N), when the fully-equipped photo-respirometer was used. This control system was preferred to on-demand CO_2 insufflation, because the pH control was very stable and the addition of acid/base solutions did not substantially modified the volume of the photo-respirometer, as discussed in section 4.1.2. Since in the basic instrumentation the pH-control could not be adopted, in those test performed with this experimental setup, it was preferred to let the pH vary rather than using a pH buffer. The initial pH was set to 7.5 (in the monitoring and model calibration protocols) or 8.5 (in the inhibition protocol), to always remain in a physiological interval.

As for the DO, its concentration was maintained around the saturation (75 - 125 % DO_{SAT}), so as to avoid avoid photo-respiration and photosynthesis inhibition at high DO. In order to bring the DO concentration back to the saturation level, non-sterile air was bubbled, either automatically (in the fully-equipped photo-respirometer) or manually (in the basic instrumentation). Using ambient air to bring back the DO to saturation was preferred rather than using N_2 or other inert gases to bring the DO to zero, as it was reported that low oxygen concetrations can limit the respiratory activity of phototrophs [53]. The use of sodium sulfite (Na_2SO_3), despite used in literature [236], was not considered during photo-respirometric tests, in order not to modify the salinity of the suspension and its dilution.

4.1.5. Evaluation of algal and bacterial contributions on oxygen dynamics

4.1.5.1. Alternation and duration of light/dark phases and acclimation of the sample

When assessing the activity of phototrophic organisms, it was essential to characterize both respiration and photosynthesis processes, in order to correctly evaluate the gross OPR. Therefore, DO dynamics were followed during light and dark phases. Indeed, all the protocols defined in this work were based on the repetition or alternation of L/D phases. During dark phases, the measured DO concentration was characterized by a much noiser signal compared to light phases. For this reason, the maximum duration of dark phases was set to 10 - 20 minutes, while 10 - 15 minutes where normally sufficient to obtain stable trends during light phases. In all cases, the first 1 - 10 minutes of data recorded after the

beginning of each phase were discarded, according to the stability of the first-order DO time derivative, identifying a pseudo steady-state, as suggested in Brindley et al. [134].

During the development of the monitoring procedure, the duration of the first light phase was initially set to 30 min to let the consortium acclimate to test conditions, in terms of light, temperature and pH. The duration of the first light phase was then brought back to 10 - 15 min, after it was decided to include a preliminary acclimation phase with the duration of 45 - 90 minutes. This timing was specifically imposed after evaluations of the photosynthetic activity of the consortium, according to PAM fluorometry experiments in which the equilibration of metabolic activities to the new light conditions was followed. During the model calibration protocol, the biomass was first incubated for 20 h under the reference conditions reported above, in order to obtain a stable activity of the consortium before modifying the conditions (see section 4.2.1.2). During this protocol, the acclimation time of 45 - 90 minutes was however respected, each time a variation in environmental parameters was imposed.

4.1.5.2. Evaluation of bacterial activity during photo-respirometric assays

As introduced in section 2.3, different methodologies can be applied to evaluate bacterial activity. In particular, it is possible to make use of selective inhibitors for bacteria or to physically separate the algal and bacterial populations. The physical separation, however, is characterized by some disadvantages, such as: the imperfect separation (filtration), the long-time requirement (natural settling) or the use of algal biomass with a particular aggregation status (e.g. immobilized microalgae). The use of selective inhibitors is a promising technique for the use in photo-respirometric assays, especially for those microalgae-bacteria systems

fed with high-strength ammonium wastewaters and characterized by a significant presence of nitrifying bacteria, such as the ones described in this work.

In this work, ATU was exploited to inhibit bacteria, and the bacterial activity was calculated by difference between the sOPR measured with and without ATU, as detailed in section 4.2.1.1. The use of ATU did not interfere with algal activity, as recently reported in literature [240], [280], [281], and also confirmed by PAM-fluorometry measurements showing no adverse effects on photosynthesis, even after 24 h exposure (data not shown). The concentration of ATU necessary to suppress the nitrifying activity was selected according to previous research works, in which the complete inhibition of AOB was achieved [125]. To this aim, a concentrated inhibitor solution (IS_1) containing 5 g ATU L^{-1} was supplied (2 μL L^{-1}) to mixed cultures of phototrophs/bacteria, obtaining a final concentration of 10 mg ATU L^{-1} in the photo-respirometer. No ATU or other bacterial inhibitors were as dosed in microalgae and cyanobacteria monocultures.

Regarding the inhibiton of NOB, other authors reported successful applications using compounds containing azide (N_3^-) or chlorate (ClO_3^-) [125], [282]. However, using sodium azide (NaN_3) at the concentration of 24 μM resulted in the complete inhibition of the photosynthetic activity in cyanobacteria samples, with possible damaging effects on cyanobacteria cells, due release of phycocyanin or other pigments providing a light-blue colour to the suspensions (data not shown). Therefore, the chemical was not exploited during the photo-respirometry assays. In an initial attempt of including the NOB activity in the nitrifying activity assessment, the "monitoring protocol" was developed by also dosing sodium nitrite to activate NOB and potassium chlorate to subsequently inhibit bacteria thus allowing to evaluate their activity as for AOB. Therefore, 30 mL L^{-1} of a concentrated inhibitor solution containing 60 g $KClO_3$ L^{-1} (IS_2) and 4 mL L^{-1} of a concentrated substrate solution containing 3.75 g $NaNO_2$ L^{-1} (SS_4) were also dosed, in order to respectively obtain 0.834 g $KClO_3$ L^{-1} (or 10 mM ClO_3^-) and 10

mg $N\text{-}NO_2$ L^{-1} in the photo-respirometer [242]. However, the protocol was later simplified, as described in section 4.2.1.1 (i.e., the NO_2^- and ClO_3^- additions were removed) because the high concentration of chlorate needed to suppress NOB resulted in increased salinity and a relevant modification of the pH during the test. On the other hand, the contribution of NOB on the overall OUR was expected to be low compared to AOB, therefore it was decided not to include the chlorate addition in any of the protocols in which inhibitors were added.

4.2. Photo-respirometric protocols and numerical methods

4.2.1. Photo-respirometric protocols

In this section, the defined photo-respirometric protocols are described in detail. The "monitoring protocol" was specifically developed to assess the activity of both phototrophic organisms and nitrifying bacteria in microalgae-bacteria consortia. The "model calibration protocol" was instead defined to provide a simple tool for the estimation of relevant parameters characterizing phototrophic populations in algae-bacteria consortia. Finally, the "inhibition protocol" was developed to specifically assess the reduction of the photosyntetic sOPR due to inhibition from inhibitory compounds (e.g. free ammonia, recalcitrant organic compounds, pesticides, herbicides or other chemicals). Those protocols are hereafter described.

4.2.1.1. Monitoring protocol

In the "monitoring protocol", the OPR and OUR by microalgae and nitrifying bacteria can be determined during the same bioassay. The protocol is

characterised by the alternation of L/D regimes and the dosage of inorganic substrates and inhibitors for nitrifying bacteria, to selectively activate/inactivate microalgal and bacterial metabolisms, as detailed below. This protocol was applied to all microalgae-bacteria cultivation systems described in materials and methods (chapter 0).

The monitoring protocol included: 1) sampling of the sample of the algae/bacteria suspension from the HRAP and transportation to the lab, 2) sample pre-treatment, 3) sample characterization, 4) acclimation to the reference conditions, 5) removal of excess DO, 6) execution of the activity test (including the addition of the nutrient and inhibitor solutions SS_1, SS_2, SS_3, IS_1), 7) data processing. The main aspects of the protocol are discussed below.

The diluted algal-bacterial suspension was then transferred into the respirometer bioreactor and ambient air was bubbled to bring the DO concentration close to saturation; DO data collection was started. Along the test duration, environmental conditions (light conditions and the presence/absence of specific substrates and/or inhibitors) were modified, identifying different light phases (L_i) and dark phases (D_i). Then the test was ended and DO data were retrieved and used to compute the OPR (positive/negative when a net production/consumption was observed) in each phase, according to the data processing and OPR calculation procedure described in section 4.2.2.1. Hereafter each phase is described, including environmental conditions and expected biological reactions affecting the DO concentration:

- L_1) Light on, addition of SS_1, SS_2 and SS_3: oxygen is produced by microalgal photosynthesis; a contribution to the oxygen variation is also expected due to the aerobic activity of nitrifying bacteria (hereafter referred to as "NIT", including both AOB and NOB), of microalgae light respiration and of

heterotrophic bacteria respiration (HB). Therefore, the net OPR of this phase ($OPR_{NET,L1}$) is made of the following contributions:

$$OPR_{NET,L_1} = OPR + OPR_{RESP} + OPR_{HB} + OPR_{NIT} \quad 4.1$$

where: OPR is the photosynthetic MA oxygen production, OPR_{RESP} is the respiration by microalgae (negative), OPR_{HB} is the oxygen production by heterotrophs (negative), OPR_{NIT} is the oxygen production by nitrifiers (negative).

– D_1) Light off: oxygen consumption by MA respiration, NIT and HB activity; therefore:

$$OPR_{NET,D_1} = OPR_{RESP} + OPR_{HB} + OPR_{NIT} \quad 4.2$$

– D_2) Light off, addition of the IS_1. NIT are inhibited and the oxygen is only modified by algal respiration and HB activity; therefore:

$$OPR_{NET,D_2} = OPR_{RESP} + OPR_{HB} \quad 4.3$$

– L_2) Light on: oxygen production due to microalgal photosynthetic activity is expected and simultaneous oxygen consumption by microalgal respiration and HB activity; therefore:

$$OPR_{NET,L_2} = OPR_{ALG} + OPR_{RESP} + OPR_{HB} \quad 4.4$$

– D_3) Same conditions as D_2: oxygen consumption by microalgae respiration and by HB activity; therefore:

$$OPR_{NET,D_3} = OPR_{RESP} + OPR_{HB} \quad 4.5$$

The OPR values of each phase (OPR_{L1}, OPR_{L2} for the two light phases; OPR_{D1}, OPR_{D2}, OPR_{D3} for the three dark phases) were determined, depending on oxygen uptake and consumption as follows:

$$OPR_{1} = OPR_{NET,L_1} - OPR_{NET,D_1} \quad 4.6$$

$$OPR_{2} = OPR_{NET,L_2} - OPR_{NET,D_2} \quad 4.7$$

$$OPR_{3} = OPR_{NET,L_2} - OPR_{NET,D_3} \quad 4.8$$

$$OPR_{NIT,1} = OPR_{NET,D_1} - OPR_{NET,D_2} \quad 4.9$$

$$OPR_{NIT,2} = OPR_{NET,L_1} - OPR_{NET,L_2} \quad 4.10$$

The OPRs values are expressed as volumetric rates (mg O_2 L^{-1} h^{-1}) and then normalized to the total biomass concentration, as detailed below (section 4.2.2.1). From Equations 4.6 to 4.10, various estimates were obtained for both microalgal photosynthetic oxygen production (OPR_1, OPR_2; OPR_3) and for the nitrifiers oxygen consumption ($OPR_{NIT,1}$, $OPR_{NIT,2}$). Mean values were then calculated (OPR_{mean}, $OPR_{NIT,mean}$). OPR_1 and the mean value of OPR_2 and OPR_3 were compared by means of heteroscedastic T-tests, as described in section 4.2.2.1. The dark oxygen consumption including MA and HB respiration was also obtained, although it gives an aggregated information (OPR_{RESP}).

The typical output of the "monitoring protocol" and its phases are reported in Figure 4.2, in which the DO profile for each phase is plotted against time.

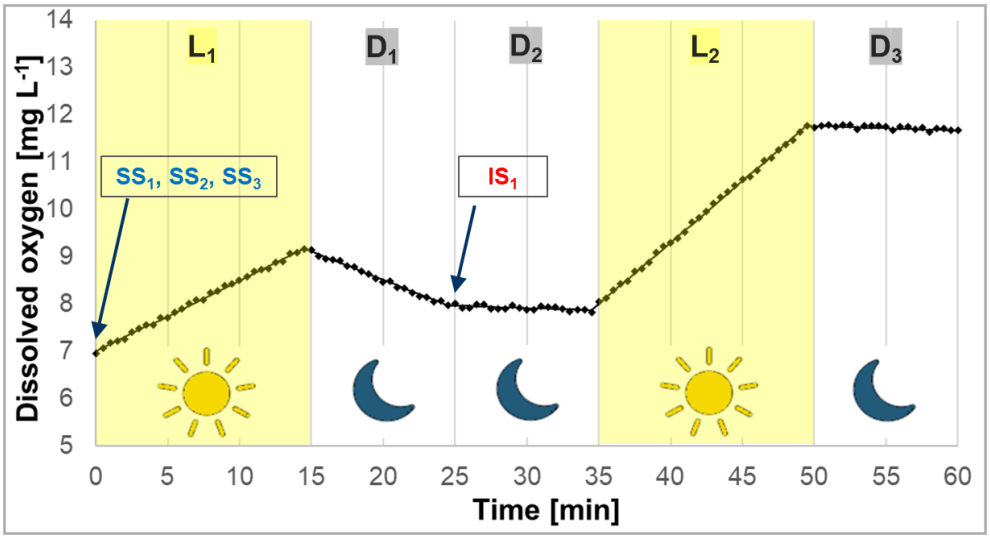

Figure 4.2. Typical result of a photo-respirometric test following the "monitoring protocol". L/D phases are reported together with the addition of substrates and inhibitors.

4.2.1.2. Model calibration protocol

The model calibration protocol aims at evaluating specific photosynthetic and respiratory OPRs under different values of the parameters under investigation. The protocol is characterised by the alternation of L/D regimes, with the dosage of nitrifying inhibitors at the beginning of the test, in order to specifically focus on the assessment of the activity of phototrophic populations.

The protocol was applied to evaluate the effects of different environmental conditions (irradiance, temperature, pH and dissolved oxygen) on the microalgae-bacteria consortium developed in the Bresso-Niguarda HRAP and fed with the LFAD, during the 2019 monitoring campaign (section 3.3.1). Two datasets (i.e. the specific photosynthetic oxygen production rates and respiratory oxygen consumption rates) were obtained for each environmental parameter. The effects of incident irradiance, temperature, pH and DO were separately investigated by evaluating the change in activity due to the variation of one parameter, while leaving the other three around reference values. The conditions

defined as reference values were: irradiance = 100 μE m^{-2} s^{-1}, temperature = 20°C, pH = 8.5 and DO = 9 mg DO L^{-1}.

The model calibration protocol included: 1) Sampling and pre-treatments (points 1 - 3 of the protocol described in section 4.2.1.1), 2) addition of bacterial inhibitors (solution IS_1), 3) addition of concentrated nutrient solutions (SS_1, SS_2 and SS_3), 4) acclimation to the reference conditions, 5) removal of excess DO, 6) execution of the activity test (repetition of L/D phases), 7) variation of the parameter under study, 8) repetition of activity tests (repetition of points 4 - 6), 9) data processing.

The activity tests started the following day, after the DO concentration had been adjusted to the saturation level by bubbling unsterilized ambient air, the parameter under investigation was set to its initial value, all other parameters were set to reference values and nutrients/inhibitors were added to the suspension. During the photo-respirometric assay, 10 minutes of illumination (L_i, light phases) were followed by 20 minutes dark (D_i, dark phases).

Each L_i/D_i cycle was repeated three times. Thus, a total duration of 1.5 h was required to assess each parameter level. After the end of the bioassay, a new level for the parameter under investigation was set and the biomass was acclimated to the new condition for a minimum time of 30 min before starting a new L_i/D_i cycle. In order to maintain the maximum activity during the activity assessment and to avoid the occurring of adaptation mechanisms, every sample was used for no longer than 8 hours. Each parameter was varied over a wide range of values, aiming at covering the conditions recorded during the outdoor monitoring campaign, and also extending them to more extreme values, when possible. The range of values recorded during the outdoor experimentation on the HRAP and those covered during the photo-respirometric study are given below.

The typical output of the "model calibration protocol" is reported in Figure 4.3, in which the DO profile is shown for each phase.

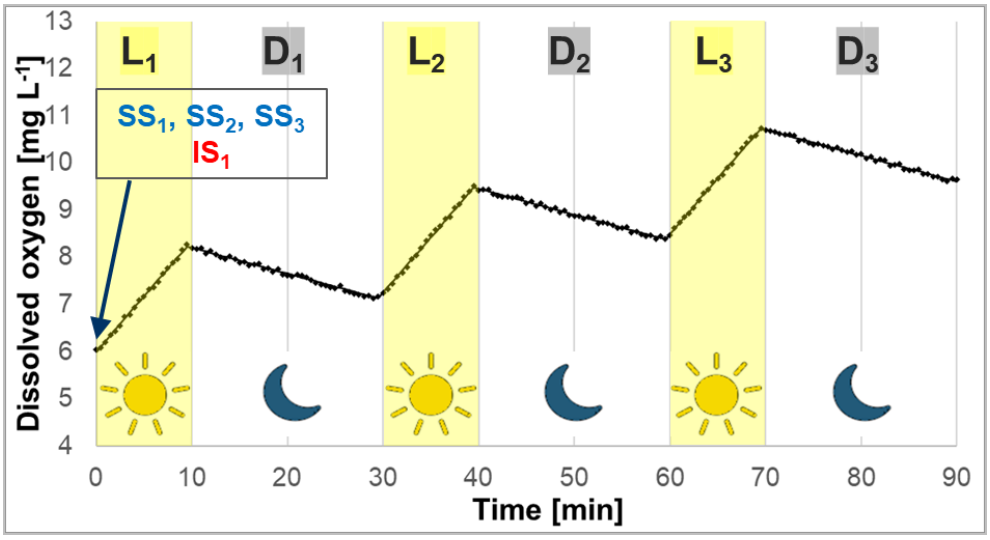

Figure 4.3. Typical result of a photo-respirometric test following the "model calibration protocol". L/D phases are reported together with the addition of substrates or inhibitors.

Irradiance tests

Irradiance tests were performed aimed at covering the entire range of values recorded at the outdoor pilot plant, where the sun radiation reaching the HRAP is partially reduced due to the presence of the roof and other surrounding trees and buildings. The incident light in photo-respirometric tests was measured along the internal surface of the glass bottle for each light configuration in 24 different positions (8 different radial directions at 3 different heights) and the average values were assumed as average incident radiation. The maximum irradiance recorded outdoor was approximately 900 μE m^{-2} s^{-1}. A total of 20 photo-respirometric tests were conducted in the irradiance of range 16-656 μE m^{-2} s^{-1}, by switching on/off the thermostatic chamber lights and by adding up to two additional LEDs, as mentioned before.

Temperature tests

Temperature tests were carried out in a wide range of values, by gradually varying the temperature of the algal-bacterial suspension through the control of the thermostatic chamber temperature. The maximum temperature variation applied to heat or cool the algal suspension were set according to the maximum temperature variations in the HRAP measured outdoor within the day (i.e., 4.8 °C h^{-1}). The recorded outdoor temperatures varied in the range 10.8 - 31.4 °C, with an average value of 21.7 °C. A total of 28 photo-respirometric tests were conducted in the temperature range 10 - 40 °C.

pH tests

The pH value was varied over the entire range of values recorded in the outdoor HRAP, also evaluating extremely acidic and alkaline conditions. After the addition of concentrated nutrient and inhibitor solutions, the pH of the algal-bacterial suspension was adjusted by dosing concentrated HCl or NaOH (0.5 - 1 M) up to the reference condition or the desired initial value. During the photo-respirometric assay, the pH was maintained at the desired set-point value by titration of the same acid/base solutions, at lower concentrations (0.1 M). During pH tests, nitrate ($NaNO_3$, 30 mg N L^{-1}) was used as nitrogen source, in order to avoid possible volatilization of ammonia at high pH or temperatures. A preliminary photo-respirometric tests was performed for comparing the two nutrient sources, showing very similar activities (data not shown). The values recorded in the HRAP during the monitoring campaign ranged from a minimum value of 4.5 to a maximum of 9.8, with an average value of 6.7. The dependence of algal activity on pH values was assessed during 22 tests, in the range: 2.5 - 10.5.

Dissolved oxygen tests

During the experimentation, high DO concentrations were tested to evaluate the effects of oxygen over-saturation on the phototrophic consortium. DO concentrations below saturation were not investigated during this phase of the research, as the main concern was the accumulation of oxygen in the HRAP. Also, technical issues made it impossible to fully exploit de-oxygenation by the DO-control system. While performing the bioassays under reference conditions, the initial DO concentration was set to oxygen saturation and the DO was maintained in the desired range (100 - 150% of the saturation value) by on-demand bubbling of ambient air. During assays conducted at oxygen over-saturation levels, the DO control was removed so as to let DO accumulate as a natural consequence of photosynthetic processes. The DO in the HRAP did not reach the high concentrations tested with the photo-respirometric procedure, ranging from 0.8 - 12.4 mg DO L^{-1}, however the estimation of activity reduction due to over-saturation was deemed to be a relevant information, as previously mentioned. Oversaturation effects were tested in 16 independent experiments (range: 9 - 18.5 mg DO L^{-1}, corresponding to approximately 100 - 205 % oxygen saturation).

4.2.1.3. Inhibition protocol

In the inhibition protocol, the inhibitory effects of compounds known to inhibit the photosynthetic and/or respiratiory activity of phototrophs, such as those described in section 2.2.1.2, could be assessed by exposing phototrophic organisms to increasing concentrations of the inhibitor. Also in this case, the protocol was characterised by applying L/D regimes and by dosing ATU at the beginning of the experiment, in order to inhibit the activity of nitrifiers. By doing so, the reduction of the photo-oxygenation potential supplied by phototrophic populations could be evaluated. In the protocol, the sOPR and sOUR of microalgae were monitored in a respirometric vessel subject L/D cycles in the absence of the inhibitor, in order to identify a reference condition for the sample (control reactor). The inhibition of photosynthesis was instead evaluated in a second reactor (inhibited reactor), in which the L/D cycles were repeated, and concentrated inhibitor solutions were dosed at the beginning of each light phase.

The inhibition protocol was in particular applied to two pilot systems (the Bresso-Niguarda HRAP and the Agropolis semi-closed PBRs, described in section 3.3.1 and section 3.4.1, respectively) and a series of lab-scale microalgae and cyanobacteria monocultures (section 3.5) were tested. FA was varied in the range 8.5 - 136 mg NH_3 L^{-1}, as detailed below. Since the tests were conducted at approximately 20°C and pH 8.5, the background FA concentration corresponding to the NH_4Cl injection was approximately 1.7 mg NH_3 L^{-1}. In order to increase the level of FA in the photo-respirometer, concentrated solutions of ammonium chloride were dosed as detailed below.

- FA_1: Ammonium chloride (0.196 g NH_4Cl L^{-1}), supplied in the proportion of 5.8 μL L^{-1} to obtain a final concentration of 8.5 mg NH_3 L^{-1} in the photo-respirometer

- FA_2: Ammonium chloride (0.392 g NH_4Cl L^{-1}), supplied in the proportion of 5.8 μL L^{-1} to obtain a final concentration of 17 mg NH_3 L^{-1} in the photo-respirometer

- FA_3: Ammonium chloride (0.784 g NH_4Cl L^{-1}), supplied in the proportion of 11.5 μL L^{-1} to obtain a final concentration of 34 mg NH_3 L^{-1} in the photo-respirometer

- FA_4: Ammonium chloride (1.568 g NH_4Cl L^{-1}), supplied in the proportion of 23.1 μL L^{-1} to obtain a final concentration of 68 mg NH_3 L^{-1} in the photo-respirometer

- FA_5: Ammonium chloride (3.135 g NH_4Cl L^{-1}), supplied in the proportion of 46.1 μL L^{-1} to obtain a final concentration of 136 mg NH_3 L^{-1} in the photo-respirometer

Cyanobacteria samples were treated with the solutions FA_1 - FA_4, while microalgae samples were exposed to higher concentrations due to the higher resistance expected, and in this case the solutions used were FA_2 - FA_5.

The typical output of the "inhibition protocol" is reported in Figure 4.4, in which the DO profile is shown for each phase.

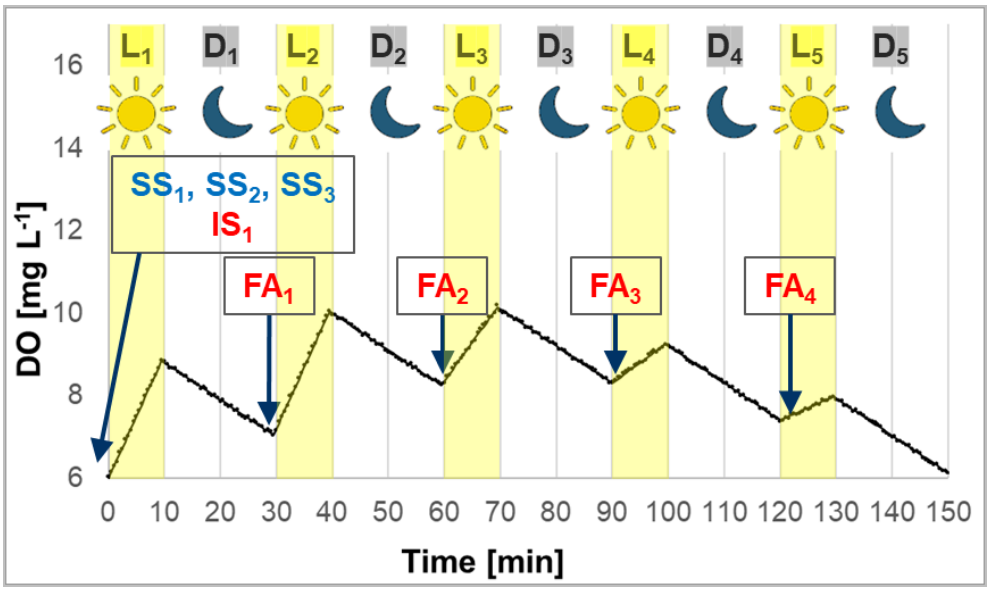

Figure 4.4. Typical result of a photo-respirometric test following the "inhibition protocol". L/D phases are reported together with the addition of substrates or inhibitors.

4.2.2. Numerical methods

In this section, numerical methods used to process DO data and to evaluate the average OPR and OUR for each test are given.

4.2.2.1. Data processing and OPR calculation

The DO dynamics was modelled by considering the concomitant occurrence of either: (i) a constant net photosynthetic oxygen production rate (during light phases) or a respiratory oxygen uptake rate (during dark phases), and (ii) the oxygen mass transfer rate at the liquid-gas interface (OTR). The resulting dynamic mass balance for the DO in the photo-respirometer is therefore (Equations 4.11 - 4.13):

$$\frac{d(DO)}{dt} = OTR + OPR_{NET,i} \quad (i=1, \ldots n) \qquad 4.11$$

$$OTR = \theta^{(T-293.15)} * k_L a_{20} * (DO_{SAT} - DO) \qquad 4.12$$

$$DO_{SAT}=pO_2*K_{H,O_2}(T)=pO_2*K_{H,O_2,\ REF}*\exp\left(-\frac{-\Delta_{SOL}H}{R}*\left(\frac{1}{T}-\frac{1}{T_{REF}}\right)\right) \quad 4.13$$

Where: DO [mg O_2 L^{-1}] is the DO concentration at the time t [h], $OPR_{NET,i}$ [mg O_2 L^{-1} h^{-1}] is the average net OPR during the phase *i* (according to Equation 2.7), n is the total number of phases constituting the protocol, DO_{SAT} [mg O_2 L^{-1}] is the DO saturation concentration at the temperature T [K], pO_2 = 0.21 [Atm] is the partial pressure of oxygen in atmosphere, T_{REF} = 298.15 [K] is the reference temperature, $K_{H,O2}(T)$ [mg O_2 L^{-1} Atm^{-3}] is the value of Henry's law solubility constant for oxygen at the temperature T, $K_{H,O2,REF}$ = 40.5 [mg O_2 L^{-1} Atm^{-1}] is the value of Henry's law solubility constant at T_{REF} [283], k_La_{20} = 0.17 ± 0.07 [h^{-1}] is the volumetric oxygen mass-transfer coefficient evaluated at 20 °C during abiotic tests, that was previously assessed for the photo-respirometer according to the nonlinear regression method [98].

To compute the average $OPR_{NET,}$ and $OPR_{RESP,}$ and k_La, nonlinear least square regression was performed using the *lsqcurvefit* function with the software MATLAB R2019b (Optimization Toolbox™, The MathWorks, Inc., USA). Raw DO data were fitted to estimate OPR_{NET} and OUR_{RESP}. The gross OPR was then calculated for each L_i/D_i determination, by subtracting the estimated OUR_{RESP} to the OPR_{NET}, and the result was divided by the total suspended solids (TSS) of the sample, measured according to Standard Methods [275], to obtain specific OPRs and OURs (sOPR and $sOUR_{RESP}$, [mg O_2 g TSS^{-1} h^{-1}]) (Equations 4.14 - 4.16):

$$OPR_i=OPR_{NET,i}-OUR_{RESP,i}\ (Phases\ 1,\ 2,\ 3) \quad 4.14$$

$$sOPR_i=\frac{OPR_i}{TSS}\ (Light\ phases,\ L_i\ i=1,\ 2,\ 3) \quad 4.15$$

$$sOUR_{RESP,i}=\frac{OUR_{RESP,i}}{TSS}\ (Dark\ phases,\ D_i\ i=1,\ 2,\ 3) \quad 4.16$$

4.2.2.2. Photosynthesis, respiration and inhibition models

Once the sOPR and $sOUR_{RESP}$ values were obtained for each condition tested, the gathered data were used to describe the influence of the tested parameters as described below.

Photosynthesis and respiration models as a function of environmental conditions

Regarding the effects of environmental parameters, several models were proposed in literature (see, for example, Béchet et al. and Shoener et al., [284] and [285]). The dependence on environmental parameters is often represented in mathematical terms by the product of different "switch" functions, each one describing the effect of a single parameter (Equations 4.17 and 4.18):

$$sOPR(I, T, pH, DO, nutrient) = sOPR_{MAX} * f_{P,I} * f_{P,T} * f_{P,pH} * f_{P,DO} * f_{P,NUTRIENT} \quad 4.17$$

$$sOUR_{RESP}(I, T, pH, DO, nutrient) = sOUR_{RESP,MAX} * f_{R,I} * f_{R,T} * f_{R,pH} * f_{R,DO} * f_{R,NUTRIENT} \quad 4.18$$

Where: $f_{P,I}$, $f_{P,T}$, $f_{P,pH}$, $f_{P,DO}$ and $f_{P,NUTRIENT}$ are the switch functions describing the effects of irradiance, temperature, pH, DO and nutrients, on photosynthesis rates, respectively, and $f_{R,I}$, $f_{R,T}$, $f_{R,pH}$, $f_{R,DO}$ and $f_{R,NUTRIENT}$ are the switch functions describing the effects of irradiance, temperature, pH, DO and nutrients on respiration rates, respectively.

A selection of commonly applied switch functions for environmental conditions (irradiance, temperature, pH and dissolved oxygen) is reported in Table 4.1 and Table 4.2. These models were applied to the photo-respirometric dataset and fitted against sOPR and $sOUR_{RESP}$ data obtained under various levels of each parameter. To obtain a better comparability of resulting fits, sOPR and $sOUR_{RESP}$ data were then normalized for the activity measured under reference conditions.

Free ammonia inhibition models

Regarding the effects of FA on photosynthesis ("inhibition protocol"), the concentration of FA was computed as a function of temperature, pH and of total ammoniacal nitrogen (TAN) concentration, as suggested by Anthonisen et al. [71] (Equation 4.19):

$$NH_3=TAN*\frac{MW_{NH_3}}{AW_N}*\frac{10^{pH}}{\exp\left(\frac{6344}{T}\right)+10^{pH}} \qquad 4.19$$

Where: TAN = NH_3 + NH_4^+ [mg N L^{-1}] is the total ammoniacal nitrogen, MW_{NH3}, is the molecular weight of ammonia [g NH_3 mol NH_3^{-1}], AW_N is the atomic weight of nitrogen [g N mol N^{-1}].

Two different inhibition models were chosen to describe the effect of FA on the photosynthesis and respiration: the non-competitive inhibition model used to evaluate FA inhibition in anaerobic digestion models [286] (Equation 4.20) and a sigmoidal logistic curve, or Hill-type model, used to describe dose-response curves [287] (Equation 4.21):

$$f_{P,NH_3}=\frac{sOPR_{NH3}}{sOPR_{CONTROL}}=\frac{1}{1+\frac{NH_3}{EC_{50,NH3}}} \qquad 4.20$$

$$f_{P,NH_3}=\frac{sOPR_{NH3}}{sOPR_{CONTROL}}=1-\frac{1}{1+\left(\frac{EC_{50,NH3}}{NH_3}\right)^N} \qquad 4.21$$

Where: $sOPR_{NH3}$ is the sOPR calculated in the reactor subject to FA inhibition [mg O_2 g TSS^{-1} h^{-1}], $sOPR_{CONTROL}$ is the sOPR calculated in the control reactor [mg O_2 g TSS^{-1} h^{-1}], NH_3 is the computed initial FA concentration [mg NH_3 L^{-1}], $EC_{50,NH3}$ is the inhibition parameter representing the FA concentration causing a 50% inhibition of the photosynthetic activity [mg NH_3 L^{-1}], N is the dimensionless shape parameter of the Hill model [-].

Table 4.1. Models describing the dependance of photosynthetic rates on local irradiance, temperature, pH and dissolved oxygen.

PHOTOSYNTHESIS MODELS				
ENVIRONMENTAL PARAMETER	**MODEL ID**	**MODEL EXPRESSION**	**MODEL PARAMETERS**	**REFERENCE**
Irradiance	f_{P,I_BR}	$sOPR(I)=sOPR_{MAX}*\frac{I}{I+\frac{sOPR_{MAX}}{\alpha}*\left(\frac{I}{I_{OPT}}-1\right)^2}$ 4.24	α, I_{OPT}	[183]
	f_{P,I_ST}	$sOPR(I)=sOPR_{MAX}*\left(\frac{I}{I_{MAX}}\right)*\exp\left(1-\frac{I}{I_{MAX}}\right)$ 4.25	I_{MAX}	[288]
	f_{P,I_LE}	$sOPR(I)=sOPR_{MAX}*\frac{I}{k_1+k_2*(I^2)}$ 4.26	k_1, k_2	[289]
Temperature	f_{P,T_RA}	$sOPR(T)=\left(b*(T-T_{MIN})*\left(1-\exp(c*(T-T_{MAX}))\right)\right)^2$ 4.27	b, c, T_{MIN}, T_{MAX}	[290]
	f_{P,T_BR}	$sOPR(T)=sOPR_{MAX}*\frac{(T-T_{MAX})*(T-T_{MIN})^2}{(T_{OPT}-T_{MIN})*((T_{OPT}-T_{MIN})*(T-T_{OPT})-(T_{OPT}-T_{MAX})*(T_{OPT}+T_{MIN}-2*T))}$ 4.28	T_{MIN}, T_{OPT}, T_{MAX}	[183]
	f_{P,T_BL}	$sOPR(T)=sOPR_{MAX}*\left(\frac{T_{MAX}-T}{T_{MAX}-T_{OPT}}\right)^{\beta}*\exp\left(-\beta*\left(\frac{T_{OPT}-T}{T_{MAX}-T_{OPT}}\right)\right)$ 4.29	β, T_{OPT}, T_{MAX}	[291]
pH	f_{P,pH_RO}	$sOPR(pH)=sOPR_{MAX}*\frac{\left(pH-pH_{MIN}\right)*(pH-pH_{MAX})}{\left((pH-pH_{MIN})*(pH-pH_{MAX})-(pH-pH_{OPT})^2\right)}$ 4.30	pH_{MIN} ,pH_{OPT}, pH_{MAX}	[52]
	f_{P,pH_IP}	$sOPR(pH)=sOPR_{MAX}*\frac{(pH-pH_{MAX})*\left(pH-pH_{MIN}\right)^2}{\left(pH_{OPT}-pH_{MIN}\right)*\left(\left(pH_{OPT}-pH_{MIN}\right)*(pH-pH_{OPT})-(pH_{OPT}-pH_{MAX})*\left(pH_{OPT}+pH_{MIN}-2*pH\right)\right)}$ 4.31	pH_{MIN} , pH_{OPT}, pH_{MAX}	[53]
	f_{P,pH_BA}	$sOPR(pH)=sOPR_{MAX}*\frac{1+2*10\text{^}(0.5*(pH_{INF}-pH_{SUP}))}{1+10^{pH-pH_{SUP}}+10\text{^}(pH_{INF}-pH)}$ 4.32	pH_{INF}, pH_{SUP}	[292]
Dissolved oxygen	f_{P,DO_CO}	$sOPR(T)=sOPR_{MAX}*\left(1-\frac{DO}{DO_{MAX}}\right)^n$ 4.33	DO_{MAX}, n	[181]
	f_{P,DO_DV}	$sOPR(T)=sOPR_{MAX}*\left(1-\frac{1}{1+\left(\frac{K_{DO}}{DO}\right)^H}\right)$ 4.34	K_{DO}, H	[293]

Table 4.2. Models describing the dependance of respiratory rates on local irradiance, temperature, pH and dissolved oxygen.

RESPIRATION MODELS					
ENVIRONMENTAL PARAMETER	**MODEL ID**	**MODEL EXPRESSION**		**MODEL PARAMETERS**	**REFERENCE**
Irradiance	f_{R,I_IP}	$sOUR(I)=sOUR_{MIN}*\frac{sOPR_{MAX}*I^n}{I_K^n+I^n}$	4.35	n, I_K	[53]
	f_{R,I_RO}	$sOUR(I)=sOUR_{MIN}+\frac{sOPR_{MAX}}{1+\exp(-a*(I-I^*))}$	4.36	a, I*	This work (Sigma function)
Temperature	f_{R,T_RA}	$sOUR(T)=\left(b*(T-T_{MIN})*\left(1-\exp(c*(T-T_{MAX}))\right)\right)^2$	4.37	b, c, T_{MIN}, T_{MAX}	[290]
	f_{R,T_BR}	$sOUR(T)=sOUR_{MAX}*\frac{(T-T_{MAX})*(T-T_{MIN})^2}{(T_{OPT}-T_{MIN})*((T_{OPT}-T_{MIN})*(T-T_{OPT})-(T_{OPT}-T_{MAX})*(T_{OPT}+T_{MIN}-2*T))}$	4.38	T_{MIN}, T_{OPT}, T_{MAX}	[183]
	f_{R,T_BL}	$sOUR(T)=sOUR_{MAX}*\left(\frac{T_{MAX}-T}{T_{MAX}-T_{OPT}}\right)^{\beta}*\exp\left(-\beta*\left(\frac{T_{OPT}-T}{T_{MAX}-T_{OPT}}\right)\right)$	4.39	β, T_{OPT} , T_{MAX}	[291]
pH	f_{R,pH_RO}	$sOUR(pH)=sOUR_{MAX}*\frac{(pH-pH_{MIN})*(pH-pH_{MAX})}{\left((pH-pH_{MIN})*(pH-pH_{MAX})-(pH-pH_{OPT})^2\right)}$	4.40	pH_{MIN}, pH_{OPT}, pH_{MAX}	[52]
	f_{R,pH_IP}	$sOUR(pH)=sOUR_{MAX}*\frac{(pH-pH_{MAX})*(pH-pH_{MIN})^2}{(pH_{OPT}-pH_{MIN})*\left((pH_{OPT}-pH_{MIN})*(pH-pH_{OPT})-(pH_{OPT}-pH_{MAX})*(pH_{OPT}+pH_{MIN}-2*pH)\right)}$	4.41	pH_{MIN}, pH_{OPT}, pH_{MAX}	[53]
	f_{R,pH_BA}	$sOUR(pH)=sOUR_{MAX}*\frac{1+2*10\text{^}(0.5*(pH_{INF}-pH_{SUP})}{1+10^{pH-pH_{SUP}}+10\text{^}(pH_{INF}-pH)}$	4.42	pH_{INF}, pH_{SUP}	[292]
Irradiance	f_{R,I_ML}	$sOPR(T)=sOPR_{MAX}*\left(\frac{DO}{K_{DO}+DO}\right)*\left(1-\frac{DO}{DO_{MAX}}\right)^n$	4.43	DO_{MAX}, n	This work (Monod + Luong model)
	f_{R,I_MS}	$sOPR(T)=sOPR_{MAX}*\left(\frac{DO}{K_{DO}+DO}\right)*\left(1-\frac{1}{1+\left(\frac{K_{DO}}{DO}\right)^H}\right)$	4.44	K_{DO}, H	This work (Monod + Hill model)

Model selection criteria

When applying both the "model calibration protocol" and the "inhibition protocol", two information criteria were used to select for the most appropriate model: the adjusted R-squared (R_{ADJ}^2, Equation 4.22) and the Akaike Information Criterion, corrected for small samples size (AIC_C, Equation 4.23). The R_{ADJ}^2 was used to evaluate how well the compared models explained the experimental data available, while the AIC_C indicator was choosen to evaluate how well each model will be able to fit new data.

$$R_{ADJ}^2 = 1 - \left(\frac{n-1}{n-p}\right) * \frac{SSE}{SST} \quad 4.22$$

$$AIC_C = \frac{SSE}{n} * (1+2*p) + 2*p* \left(\frac{1+p}{n-p-1}\right) \quad 4.23$$

Where: n is the number of experimental observations, p is the number of model parameters, SSE is the sum of squared errors and SST is the sum of squared difference between each datum and the mean value of all data.

4.2.2.1. Statistical methods

In the "monitoring protocol", mean values were calculated for the photosynthetic and nitrifying activities (OPR_{mean}, $OPR_{NIT,mean}$). OPR_1 and the mean value of OPR_2 and OPR_3 were compared by means of heteroscedastic T-tests (computed using data analysis toolbox in Microsoft Office Excel 2016) to exclude the possibility of short-term inhibition effects of ATU and chlorate on MA (section 4.2.1.1).

A principal component analysis (PCA) was also carried out on the results of the monitoring protocol, to evaluate possible qualitative correlations among the algal photosynthetic and respiratory activities and environmental (pH, averaged temperature and irradiance of the four days preceding the photo-respirometric

experiments) or operational parameters (N/P ratio and the concentrations of N-NH_4^+, N-NO_2^-, N-NO_3^-, P_PO_4^{3-}). The PCA was conducted using the software R [294]. In the "inhibition protocol", an unbalanced one-way analysis of variance (ANOVA) was applied to the datasets of experiments performed on microalgae and cyanobacteria, to evaluate statistically significant differences (α = 0.05) between calculated values of inhibition parameters for monocultures and mixed groups (section 4.2.1.3). The software MATLAB R2019b was used for this analysis (Statistics and Machine Learning Toolbox™, function *anova1*).

CHAPTER 5

RESULTS AND DISCUSSION

5. RESULTS AND DISCUSSION

The results obtained using the three proposed protocol in the study are reported in this section.

5.1. Monitoring protocol

In this section, the results obtained by applying the monitoring protocol to each cultivation system described in section 3.2 are discussed. These results are presented with a particular focus on the photosynthesis and respiration rates of phototrophic organisms and the activity of nitrifying bacteria.

5.1.1. Pilot-scale HRAP treating municipal digestate

The photo-respirometric monitoring protocol was applied to monitor the pilot-scale HRAP described in section 3.3.1. The monitoring protocol was applied over two consecutive monitoring campaigns (spring - autumn 2017 and 2018). The most relevant environmental and operational conditions recorded at the pilot plant in the period during which the photo-respirometric assays were conducted are reported in Table 5.1. As suggested by Marazzi et al. [295], average values of the four days preceding the day of test were considered for irradiance and temperature.

Relevant variations of OD_{680} were observed, as a consequence of the changing environmental conditions (Figure 5.1). Similarly, a quite high variability was observed in the oxidized nitrogen forms, though more stable ammonium concentrations were observed. The environmental conditions of the test (temperature and pH) were also variable in some cases, due to the absence of control systems during these experiments, therefore the switch functions

described in section 5.2.1 where applied to compare results. Photo-respirometric tests were performed on the MB suspension after dilution (applied dilution factors: 1:1 - 1:4), to a standardized OD_{680} of 0.4 - 0.6. During these tests, pH and temperature were not controlled. The initial pH was 7.5 and the average temperature during the monitoring tests was 23.3 ± 2.5 °C.

Table 5.1. Environmental conditions and operating parameters in the HRAP in correspondence of the photo-respirometric tests. Values are expressed as mean ± standard deviation.

MONITORING CAMPAIGN	TEST	DATE	OD_{680} [-]	TEMPERATURE [°C]	PAR [μE m^{-2} s^{-1}]	pH [-]	NH_4^+ [mg N L^{-1}]	NO_2^- [mg N L^{-1}]	NO_3^- [mg N L^{-1}]	HRT [d]
I (2017)	1	31/05/17	0.62	24.2 ± 0.9	1910 ± 26	8.1	33.0	10.9	3.1	9.5
	2	14/06/17	0.71	24.8 ± 2.2	1729 ± 235	8.4	80.9	16.4	2.0	9.0
	3	28/06/17	1.05	25.0 ± 2.5	1827 ± 149	7.3	60.9	107.0	12.0	9.5
	4	12/07/17	1.37	25.8 ± 1.7	1753 ± 167	7.1	43.2	109.0	7.1	9.5
	5	26/07/17	1.41	24.9 ± 1.4	1934 ± 119	7.3	65.9	145.0	12.0	9.5
	6	04/08/17	1.68	29.0 ± 1.8	1740 ± 40	7.2	60.9	157.0	12.4	10.0
	7	25/08/17	1.79	24.1 ± 1.4	1721 ± 95	7.6	40.2	146.0	13.2	10.0
II (2018)	1	11/06/2018	1.52	22.8 ± 1.5	1727 ± 317	6.7	78.4	226.5	64.5	20.7
	2	15/06/2018	1.65	22.5 ± 1.4	1572 ± 338	7.1	92.2	207.0	60	11.8
	3	18/06/2018	1.59	23.8 ± 1.1	1928 ± 149	7.8	92.0	214.0	61.5	11.8
	4	22/06/2018	1.67	25.7 ± 0.8	1904 ± 109	6.6	84.2	230.5	59.5	11.8
	5	25/06/2018	1.76	23.6 ± 2.3	1809 ± 94	6.5	97.0	215.0	79.76	11.8
	6	29/06/2018	1.85	23.1 ± 1.0	1973 ± 126	7.0	101.0	165.5	159	11.8
	7	02/07/2018	2.06	25.5 ± 1.5	1934 ± 132	6.0	96.9	12.4	235.8	11.8
	8	06/07/2018	1.67	25.0 ± 1.6	1877 ± 137	6.4	102.0	0.3	274	11.8
	9[a]	09/07/2018	1.66	24.3 ± 1.0	1938 ± 110	5.8	89.7	0.4	265.5	-
	10[a,b]	11/07/2018	-	24.7 ± 1.2	1925 ± 67	3.5	-	-	-	-
	11	13/07/2018	2.13	24.5 ± 1.3	1845 ± 82	6.7	42.0	28.3	363	20.7
	12[c]	16/07/2018	1.96	24.4 ± 1.2	1729 ± 154	6.8	26.5	8.4	282.5	20.7

Notes: a) The HRAP was operated in batch; b) The pH dropped due to technical problems, the characterization of the suspension was not available; c) The influent was a mixture of LFAD (50%) and primary WW (50%).

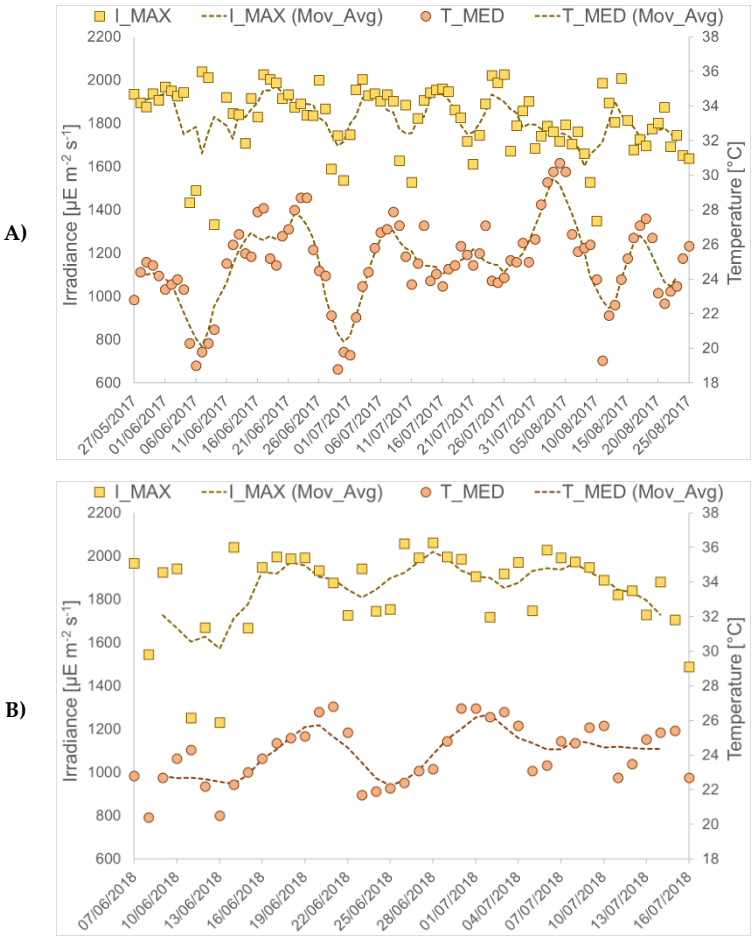

Figure 5.1. Temperature and irradiance during the HRAP monitoring campaigns and their 5-points moving average (A: 2017 monitoring campaign, B: 2018 monitoring campaign).

The sOPRs assessed by respirometric tests are summarized in Figure 5.2. As for the MA, $sOPR_{mean}$ are reported together with the standard deviation on the three measurements (i.e. computed from OPR_1, OPR_2, OPR_3). A very satisfactory reproducibility was obtained, with an average coefficient of variation (CV) of 7.8%.

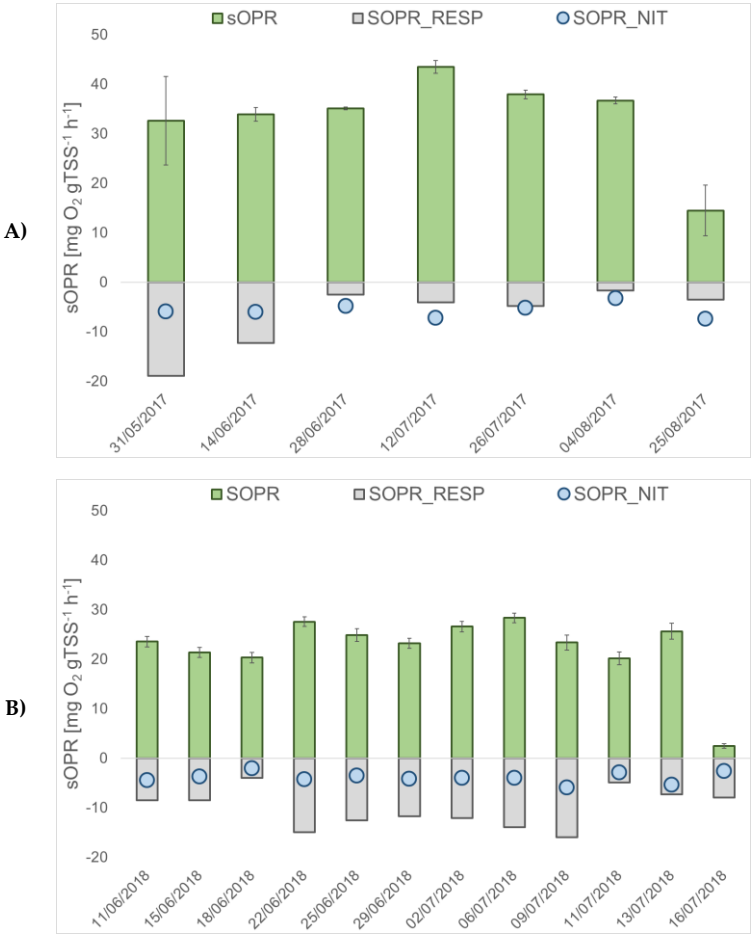

Figure 5.2. Microalgae and bacteria activities measured during monitoring tests: comparison between specific OPR by microalgal photosynthesis (sOPR), microalgal respiration ($sOPR_{RESP}$) and nitrification ($sOPR_{NIT}$) during the two monitoring campaigns (A: 2017 monitoring campaign, B: 2018 monitoring campaign)

Apart from three tests, in which the CV was higher than 20% probably due to a particularly unstable phototrophic activity or to minimal differences in the sampling time, the average CV computed on the remaining tests was 4.1 ± 1.6%, indicating a very good reproducibility for the assessment of photosynthesis using the monitoring protocol.

The precision obtained for this method is similar to that calculated by Rozzi et al. [134] for determining microalgal photosynthetic rates, where values of 2.8 – 7.6% were obtained during repeatability tests. An average CV of 8 - 10% was observed by Rozzi et al. [296] while applying respirometric tests on heterotrophic bacteria in activated sludge samples, using three different respirometric protocols. Results are also consistent with the study of Ricco et al. [297], in which coefficient of variation of 2 - 10% where determined during toxicity assessments for xenobiotic compounds in a closed respirometer.

As depicted in Figure 5.2, the specific oxygen production was quite constant during the two monitoring periods, with specific OPRs ranging from approximately 20 - 45 mg O2 g TSS^{-1} L^{-1}. A significant decrease in activity was recorded in the last monitoring tests of both campaigns. In the first case (Figure 5.2A), the test was executed at the end of the summer, when the outdoor irradiance and temperature were lower than in July and August, thus justifying a lower OPR. During the second monitoring campaign (Figure 5.2B), the lower sOPR recorded during the last test could be attributed to a generally low activity of the biomass, as in that period the HRAP was subject to malfunctioning in the feeding system and the HRAP was operated in batch for a few days. The volumetric OPR of microalgae during light phases was 10 - 25 mg O_2 L^{-1} h^{-1}, similar to that obtained by Decostere et al. [139]. Results are also consistent with that obtained for *Chlorella vulgaris* by Tang et al. [144], under similar conditions. In general terms, during the 2017 monitoring campaign a slightly higher photosynthetic sOPR was assessed if compared to 2018, possibly due to the pH values recorded during the two experimental periods. Indeed, during the 2017 monitoring campaign, the average pH value measured in the HRAP was 7.7 ± 0.5, which is in the range of the typical optimal pH values for phototrophs [53], [181]. On the contrary, during the 2018 photo-respirometric campaign, the average pH was 6.7 ± 0.4, thus resulting in lower activity at the pH value

maintained during photo-respirometric assays. Another difference between the two datasets is represented by the temperature (sligthly higher during the 2017 monitoring campaign), which may have contributed to the differences found. The photosynthetic activity of MA detected by the respirometric assay could not be directly linked to any calculated parameter in the open pond. Indeed, the variation rate of the biomass concentration (expressed as TSS or VSS) or turbidity are not appropriate indicators of the algal biomass alone, due to the fact that the apportioning among the algal and bacterial populations is expected to be higly dynamic over time. On the contrary, the rate of variation of OD_{680} deriving from the application of a mass balance to the cultivation PBR (rOD_{680}, calculated according to Equation 2.3) is directly related to the concentration of microalgal biomass, since it represents an indirect measure of the chlorophill content, provided that no relevant changes in the pigment composition of the cell occur [298]. The comparison of the obtained data with the rOD_{680} (Figure 5.3) suggests that the protocol is a reliable tool to follow the evolution of microalgae activity in the HRAP. The few discrepancies with experimental data could be justified by the fact that the microalgae growth rate in the raceway is assessed across a period of 3 - 7 days, while the OPR value is an instantaneous response under reference conditions, therefore discrepancies are expected, especially during highly dynamic periods.

The specific oxygen consumption during dark phases ($sOPR_{RESP}$), representing the light respiration of microalgae, varied significantly over time (2 – 19 mg O_2 g TSS^{-1} h^{-1}). During the first two tests of the 2017 monitoring campaign, some of the highest results were recorded. Later, microalgal dark respiration decreased, reaching stable values of approximately 2 - 5 mg O_2 g TSS^{-1} h^{-1}. The latter interval is coherent with the values obtained by Ruiz-Martinez et al. [299].

The initial higher respiratory activity the first two tests might be explained with a fast microalgal growth, resulting in an increased energy requirement, as suggested by Kliphuis et al. [153]. Respiration rates higher than 10 mg O_2 g TSS^{-1} h^{-1} were also recorded during the central phase of the 2018 monitoring campaign (22/06/2018 - 09/07/2018). This could be associated to a generally higher activity, as the sOPR was also slightly higher in this period, possibly due to particularly favorable weather conditions (Figure 5.3). When evaluating respiratory activities, it should be considered that algal respiration may also include heterotrophic oxygen uptake, although its contribution to the overall oxygen consumption is not expected to be relevant because of the recalcitrant nature of the organic matter in the LFAD, that was used to feed the raceway.

The sOPR recorded for nitrifiers during the 2017 and 2018 monitoring campaigns are reported in Figure 5.3C and Figure 5.3D. Results suggests that the activity of nitrifying bacteria was substantially stable in the HRAP in both the experimental periods (5.7 ± 1.3 and 3.9 ± 1.0 mg O_2 $gTSS^{-1}$ h^{-1}, obtained during the first and second monitoring campaigns, respectively). This is also in agreement with the stable concentration of NO_X (NO_2^- + NO_3^-) measured in the HRAP (see Table 5.1). From the NO_X concentration trend assessed in the HRAP, and assuming a conventional stoichiometric DO request for nitrification, the OUR by nitrifiers could be estimated and compared to the volumetric oxygen uptake rate evaluated with the photo-respirometric assay (see Equations 2.3 - 2.6). The nitrifying OUR detected with photo-respirometry (Figure 5.3C and Figure 5.3D) seemed to be very well correlated to the estimated average level of DO uptake rate by nitrifiers, both for the 2017 and 2018 monitoring campaigns. Only the first OUR value was slightly negative in the first test of the 2017 monitoring campaign, indicating that the nitrifying activity was scarce and the quite low DO consumption was poorly detected with the procedure.

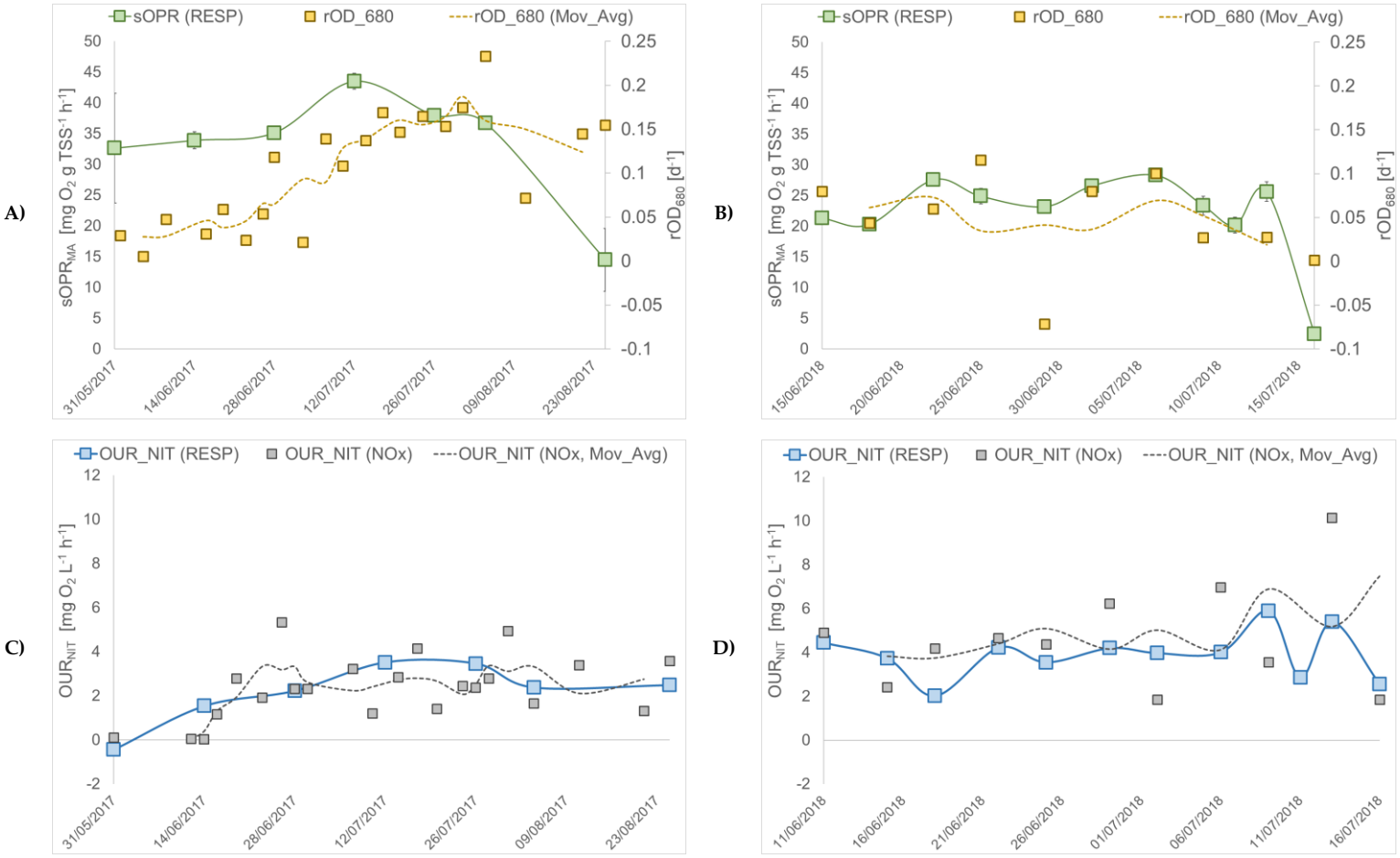

Figure 5.3. Microalgae and bacteria activities measured during monitoring tests: A,C)) Comparison between microalgae OPR rates calculated by photo-respirometric tests (OPR (RESP)), rate of variation of the optical density at 680 nm (rOD_{680}) and its 3-points moving average (rOD_{680},Mov_Avg) (A: 2017 monitoring campaign, C: 2018 monitoring campaign); B, D) Comparison between nitrification rates calculated by photo-respirometric tests (OUR_{NIT} (RESP)), monitoring data (OUR_{NIT} (NO_X)) and its 3-points moving average OUR_{NIT} (NO_X,Mov_Avg) (B: 2017 monitoring campaign, D: 2018 monitoring campaign).

It is also interesting to notice that, during the 2018 monitoring campaign, a stable nitrification only occurred after July, but this process could not be completely described using the photo-respirometric procedure. Indeed, the analysis of the NO_X concentrations indicate that only partial nitrification took place during the first part of the experimentation, while the complete oxidation to NO_3^- was achieved in the HRAP until the end of the monitoring campaign. As previously mentioned (section 4.1.5.2), during the monitoring protocol, the inhibition of AOB is achieved by dosing ATU, while NOB activity is not detected, due to the fact that this population was not inhibited during the test. However, both the OUR_{NIT} calculated from r_{NIT} and from the photo-respirometric procedure are consistent, suggesting that the OUR by NOB did not have a large influence on the overall oxygen demand. This is coherent with the low NOB concentrations that are expected in these kind of treatment systems [300]. These results suggest that a more exhaustive characterization of nitrification processes taking place in microalgae-bacteria systems should be carried out, possibly also exploiting molecular tools. FISH analyses performed on samples from the 2018 monitoring campaign also confirmed a stable occurrence of AOB in the MB suspensions (Figure 5.4).

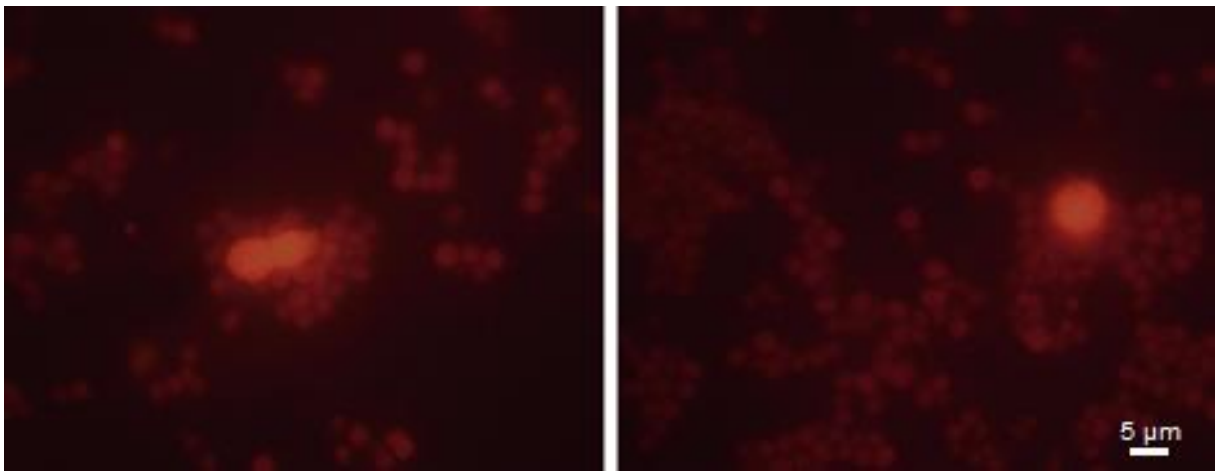

Figure 5.4. Results of the FISH analysis: microalgae (dark red) and AOB colonies (light red) observed in samples collected from the HRAP using a fluorescent microscope.

5.1.2. Pilot-scale bubble-column treating municipal digestate

The monitoring protocol was applied to the bubble-column described in section 3.3.2, treating the effluent of the HRAP described in the previous section 5.1.1. The monitoring protocol was applied in four different tests conducted in duplicate during the period October - November 2019. During this period, the column was contaminated by cyanobacteria, whose development was probably favored by environmental conditions that were less favorable to microalgae. Indeed, higher thermal excursions could be calculated in the bubble-column (13 °C on average), while lower variations were obtained in the HRAP (8.3 °C), during the monitoring campaign of the two reactors (July - August 2019). This may have contributed to the proliferation of cyanobacteria, due to their higher capacity of adapting at both low and high temperatures, by regulating the inernal pigment contents or their carbon fixation mechanisms [301].

The results of the monitoring protocol applied to the bubble-column treating the effluent of the HRAP are reported in Figure 5.6. As can be observed, the photosynthetic sOPR reached values of approximately 12 - 24 mg O_2 g TSS^{-1} h^{-1}. The sOPR determined during the first test was slightly higher than the other tests, possibly due to the fact that the environmental conditions a declined during the following tests, especially in terms of light availability. In general terms, the photosynthetic activity was lower than the values obtained in the HRAP during the monitoring described before. A lower photosynthetic activity in the bubble-column was indeed expected, due to the fact that the column was fed using the effluent of the HRAP as nutrient source, where the ammonium initially present in the influent LFAD was mostly oxidized to nitrate and/or nitrite. The variability of the microalgal sOPR was comparable with the results reported in the previous section 5.1.1. Indeed, the CV obtained for this series of experiments ranged from 1.7 - 10.0% (4.5 ± 2.7%, on average).

The specific respiration rates were also coherently lower, with values in the range 2 - 3 mg O_2 $gTSS^{-1}$ h^{-1}. However, a slightly lower respiration rate was obtained, compared to the photosynthetic rate. In the bubble-column, the $sOPR_{RESP}$/sOPR ratio was on average 17 ± 7%, compared to an average value of 34 ± 19% obtained in the HRAP during the previous monitoring campaigns. Since cyanobacteria were the dominant population of the bubble-column, these findings are consinstent with Geider and Osborne [136], in which lower respiration to photosynthesis ratios for cyanobacteria compared to green algae (*chlorophyceae*) were suggested. However, it should be also noticed that different respiration to photosynthesis ratios might be also connected to the different environmental conditions, since the monitoring campaign of the bubble-column was conducted during autumn while the HRAP was monitored through photo-respirometry during the summer period.

Regarding the bacterial activity measured in the column, nitrification could be detected at a very low rate. Indeed, the DO uptake rate of nitrifying activity were always in the range 0.3 - 0.6 mg O_2 $gTSS^{-1}$ h^{-1}., corresponding to an average volumetric rate always lower than 0.1 mg O_2 L^{-1} h^{-1}. A very low activity was expected in this case, due to the fact that the main nitrogen source was represented by oxidized nitrogen (nitrate), and the ammonium concentration was quite low (see Table 3.2). Indeed, the nitrification rates calculated from the trend of NO_X compounds yielded an average value of approximately 0.05 mg O_2 L^{-1} h^{-1}.

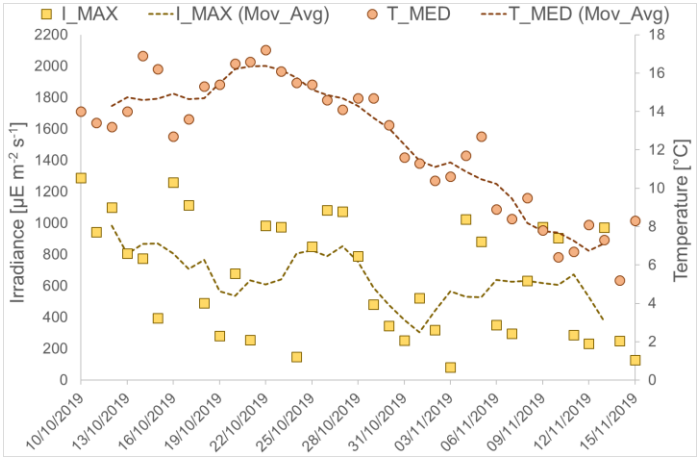

Figure 5.5. Temperature and irradiance during the HRAP monitoring campaigns and their 5-points moving average (A: 2017 monitoring campaign, B: 2018 monitoring campaign).

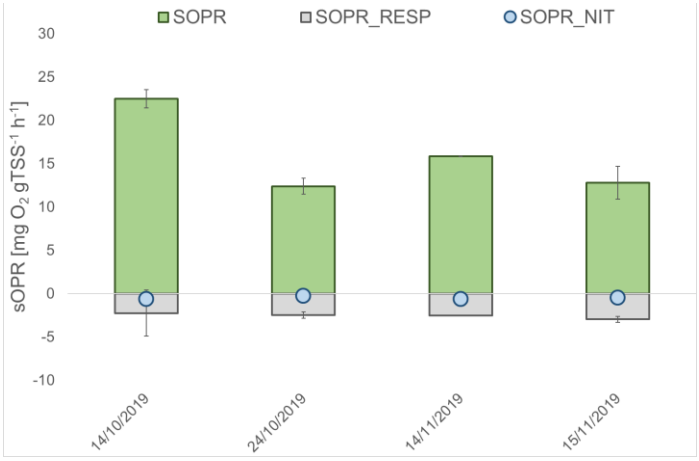

Figure 5.6. Microalgae and bacteria activities measured during monitoring tests performed on the pilot-scale bubble-column: comparison between specific OPR by microalgal photosynthesis (sOPR), microalgal respiration ($sOPR_{RESP}$) and nitrification ($sOPR_{NIT}$).

5.1.3. Pilot-scale bubble-column treating agricultural digestate

The photo-respirometric monitoring protocol was on the suspensions sampled from the pilot-scale bubble-column described in section 3.3.3. In this case, the experiments were conducted during three consecutive days, in two different periods corresponding to different atmospheric conditions (autumn and winter conditions).

The specific photosynthetic activity obtained with the suspension growing on agro-industrial LFAD was on average 33.7 ± 2.1 mg O_2 g TSS^{-1} h^{-1} during autumn and 12.9 ± 2.0 mg O_2 g TSS^{-1} h^{-1} during the winter period. The photosynthetic activity of the consortium was very low during the winter, as a consequence of the poor environmental conditions and despite the higher HRT imposed during this season to increase the removal efficiency of the system (approximately 15 days, compared to the average HRT of 10 days maintained during autumn). It should be noticed that during these tests, the biomass was acclimated for only 30 minutes prior to the execution of the experiments, and the lack of adaptation could have led to the differences found, again highlighting the importance of acclimation phase.The obtained volumetric rates (9.5 ± 0.8 mg O_2 L^{-1} h^{-1} and 4.9 ± 0.6 mg O_2 L^{-1} h^{-1},during autumn and winter, respectively) were however comparable to the results obtained by Decostere et al. [139], [182], in which the gross OPR was found to be lower than 10.4 mg O_2 L^{-1} h^{-1}. Also in these experiments, the variability found for the determination of the microalgal sOPR was quite low (7.3 ± 3.6%, on average), thus confirming the adequacy of the experimental protocols.

In the pilot-scale bubble-column systems, the nitrifying activity was present at a higher level compared to the algae-bacteria reactors previously shown (2.8 - 8.2 mg O_2 g TSS^{-1} h^{-1}, or 0.8 - 3.1 mg O_2 L^{-1} h^{-1}). The presence of such a nitrifying activity in the algal-bacterial community of the pilot-scale column was confirmed

by the presence of oxidized nitrogen forms (both as nitrite and nitrate) in the suspension. Indeed, the nitrifying activity was in the range 0.7 - 6.1 mg O_2 L^{-1} h^{-1} and 1.8 - 4.5 mg O_2 L^{-1} h^{-1} respectively during autumn and winter.

Results about algal respiration during the dark phases (4.3 - 5.9 mg O_2 g TSS^{-1} h^{-1}) were very similar to those obtained in the previous experiments. Microalgal dark respiration rates were also coherent with those indicated by Ruiz-Martinez et al. [299] (0.9 - 5.1 mg O_2 $gTSS^{-1}$ h^{-1}).

Table 5.2. Environmental conditions and operating parameters in the pilot-scale bubble-column in correspondence of the photo-respirometric tests. Values are expressed as mean ± standard deviation.

PERIOD	TEST	DATE	OD_{680} [-]	TEMPERATURE [°C]	PAR [μE m^{-2} s^{-1}]	NH_4^+ [mg N L^{-1}]	NO_2^- [mg N L^{-1}]	NO_3^- [mg N L^{-1}]	HRT [d]
Autumn 2016	1	07/09/2016	0.37	24.8 ± 1.4	1586 ± 117	19.9	182.0	20.6	10
	2	08/09/2016	0.38	24.5 ± 1.1	1592 ± 115	21.3	179.8	19.6	10
	3	09/09/2016	0.32	24.4 ± 1.0	1618 ± 68	17.7	181.2	22.8	10
Winter 2017	1	22/02/2017	0.58	6.1 ± 0.6	890 ± 274	3.3	0.5	325.5	15
	2[a]	23/02/2017	-	6.0 ± 0.3	750 ± 331	-	-	-	15
	3	24/02/2017	0.97	6.8 ± 1.8	634 ± 284	6.9	0.0	302.1	15

Notes: a) The characterization of the suspension was not available

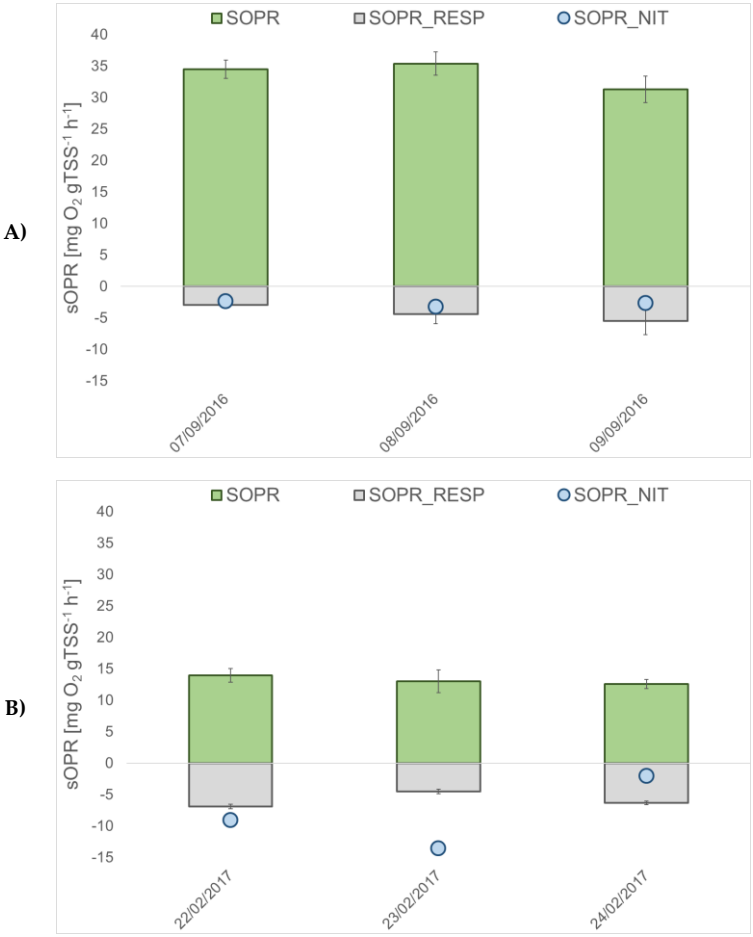

Figure 5.7. Microalgae and bacteria activities measured during monitoring tests performed on the pilot-scale bubble-column: comparison between specific OPR by microalgal photosynthesis (sOPR), microalgal respiration ($sOPR_{RESP}$) and nitrification ($sOPR_{NIT}$) during two series of tests (A: autumn 2016, B: winter 2017).

5.1.4. Lab-scale PBRs treating agricultural digestate

The monitoring protocol was applied in triplicate to the lab-scale photobioreactors described in section 3.3.4, fed on agricultural digestate as previously described.

The sOPR obtained for the microalgae-bacteria consortium developed in the lab-system was on average 12.3 ± 1.9 mg O_2 g TSS^{-1} h^{-1} (5.1 ± 0.8 mg O_2 L^{-1} h^{-1}), very similar to that obtained in the pilot-scale column previously described (section 5.1.3), as expected due to the similar composition of the LFAD used to grow the

algae-bacteria consortia. Similarly to what found previously, the calculated CV was on average 7.8 ± 5.6%, with a maximum value of 14.2%.

The nitrifying activity (5.4 mg O_2 g TSS^{-1} h^{-1}) was similar to that obtained in the HRAP treating LFAD from a municipal source and slightly lower to that obtained in the pilot-scale bubble-column treating a similar wastewater. Compared to the results obtained for the pilot-scale system treating the same influent, however, a lower variability was found coherently with the higher variability in the environmental conditions in the outdoor column.

Results about algal respiration during the dark phases (OPR_{RESP}) were very similar to those obtained in the experiments on the pilot system (4.1 ± 0.9 mg O_2 g TSS^{-1} h^{-1}). As previously mentioned, the endogenous respiration of heterotrophic biomass cannot be computed, and it is eventually embedded in the measurement of the $OPR_{RESP.}$

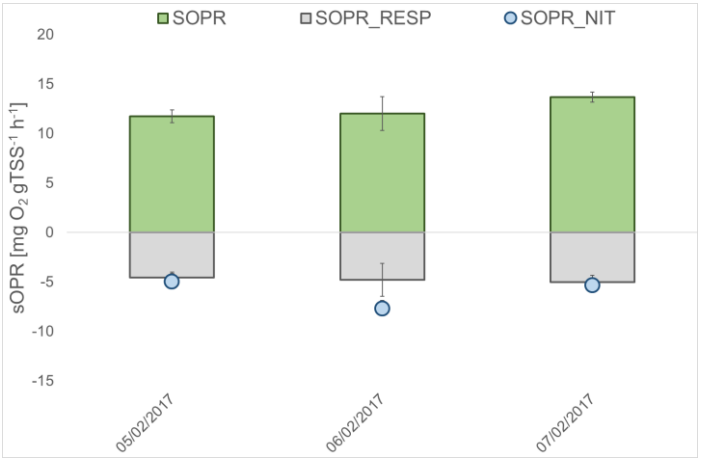

Figure 5.8. Microalgae and bacteria activities measured during monitoring tests performed on lab-scale PBRs: comparison between specific OPR by microalgal photosynthesis (sOPR), microalgal respiration ($sOPR_{RESP}$) and nitrification ($sOPR_{NIT}$) during two series of tests.

5.1.5. Demonstrative-scale semi-closed PBRs treating agricultural runoff

A further validation of the monitoring protocol was carried out in the set of semi-closed PBRs described in section 3.4.1 that were operated for more than one year (may 2017 - December 2018) to treat water from agricultural runoff. The photo-respirometric monitoring campaign had a duration of three months (September - December 2018) and the samples were analyzed weekly, following the photo-respirometric monitoring protocol. Also in this case, the switch functions obtained with the model calibration protocol were applied to allow for results comparison (see section 5.2).

The environmental conditions recorded during the photo-respirometric monitoring are reported in Figure 5.9. The overall trends of sOPR, $sOPR_{RESP}$ and $sOPR_{NIT}$ are reported in Figure 5.10 for the entire photo-respirometry monitoring period. In general terms, the sOPRs due to photosynthesis and respiration by cyanobacteria in the semi-closed PBR 1 were much lower than the results obtained with the other two PBRs. This was probably due to the fact that cyanobacteria aggregates in PBR 1 had a very compact structure, resulting in lower specific rates due to the flocculent nature of the TSS. In addition, in the first PBR no additional inorganic carbon was provided, while it was dosed in the other two reactors, possibly contributing to the higher rates measured. However, the specific OPR by phototrophs in all semi-closed PBRs were always in the range 0.8 - 5.5 mg O_2 g TSS^{-1} h^{-1} (Figure 5.10), thus being lower than the values obtained for all other systems. This is partially explained by the fact that the PBRs were fed using a wastewater with very low nutrient concentrations (see section 3.4.1), therefore a low activity was expected in all PBRs. In addition, the environmental conditions were suboptimal, due to the fact that the experiments were carried out during the autumn, when temperature and irradiance rapidly tended to very low values (Figure 5.9). In this viewpoint, it seems counter-intuitive to see that,

despite the large variations in the temperature and irradiance values, no particular decrease was recorded in the phototrophic activity. On the contrary, the trend of photosynthetic and respiratory processes seem to increase over time. These phenomena can be possibly explained by the fact that the biomass was acclimated to test conditions for at least 45 minutes, and the tests always took place at physiological temperatures. It is also possible to speculate on the fact that the increasing trend in the phototrophic activity may be due to the fact that the light intensity in the lab was kept constant at a non-saturating level, while the outdoor irradiance gradually tended to this value, possibly producing the observed effect. However, a better comprehension of acclimation processes is required to better ascertain this aspect. Regarding the variability of experimental sOPR determinations, the overall CVs (by considering the entire dataset, thus including the three semi-closed PBRs) was similar to that of previous systems (8.3 ± 4.7%, on average). The variabilities were also very similar among the three PBRs (7.5 ± 4.7%, 8.8 ± 5.2% and 8.7 ± 4.7%, for the first, second and third PBRs, respectively).

The nitrifying activity was almost absent in all cases, with maximum values of oxygen uptake rates of approximately 0.5, 1.2 and 1.3 mg O_2 g TSS^{-1} h^{-1} in PBR 1, PBR 2, and PBR 3, respectively. The absence of nitrification was indeed expected, as the system was fed on nitrate as nitrogen source. The slightly higher nitrifying activity in the second and third PBRs can be associated to the fact that inorganic carbon was added to PBR 2 and PBR 3, possibly resulting in non-limited carbon availability for nitrifiers.

The respiration of phototrophic organisms during dark phases was substantially stable and correlated with the specific OPR by phototrophs. During dark phases, the specific oxygen consumption was in the range of 0.6 - 1.2 mg O_2 g TSS^{-1} h^{-1}, 1.0 - 3.2 mg O_2 g TSS^{-1} h^{-1} and 1.0 - 3.4 mg O_2 g TSS^{-1} h^{-1} for PBR 1, PBR 2, and PBR 3, respectively. These results are similar to those obtained with the other systems

described and unexpectedly high, considered low photosynthetic rates measured during the experimentation. Indeed, respiration to photosynthesis ratios for the three PBRs were on average 61.8 ± 10.0%, 67.6 ± 6.3% and 80.5 ± 2.9%. These were the highest found in the entire dataset; possibly, the increased respiratory activities were associated to stressing operational conditions applied, namely the nutrient deprivation for stimulating the accumulation of bio-polymers in the biomass.

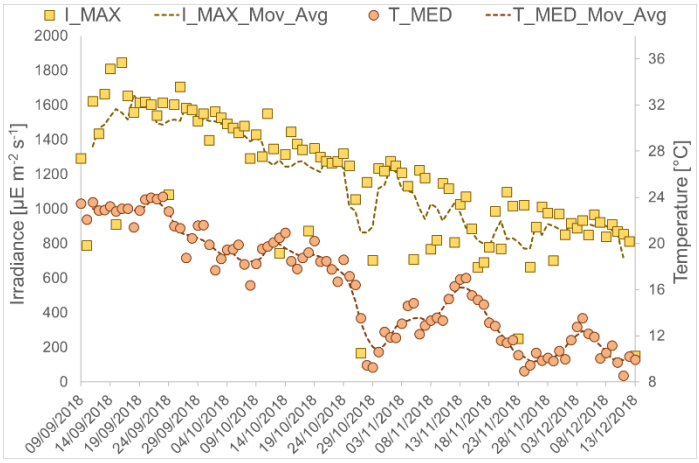

Figure 5.9. Temperature, irradiance and their 5-days moving average during the monitoring campaign of the demonstrative-scale PBRs.

Table 5.3. Environmental conditions and operating parameters in the demonstrative-scale semi-closed PBRs in correspondence of the photo-respirometric tests. Values are expressed as mean ± standard deviation.

DATE	TEMPERATURE	PAR	pH[a] [-]			NH_4^{+a} [mg N L^{-1}]			NO_3^{-a} [mg N L^{-1}]		
	[°C]	[µE m^{-2} s^{-1}]	PBR_1	PBR_2	PBR_3	PBR_1	PBR_2	PBR_3	PBR_1	PBR_2	PBR_3
13/09/2018	23.0 ± 0.6	1360 ± 352	9.5	7.8	7.8	0.6	0.1	0.0	1.8	0.0	1.5
19/09/2018	22.6 ± 0.7	1516 ± 356	9.0	8.0	8.0	0.5	0.4	0.3	2.4	0.0	0.0
26/09/2018	22.7 ± 1.3	1509 ± 245	8.0	9.1	9.1	0.2	0.3	0.2	0.0	0.0	7.8
03/10/2018	19.9 ± 1.7	1509 ± 66	9.2	9.0	8.2	0.4	0.0	0.4	0.0	-	-
10/10/2018	18.5 ± 1.4	1390 ± 85	9.2	8.7	8.4	0.2	0.3	0.0	3.7	1.6	0.0
17/10/2018	19.3 ± 1.3	1244 ± 284	9.2	-	8.3	0.0	-	0.3	19.6	0.0	0.0
18/10/2018[b]	19.1 ± 1.2	1271 ± 227	-	-	-	-	-	-	-	-	-
24/10/2018	18.0 ± 0.8	1288 ± 22	8.2	8.5	8.4	-	-	-	-	-	-
01/11/2018	10.7 ± 1.4	1118 ± 235	-	8.3	8.4	0.0	2.4	0.0	3.4	1.8	0.0
07/11/2018	13.5 ± 1.2	1091 ± 216	8.4	8.3	8.5	0.3	1.1	0.0	4.0	1.7	0.0
14/11/2018	15.8 ± 1.5	1034 ± 135	8.0	8.1	8.4	0.1	0.0	0.0	0.0	0.0	0.0
21/11/2018	12.8 ± 1.3	865 ± 170	8.1	8.1	8.5	0.3	0.0	0.0	2.1	0.0	0.0
28/11/2018	9.8 ± 0.6	914 ± 149	8.1	-	8.2	0.1	-	0.0	1.7	0.0	0.0
05/12/2018	12.0 ± 1.3	888 ± 38	8.1	8.1	8.2	0.3	0.0	0.0	0.0	0.0	0.0
13/12/2018	9.9 ± 0.9	720 ± 320	8.0	7.8	7.9	2.9	0.0	0.0	0.0	0.0	0.0

Notes: a) The analyses are referred to the day before, b) The characterization of the suspension was not available

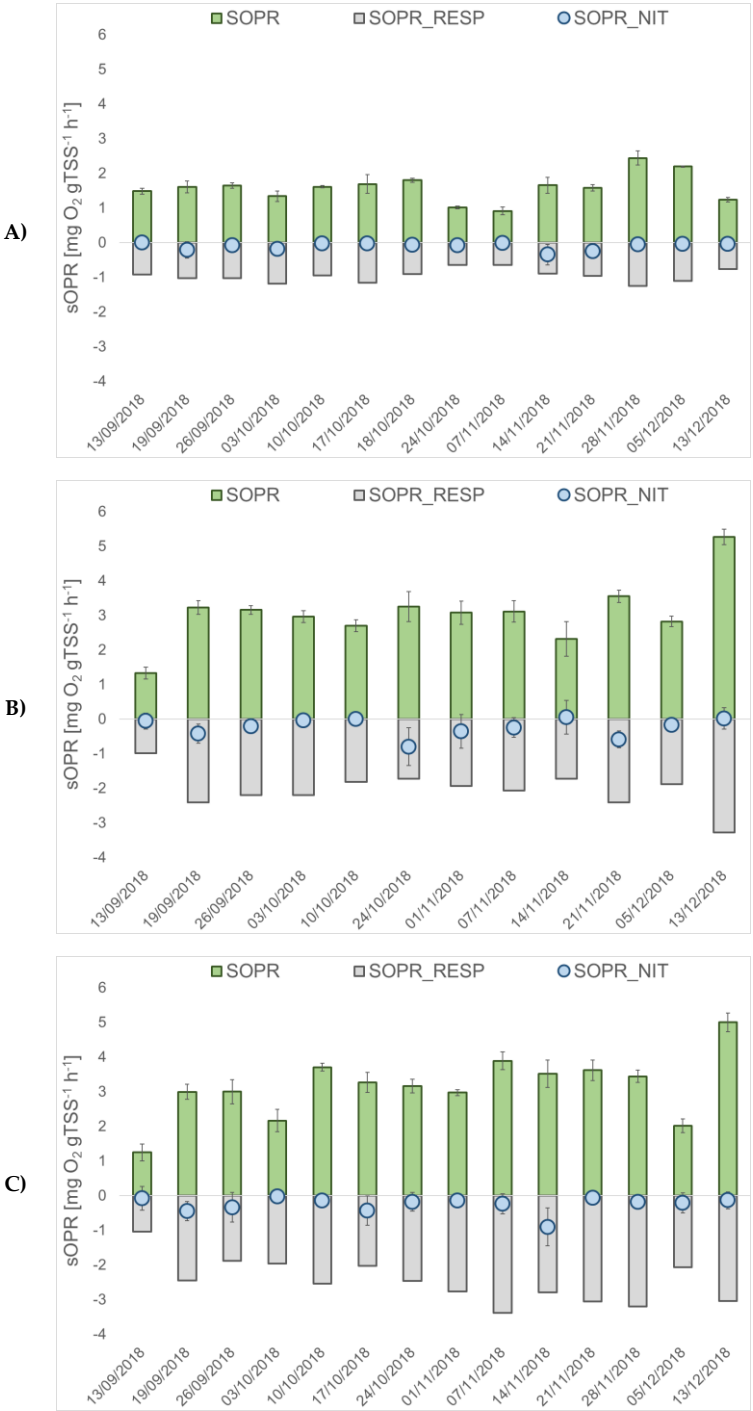

Figure 5.10. Microalgae and bacteria activities measured during monitoring tests performed on the demonstrative-scale semi-closed PBRs: comparison between specific OPR by microalgal photosynthesis (sOPR), microalgal respiration ($sOPR_{RESP}$) and nitrification ($sOPR_{NIT}$) (A: Semi-closed PBR 1, B: Semi-closed PBR 2, C: Semi-closed PBR 3).

5.1.6. Lab-scale PBRs treating aquaculture and piggery wastewaters

The monitoring protocol was applied to monitor the biological activity in a lab-scale system in which both aquaculture and piggery wastewaters were used as nutrient sources. During these experimentations, the cultivation system described in section 3.4.2 was used.

The green alga *T.Suecica* was grown to treat aquaculture wastewaters. The monitoring protocol was applied in three single tests performed in duplicate. The sOPR, $sOPR_{RESP}$ and $sOPR_{NIT}$ trends are reported in Figure 5.11. The photosynthetic sOPRs were in the range 20 - 35 mg O_2 g TSS^{-1} h^{-1}, similar to the values obtained with the other pilot-scale systems presented. The volumetric activities obtained, ranging from 10 - 16 mg O_2 L^1 h^{-1}, are also comparable with those previously obtained by other authors [232], [302]. In this set of experiments, the variability of sOPR determinations among different phases was slightly lower than in the other systems tested, although a very similar CV was found (6.1 ± 3.5%, on average). The different values of the average sOPRs obtained among the different tests can be explained by the different OD_{680} values. Indeed, the highest sOPR was obtained during the second experiment and the correspondent OD_{680} was slightly lower in this test (0.51) than in the other two tests (0.61 and 0.65, on average). This result further highlights the importance of performing the photo-respirometric activity assessment under standardized conditions, especially in terms of light availability.

The nitrifying activity was present, although very low values were recorded (0.5 - 0.8 mg O_2 g TSS^{-1} h^{-1}), coherently with the fact that almost negligible ammonium concentration were present in the feed (Table 3.5), and nitrate was supplemented in order to adjust the N:P ratio of the influent wastewater.

The algal respiration was in the range 6.4 - 8.9 mg O_2 g TSS^{-1} h^{-1}, with a respiration to photosynthesis ratios of 29.7 ± 4.0%, in line with the other systems tested.

During another experimental phase, the lab-scale cultivation system was finally applied to two different microalgae-bacteria consortia fed on the pre-treated piggery wastewater described in Table 3.6. As previously mentioned, a control PBR was only inoculated with a microalgae-bacteria suspension (Reactor A) while a second PBR was also inoculated with filamentous green algae (Reactor B), as described in section 3.4.2. The monitoring protocol was applied to the cultivation system for approximately one month (10/11/17 - 06/12/17). During the cultivation the pH was set to 7.5 by bubbling CO_2, although some failures of the pH-control system allowed the pH to vary between 6.8 - 9.8.

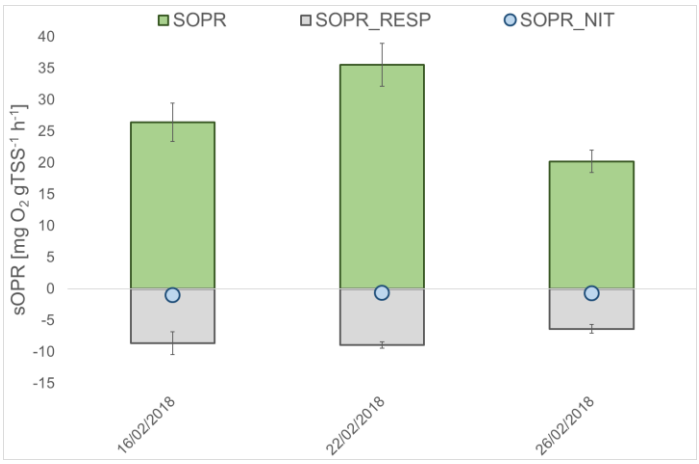

Figure 5.11. Microalgae and bacteria activities measured during monitoring tests performed on the lab-scale PBRs treating aquaculture wastewater: comparison between specific OPR by microalgal photosynthesis (sOPR), microalgal respiration ($sOPR_{RESP}$) and nitrification ($sOPR_{NIT}$).

The cultivation temperature was on average 30.0 ± 0.5°C. During the execution of these photo-respirometric monitoring campaigns, samples were not adapted to light and the tests were performed within approximately 5 - 15 minutes after

the sample dilution, which can explain part of the variability of the results presented below.

The photosynthetic and respiratory rates and the nitrifying activities measured during the monitoring protocol are summarized in Figure 5.12. The specific oxygen production varied widely during the monitoring tests. Indeed, the specific OPR varied within 2.7 - 16.0 mg O_2 g TSS^{-1} h^{-1} in the microalgae-bacteria control reactor and between 4.6 - 20.0 mg O_2 g TSS^{-1} h^{-1} in the PBR contaminated with filamentous green algae.

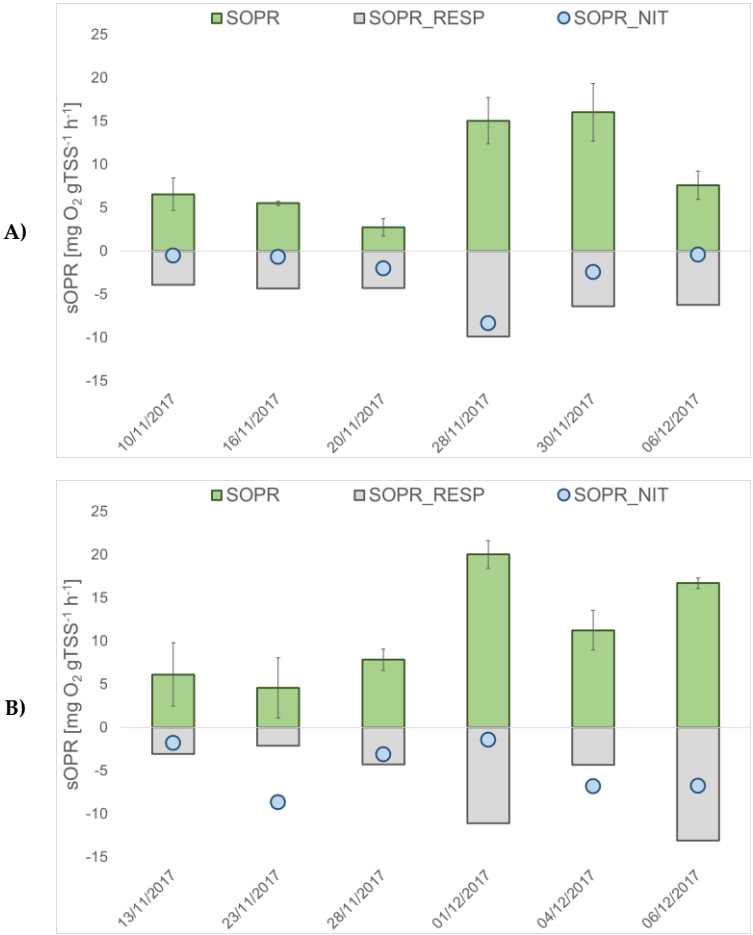

Figure 5.12. Microalgae and bacteria activities measured during monitoring tests: comparison between specific OPR by microalgal photosynthesis (sOPR), microalgal respiration ($sOPR_{RESP}$) and nitrification ($sOPR_{NIT}$) in a microalgae-bacteria consoritum (A) and in a microalgae-bacteria consortium contaminated with filamentous green algae (B).

The photosynthetic activity was particularly low during the first three tests, as a consequence of the higher pH reached in both reactors. On the contrary, during the last three tests, the pH control worked properly and the sOPR consequently increased. A large variability could be found among the different determinations (CV = 26.2 ± 22.0%, on average). This variability was the highest recorded among all the samples, again highlighting the importance of the sample acclimation in the photo-respirometric activity assessment.

During the dark phases of the monitoring protocol, the $sOPR_{RESP}$ varied proportionally to sOPR. During the first three tests, respiration rates were lower than 5 mg O_2 $gTSS^{-1}$ h^{-1}, comparable to the rates obtained in this work and in Ruiz-Martinez et al. [299]. During the last three tests, the respiration rates increased with the same trend of the photosynthetic rate. The respiration to photosynthesis ratio was high during the whole experimentation and strongly varying over time, probably due to the absence of light acclimation or the stress induced by high pH in the cultivation reactor. Indeed, the $sOPR_{RESP}$ to sOPR ratio was on average 80.3 ± 40.2% in the control reactor and 53.8 ± 13.5% in the filamentous-contaminated reactor.

The nitrifying oxygen consumption rates ranged from 0.4 - 8.3 mg O_2 $gTSS^{-1}$ h^{-1} in the control reactor and 1.5 - 8.7 mg O_2 $gTSS^{-1}$ h^{-1} in the other reactor. Nitrification seemed to only occur sporadically in the control reactor, while an almost stable nitrification rate was recorded in the reactor contaminated with filamentous algae, starting from the second test. The higher nitrifying activity could be due to the fact that the inoculum of the reactor also contained filamentous algae sampled from algal biofilm, possibly containing a higher concentration of nitrifying bacteria. The comparison of average volumetric OPRs obtained for nitrifiers through the photo-respirometric protocol were almost the same as those calculated with the conventional stoichiometry. Indeed, the

averaged volumetric nitrification rate obtained experimentally was 1.8 ± 1.6 mg O_2 L^{-1} h^{-1}, while the rate calculated from NO_X variation was on average 1.9 ± 1.3 mg O_2 L^{-1} h^{-1}, again confirming that the defined protocol is higly suitable for the simultaneous determination of algal and nitrifying activities.

5.1.7. Results and discussion

In this section, results obtained with the monitoring protocol are discussed. Table 5.4 reports a comparison with literature works performed in similar microalgae-bacteria systems. Although many studies reported the presence of nitrifiers in algae-bacteria consortia [79], [233], only a few studies provided direct estimations of bacterial rates in systems fed with real wastewaters [240], [245], [247]. However, among these studies the measurement units are not always consistent with those adopted in this work. In addition, most of the available nitrification data in algae-bacteria systems were based on the analysis of growth curves [79] or NO_X production rates [235], hindering a direct comparison. Results presented in this section shows that the highest nitrifying activities were measured in bioremediation of piggery wastewaters (both pre-treated wastewater and LFAD), followed by the LFAD from municipal sources, due to the higher ammonium loading rates applied in these systems compared to the others. On the contrary, the samples from the bubble-column treating the effluent of the HRAP, the lab-scale system treating aquaculture wastewaters and the demonstrative scale system treating agricultural runoff showed almost no nitrifying activity, as expected due to the low-strength ammonium influent. When analyzing data obtained for algae-bacteria consortia treating high-strength wastewaters, a direct correlation between photosynthesis and nitrification rates was found (Figure 5.14), suggesting that the conditions promoting the growth of

phototrophs in microalgae-bacteria systems are well suitable for nitrifying bacteria too.

According to the results obtained for the photosynthetic oxygen production rate, this was higher than the nitrifying bacteria DO request in almost all cases, thus confirming that the process of photo-oxygenation was able to sustain the oxygen request by nitrifying bacteria in all systems tested. The highest photosynthetic rates were obtained in the pilot-scale HRAP, in the pilot-column treating LFAD from piggery wastewaters and in the algae-bacteria cultivation treating aquaculture wastewater, which have been indeed proposed as suitable substrates for the cultivation of microalgae [49], [303]. All the rates obtained in these systems were comparable with reported photosynthetic activities obtained with photo-respirometry procedures using synthetic media or wastewaters, [75], [239] and [234]. Results obtained by Arbib et al. [232] were instead lower, although the same type of wastewater was used. In this case, the rates were obtained by evaluating the DO variations directly in the cultivation bioreactor, possibly explaining the differences found. Volumetric photosynthesis rates obtained for the systems in which LFAD and aqualculture wastewaters were treated were in the same order of magnitude of previous works, [229], [246] and [232]. Rada-Ariza [240] reported much higher photosynthtic activities, which can be linked to the higher irradiance maintained during photo-respirometry. During the application of the photo-respirometric monitoring protocol, the lowest activities could be recorded in the demonstrative-scale PBRs treating runoff wastewater, possibly due to the flocculent nature of the suspension, the higher TSS concentrations and the potential limitation from carbon deficiency. Indeed, the overall correlation among the experimental OPR and TSS concentrations in the PRT sample could be described by using a power law to a satisfactory extent ($R^2 > 0.7$), as depicted in Figure 5.13. Low photosynthetic activities were also measured in some tests performed on the HRAP and in the lab-scale system

treating piggery wastewater, which were associated to poor environmental conditions in the first case and to the high cultivation pH which may have reduced the availability of inorganic carbon in the second case.

In general terms, the variability of the estimated photosynthetic activity was low, as demonstrated by the low average CVs calculated, that were almost always included in the range 4.5 - 8.8%, never exceeding these values except for a few cases (see sections 5.1.1 and 5.1.6). The average CV considering all the PRTs performed is also comparably low (9.9 ± 11.2%), thus further confirming the suitability of the method. The small variability calculated among tests performed in consecutive days (sections 5.1.3, 5.1.4 and 5.1.6) might be attributed to a combination of biotic and abiotic factors, such as small differences in: i) the biomass concentration and/or the average light intensity received by the biomass, ii) the hour at which the sampling was performed, iii) the sample storage time of the sample prior to testing, and iv) the duration of the acclimation phase.

The specific respiration rates were generally lower than 10 mg O_2 g TSS^{-1} h^{-1}, with a few exceptions calculated for some tests performed on the HRAP and the lab-scale system treating aquaculture wastewaters. Both the specific and volumetric respiration rates were in line with the results reported in literature for similar systems. In particular, the respiration rates measured for the HRAP were coherent with those reported by Arbib et al. [232], in which a systems treating the same type of influent was studied. The volumetric rates reported by Wang et al. and El Ouarghi et al., [246] and [229], were slightly higher than respiration rates obtained following the monitoring protocol, probably due to the fact that the consortia were exploited for the treatment of municipal wastewaters, and the respiration rates could include heterotrophic activity. Similarly, the specific rates found by Sforza et al. and Pastore et al., [75] and [239], are considerably higher, which may be associated to the fact that mixotrophic conditions were

investigated, with higher oxygen consumption rates expected. When analyzing photosynthesis and respiration rates obtained with photo-respirometry, it should be noticed that the conditions applied during photo-respirometry vary sligthly among sets (Table 5.4), therefore photosynthesis and respiration data were normalized by using the switch functions described in section 5.2 for pH, temperature and irradiance.

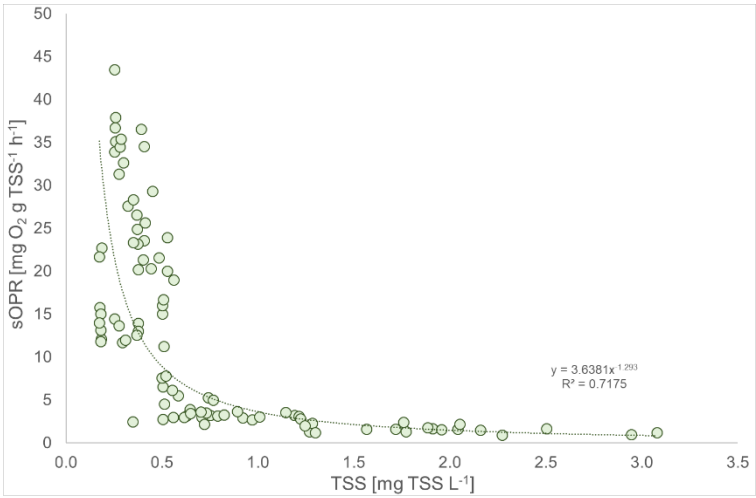

Figure 5.13. Correlation between sOPR measured in photo-respirometic tests and TSS of the photo-respirometric test.

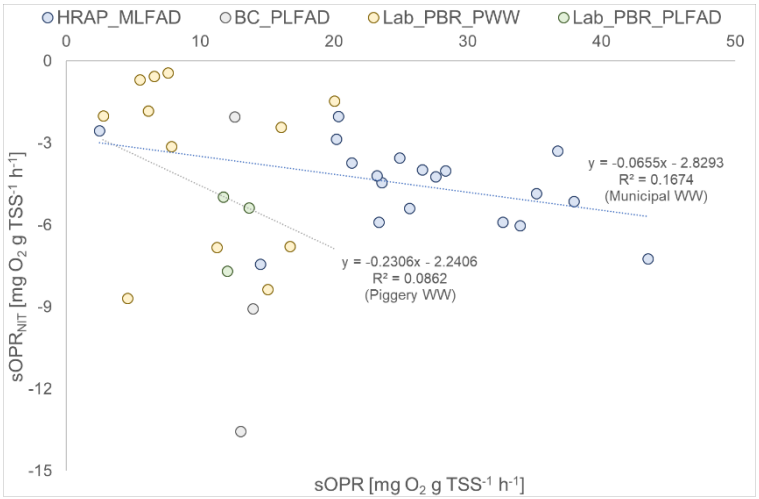

Figure 5.14. Correlation between specific nitrfication rates ($sOPR_{NIT}$) and specific photosynthesis rates (sOPR) in tests performed on systems treating municipal and piggery wastewaters.

Table 5.4 Summary of the results obtained following the photo-respirometric monitoring protocol and comparison with literature results. Values are expressed as mean ± standard deviation (minimum, maximum).

PBR	FEED	N/P	CO_2	DOMINANT PHOTOTROPHIC ORGANISMS	PBR	PHOTO-RESPIROMETRY			VOLUMETRIC RATES ($mg\ O_2\ L^{-1}\ h^{-1}$)			SPECIFIC RATES ($mg\ O_2\ g\ TSS^{-1}\ h^{-1}$)			REF
					IRRADIANCE ($\mu E\ m^{-2}\ s^{-1}$), TEMPERATURE (°C), pH (-)	IRRADIANCE ($\mu E\ m^{-2}\ s^{-1}$), TEMPERATURE (°C), pH (-)	OD_{680}	TSS ($g\ L^{-1}$)	OPR	OUR_{RESP}	OUR_{NIT}	sOPR	$sOUR_{RESP}$	$sOUR_{NIT}$	
HRAP (1.2 m^3)	MLFAD (NH_4^+)	45	Air	CHL, SCE, CHLAM	I: 1820 ± 155 (1332 - 2040), T: 25 ± 2 (19 - 31), pH:7.2 ± 1.2 (5.2 - 10.1)	I: 81 ± 23 (43 – 101), T: 26 ± 2 (22 - 29), pH: 7.6 ± 0.2 (7.3 - 7.8)	0.53 ± 0.08 (0.41 - 0.64)	0.33 ± 0.06 (0.25 - 0.44)	8.5 ± 2.4 (0.7 - 11.5)	3.0 ± 1.7 (0.4 - 5.6)	1.8 ± 1.0 (0.4 -4.0)	26.4 ± 9.4 (1.9 - 44.5)	8.9 ± 5.1 (1.7 - 18.9)	4.6 ± 1.5 (2.0 - 7.4)	This work
BC (80 L)	MLFAD (NO3-)	75	-	CHL, SCE, CHLAM, FCB	I: 312 ± 173 (39 - 614), T: 12 ± 3 (5 - 17), pH: 7.0 ± 0.8 (6.0 - 8.8)	I: 110 ± 5 (102 - 117), T: 20, pH: 8.5	0.21 ± 0.02 (0.20 - 0.23)	0.18 ± 0.02 (0.17 - 0.20)	2.0 ± 0.8 (2.0 - 4.3)	0.5 ± 0.2 (0.1 - 0.7)	0.1 ± 0.1 (-0.1 - 0.2)	15.8 ± 4.3 (11.0 - 23.7)	2.5 ± 1.0 (0.4 - 4.0)	0.5 ± 0.3 (0.1 - 1.0)	This work
BC (80 L)	PLFAD (NH_4^+)	19	-	CHL, SCE	I: 715 ± 450 (79 - 1712), T: 9 ± 7 (-2 - 26), pH: 7.9 ± 0.7 (6.2 - 9.0)	I: 42 ± 7 (38 – 50), T: 23 ± 2 (21 - 24), pH: 7.2 ± 0.5 (6.6 - 7.7)	0.47 ± 0.11 (0.36 - 0.58)	0.33 ± 0.05 (0.28 - 0.38)	7.2 ± 2.5 (4.4 - 10.7)	1.7 ± 0.7 (2.6 - 0.8)	1.9 ± 1.8 (0.1 - 5.7)	23.5 ± 10.8 (27.9 - 34.6)	5.1 ± 1.4 (3.0 - 6.9)	5.5 ± 4.7 (3.8 - 10.8)	This work
LPBR (2 L)	PLFAD (NH_4^+)	15	-	CHL, SCE	I: ± 59 ± 7 (50 - 68), T: 24 ± 0 (23 - 24), pH: 6.5 ± 0.8 (5.9 - 8.6)	I: 59 ± 3 (56 – 62), T: 22 ± 1 (21 - 24), pH: 7.9 ± 0.2 (7.8 - 8.1)	0.40 ± 0.04 (0.36 - 0.43)	0.29 ± 0.02 (0.28 - 0.31)	3.6 ± 0.3 (3.1 - 4.1)	1.4 ± 0.1 (1.4 - 1.5)	1.8 ± 0.6 (1.2 - 2.9)	12.5 ± 1.4 (10.1 - 14.2)	4.8 ± 0.2 (4.5 - 5.0)	6.0 ± 1.8 (4.0 - 9.3)	This work
SCPBR (13.6 m3)	ARWW (NO3-)	18.5	CO_2	CYS, COC, LEP	I: 1157 ± 354 (151 - 1845), T: 16 ± 5 (9 - 24), pH: 8.4 ± 0.5 (7.2 - 9.5)	I: 105 ± 6 (101 - 116), T: 23 ± 1 (21 - 25), pH: 8.5	-[a]	1.33 ± 0.67 (0.56 - 3.08)	2.9 ± 0.8 (1.3 - 4.8)	1.9 ± 0.4 (1.2 - 2.8)	0.2 ± 0.3 (0.0 - 1.4)	2.6 ± 1.1 (0.8 - 5.5)	1.8 ± 0.8 (0.6- 3.4)	0.2 ± 0.3 (0.0 - 1.3)	This work
LPBRs (3.5 L)	AWW (NO3-)	1.8	CO_2	TETR	I: 119 ± 28 (82 - 179), T: 27 ± 1 (26 - 29), pH: 8.2 ± 0.5 (7.9 - 8.5)	I: 113 ± 2 (110 - 116), T: 24 ± 1 (24 - 25), pH: 8.1 ± 0.1 (7.9 - 8.3)	0.58 ± 0.09 (0.50 - 0.65)	0.47 ± 0.07 (0.39 - 0.56)	12.6 ± 1.7 (9.9 - 16.0)	3.7 ± 0.5 (3.3 - 4.5)	0.4 ± 0.3 (0.0 - 0.9)	27.5 ± 7.0 (18.5 - 40.9)	8.0 ± 1.6 (5.9 - 10.0)	0.8 ± 0.7 (0.0 - 2.0)	This work
LPBRs (3.5 L)	PWW (NH_4^+)	14	CO_2	CHL, SCE, CHLAM, TRIB, STIG	I: 119 ± 28 (82 - 179), T: 30 ± 1 (28 - 31), pH: 8.2 ± 1.1 (5.9 - 9.8)	I: 101 ± 8 (89 - 115), T: 23 ± 2 (20 - 25), pH: 8.0 ± 0.3 (7.8 - 8.4)	0.58 ± 0.12 (0.52 - 0.88)	0.51 ± 0.02 (0.48 - 0.55)	5.2 ± 2.9 (0.9 - 11.1)	3.1 ± 1.7 (1.1 - 6.7)	1.8 ± 1.6 (0.2 - 4.5)	10.0 ± 5.8 (1.7 - 21.1)	3.6 ± 3.1 (0.4 - 8.7)	6.1 ± 3.4 (2.1 - 13.1)	This work
HRAP (9.6 m3)	MLFAD (NH_4^+)	-	-	WILD (COEL)	I: 261 - 716	I: 261 - 716	-	-	4.8 - 9.5	-	2.0 - 3.9	2.9 - 3.8[b]	-	-	[232]
PSBR (2 L)	PLFAD (NH_4^+)	13.6	-	WILD (CHL, SCE, STI)	I: 200 - 400, T: 21	I: 200 - 400, T: 21	-	-	8.0	7.6		-	-	-	[246]
HRAP (2.5-5.3 m3)	FPWW	-	-	SCE	I: 0 - 1960, T: 6.5 - 25	I: 0 - 1960, T: 6.5 - 25	-	-	-	-	-	-	0.4 - 1.5[b]	-	[231]

(continued)

Table 5.4 (continued)

HRAP (500 m3)	MWW	-	-	-	pH: 7.5	-	-	-	25	8	-	-	-	-	[229]
LPBRs (250 mL)	MWW, SW (NH_4^+)	7.5 - 13.1	Air + CO_2	MIX (CHL)	I: 30, T: 24	I: 45, T: 25, pH: 8	-	0.44	-	-	-	6 - 39[c]	12 - 39[c]	-	[75]
PSBR (9.2 L)	SW (NH_4^+)	11.1	-	MIX (CHL)	I: 92 - 183, T: 26	I: 92 - 183, T: 26	-	-	-	-	-	6.7 - 22.6	-	-	[234]
LPBRs	SW (NH_4^+)	4.1	-	CHL	I: 100, T: 24	I: 10 - 130, T: 25, pH: 8	-	0.44	-	-	-	6.6 - 31.2[c]	13.8 - 31.8[c]	-	[239]
PSBR (4 L)	MM (NH_4^+)	8	-	MIX	I: 766.5, T:25, pH: 7.5	I: 300, T: 25, pH: 7.5	-	-	20 - 130	-	-	-	-	-	[240]

Since these functions were only calibrated on the HRAP consortium, in which *Chlorella* sp. and *Scenedesmus* sp. were the dominant phototrophic organisms, the normalization procedure could be applied only to those systems in which similar phototrophic communities developed (i.e. with green microalgae as dominant organisms). Normalization consisted in evaluating the switch functions for environmental conditions, in order to refer all the results to the same reference conditions (irradiance: 110 μE/m²/s, Temperature: 20°C, pH: 8.5 and DO: 10 mg DO L^{-1}, see section 4.2). Results of the normalization procedure are reported in Table 5.5. In particular, the photosynthetic activity of the consortium developed in the bubble column treating LFAD from piggery wastewaters was the highest, followed by that of the HRAP, contrarily to what reported before (Table 5.4). These results remark two different aspects to be considered in the interpretation of photo-respirometric results: i) the importance of normalizing the rates obtained by photo-respirometry when comparing experiments performed at different conditions and ii) the importance of thoroughly reporting the test conditions applied, in order to facilitate the comparison with literature results. An explorative analysis was also conducted to evaluate possible correlations of the environmental and operational parameters on the normalized rates measured by photo-respirometry. To this aim, a PCA was carried out on the experimental data obtained for the HRAP and the bubble-column treating digestates.

Table 5.5. Normalized photosynthesis and respiration rates in tests performed on systems treating municipal and piggery wastewaters with green microalgae as dominant phototrophic organisms. Values are expressed as mean ± standard deviation (minimum, maximum).

PHOTOBIOREACTOR	FEED AND NUTRIENT SOURCE	DOMINANT PHOTOTROPHIC ORGANISMS	NORMALIZED RATES (mg O_2 g TSS^{-1} h^{-1})	
			sOPR	$sOUR_{RESP}$
HRAP (1.2 m^3)	MLFAD (NH_4^+)	*Chlorella sp., Scenedesmus sp., Chlamydomonas sp.*	37.6 ± 23.7 (2.5 - 91.8)	11.2 ± 6.4 (2.3 - 25.9)
BC (80 L)	PLFAD (NH_4^+)	*Chlorella sp., Scenedesmus sp.*	60.2 ± 27.9 (27.8 - 89.4)	7.4 ± 2.1 (4.3 - 10.0)
Lab-PBR (2 L)	PLFAD (NH_4^+)	*Chlorella sp., Scenedesmus sp.*	21.9 ± 0.8 (21.0 - 22.7)	6.5 ± 0.3 (6.2 - 6.8)
Lab-PBRs (3.5 L)	PWW (NH_4^+)	*Chlorella sp., Scenedesmus sp., Chlamydomonas sp., Tribonema sp., Stigeoclonium sp.*	10.1 ± 5.7 (2.7 - 20.0)	7.3 ± 4.2 (2.5 - 16.2)

The analysis was specifically conducted to evaluate the correlation between the sOPR and $sOPR_{RESP}$ and different variables, including: the average N/P ratio of the influent wastewater, the pH of the suspension in the day of the test and the irradiance and temperatures values averaged on the four days preceeding the test (I_4d and T_4d). Results reported in Figure 5.15 show that only a direct proportionality between sOPR and the pH could be found, while the other parameters seemed not to particularly influence the photosynthetic rate. Regarding the respiration rate, $sOPR_{RESP}$ was not influenced by any of the parameters studied.

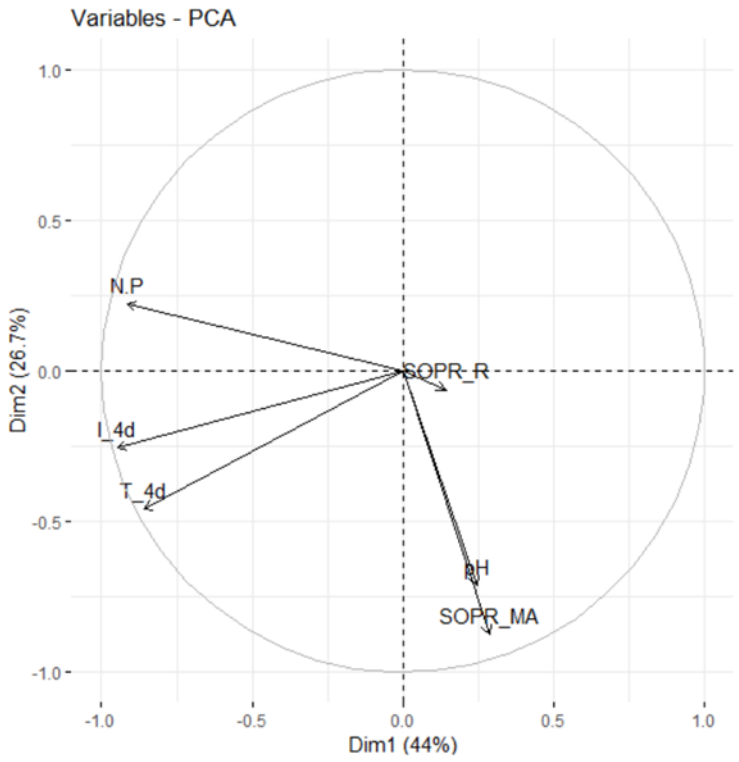

Figure 5.15. Results of the principal component analysis applied to the pilot-scale HRAP and bubble-column treating digestates (I_4d: average irradiance on the four days preceeding the test, T_4d: average irradiance on the four days preceeding the test).

5.2. Model calibration protocol

The model calibration protocol was applied to the HRAP described in section 3.3.1, during the 2019 monitoring campaign. The models described in Table 4.1 and Table 4.2 were fitted to each corresponding dataset, in order to identify the optimal model parameters. Results of the data-fitting exercise are reported in the following sections (5.2.1 and 5.2.2), in which, the effect of the factors under study (irradiance, temperature, pH, DO) on both photosynthesis and respiration rates are separately discussed. For the sake of simplicity, in this section the $sOUR_{RESP}$ is simply referred to as sOUR, as no other oxygen consumption terms are practically involved.

5.2.1. Selection of photosynthesis models

5.2.1.1. Irradiance models

Respirometric data were used to plot PI curves for the microalgae-bacteria consortium (Figure 5.16A). Experimental data are correctly described by the three considered models. In particular, according to the AICc criterion alone, the model by Lee et al. [289] should be preferred, as it is characterized by the lowest AICc value. The model by Bernard and Rémond [183], however, seems to be the most appropriate to interpret all relevant aspects of the PI curve: (i) the initial slope of the curve, (ii) the optimal irradiance, and especially (iii) the photoinhibition effect. This model is also characterized by the highest value of R_{ADJ}^2 (0.9525) and the lowest SSE (Table 5.6) and it is therefore chosen to describe the effect of irradiance on the photosynthetic oxygen production.

5.2.1.2. Temperature models

Respirometric data obtained at different temperatures follows the typical trends obtained for microbial cultures. The dependence of photosynthetic activity on temperature was well described by the three models (Figure 5.16B). Indeed, the information criteria (Table 5.6) were best satisfied by the cardinal temperature model with inflection [183], that was selected to describe the temperature dependence, although the other two equations could be used with a similar accuracy (all R_{ADJ}^2 are between 0.8907 and 0.8975).

5.2.1.3. pH models

The effect of pH on photosynthetic oxygen production was highly variable and model fitting was slightly less satisfactory (R_{ADJ}^2 between 0.7481 and 0.8043). Nevertheless, both the cardinal pH model (CPM) by Rosso et al. [52] and the cardinal pH model with inflection (CPMI) by Ippoliti et al. [53] seem to accurately represent experimental data. The empirical expression adopted by [292] to model the effects of pH on the anaerobic digestion process was also adequate to fit photo-respirometric data in the optimal pH range (Figure 5.16C). The goodness of fit for the model by [292] was also confirmed by the high value of the adjusted R^2 and the low values of both SSE and AICc (Table 5.6). Nevertheless, the model does not allow a direct estimation of cardinal pH values, and a subsequent numerical estimation is needed to evaluate these values. For this reason, it was chosen to describe the effects of pH variations on the photosynthetic activity using the cardinal model originally proposed by Rosso et al. [52].

5.2.1.4. Dissolved oxygen models

Normalized sOPRs at DO concentrations exceeding the oxygen saturation level are reported in Figure 5.16D. Experimental data could be described by the two selected models: the hyperbolic model with no inhibition proposed by Ippoliti et al. [53] and the generic Hill model described by di Veroli et al. [293]. Both models can simulate the inhibitory response to DO in a similar way, as confirmed by the almost identical values of all information criteria (Table 5.6). Although the model proposed by Ippoliti et al. [53] met selection criteria slightly better than the other model (R_{ADJ}^2 = 0.7186), the Hill curve is characterized by a smoother shape at high DO concentrations, which seems to be more adequate to reduce numerical instability in complex mathematical models. The Hill equation [293] is therefore preferred to model the evolution of the sOPR at different DO concentrations.

5.2.2. Selection of respiration models

5.2.2.1. Irradiance models

Respiration data as a function of the irradiance received during the previous light phase varied widely over the range or irradiance values tested. Such variability is particularly relevant in the irradiance range 300-550 μE/m²/s and could be partially explained by the presence of endogenous respiration by heterotrophic bacteria, which could have affected the test output. The reference model [53] was compared to the sigma function proposed in this work (Figure 5.17A). The two models similarly predict the trend in experimental data and the information criteria are accordingly very similar. The sigma function is however preferred to describe the respiration rate as a function of the received light, according to the calculated AICc and adjusted R^2 (Table 5.7).

5.2.2.2. Temperature models

The dependence of algal respiration on the temperature of the suspension could be represented with all the selected temperature-dependence models (Figure 5.17B): the square-root model [290], the CTMI [183] and the Blanchard model [291]. Among the three, the cardinal model seems to better represent the decrease in the specific OUR at high temperatures and it is also characterized by a better score in terms of model selection criteria (Table 5.7), therefore it is selected as the optimal model equation.

It is interesting to notice that the temperature had a greater effect on the respiration rate (Figure 3B) rather than on the photosynthetic rate (Figure 2B), with an increase in respiratory oxygen uptake rates reaching up to three times the rate measured at the reference condition (20 °C).

5.2.2.3. pH models

The measured and modelled pH-dependent respiration rates are reported in Figure 5.17C. Also in this case, the model proposed by Batstone et al. [292] was suitable to describe respiration data: compared to the two cardinal models, the Batstone model ranked better in terms of corrected AIC and it seems to better describe the data in the interval around the optimum values. Interestingly, also in the case of respiration rates, the CPM equation better represented experimental trends, compared to the CPMI. In general, as shown by the poor values of adjusted R^2 (Table 5.7), experimental sOURs were characterized by a high variability, especially in the operational range 4.5 - 8.5. The execution of additional experiments is here suggested, in order to better understand and to achieve a more robust model of the pH effect on the respiration dynamics.

5.2.2.4. Dissolved oxygen models

Since only DO oversaturation data were collected in this study, it was not possible to estimate all parameters characterizing the proposed switch functions at different DO concentrations. Nevertheless, parameter estimation was computed using respiration data, by assuming constant values for the parameters located outside of the range of experimental DO. For this reason the half-saturation constant for oxygen was set at a constant value ($K_{S,DO}$ = 0.2 mg DO L^{-1}) since it could not be estimated as a fitting parameter. As shown in Table 5.7, only a small difference in the information criteria was found between the modified Luong and the Hill models, and the first model was chosen, for the same reasons described for photosynthetic rates.

5.2.3. Data fitting considering all parameters

During the bioassays, reference conditions were maintained as fixed as possible for all the parameters but the one under study. However, the impossibility of achieving a perfect control on experimental conditions during the bioassay, and the unavoidable DO accumulation during light phases caused this parameter to vary more significantly than all other ones. Indeed, these conditions resulted in the overestimation of effects attributed to each parameter under investigation since a slight potential inhibition from oversaturated DO level were ascribed to that parameter. To include the effects of all environmental parameters at the same time, a second run of the least squares minimization method was carried out, considering the variation of all conditions simultaneously.

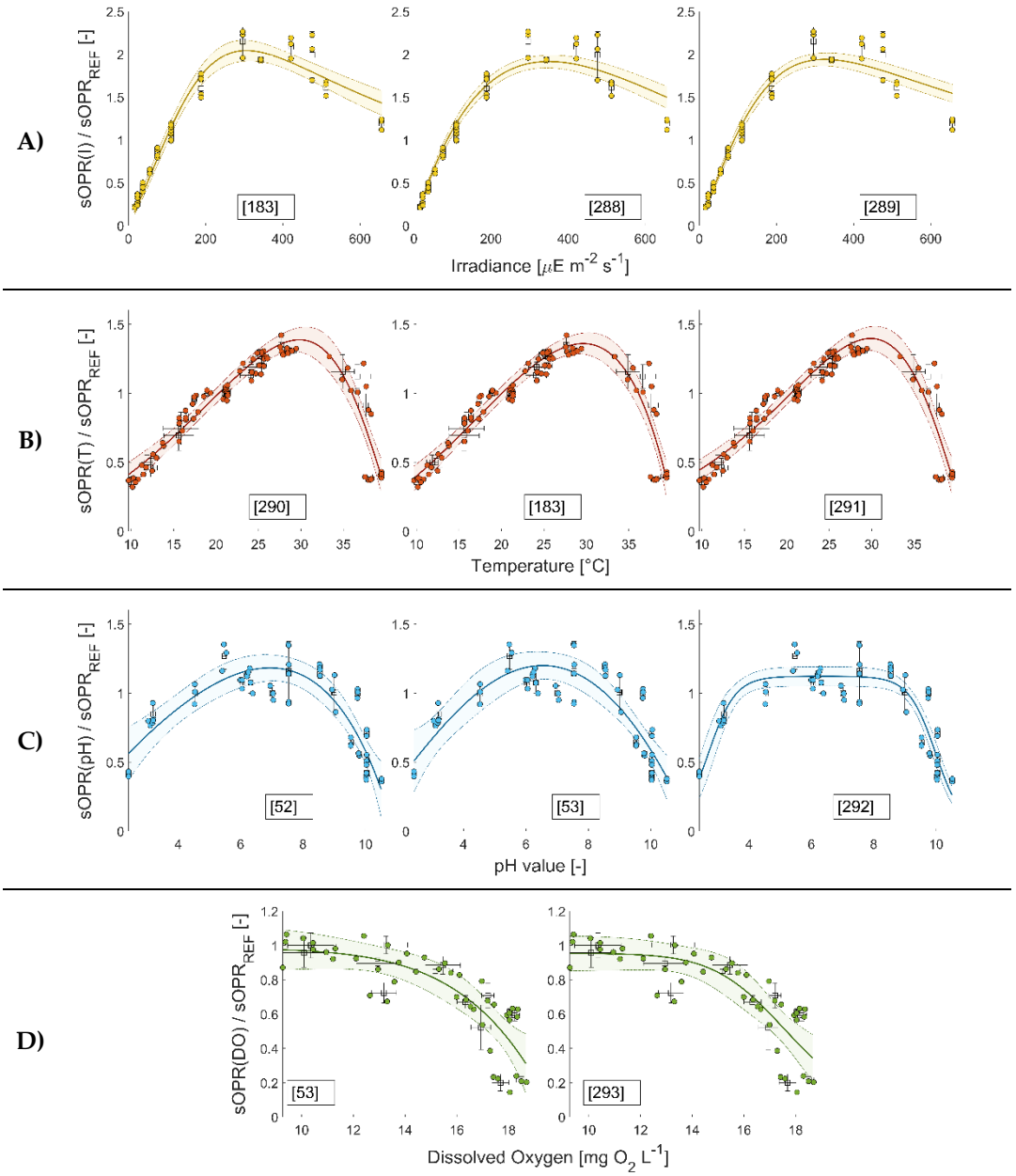

Figure 5.16. Fit of different photosynthesis models to normalized sOPR data: irradiance (A), temperature (B), pH (C) and DO (D) (error bars indicate standard deviations for three sOPR determination, shaded areas indicate 95% confidence intervals for fitting functions).

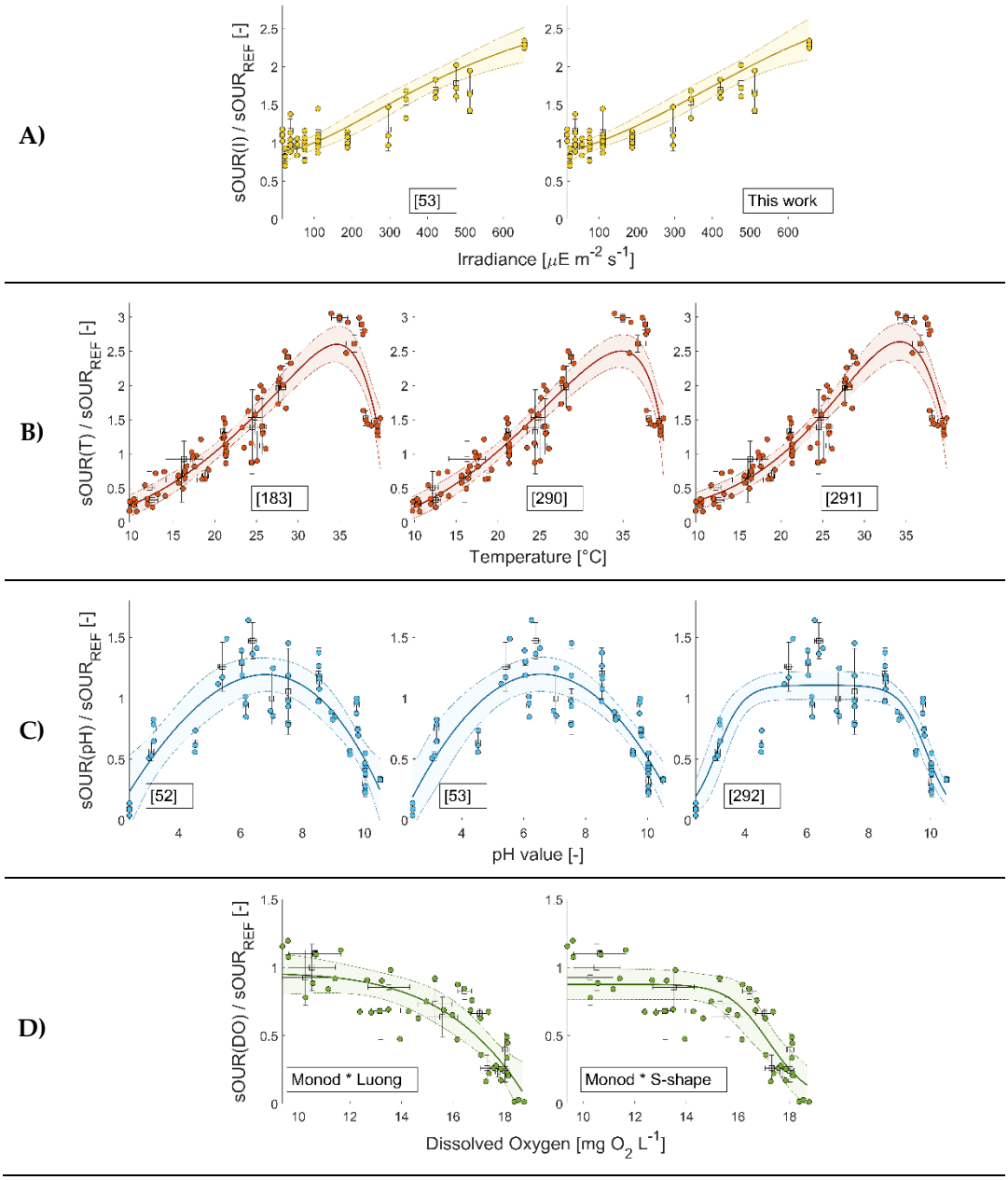

Figure 5.17. Fit of different respiration models to normalized sOUR data: irradiance (A), temperature (B), pH (C) and DO (D) (error bars indicate standard deviations for three sOUR determination, shaded areas indicate 95% confidence intervals for fitting functions).

Table 5.6. Estimated parameters and information criteria for the described photosynthesis models (data in square brackets indicate 95% confidence intervals for the estimated value).

ENVIRONMENTAL PARAMETER	MODEL ID	NUMBER OF OBSERVATIONS (n)	NUMBER OF PARAMETERS (p)	PARAMETER ESTIMATES	SSE	R_{ADJ}^2	AICc
Irradiance	f_{P,I_BR}	60	2	α = 0.16 mg O2/g TSS/h [0.14, 0.18] I_{OPT} = 305.4 µE m^{-2} s^{-1} [288.6, 322.1]	293.89	0.9525	143.74
	f_{P,I_ST}	60	1	I_{MAX} = 349.8 µE m^{-2} s^{-1} [328.8, 370.9]	358.39	0.9430	138.20
	f_{P,I_LE}	60	2	k_1 = 90.4 W h m^{-2} [85.1, 95.8] k_2 = 0.0038 m^2 h W^{-1} [0.0035, 0.004]	351.94	0.9441	137.55
Temperature	f_{P,T_RA}	84	4	b = 0.152 [0.123, 0.18] c = 0.149 [0.100, 0.198] T_{MIN} = - 7.8 °C [-11.9, -3.6] T_{MAX} = 42.5 °C [41.6, 43.4]	275.82	0.8949	204.07
	f_{P,T_BR}	84	3	T_{MIN} = -3.7 °C [-6.8, -0.6] T_{OPT} = 29.6 °C [28.8, 30.4] T_{MAX} = 40.8 °C [40.3, 41.4]	269.11	0.8975	203.47
	f_{P,T_BL}	84	3	β = 1.71 [0.99, 2.43] T_{OPT} = 29.9 °C [29.1, 30.6] T_{MAX} = 42.1 °C [40.1, 44.2]	286.83	0.8907	205.04
pH	f_{P,pH_RO}	66	3	pH_{MIN} = 0.21 [-0.9, 1.4] pH_{OPT} = 6.94 [6.5, 7.4] pH_{MAX} = 10.93 [10.6, 11.3]	396.96	0.7651	174.90
	f_{P,pH_IP}	66	3	pH_{MIN} = 0.0 [-2.7, 2.7][a] pH_{OPT} = 6.5 [6.03, 7.1] pH_{MAX} = 11.3 [10.9, 11.8]	425.63	0.7481	176.92
	f_{P,pH_BA}	66	2	pH_{INF} = 2.69 [2.51, 2.87] pH_{SUP} = 10.0 [9.9, 10.1]	335.92	0.8043	159.18
Dissolved Oxygen	f_{P,DO_CO}	48	2	DO_{MAX} = 19.6 mg O_2 L^{-1} [18.7, 20.5] n = 7.13 [3.49, 10.78]	305.26	0.7186	121.24
	f_{P,DO_DV}	48	2	K_{DO} = 17.8 mg O_2 L^{-1} [17.3, 18.2] H = 12.7 [6.82, 18.6]	310.61	0.7137	121.67

Notes: a) The parameter was constrained to: pH ≥ 0. The original fitted value was: pH_{MIN} = -2.9 [-5.8, 0.0]

Table 5.7. Estimated parameters and information criteria for the described respiration models (data in square brackets indicate 95% confidence intervals for the estimated value).

ENVIRONMENTAL PARAMETER	MODEL ID	NUMBER OF OBSERVATIONS (n)	NUMBER OF PARAMETERS (p)	PARAMETER ESTIMATES	SSE	R_{ADJ}^2	AICc
Irradiance	f_{R,I_IP}	60	2	n = 1.70 [1.23, 2.18] I_K = 565.3 µE m^{-2} s^{-1} [490.3, 640.3]	11.200	0.8291	109.77
	f_{R,I_RO}	60	2	a = 0.0043 [0.0035, 0.0052] I* = 385.8 µE m^{-2} s^{-1} [216.9, 554.6]	10.795	0.8352	109.71
Temperature	f_{R,T_RA}	84	4	b = 0.031 [0.026, 0.035] c = 0.333 [0.204, 0.463] T_{MIN} = -0.1 °C [-3.4, 3.2] T_{MAX} = 42.2 °C [41.2, 43.3]	41.066	0.8522	180.16
	f_{R,T_BR}	84	3	T_{MIN} = 1.5 °C [-1.7, 4.8] T_{OPT} = 34.8 °C [34.0, 35.6] T_{MAX} = 40.9 °C [40.1, 41.7]	40.099	0.8557	180.05
	f_{R,T_BL}	84	3	β= 1.176 [0.482, 1.869] T_{OPT} = 34.3 °C [33.5, 35.0] T_{MAX} = 41.7 °C [39.8, 43.7]	43.507	0.8434	180.45
pH	f_{R,pH_RO}	66	3	pH_{MIN} = 1.8 [1.2, 2.5] pH_{OPT} = 6.8 [6.2, 7.4] pH_{MAX} = 10.9 [10.5, 11.4]	13.134	0.6871	139.52
	f_{R,pH_IP}	66	3	pH_{MIN} = 2.0 [1.3, 3.2] pH_{OPT} = 6.6 [6.3, 6.9] pH_{MAX} = 11.1 [10.8, 11.4]	13.272	0.6839	139.54
	f_{R,pH_BA}	66	2	pH_{INF} = 3.1 [2.8, 3.4] pH_{SUP} = 9.9 [9.7, 10.0]	13.440	0.6849	120.85
Dissolved Oxygen	f_{R,DO_ML}	48	2	DO_{MAX} = 19.0 mg O_2 L^{-1} [18.3, 19.6] n = 6.22 [2.94, 9.49]	2.3711	0.7281	86.944
	f_{R,DO_MS}	48	2	K_{DO} = 17.3 mg O_2 L^{-1} [16.9, 17.6] H = 21.2 [10.4, 32.0]	2.6139	0.7003	86.984

This time, all the parameters were estimated together, using the entire sOPR and sOUR datasets for the calibration of all parameters of the pre-selected models (i.e. those selected on each sub-set of data in paragraphs 5.2.1 and 5.2.2). A new set of parameters was obtained and is reported in Table 5.8.

The overall correlation obtained between experimental and simulated sOPR was very poor for the first modelling round. i.e. by using parameters reported in Table 5.6 for each selected model. Indeed, by fitting the model predictions versus the experimental data to a straight line a slope of m = 0.5788 was obtained and the coefficient of determination was $R^2 = 0.7954$.

After the second run, the capability of predicting the experimental sOPR and sOUR improved, as the regression parameters became: m = 0.9616 and $R^2 = 0.8726$. Regarding respiration rates, the correlation between experimental and calculated data was lower than that obtained for photosynthesis, also reflecting the higher variability measured in the experimental sOUR during dark phases. After including the interactions among different environmental parameters, however, the slope of the measured vs. calculated respiration rates strongly increased, from m = 0.3996 indicating a very poor capability of reproducing the variation of all parameters, up to m = 0.9310, slightly lower than the slope obtained using photosynthetic rates but very close to one. The statistical correlation also improved, as demonstrated by the increased coefficient of determination ($R^2 =$ 0.7763 and 0.8162, during the first and second estimation routines, respectively).

The regression parameters calculated for photosynthesis are very close to the values reported by Costache et al. and Ippoliti et al., [181] and [53], and the results related to respiration rates are also consistent to those reported by Ippoliti et al. [53]. These studies were possibly conducted in the absence of a relevant bacterial contamination, as synthetic media were used for the cultivation. On the contrary,

during this study, the system was operated to specifically grow a consortium of microalgae and bacteria which was fed with the undiluted LFAD. A minimum heterotrophic activity due to the presence of residual COD can partially explain anomalous data found in experimental respiration rates since some heterotrophic respiration cannot be excluded. The expected heterotrophic activity could be estimated by considering the theoretical biomass fractionation which was estimated by using a comprehensive growth model. To this purpose the ALBA (algae-bacteria) model that was described in recent studies was used [300]. The model was ran using typical daily patterns for irradiance and temperature and with the average nutrient concentrations of the influent wastewater described in section 2.1. Under these conditions, the expected concentrations of phototrophs (X_{ALG}), heterotrophic bacteria (X_H), ammonia-oxidizers (X_{AOB}) and nitrite-oxidizers (X_{NOB}) could be assessed as a percentage of the total biomass solids ($X_{TOT} = X_{ALG} + X_H + X_{AOB} + X_{NOB}$). The obtained ratios ($X_{ALG}/X_{TOT}$ = 92.2%, X_H/X_{TOT} = 5.8%, X_{AOB}/X_{TOT} = 1.4% and X_{NOB}/X_{TOT} = 0.6%, respectively) were used to initialize the biomass composition that was used in the respirometric tests. The theoretical OURs were then simulated by taking into account the applied environmental conditions during respirometric tests (COD-free medium, applied values of pH, T, DO). Under these conditions, the expected contribution of heterotrophic bacteria on the overall respiration rate were non-negligible though lower than the contribution from microalgae [300] respiration (OUR_H/OUR_{TOT} = 25%). These results suggest that a more exhaustive investigation should be conducted on this topic, possibly complemented with the use of selective inhibitors for heterotrophic bacteria or wide-spectrum antibiotics to suppress this biological interference, in order to fully exploit the advantages of the proposed photo-respirometric method. In this viewpoint, results presented in this work are encouraging and suggest that a more complete understanding of the behaviour of phototrophic organisms grown on wastewater can be obtained using the

proposed method, e.g. to model limitation/inhibition effects due to dissolved inorganic/organic components, or to evaluate the adaptation mechanisms of the consortium at different pH values and temperatures. The estimated values of model parameters and their respective confidence regions obtained considering the entire dataset for photosynthesis/respiration rates are available in Table 5.8. In the majority of cases, by using the entire dataset, the confidence intervals for fitted coefficients are reduced and the new estimated values falls in the confidence interval determined during the first round of modelling, again confirming the reliability of the estimation procedure.

Results presented in Table 5.8 are of particular interest, as they are referred to a mixed consortium treating real wastewater, instead of an axenic culture fed with synthetic media, as normally found in the scientific literature [53], [181], [304].

Table 5.8. Estimated parameter values for selected models considering the interactions among all environmental parameters (data in square brackets indicate 95% confidence intervals for the estimated value).

PHOTOSYNTHESIS			RESPIRATION		
MODEL ID	**SYMBOL**	**VALUE**	**MODEL ID**	**SYMBOL**	**VALUE**
f_{P,I_BR}	α	0.394 [0.341, 0.447]	f_{R,I_RO}	a	0.010 [0.004, 0.016]
	I_{OPT}	301.1 [265.2, 337.0]		I*	333.1 [208.3, 458.0]
f_{P,T_BR}	T_{MIN}	-0.1 [-4.9, 4.6]	f_{R,T_BR}	T_{MIN}	4.9 [2.3, 7.6]
	T_{OPT}	27.6 [26.6, 28.6]		T_{OPT}	35.5 [34.6, 36.1]
	T_{MAX}	42.5 [41.1, 43.9]		T_{MAX}	40.8 [40.1, 41.5]
f_{P,pH_RO}	pH_{MIN}	0.0 [-1.3, 1.3][a]	f_{R,pH_RO}	pH_{MIN}	1.5 [0.1, 2.9]
	pH_{OPT}	7.4 [7.1, 7.7]		pH_{OPT}	7.8 [7.3, 8.4]
	pH_{MAX}	10.9 [10.6, 11.3]		pH_{MAX}	10.7 [10.2, 11.1]
f_{P,DO_DV}	K_{DO}	17.9 [17.5, 18.2]	f_{R,I_IP}	K_{DO}	16.3 [15.8, 16.9]
	H	17.5 [9.8, 25.2]		H	21.8 [8.7, 34.9]

Notes: a) The parameter was constrained to: $pH \geq 0$. The original fitted value was: pH_{MIN} = -1.8 [-3.0, 0.4]

All the results can be considered reliable, as they fall in the range of previously reported studies. The maximum photosynthetic rate was found at an irradiance level of approximately 300 μE m^{-2} s^{-1} and the photo-inhibition was practically negligible, contrarily to what was suggested by the first round of the fitting procedure. A complete absence or very low level of photo-inhibition was documented in previous studies, although performed on axenic cultures of *Pheodactylum* sp. [305], Chlorella sp. [165], [306], [307] and Scenedesmus sp. [143], [187], [308]. The optimal temperature to which the the microalgae-bacteria consortium exhibited the maximum sOPR was approximately 28 °C, which is in the range of parameters reviewed by other authors [309], [310] and [311]. The obtained results were slightly lower than the optimal temperature estimated with previous photo-respirometric studies [53], [143], [181], [187], [304] and growth experiments [305], [308], [312]. In these studies, optimal temperatures ranged from 30 to 35 °C. The fact that the dependence of photosynthetic activities on temperature is species-specific [50], [311] is a partial explanation of this low optimal temperature determined for the microalgae-bacteria consortium. Another important consideration is that the biomass was grown outdoor, and the temperature of the water rarely exceeded 30°C (Table 5.1), which may have caused an acclimation or a selection of species more adapted to lower temperatures. Regarding the pH value, the optimum determined using the model calibration protocol was 7.4, that is quite similar to the values obtained with similar procedures, [53], [181], [187]. The value also falls in the range obtained in dedicated growth experiments, [305], [312], [313]. Finally, the observed effect of DO on the photosynthetic rate is consistent with the sOPR reduction evaluated at DO concentrations in the range 20 - 30 mg O_2 L^{-1} [53], [181], [187], [314]., regarding the effects of environmental parameters on the microalgal respiration rate, the highest values are consistent with the results obtained by Ippoliti et al. and Cortés Téllez et al., [53], [315].

5.3. Inhibition protocol

The inhibition protocol was applied to the previously described HRAP (section 3.3.1) in the 2019 monitoring campaign. In the following sections the results are reported. Table 5.9 reports the tests performed during the inhibition protocol.

5.3.1. Selection of free ammonia inhibition models

The experimental sOPR values were calculated as described in section 4.2.2.1 and the dataset obtained from PRTs was used to fit to the non-competitive inhibition model (Equation 4.20) and to the sigmoidal logistic curve (Equation 4.21). Model information criteria (R_{ADJ}^2 and cAIC) are shown in Table 5.10. Both models can describe the entire photo-respirometric dataset and show a high value of R_{ADJ}^2 (all higher than 0.98). Regarding cAICs values, low differences among models are observed, however the non-competitive model was preferred because a similar predicting ability was obtained with one parameter less, thus reducing computational costs and facilitating parameter estimation. The predicting ability of this model was able to correctly describe the inhibition process for both mono and mixed cultures. However, the variability of some estimated parameter was quite high, as proven by the large extension of 95% confidence bounds.

Predictions for cyanobacterial monocultures were more accurate than for microalgae. The highest variabilities were found for *Scenedesmus quadricauda* and *Chlorella sorokiniana.* With respect to this variability, decreasing the measurement noise (e.g. by reducing/eliminating gas-liquid transfer) and/or adjusting the experimental protocol (e.g. by increasing the number of replications to obtain more robust inhibition data) could be desirable improvements to the proposed methodology. Moreover, the variability of estimated parameters was generally

higher in PRTs performed on mixed consortia, compared to monocultures (especially for the sample from the microalgae-bacteria system).

Table 5.9. Free ammonia inhibition tests performed and conditions applied. Temperature and irradiance data are reported as mean ± standard deviation.

Test ID	Cultivation system (volume)	Type of culture and dominant phototrophs	Species	Growth substrate (N-source)	Free ammonia concentration	Temperature	Irradiance
-	-	-	-	-	mg NH_3 L^{-1}	°C	μE m^{-2} s^{-1}
MB	HRAP (1.2 m^3)	Phototrophs-bacteria	*Chlorella/Scenedesmus sp.*	LFADM (NH_4)	17, 34, 68, 134	20.3 ± 0.2	108 ± 16
CB_1	SCPBRs (11.7 m^3)	Phototrophs-bacteria	*Synechocystis sp., Synechococcus sp.*	ARWW (NO_3)	8.5, 17, 34, 68	21.5 ± 0.3	116 ± 23
CB_2	SCPBRs (11.7 m^3)	Phototrophs-bacteria	*Synechocystis sp., Synechococcus sp.*	ARWW (NO_3)	8.5, 17, 34, 68	21.6 ± 0.3	116 ± 23
CB_3	SCPBRs (11.7 m^3)	Phototrophs-bacteria	*Synechocystis sp., Synechococcus sp.*	ARWW (NO_3)	8.5, 17, 34, 68	21.8 ± 0.4	116 ± 23
M_1	LPBR (1 L)	Green algae monoculture	*Chlorella vulgaris*	MBBM (NO_3)	17, 34, 68, 134	19.6 ± 0.1	108 ± 16
M_2	LPBR (1 L)	Green algae monoculture	*Scenedesmus quadricauda*	MBBM (NO_3)	17, 34, 68, 134	19.7 ± 0.1	108 ± 16
M_3	LPBR (1 L)	Green algae monoculture	*Chlorella sorokiniana*	MBBM (NO_3)	17, 34, 68, 134	19.9 ± 0.1	108 ± 16
M_4	LPBR (1 L)	Green algae monoculture	*Scenedesmus obliquus*	MBBM (NO_3)	17, 34, 68, 134	20 ± 0.0	108 ± 16
C_1	LPBR (1 L)	Cyanobacteria monoculture	*Synechocystis sp.*	BG11 (NO_3)	8.5, 17, 34, 68	20.0 ± 0.4	116 ± 23
C_2	LPBR (1 L)	Cyanobacteria monoculture	*Synechococcus sp.*	BG11 (NO_3)	8.5, 17, 34, 68	20.6 ± 0.3	116 ± 23
C_3	LPBR (1 L)	Cyanobacteria monoculture	*Leptolyngbia sp.*	BG11 (NO_3)	8.5, 17, 34, 68	20.8 ± 0.3	116 ± 23

This variability can be due to the presence of other microorganisms in the suspension, possibly contributing to the DO mass balance (protozoa, heterotrophic bacteria) and constituting an additional biological noise. In order to improve data reliability, further research is suggested regarding the pre-treatment of the sample and the possibility of using wide spectrum inhibitors/antibiotics to suppress undesired in biological activities.

5.3.1. Effects of free ammonia on axenic microalgae and cyanobacteria

Experimental $sOPR_{NH3}/sOPR_{CONTROL}$ values quantifying the reduction of photosynthetic activity due to the exposure to free ammonia for microalgae and cyanobacteria monocultures are shown in Figure 5.18, together with the fit of the non-competitive inhibition model.

The photosynthetic activities of all monocultures decreased at increasing FA, as expected due to the inhibitory effects on photosynthesis, and no stimulatory effects due to ammonia assimilation were observed. FA only affected the $sOPR_{NET}$, and the observed $sOUR_{RESP}$ did not vary significantly regardless of the FA concentration applied (data not shown), coherently with previous findings [215].

Regarding results on microalgae monocultures (Table 5.10), the value of $EC_{50,NH3}$ for *Chlorella vulgaris* (60.9 mg NH_3 L^{-1}) was close to 54 mg NH_3 L^{-1} obtained by [74] under similar conditions. An $EC_{50,NH3}$ = 96.3 mg NH_3 L^{-1} was obtained for *Chlorella Sorokiniana*, coherently with the absence of inhibition reported by Gutierrez et al. [201], and with the higher concentrations obtained for different *Chlorella Sorokiniana* strains by Wang et al. [220]. The inhibition parameter for *Scenedesmus quadricauda* was 77.7 mg NH_3 L^{-1}, but literature values are not available for this species and a direct comparison is not possible. The value obtained for *Scenedesmus obliquus* (52.6 mg NH_3 L^{-1}) is instead very similar to that obtained at the same pH by Abeliovich and Azov [215] (51 mg NH_3 L^{-1}).

Table 5.10. Selection criteria and estimated parameters for selected free ammonia inhibition models. 95% confidence intervals on estimated parameters are reported in square brackets. Averaged data are reported as mean ± standard deviation.

CYANOBACTERIA						
Test ID	**Model 1 (non-competitive inhibition)**			**Model 2 (sigmoidal logistic function)**		
-	**cAIC**	**R_{ADJ}^2**	**Estimated parameters**	**cAIC**	**R_{ADJ}^2**	**Estimated parameters**
C_1	-16.7	0.9478	$EC_{50,NH3}$ = 17.5 mg NH_3 L^{-1} [9.9, 25.0]	-17.8	0.9820	$EC_{50,NH3}$ = 18.5 mg NH_3 L^{-1} [14.7, 22.2], N = 1.43 [0.96, 1.89]
C_2	-19.7	0.9990	$EC_{50,NH3}$ = 13.1 mg NH_3 L^{-1} [8.8, 17.5]	-16.1	0.9993	$EC_{50,NH3}$ = 11.8 mg NH_3 L^{-1} [6.1, 17.5], N = 0.78 [0.34, 1.21]
C_3	-21.0	0.9982	$EC_{50,NH3}$ = 11.7 mg NH_3 L^{-1} [8.2, 15.2]	-15.3	0.9981	$EC_{50,NH3}$ = 12.3 mg NH_3 L^{-1} [7.9, 16.6], N = 1.15 [0.58, 1.71]
Avg	-	-	*$EC_{50,NH3}$ = 14.1 ± 3.0 mg NH_3 L^{-1}*	-	-	*$EC_{50,NH3}$ = 14.2 ± 3.7 mg NH_3 L^{-1}, N = 1.12 ± 0.32*
CB_1	-10.3	0.9972	$EC_{50,NH3}$ = 21.8 mg NH_3 L^{-1} [4.4, 39.2]	-17.6	0.9998	$EC_{50,NH3}$ = 21.4 mg NH_3 L^{-1} [17.8, 25.0], N = 2.01 [1.37, 2.67]
CB_2	-16.6	0.9983	$EC_{50,NH3}$ = 32.4 mg NH_3 L^{-1} [18.4, 46.5]	-10.4	0.9979	$EC_{50,NH3}$ = 31.6 mg NH_3 L^{-1} [15.3, 47.9], N = 1.12 [0.33, 1.91]
CB_3	-9.3	0.9832	$EC_{50,NH3}$ = 24.4 mg NH_3 L^{-1} [2.8, 46.1]	-7.4	0.9903	$EC_{50,NH3}$ = 22.7 mg NH_3 L^{-1} [11.8, 33.6], N = 1.92 [0.23, 3.61]
Avg	-	-	*$EC_{50,NH3}$ = 26.2 ± 5.5 mg NH_3 L^{-1}*	-	-	*$EC_{50,NH3}$ = 25.2 ± 5.6 mg NH_3 L^{-1}, N = 1.68 ± 0.49*
MICROALGAE						
Test ID	**Model 1 (non-competitive inhibition)**			**Model 2 (sigmoidal logistic function)**		
-	**cAIC**	**R_{ADJ}^2**	**Estimated parameters**	**cAIC**	**R_{ADJ}^2**	**Estimated Parameters**
M_1	-18.8	0.9996	$EC_{50,NH3}$ = 60.9 mg NH_3 L^{-1} [39.7, 82.1]	-12.4	0.9995	$EC_{50,NH3}$ = 60.3 mg NH_3 L^{-1} [34.5, 86.1], N = 1.08 [0.42, 1.75]
M_2	-15.1	0.9996	$EC_{50,NH3}$ = 77.7 mg NH_3 L^{-1} [37.7, 117.7]	-13.6	0.9998	$EC_{50,NH3}$ = 71.1 mg NH_3 L^{-1} [49.0, 93.1], N = 1.49 [0.73, 2.24]
M_3	-12.7	0.9960	$EC_{50,NH3}$ = 96.3 mg NH_3 L^{-1} [31.2, 161.3]	-9.5	0.9972	$EC_{50,NH3}$ = 54.2 mg NH_3 L^{-1} [34.2, 74.2], N = 1.80 [0.62, 2.97]
M_4	-19.6	0.9993	$EC_{50,NH3}$ = 52.6 mg NH_3 L^{-1} [26.1, 66.4]	-15.3	0.9994	$EC_{50,NH3}$ = 52.4 mg NH_3 L^{-1} [37.1, 67.7], N = 1.20 [0.68, 1.73]
MB	-14.2	0.9994	$EC_{50,NH3}$ = 88.4 mg NH_3 L^{-1} [37.9, 138.9]	-16.6	0.9999	$EC_{50,NH3}$ = 78.7 mg NH_3 L^{-1} [61.5, 95.9], N = 1.63 [1.01, 2.26]
Avg	-	-	*$EC_{50,NH3}$ = 75.2 ± 18.3 mg NH_3 L^{-1}*	-	-	*$EC_{50,NH3}$ = 63.3 ± 11.3 mg NH_3 L^{-1}, N = 1.44 ± 0.30*

$EC_{50,NH3}$ for *Scenedesmus obliquus* (60.9 mg NH_3 L^{-1}) are slightly lower, but in the same order of magnitude, than what reported by Azov and Goldman and by Collos and Harrison, [73] and [72].

Regarding cyanobacterial monocultures, estimated inhibition parameters and model fits are reported in Figure 5.18 B. As mentioned, contrarily to other findings [72], the adverse effect of FA on photosynthesis was more pronounced in cyanobacteria than in microalgae. This is confirmed by comparing the average $EC_{50,NH3}$ for the two types of organisms (Table 5.10).

For cyanobacterial monocultures, the average $EC_{50,NH3}$ was 14.1 mg NH_3 L^{-1}, with similar values among the different strains adopted. Unluckily, only a few authors reported inhibition parameters for cyanobacteria, and most available data are for the strain *Arthrospira platensis sp.*, typically characterized by a high resistance to

FA [74], [214]. However, all the values obtained for cyanobacterial monocultures and mixed populations fall in the range indicated by Collos and Harrison [72] (4.3 - 34.8 mg NH_3 L^{-1}).

5.3.2. Effects of free ammonia on mixed algae-bacteria consortia

The value of $EC_{50,NH3}$ for the mixed microalgae-bacteria consortium was among the highest and also the coefficients determined for cyanobacteria mixed cultures were higher than those obtained from monocultures data. Due to the increase in the $EC_{50,NH3}$ for both microalgae and cyanobacteria monocultures to mixed cultures (Table 5.10), a first interpretation of results would suggest that the environmental conditions in which the mixed cultures are grown selected phototrophic strains that are more robust and tolerant to adverse conditions, including inhibitory compounds. Unravelling this aspect would contribute to a better understanding of the interactions between microorganisms in wastewater treatment processes with microalgae-bacteria (e.g., optimizing influent TAN loading rates, or adopting dynamic pH setpoints based on TAN). However, the difference in the effect of FA on microalgae mixed and monocultures could not be explained by ANOVA (*p-value* = 0.501), therefore microalgae monocultures and mixed consortia could be described by an average value of $EC_{50,NH3}$ = 75 mg NH_3 L^{-1}. On the contrary, cyanobacteria growing in monocultures and mixed cultures were characterized by statistically different values of the inhibition parameter. In this case, an average value of $EC_{50,NH3}$ = 14 mg NH_3 L^{-1} was estimated for monocultures, which is significantly different from the $EC_{50,NH3}$ of 26 mg NH_3 L^{-1} obtained for mixed cultures (*p-value* = 0.029). As a comparison, nitrifying bacteria were also reported to be inhibited by FA, with a differential effect on AOB and NOB. Indeed, previous works indicated that AOB are less susceptible to high levels of FA, with the inhibition occurring in the range of

12.1 - 182.1 mg NH_3 L^{-1}; on the contrary, NOB are more sensitive to FA, and inhibited growth has been reported in presence of 0.12 - 1.2 mg NH_3 L^{-1}[316]–[319].

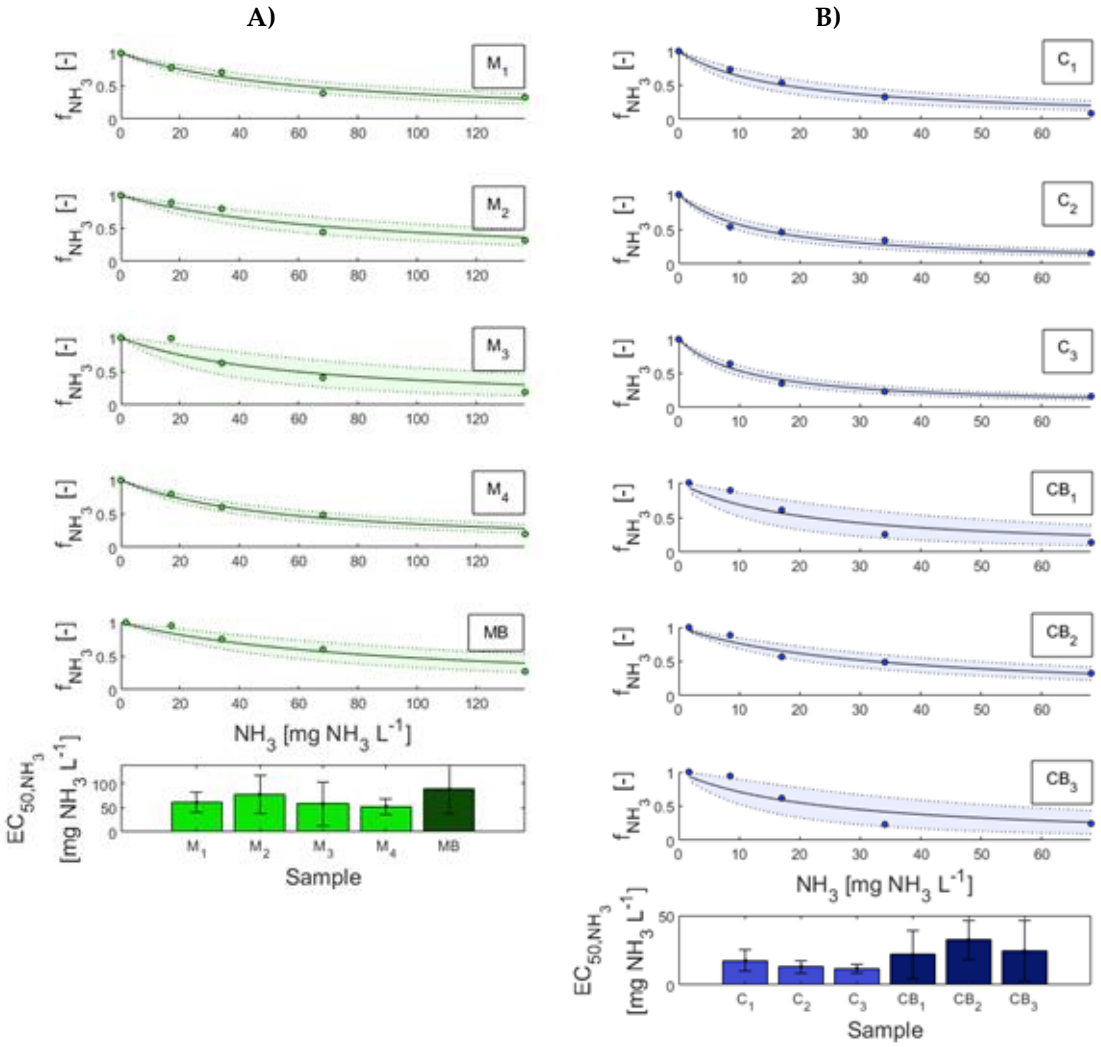

Figure 5.18. Effects of free ammonia inhibition on microalgae and cyanobacteria: reduction of fNH3, non-competitive inhibition model fit and estimated model parameters (A: Microalgae, B: Cyanobacteria, samples abbreviations: M1 = Chlorella vulgaris, M2 = Scenedesmus quadricauda, M3 = Chlorella sorokiniana, M4 = Scenedesmus obliquus, MB = Sample from the HRAP; C1 = Synechocystis, C2 = Synechococcus, C3 = Leptolyngbya, CB1 = Sample from the semi-closed PBR1, CB2 = Sample from the semi-closed PBR2, CB3 = Sample from the semi-closed PBR3. Shaded areas and error bars represent 95% confidence intervals).

5.3.3. Free ammonia inhibition scenarios in microalgae-based wastewater treatment

To evaluate the need for considering FA inhibition in algae/bacteria modelling, several scenarios were analysed by calculating theoretical FA concentration profiles during typical operational days in the pilot plants. Scenarios were defined by varying: i) the season (spring, summer and autumn), ii) the setpoint of the pH-control system (7, 8 and 9 for microalgae and 8.5, 9.5 and 10.5 for cyanobacteria) and iii) the initial TAN concentration in the suspension (5, 10 and 20 mg N-TAN L^{-1} for cyanobacteria and 35, 70 and 140 mg N-TAN L^{-1} for microalgae). Typical daily patterns were defined for incident PAR and water temperature, by averaging hourly data collected over a long-term period (January 2017 - November 2019) in the two pilot-scale systems in which FA inhibition was assessed, namely the Bresso-Niguarda HRAP and the Agropolis semi-closed PBRs. Irradiance data were collected from the closest weather stations located near each pilot-plant site, and water temperature was logged by temperature probes in pilot reactors. Daily average trends for each season are shown in Figure 5.19. pH setpoints and TAN concentrations were chosen according to values measured in pilot plants during the photo-respirometric campaigns, in order to reflect relevant conditions that are commonly met in wastewater-treating outdoor PBRs. The measured pH value in the microalgae-bacteria system was on average 7.0 (maximum pH: 8.5), because of the high nitrification rates reported [269] and compared with the higher values measured in the cyanobacteria-bacteria systems (average pH = 8.4, maximum pH = 9.5). Likewise, the measured TAN concentration in the microalgae-bacteria system was on average = 34 mg N-TAN L^{-1} (maximum TAN = 71 mg N-TAN L^{-1}). This condition reflects the high concentration of NH_4^+ in the LFAD (240 ± 55 mg N-NH_4^+ L^{-1}, on average) and the presence of residual NH_4^+ concentration in the suspension, possibly due to low transitory algal activities. On the contrary,

cyanobacteria scenarios were characterized by lower TAN concentrations, as the influent agricultural runoff was a low strength wastewater stream [273]. The biomass was subjected to starvation to promote the accumulation of biopolymers and fed with nitrate as nitrogen source, with the ammoniacal nitrogen being almost absent during the entire experimentation (average TAN = 0.3 mg N-TAN L^{-1}, maximum TAN = 2.9 mg N-TAN L^{-1}).

In addition to modelling FA inhibition, to describe a more realistic photosynthetic sOPR trend during typical days, the switch functions describing the dependence on light, temperature and pH were also evaluated, according to the previously described selection criteria and using the estimated model parameters.

The model describing the overall trend of oxygen production can be represented in two different ways: by using the product of the mentioned switch functions (i.e. Equation 4.20 and Equations 4.24, 4.28 and 4.30) (f_{TOT}, Equation 5.1), or by considering the minimum value assumed by each switch function ($f_{P,TOT,MIN}$, Equation 5.2). Since during photo-respirometric tests performed in this work nutrient solutions were added at the beginning of each experiment, the nutrient switch function present in Equation 4.17 was theoretically equal to one and it was neglected. $f_{P,pH}$ was constant, as a pH-control is implemented. No light/solute-gradients were included (0-D model), therefore an average irradiance and a perfect mixing were considered. The switch function describing the dependence on DO was also not considered in this evaluation, under the hypothesis that an efficient degassing unit is also available.

The overall switch functions, $f_{P,TOT}$, and $f_{P,TOT,MIN}$, were therefore represented as:

$$f_{P,TOT} = f_{P,I} * f_{P,T} * f_{P,pH} * f_{P,NH_3} \quad 5.1$$

$$f_{P,TOT;MIN} = \min(f_{P,I} * f_{P,T} * f_{P,pH} * f_{P,NH_3}) \quad 5.2$$

The parameters characterizing the described switch functions were calibrated for the microalgae-bacteria consortium in the Bresso-Niguarda HRAP (as the main result of the "model calibration protocol"). However, since no experimental data were available to describe the effects of environmental conditions on cyanobacteria, and the optimal conditions for cyanobacteria are not always available in literature, possibly being very different from microalgal optima [320], the evolution of switch functions was only modelled for the HRAP case study.

Since during photo-respirometric tests performed in this work nutrient solutions were added at the beginning of each experiment, the nutrient switch function present in Equation 4.17 was theoretically equal to one and it was neglected. $f_{P,pH}$ was constant, as a pH-control is implemented. No light/solute-gradients were included (0-D model), therefore an average irradiance and a perfect mixing were considered. The switch function describing the dependence on DO was also not considered in this evaluation, under the hypothesis that an efficient degassing unit is also available. The overall switch functions $f_{P,TOT}$ (Equation 5.3) and $f_{P,TOT,MIN}$ (Equation 5.4) were therefore represented as:

$$f_{P,TOT} = f_{P,I} * f_{P,T} * f_{P,pH} * f_{P,NH_3} \quad 5.3$$

$$f_{P,TOT;MIN} = \min(f_{P,I} * f_{P,T} * f_{P,pH} * f_{P,NH_3}) \quad 5.4$$

The parameters characterizing the described switch functions were calibrated for the microalgae-bacteria consortium in the Bresso-Niguarda HRAP (as the main result of the "model calibration protocol").

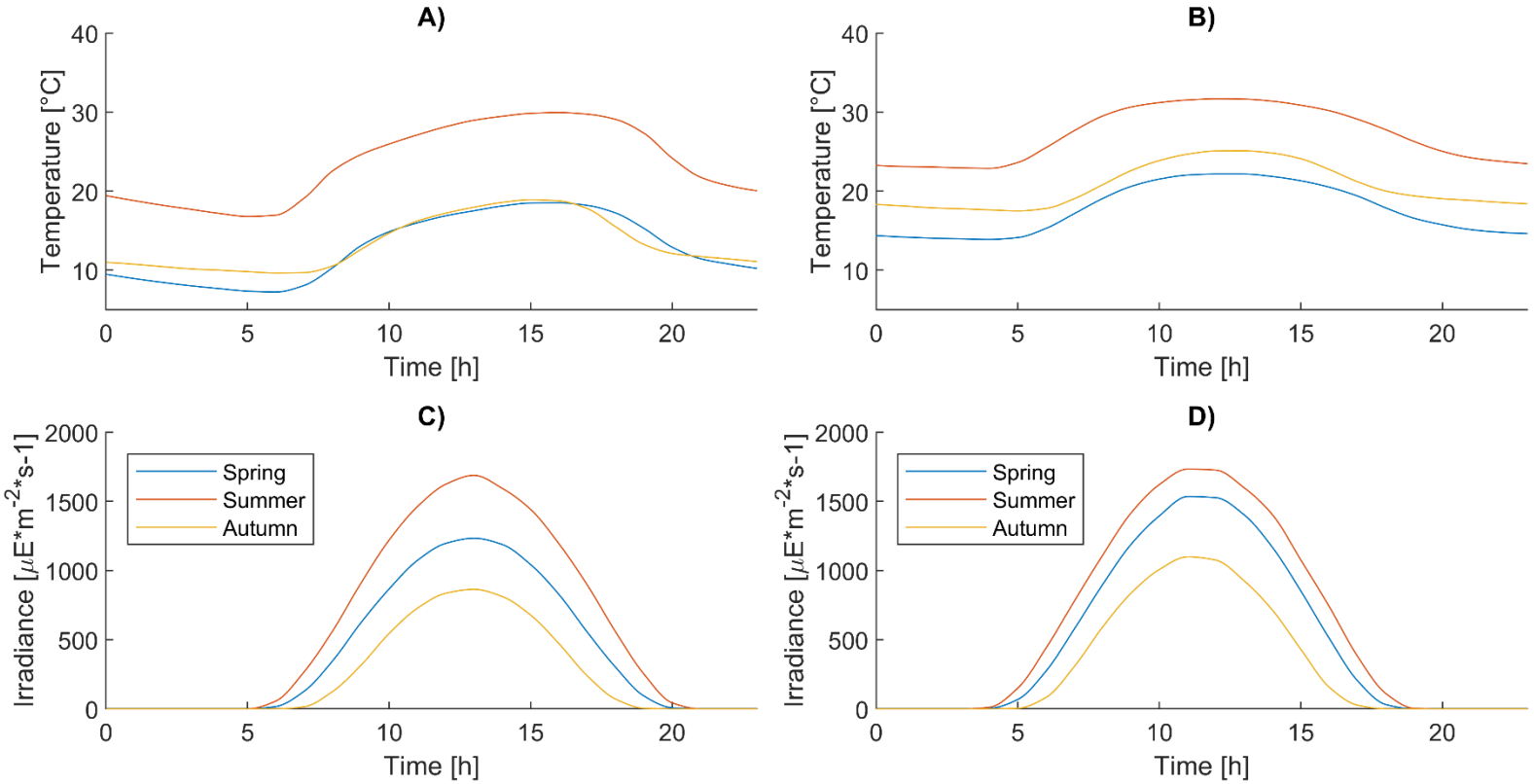

Figure 5.19. Typical daily variations of water temperature and irradiance for different seasons (A = water temperature in the HRAP, B = water temperature in semi-closed PBRs, C = irradiance data for the HRAP, dataset: January 2017 - November 2019).

However, since no experimental data were available to describe the effects of environmental conditions on cyanobacteria, and the optimal conditions for cyanobacteria are not always available in literature, possibly being very different from microalgal optima [320], the evolution of switch functions was only modelled for the HRAP case study.

The utilization of parameter estimates for the obtained FA inhibition model can be particularly useful to evaluate the extent of the inhibition due to FA in several common operational conditions of the phototrophs-bacteria cultivation processes. For example, rising TAN concentrations can result from limited removal rates during start-up periods or due to adverse atmospheric conditions. Similarly, the pH value can rise during the day, as a result of the photosynthetic activity. As an example, the photosynthesis inhibition model was run using the time-series describing the daily evolution of FA during typical days in each scenario (i.e. by varying the season, the average pH and total TAN). To predict the FA response, Equation 4.19 was used with the estimated values of inhibition parameters (i.e., $EC_{50,NH3}$ = 88.4 mg NH_3 L^{-1} for microalgae-bacteria and $EC_{50,NH3}$ = 26.2 mg NH_3 L^{-1} for cyanobacteria-bacteria). The evolution of the inhibition function (f_{NH3}) under the identified environmental/operational conditions is depicted in Figure 5.20 for microalgae and cyanobacteria. Although the value of the microalgae-bacteria inhibition parameter is high, which means a high resistance to FA, severe inhibition levels can be reached under the worst conditions. In particular, the values of f_{NH3} during autumn indicate a photosynthesis inhibition of 30%, while the inhibition can reach values higher than 40%, during summer times. Temperature variations seem to have a lower influence on FA production, compared to the other parameters. When comparing summer and autumn, maximum f_{NH3} variations fall within 30% due to temperature variations, while larger effects are associated to the variation of other parameters (TAN and pH). At low and average pH, f_{NH3} is close to one,

regardless of the TAN concentration or the seasonal condition imposed. A drastic drop in photosynthetic sOPRs occurs with higher pH values. Similarly, in the cyanobacterial mixed culture, the inhibition function can result in a limited photosynthetic oxygen evolution during the day, due to the high pH values and temperatures. f_{NH3} can reach very low values (up to 75% inhibition), thus depicting severe inhibition, even if the considered TAN concentrations are seven times lower than those expected in HRAP scenarios. This clearly indicates the high influence of pH on FA generation, confirming that pH should be strictly controlled in wastewater treatment PBRs, to prevent reductions in the photosynthetic oxygenation by phototrophs. For the microalgae-bacteria consortium case study, the trends for f_{TOT} and for the functions expressing the dependence of photosynthesis on FA and environmental conditions were also constructed. Switch functions are shown in Figure 5.21, for a TAN concentration of 60 mg N-TAN L^{-1} and for different seasons and pH conditions. Among the studied variables, temperature is the one most directly affecting photosynthetic sOPR: the value assumed by the f_T switch function is always the lowest (excluding the irradiance switch function, which is obviously zero during the night). This is particularly evident during autumn (Figure 5.21B and Figure 5.21D), when temperature is lower than the optimum.

During summer, temperature approaches the optimal value, resulting in f_T close to one for almost all the daytime. Although summer temperatures are close to optimal values resulting in higher f_T values, the increase in temperature also favours the FA formation, what inhibits photosynthesis (Figure 5.21A and Figure 5.21B).

The combined effects of temperature and pH are evident when the pH is 9 (Figure 5.21C and Figure 5.21D): f_{TOT} reaches approximately 0.6-0.65 during summer and is reduced to approximately 0.5 during autumn. Regarding f_{NH3}, it has

comparable or lower values than the f_T during summer, indicating that under these conditions the inhibition due to FA is the most relevant limitation occurring in the reactor. It is also important to notice that the pH value can be responsible for a reduction of the photosynthetic activity in itself. This reduction is negligible at pH 7, but at a pH of 9 causes a reduction of approximately 15% of the sOPR.

Regarding the choice of the most suitable switch function to describe the combined effects of environmental parameters and FA, similar results were obtained by using both $f_{P,TOT}$ and $f_{P,TOT,MIN}$ (Figure 5.22). The difference among the two models is more emphasized when the values of the single switch functions is higher. This can be noticed by comparing the results obtained at pH 7 (Figure 5.22A and Figure 5.22B) and at pH 9 (Figure 5.22C and Figure 5.22D): as the switch functions for pH and FA decrease, the difference among Equation 5.3 and Equation 5.4 becomes larger. Although the observed difference among the two models is small, a possible magnification of the sOPR reduction should be expected when using Equation 5.3, especially in the caase in which several switch functions are present to describe the effects of several nutrients and environmental conditions. Choosing this function is however cautelative, in view of estimating the DO availability for bacteria. In addition, the function has a smoother shape compared to the minimum function, due to the fact that local first-order derivative has no discontinuity, thus improving the stability of numerical simulations.

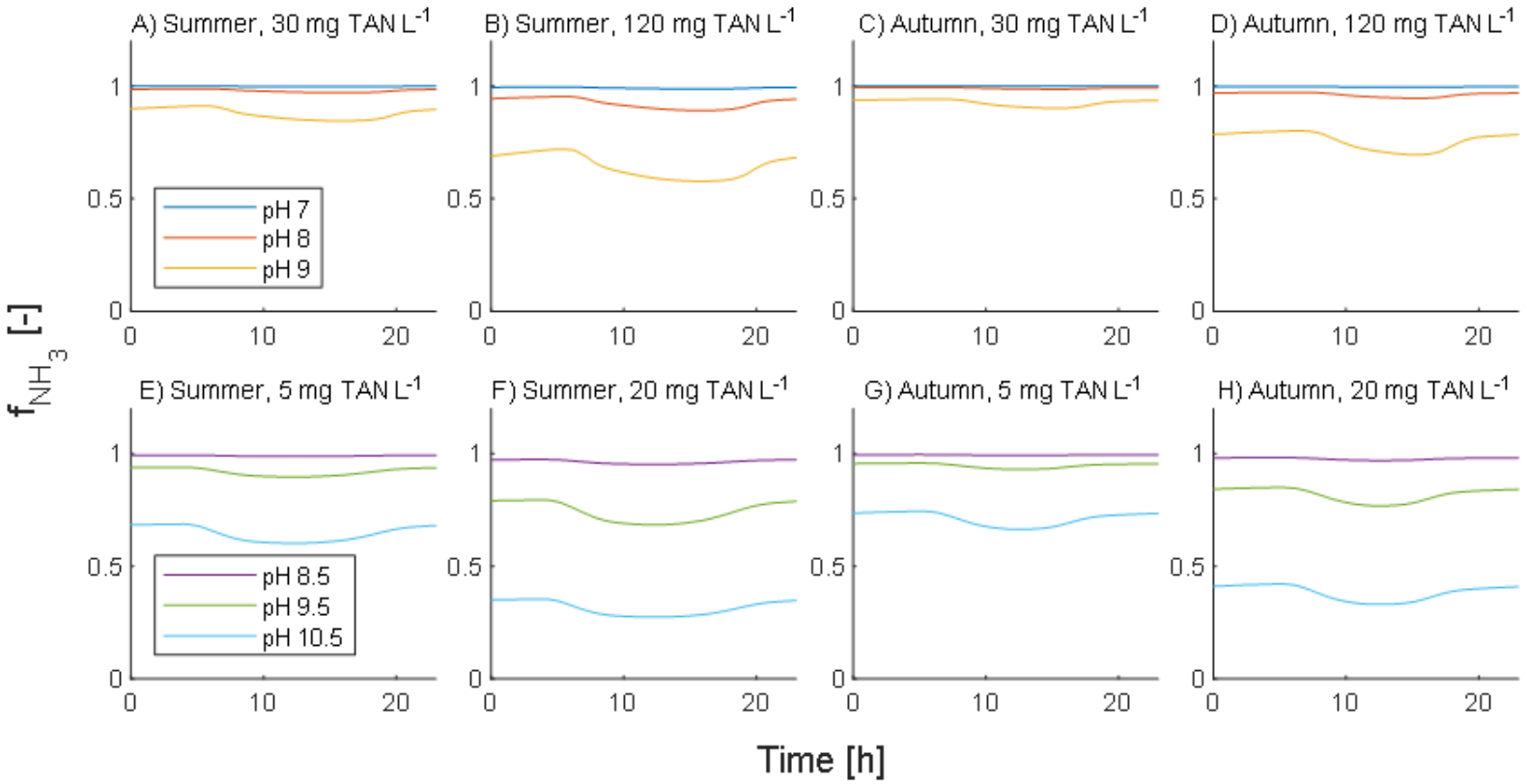

Figure 5.20. Simulated evolution of the inhibition function (f_{NH3}) under typical daily variations for different seasons, pH values and TAN concentrations. Inhibition functions are calculated considering microalgae (A - D) and cyanobacteria (E - H) as dominant species in mixed phototrophs-bacteria consortia.

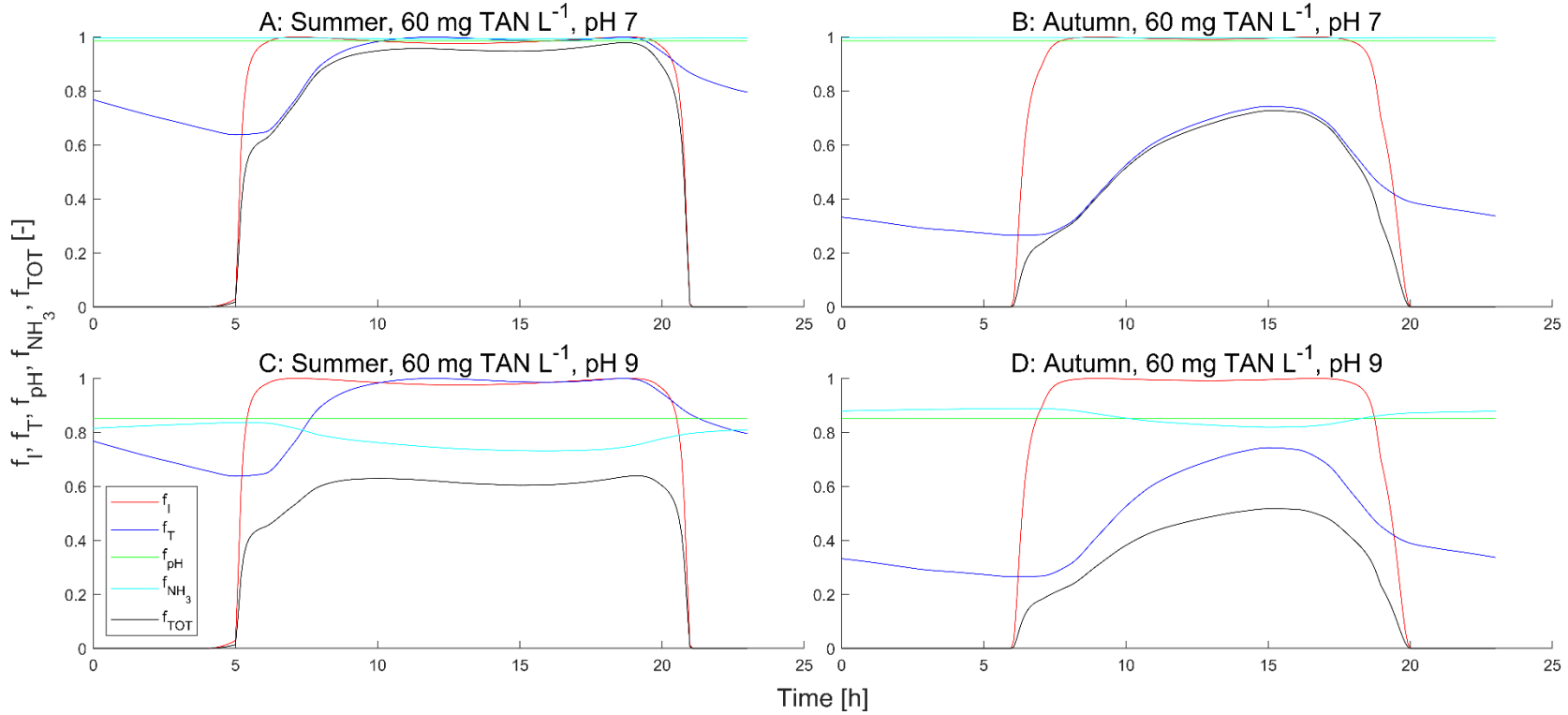

Figure 5.21. Simulated evolution of switch functions in the HRAP at 60 mg N-TAN L-1 for different seasons and pH values (A = summer, low pH, B = autumn, low pH, C = summer, high pH, D = autumn, high pH).

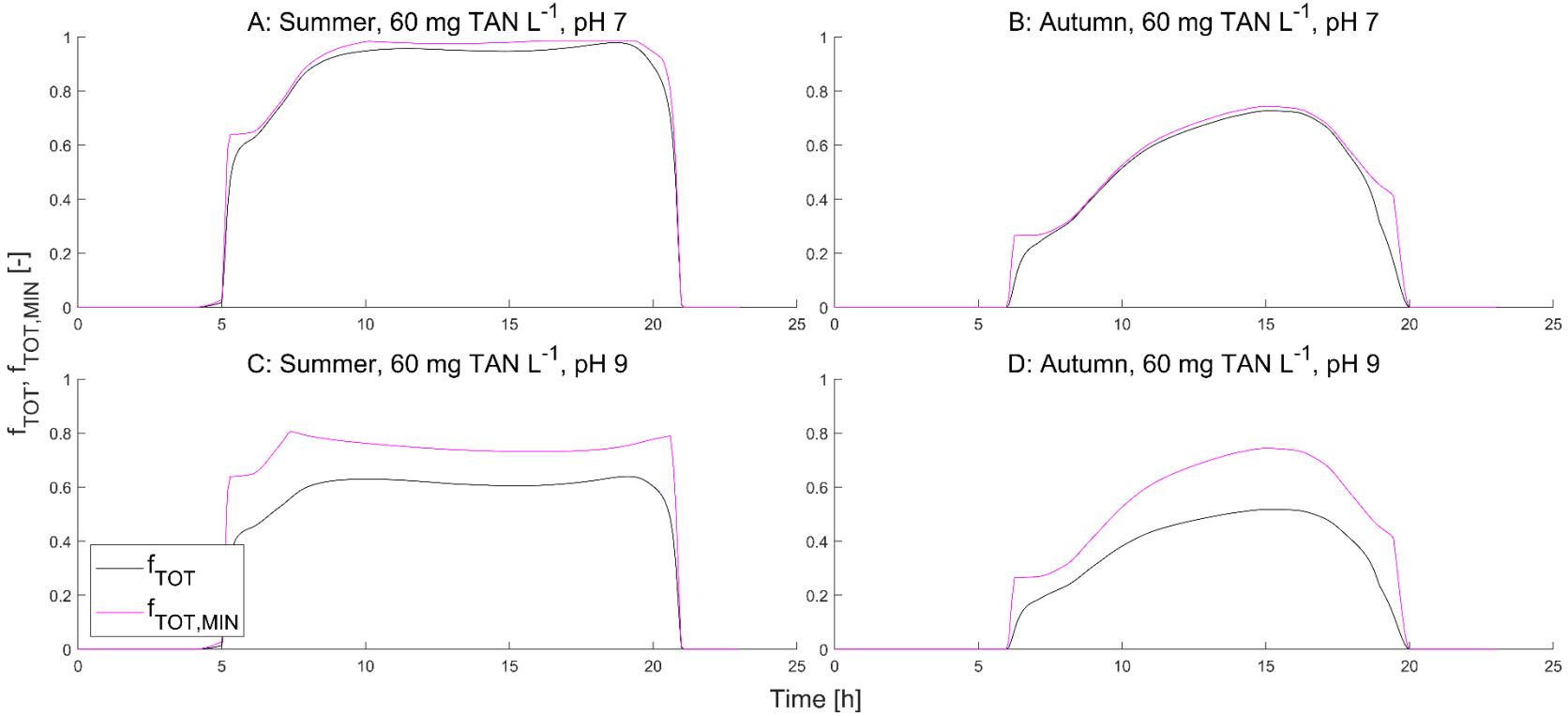

Figure 5.22. Simulated evolution of different switch functions to to describe the combined effects of environmental parameters and free ammonia: product of all the switch functions (black) and minimum of each switch function (magenta) (A = summer, low pH, B = autumn, low pH, C = summer, high pH, D = autumn, high pH).

CHAPTER 6

CONCLUSIONS AND PERSPECTIVES

6. CONCLUSIONS AND PERSPECTIVES

6.1. Conclusions

Respirometry has been extensively applied for characterizing the activity of biological suspensions exploited during wastewater treatment, as remarked in Chapter 2. The flexibility provided by respirometric measurement, combined with the high repeatability of the experiments, strongly contributed to the diffusion of monitoring and modelling techniques for conventional biological treatment processes. As reported in the scientific literature, photo-respirometry has been also extensively adopted for estimating the dependence of microalgal photosynthesis and respiration on several environmental parameters. However the versatility of the photo-respirometric method, combined with the absence of standardized protocols, eventually led to the definition of extremely diversified procedures in the literature, with different authors adopting different experimental setups and biomass monitoring techniques, thus hindering the results comparability. Similar difficulties rise when applying photo-respirometry to microalgae-bacteria consortia. In addition, as higlighted in Chapter 1, microalgae-bacteria consortia are quite complex biological systems, what makes the interpretation and comparison of photo-respirometric results even more. Discerning phototrophic/bacterial contributions to DO dynamics has been previously attempted only by a few authors. A description of proposed protocols and photo-respirometric devices was however lacking in literature. Therefore, experimental methods for activated sludge bacteria, phototrophic organisms and microalgal-bacterial consortia were reviewed, eventually representing a starting point for future photo-respirometry studies to characterize algae-bacteria consortia using standardized photo-respirometric protocols.

The review presented in Chapter 2 was particularly focused on the potential application of (photo-)respirometry-based techniques, and on the most important challenges faced in this research line. The knowledge gathered from the literature analysis could be put in practice with the definition of three photo-respirometric protocols to be applied to existing microalgae-bacteria units treating real wastewaters (the *monitoring*, *model calibration* and *inhibition* protocols). These protocols were defined contextually to a series of indications, aimed at obtaining standardized methodologies to conduct the experiments under replicable conditions, to facilitate the comparison with literature and to avoid common mistakes in the execution of photo-respirometry assays. These protocols were based on the implementation of changing environmental conditions and the use of selective compounds for inhibiting the nitrifying bacteria and evaluate the main contributions to oxygen dynamics. Each protocol was optimized in order to balance the test duration and reliability of results. A fully equipped photo-respirometer was eventually designed and used to assess microbial activity, the system being characterized by a high data logging resolution and setup flexibility. The photo-respirometer included different options for the control of environmental conditions, such as gas bubbling and the dosage of concentrated solutions. When possible, tests were also performed inside a thermo-incubator to also gain complete control over the temperature and irradiance conditions. However, all the protocols proposed in this work for monitoring and modelling microalgae-bacteria systems can be equally executed using a simple instrumentation, including a light source and a DO probe equipped with data logging.

In order to standardize the photo-respirometric protocols, several challenges were faced, and different expedients were proposed to maximize the precision. These improvements included: i) the standardisation of environmental test conditions thanks to appropriate control-systems, ii) the standardisation of the

initial biomass concentration and light penetration in the sample, iii) the choice of appropriate acclimation times and duration of L/D phases, and iv) the standardisation of initial nutrient and inhibitor concentrations. The mentioned protocols were applied on a broad range of microalgae-bacteria consortia, grown on wastewaters from both municipal and industrial sources (anaerobic digestates from municipal wastewaters and from piggery wastewaters, aquaculture wastewaters, agricultural runoff wastewaters, and pre-treated piggery wastewaters). The size of the cultivation photobioreactors tested ranged from the lab-scale (2 - 3.5 L) to pilot-scale (80 L - 1.2 m^3) and pre-industrial-scale systems (approximately 36 m^3). The dominant phototrophs in these systems were consortia of green microalgae (mainly *Chlorella* sp. and *Scenedesmus* sp.) or cyanobacteria (*Synechocystis* sp. and *Synechococcus* sp.), which are commonly found in outdoor algae-bacteria systems and exploited for wastewater treatment. Therefore, the results obtained in this work could serve as a reference point in the analysis of existing algae-bacteria systems or to make important assumptions, during the design of new systems.

The main feature of the monitoring protocol was the possibility of simultaneously retrieving information about the algal and bacterial oxygen production/consumption rates. Indeed, with the application of the protocol, the specific oxygen production or consumption rates deriving from the metabolisms of the different microbial guilds involved could be successfully distinguished in the wide range of cultivation conditions tested. To the best knowledge of the author, a similar overview of bacterial activities in different microalgae-bacteria systems treating wastewater was missing in the specialized literature. For this reason, the development of a protocol allowing to obtain information about nitrification rates in a fast and standardized way represents an important advance in monitoring microalgae-bacteria bioprocesses.

The model calibration protocol was defined to determine the effects of environmental conditions on the photosynthetic and respiratory rates of an algal-bacterial consortium upon inhibition of nitrifiers by ATU and was specifically applied to study the relevance of irradiance, temperature, pH and DO on the photo-oxygenation process, within a wide range of conditions including common outdoor conditions measured at the pilot site were the consortium was cultivated. Two novel datasets were obtained for phosynthesis and respiration on non-axenic cultures. Indeed, the application of the proposed protocol allowed to assess the optimum conditions directly on the algal-bacterial consortium, in a fast and reliable way. These data were used to compare different mathematical models to select the most suitable equations to describe the experimental data. Following this procedure, a comprehensive dataset of calibrated and reliable models (with adjusted R^2 ranging from to 0.69 to 0.95) were obtained, to be used for further modelling studies.

The inhibition protocol was defined to assess the effect of a potential inhibitor to the photosynthetic activity and it was specifically applied to the case of free ammonia inhibition. The nitrifying activity was inhibited, as it was done in the model calibration protocol. In the inhibition protocol, the decrease in sOPR was followed at increasing free ammonia concentrations, while a control reactor was utilized to determine reference activities. The protocol was applied to the consortium developed in the pilot system treating the liquid fraction of anaerobic digestates and on cyanobacteria grown on agricultural runoff water. Monocultures were also tested for providing a comparison between organisms growing under controlled lab-scale conditions and in consortia with bacteria in outdoor conditions. Results showed that microalgae and cyanobacteria were differently inhibited by free ammonia, with microalgae showing higher resistance than cyanobacteria and suggested that photosynthetic activities were less affected by FA in algae-bacteria systems than in monocultures, probably

because the biomass grown in outdoor systems developed a higher tolerance to adverse conditions. Although no evident effects of free ammonia on respiration rates was recorded in the organisms tested, the inhibition protocol allows to identify short-term inhibition effects on the respiration too. These findings are of high interest, especially due to the lack of literature information regarding ammonia inhibition in mixed algae-bacteria consortia, for which the cultivation conditions typically promote the its formation. In addition, the proposed procedure was standardized to generate a dataset of comparable EC_{50} values and theoretical dose-response curves, useful for further modelling studies. The protocol can be easily extended to different chemicals known to be inhibitory for the algal-bacterial biomass (e.g. herbicides/pesticides or aromatic compounds). This would allow to improve the predicting ability of existing mathematical models. Indeed, the simulation of different weather/operational conditions showed that free ammonia can drastically impact photo-oxygenation during wastewater bioremediation. The results obtained suggest that considering free ammonia inhibition in existing mathematical models would lead to more reliable predictions.

It is finally important to stress that the protocols can be adapted to be exploited to analyze other relevant aspects of the microalgae-bacteria cultivation process than those mentioned in this work. For example, the monitoring protocol can be modified to include the assessment of heterotrophic bacteria respiration, once an effective way to inhibit either heterotrophs or phototrophs is found (see section 6.2). Similarly, the model calibration protocol can be theoretically applied/modified to determine important kinetic or stoichiometric parameters of phototrophic organisms (such as the maximum growth rate or the half-saturation constants for nutrients), by adapting the experimental procedure to the specific aim and by coupling photo-respirometric data to a comprehensive mathematical growth model. In a similar way, the inhibition protocol can be potentially applied

to obtain information regarding any inhibitory compound/wastewater or stressing condition (e.g. increased salinity).

6.2. Further research required

In this research work, the proposed photo-respirometric protocols were successfully applied, achieving the main goals of the thesis, i.e. to define and validate standardized operational procedures and laboratory equipment necessary to describe the algal and bacterial metabolisms in microalgae-bacteria PBRs currently operated for wastewater treatment. The procedure allowed obtaining robust datasets for systems treating real wastewaters.

However, some aspects of the respirometric protocols defined still require further in-depth analyses as summarized hereafter:

i) Better characterizing the activities of heterotrophic bacteria and the occurrence of algal mixotrophic growth,

ii) Exploiting selective inhibitors for other organisms (i.e. for microalgae and/or heterotrophic and for nitrite-oxidizing bacteria) during photo-respirometric tests,

iii) Evaluating possible adverse effects of biomass pre-treatments.

The presence of heterotrophic bacteria in microalgae-bacteria systems complicates the separation of algal and bacterial contributions on the overall respiration process due to bacteria respiration and algal dark respiration or mixotrophic growth. This aspect represents the most important research need to be faced, in order to fully exploit the potentiality of the proposed protocols and to exteend their applications also to those systems in which the growth of heterotrophic bacteria and the algal mixotrophy cannot be ruled out. In this

sense, having the possibility of exploiting selective inhibitors for heterotrophic bacteria and/or for phototrophs would allow for a faster and easier distinction between heterotrophic OUR and phototrophic respiration. Unluckily, an inhibitor with such characteristics has not been identified in literature, although potentially suitable compounds were already proposed and applied to suppress the heterotrophic activity (such as peracetic acid, PAA) or the phototrophic activity alone (e.g. using wide-spectrum antibiotics or herbicides). In preliminary tests performed on activated sludge, microalgae and microalgae-bacteria suspensions, PAA seemed to show interesting properties, being the photosynthetic activity of microalgae almost unaffected at the concentrations to which the disinfectant is expected to suppress heterotrophic activity (2 - 5 mg PAA L^{-1}). In this viewpoint, a deeper characterization of PAA dose-response curves is definitely required, prior to adapting the proposed photo-respirometric protocols for the utilization of PAA in the bioassay.

Such an inhibitor would path the way toward new applications. Indeed, the flexibility of photo-respirometric methods allows to design experiments in which the variation of sOPR and sOUR of the algae-bacteria consortium are characterized under conditions promoting the mixotrophic growth. Indeed, previous findings confirmed that particular combinations of irradiance, biodegradable COD and inorganic carbon influenced one metabolism over the other, with subsequent variation in the overall sOPR and sOUR. However, no clear and uniform indications are available on which combination of factors effectively promote this metabolism over the phototrophic one in real systems. Therefore, specific experiments could be designed in order to evaluate the occurrence of mixotrophy at the test conditions.

In this work, the use of ATU was proven to be effective to stop the activity of AOB and did not substantially modify the photosynthetic activity of the

consortium, coherently with other studies cited. However, information is scarce regarding the inhibition of photosynthesis due to ATU in the short and long term. A complete screening of ATU effects on the main species of green algae and cyanobacteria used for the bioremediation of wastewaters would be useful to determine if inhibition processes may occur. In the first attempts to define the monitoring protocol, the activity of both AOB and NOB were included in the mass balance, and the inhibitor $KClO_3$ was dosed to calculate the activity of NOB. However, this idea was later discarded since the NOB activity was practically undetectable, and the dosage of the inhibitor substantially modified the salinity and pH of the suspension. In any case, evaluating the NOB activity remains of great interest, as the accumulation of nitrite is a commonly described feature of microalgae-bacteria systems treating wastewaters from both municipal and industrial sources. In addition, although the NOB activity is expected to scarcely impact the overall OUR of the consortium, the use of such an inhibitor for NOB would allow for a more exhaustive description of the system's behaviour and for a more accurate calibration of mathematical models. Therefore, a screening of commonly used NOB inhibitors should be also carried out on microalgae-bacteria and enriched NOB suspensions to evaluate the possibility of reintroducing it in the protocol.

Regarding the effect of pretreatments on the algal biomass, as already pointed out the algal respiration can vary as a result of stress conditions of the biomass, due for example to osmotic stress or the application of shear stress. In this viewpoint, the effects of biomass pre-treatments should be also assessed, in order to avoid erroneous estimations of the algal activity. In particular, possible salinity stress associated with the dilution/resuspension in synthetic media with significant alterations in the ionic composition should be evaluated. For the same reason, it is important to estimate if there is any stress induced by the centrifugation of the sample.

Besides these aspects for which a further research is strongly suggested, the application of the proposed protocols would allow exploring other interesting aspects of microalgae-bacteria systems. In particular, photo-respirometry could be applied for:

i) Assessing the variability of optimal growth conditions during different seasons and at different nutrient availability conditions,

ii) Better characterizing the occurrence of acclimation processes in outdoor PBRs for microalgae/cyanobacteria cultivations

iii) Obtaining a better characterization of light and dark respiration processes.

Indeed, as previously observed by other researchers, the optimal conditions identified for phototrophic organisms can vary as a consequence of different environmental/operational conditions applied. For example, cardinal parameters describing the growth of phototrophs can be subject to an evolution during different seasons, as a consequence of adaptive mechanisms or due to nutrient starvation conditions. For these reasons, the model calibration protocol should be repeated as frequently as possible during the year, in order to catch the seasonal variations and to identify any trend in model parameters as a result of changes in the algal community or of adaptation. Finally, as highlighted in some of the studies reviewed, different respiration rates can be measured in the phototrophic algal metabolism, according to the light conditions applied. Indeed, an increased respiration rate can be measured in algal cells immediately after their exposure to light, which is the algal light respiration, while a long-term exposure to dark conditions is known to cause a lower respiration rate, which cannot be measured during the short-time of the proposed protocols. Nonetheless, photo-respirometry is particularly suitable for the determination of

oxygen consumption rates. For this reason, the design of a specific protocol and the execution of an extensive photo-respirometry campaign would allow characterizing the dark respiration processes, representing a desirable extension to the proposed techniques to better estimate oxygen consumption during nighttime, providing additional predicting ability to mathematical models.

BIBLIOGRAPHY

[1] Eurostat, *Energy, Transport and environment statistics. 2019 edition*. 2019.

[2] I. Sanseverino, D. Conduto, L. Pozzoli, S. Dobricic, and T. Lettieri, 'Algal bloom and its economic impact', 2016.

[3] M. Henze, W. Gujer, M. Takashi, and M. van Loosdrecht, *Activated sludge models ASM1, ASM2, ASM2d and ASM3*. IWA Publishing, London, UK, 2000.

[4] J. Alex *et al.*, 'Benchmark Simulation Model no. 1 (BSM1)', 2008.

[5] M. C. M. van Loosdrecht, P. H. Nielsen, C. M. Lopez-Vazquez, and D. Brdjanovic, *Experimental Methods in Wastewater Treatment*. IWA Publishing, London, UK, 2016.

[6] A. K. Plappally and J. H. V Lienhard, 'Energy requirements for water production, treatment, end use, reclamation, and disposal', *Renew. Sustain. Energy Rev.*, vol. 16, no. 7, pp. 4818–4848, 2012.

[7] S. Longo *et al.*, 'Monitoring and diagnosis of energy consumption in wastewater treatment plants. A state of the art and proposals for improvement', *Appl. Energy*, vol. 179, pp. 1251–1268, 2016.

[8] J. L. Campos, D. Valenzuela-Heredia, A. Pedrouso, A. Val del Río, M. Belmonte, and M.-C. A, 'Greenhouse Gases Emissions from Wastewater Treatment Plants : Minimization, Treatment, and Prevention', *J. Chem.*, vol. 2016, 2016.

[9] S. Bringezu and R. Bleischwitz, *Sustainable resource management : global trends, visions and policies*. New York, USA: Taylor & Francis, 2009.

[10] J. H. J. Spiertz, 'Nitrogen, Sustainable Agriculture and Food Security: A Review', *Sustain. Agric.*, vol. 30, pp. 43–55, 2010.

[11] J. S. Guest *et al.*, 'A new planning and design paradigm to achieve sustainable resource recovery from wastewater', *Environ. Sci. Technol.*, vol. 43, no. 16, pp. 6126–6130, 2009.

[12] W. Mo and Q. Zhang, 'Energy-nutrients-water nexus: Integrated resource recovery in municipal wastewater treatment plants', *J. Environ. Manage.*, vol. 127, pp. 255–267, 2013.

[13] K. E. Holmgren, H. Li, W. Verstraete, and P. Cornel, 'State of the Art Compendium Report on Resource Recovery from Water Preface', London, UK, 2016.

[14] R. Latimer *et al.*, 'Towards a Renewable Future: Assessing Resource Recovery as a Viable Treatment Alternative State of the Science and Market Assessment', 2016.

[15] M. C. Chrispim, M. Scholz, and M. A. Nolasco, 'Phosphorus recovery from municipal wastewater treatment: Critical review of challenges and opportunities for developing countries', *J. Environ. Manage.*, vol. 248, no. February, p. 109268, 2019.

[16] S. T. Harrison *et al.*, 'Towards Wastewater Biorefineries : integrated bioreactor and process design for combined water treatment and resource productivity', 2016.

[17] D. J. Batstone, T. Hülsen, C. M. Mehta, and J. Keller, 'Platforms for energy and nutrient recovery from domestic wastewater: A review', *Chemosphere*, vol. 140, pp. 2–11, 2015.

[18] N. Diaz-Elsayed, N. Rezaei, T. Guo, S. Mohebbi, and Q. Zhang,

'Wastewater-based resource recovery technologies across scale: A review', *Resour. Conserv. Recycl.*, vol. 145, no. February, pp. 94–112, 2019.

[19] K. W. Chew *et al.*, 'Microalgae biorefinery: High value products perspectives', *Bioresour. Technol.*, vol. 229, pp. 53–62, 2017.

[20] L. T. Arashiro, A. M. Rada-ariza, M. Wang, P. Van Der Steen, and S. J. Ergas, 'Modelling shortcut nitrogen removal from wastewater using an algal – bacterial consortium', *Water Sci. Technol.*, vol. 75, no. 4, pp. 782–792, 2018.

[21] R. Munoz and B. Guieysse, 'Algal – bacterial processes for the treatment of hazardous contaminants : A review', *Water Res.*, vol. 40, pp. 2799–2815, 2006.

[22] T. Cai, S. Y. Park, and Y. Li, 'Nutrient recovery from wastewater streams by microalgae: Status and prospects', *Renew. Sustain. Energy Rev.*, vol. 19, pp. 360–369, 2013.

[23] Campos *et al.*, 'Multiple analysis reprogrammable titration analyser for the kinetic characterization of nitrifying and autotrophic denitrifying biomass', *Biochem. Eng. J.*, vol. 26, no. 2–3, pp. 176–183, 2005.

[24] W. J. Oswald *et al.*, 'Algae Symbiosis in Oxidation Ponds : III . Photosynthetic Oxygenation', *Sewage Ind. Waste.*, vol. 25, no. 6, pp. 692–705, 1953.

[25] K. D. Fagerstone, J. C. Quinn, T. H. Bradley, S. K. De Long, and A. J. Marchese, 'Quantitative measurement of direct nitrous oxide emissions from microalgae cultivation', *Environ. Sci. Technol.*, vol. 45, no. 21, pp. 9449–9456, 2011.

[26] N. G. A. I. Karya, N. P. van der Steen, and P. N. L. Lens, 'Photo-oxygenation

to support nitrification in an algal-bacterial consortium treating artificial wastewater', *Bioresour. Technol.*, vol. 134, pp. 244–250, 2013.

[27] P. Praveen and K. C. Loh, 'Photosynthetic aeration in biological wastewater treatment using immobilized microalgae-bacteria symbiosis', *Appl. Microbiol. Biotechnol.*, vol. 99, no. 23, pp. 10345–10354, 2015.

[28] M. Muys, J. Coppens, N. Boon, and S. E. Vlaeminck, 'Photosynthetic oxygenation for urine nitrification', *Water Sci. Technol.*, vol. 78, no. 1, pp. 183–194, 2018.

[29] E. Uggetti, B. Sialve, E. Trably, and Jean-Philippe Steyer, 'Integrating microalgae production with anaerobic digestion: a biorefi nery approach Enrica', *Biofuels, Bioprod. Biorefining*, vol. 6, no. 3, pp. 246–256, 2012.

[30] F. Passos, E. Uggetti, H. Carrère, and I. Ferrer, 'Pretreatment of microalgae to improve biogas production: A review', *Bioresour. Technol.*, vol. 172, pp. 403–412, 2014.

[31] L. Moreno-garcia, K. Adjallé, S. Barnabé, and G. S. V Raghavan, 'Microalgae biomass production for a biore fi nery system: Recent advances and the way towards sustainability', *Renew. Sustain. Energy Rev.*, vol. 76, no. May 2016, pp. 493–506, 2017.

[32] R. Díez-Montero, A. Solimeno, E. Uggetti, M. J. García-Galán, and J. García, 'Feasibility assessment of energy-neutral microalgae-based wastewater treatment plants under Spanish climatic conditions', *Process Saf. Environ. Prot.*, vol. 119, pp. 242–252, 2018.

[33] F. G. Acién, C. Gómez-Serrano, M. M. Morales-Amaral, J. M. Fernández-Sevilla, and E. Molina-Grima, 'Wastewater treatment using microalgae: how realistic a contribution might it be to significant urban wastewater

treatment?', *Appl. Microbiol. Biotechnol.*, vol. 100, no. 21, pp. 9013–9022, 2016.

[34] R. Whitton, F. Ometto, M. Pidou, P. Jarvis, R. Villa, and B. Jefferson, 'Microalgae for municipal wastewater nutrient remediation: mechanisms, reactors and outlook for tertiary treatment', *Environ. Technol. Rev.*, vol. 4, no. 1, pp. 133–148, 2015.

[35] G. Markou and D. Georgakakis, 'Cultivation of filamentous cyanobacteria (blue-green algae) in agro-industrial wastes and wastewaters: A review', *Appl. Energy*, vol. 88, no. 10, pp. 3389–3401, 2011.

[36] O. Fenton and D. Ó hUallacháin, 'Agricultural nutrient surpluses as potential input sources to grow third generation biomass (microalgae): A review', *Algal Res.*, vol. 1, no. 1, pp. 49–56, 2012.

[37] E. J. Olguín, 'Dual purpose microalgae-bacteria-based systems that treat wastewater and produce biodiesel and chemical products within a Biorefinery', *Biotechnol. Adv.*, vol. 30, no. 5, pp. 1031–1046, 2012.

[38] S. L. Lim, W. L. Chu, and S. M. Phang, 'Use of Chlorella vulgaris for bioremediation of textile wastewater', *Bioresour. Technol.*, vol. 101, no. 19, pp. 7314–7322, 2010.

[39] Y. Wang, J. Liu, D. Kang, C. Wu, and Y. Wu, 'Removal of pharmaceuticals and personal care products from wastewater using algae-based technologies: a review', *Rev. Environ. Sci. Biotechnol.*, vol. 16, no. 4, pp. 717–735, 2017.

[40] L. Lin, G. Y. S. Chan, B. L. Jiang, and C. Y. Lan, 'Use of ammoniacal nitrogen tolerant microalgae in landfill leachate treatment', *Waste Manag.*, vol. 27, no. 10, pp. 1376–1382, 2007.

[41] A. Xia and J. D. Murphy, 'Microalgal Cultivation in Treating Liquid Digestate from Biogas Systems', *Trends Biotechnol.*, vol. 34, no. 4, pp. 264–275, 2016.

[42] R. Muñoz, L. Meier, I. Diaz, and D. Jeison, 'A review on the state-of-the-art of physical/chemical and biological technologies for biogas upgrading', *Rev. Environ. Sci. Biotechnol.*, vol. 14, no. 4, pp. 727–759, 2015.

[43] H. W. Yen, S. H. Ho, C. Y. Chen, and J. S. Chang, 'CO2, NOx and SOx removal from flue gas via microalgae cultivation: A critical review', *Biotechnol. J.*, vol. 10, no. 6, pp. 829–839, 2015.

[44] D. M. Thomas, J. Mechery, and S. V. Paulose, 'Carbon dioxide capture strategies from flue gas using microalgae: a review', *Environ. Sci. Pollut. Res.*, vol. 23, no. 17, pp. 16926–16940, 2016.

[45] N. Abdel-Raouf, A. A. Al-Homaidan, and I. B. M. Ibraheem, 'Microalgae and wastewater treatment', *Saudi J. Biol. Sci.*, vol. 19, no. 3, pp. 257–275, 2012.

[46] F. Marazzi, M. Bellucci, S. Rossi, R. Fornaroli, E. Ficara, and V. Mezzanotte, 'Outdoor pilot trial integrating a sidestream microalgae process for the treatment of centrate under non optimal climate conditions', *Algal Res.*, vol. 39, p. 101430, 2019.

[47] S. Abinandan and S. Shanthakumar, 'Challenges and opportunities in application of microalgae (Chlorophyta) for wastewater treatment: A review', *Renew. Sustain. Energy Rev.*, vol. 52, pp. 123–132, 2015.

[48] A. F. Mohd Udaiyappan, H. Abu Hasan, M. S. Takriff, and S. R. Sheikh Abdullah, 'A review of the potentials, challenges and current status of microalgae biomass applications in industrial wastewater treatment', *J.*

Water Process Eng., vol. 20, no. August, pp. 8–21, 2017.

[49] A. L. Gonçalves, J. C. M. Pires, and M. Simões, 'A review on the use of microalgal consortia for wastewater treatment', *Algal Res.*, vol. 24, no. B, pp. 403–415, 2016.

[50] M. Ras, J.-P. Steyer, and O. Bernard, 'Temperature effect on microalgae : a crucial factor for outdoor production', *Rev. Environ. Sci. Bio/Technology*, vol. 12, pp. 153–164, 2013.

[51] G. M. Grimaud, F. Mairet, A. Sciandra, and O. Bernard, 'Modeling the temperature effect on the specific growth rate of phytoplankton : a review', *Rev. Environ. Sci. Bio/Technology*, vol. 16, pp. 625–645, 2017.

[52] L. Rosso, J. R. Lobry, S. Bajard, C. Bernard, and J. P. Flandrois, 'Convenient Model To Describe the Combined Effects of Temperature and pH on Microbial Growth', *Appl. Environ. Microbiol.*, vol. 61, no. 2, pp. 610–616, 1995.

[53] D. Ippoliti, C. Gómez, M. del Mar Morales-Amaral, R. Pistocchi, J. M. Fernández-Sevilla, and F. G. Acién, 'Modeling of photosynthesis and respiration rate for Isochrysis galbana (T-Iso) and its influence on the production of this strain', *Bioresour. Technol.*, vol. 203, pp. 71–79, 2016.

[54] C. Sousa, 'Oxygen accumulation in photobioreactors', Ph.D. thesis, Wageningen University, Wageningen, NL, 2013.

[55] L. Peng, C. Q. Lan, and Z. Zhang, 'Evolution , Detrimental Effects , and Removal of Oxygen in Microalga Cultures : A Review', *Environ. Prog. Sustain. Energy*, vol. 32, no. 4, pp. 982–988, 2013.

[56] F. M. I. Natrah, P. Bossier, P. Sorgeloos, F. M. Yusoff, and T. Defoirdt, 'Significance of microalgal-bacterial interactions for aquaculture', *Rev.*

Aquac., vol. 6, no. 1, pp. 48–61, 2014.

[57] A. L. Gonçalves, J. C. M. Pires, and M. Simões, 'The effects of light and temperature on microalgal growth and nutrients removal- an experimental and mathematical approach', *RSC Adv.*, vol. 6, no. 27, pp. 22896–22907, 2016.

[58] C. Vasseur *et al.*, 'Carbon conversion efficiency and population dynamics of a marine algae-bacteria consortium growing on simplified synthetic digestate: First step in a bioprocess coupling algal production and anaerobic digestion', *Bioresour. Technol.*, vol. 119, pp. 79–87, 2012.

[59] N. M. Jais, R. M. S. R. Mohamed, A. A. Al-Gheethi, and M. K. A. Hashim, 'The dual roles of phycoremediation of wet market wastewater for nutrients and heavy metals removal and microalgae biomass production', *Clean Technol. Environ. Policy*, vol. 19, no. 1, pp. 37–52, 2017.

[60] E. M. Ferrero, I. de Godos, E. M. Rodríguez, P. A. García-Encina, R. Muñoz, and E. Bécares, 'Molecular characterization of bacterial communities in algal-bacterial photobioreactors treating piggery wastewaters', *Ecol. Eng.*, vol. 40, pp. 121–130, 2012.

[61] I. Krustok *et al.*, 'Characterization of algal and microbial community growth in a wastewater treating batch photo-bioreactor inoculated with lake water', *Algal Res.*, vol. 11, pp. 421–427, 2015.

[62] K. Tait *et al.*, 'Characterisation of bacteria from the cultures of a Chlorella strain isolated from textile wastewater and their growth enhancing effects on the axenic cultures of Chlorella vulgaris in low nutrient media', *Algal Res.*, vol. 44, no. February, p. 101666, 2019.

[63] Y. Anjaneyulu, N. Sreedhara Chary, and D. Samuel Suman Raj,

'Decolourization of industrial effluents - Available methods and emerging technologies - A review', *Rev. Environ. Sci. Biotechnol.*, vol. 4, no. 4, pp. 245–273, 2005.

[64] F. Marazzi *et al.*, 'A novel option for reducing the optical density of liquid digestate to achieve a more productive microalgal culturing', *Algal Res.*, vol. 24, pp. 19–28, 2017.

[65] E. Marañón, L. Castrillón, Y. Fernández-Nava, A. Fernández-Méndez, and A. Fernández-Sánchez, 'Colour, turbidity and COD removal from old landfill leachate by coagulation-flocculation treatment', *Waste Manag. Res.*, vol. 28, no. 8, pp. 731–737, 2010.

[66] B. V. Raghunath, A. Punnagaiarasi, G. Rajarajan, A. Irshad, A. Elango, and G. M. Kumar, 'Impact of Dairy Effluent on Environment—A Review', in *Integrated Waste Management in India*, 2016, pp. 239–249.

[67] C. O'Neill, F. R. Hawkes, D. L. Hawkes, N. D. Lourenço, H. M. Pinheiro, and W. Delée, 'Colour in textile effluents - Sources, measurement, discharge consents and simulation: A review', *J. Chem. Technol. Biotechnol.*, vol. 74, no. 11, pp. 1009–1018, 1999.

[68] D. Pant and A. Adholeya, 'Biological approaches for treatment of distillery wastewater: A review', *Bioresour. Technol.*, vol. 98, no. 12, pp. 2321–2334, 2007.

[69] D. Pokhrel and T. Viraraghavan, 'Treatment of pulp and paper mill wastewater - A review', *Sci. Total Environ.*, vol. 333, no. 1–3, pp. 37–58, 2004.

[70] D. Orhon and E. U. Cokgor, 'COD Fractionation in Wastewater Characterization — The State of the Art', *J. Chem. Tech. Biotechnol.*, vol. 68, pp. 283–293, 1997.

[71] A. C. Anthonisen, R. C. Loehr, P. T. B. S, and E. G. Srinath, 'Inhibition of nitrification by ammonia and nitrous acid', *Water Pollut. Control Fed.*, vol. 48, no. 5, pp. 835–852, 1976.

[72] Y. Collos and P. J. Harrison, 'Acclimation and toxicity of high ammonium concentrations to unicellular algae', *Mar. Pollut. Bull.*, vol. 80, pp. 8–23, 2014.

[73] Y. Azov and J. C. Goldman, 'Free ammonia inhibition of algal photosynthesis in intensive cultures.', *Appl. Environ. Microbiol.*, vol. 43, no. 4, pp. 735–9, 1982.

[74] G. Markou, O. Depraetere, and K. Muylaert, 'Effect of ammonia on the photosynthetic activity of Arthrospira and Chlorella: A study on chlorophyll fluorescence and electron transport', *Algal Res.*, vol. 16, pp. 449–457, 2016.

[75] E. Sforza, M. Pastore, A. Spagni, and A. Bertucco, 'Microalgae-bacteria gas exchange in wastewater: how mixotrophy may reduce the oxygen supply for bacteria', *Environ. Sci. Pollut. Res.*, vol. 25, no. 28, pp. 28004–28014, 2018.

[76] M. Karvelas, A. Katsoyiannis, and C. Samara, 'Occurrence and fate of heavy metals in the wastewater treatment process', *Chemosphere*, vol. 53, no. 10, pp. 1201–1210, 2003.

[77] K. K. I. U. Arunakumara and X. Zhang, 'Heavy metal bioaccumulation and toxicity with special reference to microalgae', *J. Ocean Univ. China*, vol. 7, no. 1, pp. 60–64, 2007.

[78] S. Park, J. Kim, Y. Yoon, Y. Park, and T. Lee, 'Blending water- and nutrient-source wastewaters for cost-effective cultivation of high lipid content microalgal species Micractinium inermum NLP-F014', *Bioresour. Technol.*,

vol. 198, pp. 388–394, 2015.

[79] I. de Godos *et al.*, 'A comparative evaluation of microalgae for the degradation of piggery wastewater under photosynthetic oxygenation', *Bioresour. Technol.*, vol. 101, no. 14, pp. 5150–5158, 2010.

[80] M. Rizwan, G. Mujtaba, S. A. Memon, K. Lee, and N. Rashid, 'Exploring the potential of microalgae for new biotechnology applications and beyond: A review', *Renew. Sustain. Energy Rev.*, vol. 92, no. April, pp. 394–404, 2018.

[81] O. Uysal, F. O. Uysal, and K. Ekinci, 'Evaluation of Microalgae as Microbial Fertilizer', *Eur. J. Sustain. Dev.*, vol. 4, no. 2, pp. 77–82, 2015.

[82] M. Bilal, T. Rasheed, I. Ahmed, and H. M. N. Iqbal, 'High-value compounds from microalgae with industrial exploitability - A review', *Front. Biosci. - Sch.*, vol. 9, no. 3, pp. 319–342, 2017.

[83] H. Spanjers and P. Vanrolleghem, 'Respirometry as a tool for rapid characterization of wastewater and activated sludge', *Water Sci. Technol.*, vol. 31, no. 2, pp. 105–114, 1995.

[84] H. Spanjers and P. A. Vanrolleghem, 'Respirometry', in *Experimental Methods in Wastewater Treatment*, IWA Publishing, London, UK, 2016.

[85] H. Spanjers, 'Respirometry in Activated Sludge', Ph.D. thesis, Wageningen Agricultural University, 1993.

[86] V. Mahendraker and T. Viraraghavan, 'Respirometry in environmental engineering', *J. Environ. Sci. Heal. Part A Environ. Sci. Eng. Toxicol.*, vol. 30, no. 4, pp. 713–734, 1995.

[87] E. M. Contreras, M. E. Albertario, N. C. Bertola, and N. E. Zaritzky,

'Modelling phenol biodegradation by activated sludges evaluated through respirometric techniques', *J. Hazard. Mater.*, vol. 158, no. 2–3, pp. 366–374, 2008.

[88] V. Pambrun, A. Marquot, and Y. Racault, 'Characterization of the toxic effects of cadmium and 3.5-dichlorophenol on nitrifying activity and mortality in biologically activated sludge systems - Effect of low temperature', *Environ. Sci. Pollut. Res.*, vol. 15, no. 7, pp. 592–599, 2008.

[89] M. Linaric, M. Markic, and L. Sipos, 'High salinity wastewater treatment', *Water Sci. Technol.*, vol. 68, no. 6, pp. 1400–1405, 2013.

[90] A. Ismail, M. C. Wentzel, and F. Bux, 'Using Respirometric Techniques and Fluorescent In Situ Hybridization to Evaluate the Heterotrophic Active Biomass in Activated Sludge', *Biotechnol. Bioeng.*, vol. 98, no. 3, pp. 561–568, 2007.

[91] J. M. Choubert *et al.*, 'Rethinking wastewater characterisation methods for activated sludge systems - A position paper', *Water Sci. Technol.*, vol. 67, no. 11, pp. 2363–2373, 2013.

[92] E. Ficara, A. Rozzi, and P. Cortelezzi, 'Theory of pH-stat titration', *Biotechnol. Bioeng.*, vol. 82, no. 1, pp. 28–37, 2003.

[93] M. A. Hoque, V. Aravinthan, and N. M. Pradhan, 'Calibration of biokinetic model for acetate biodegradation using combined respirometric and titrimetric measurements', *Bioresour. Technol.*, vol. 101, no. 5, pp. 1426–1434, 2010.

[94] M. Mora, L. R. López, X. Gamisans, and D. Gabriel, 'Coupling respirometry and titrimetry for the characterization of the biological activity of a SO-NR consortium', *Chem. Eng. J.*, vol. 251, pp. 111–115, 2014.

[95] A. K. Gernaey, B. Petersen, J. P. Ottoy, and P. Vanrolleghem, 'Activated sludge monitoring with combined respirometric-titrimetric measurements', *Water Res.*, vol. 35, no. 5, pp. 1280–1294, 2001.

[96] B. Petersen, K. Gernaey, M. Henze, and P. A. Vanrolleghem, 'Calibration Of Activated Sludge Models: A Critical Review Of Experimental Designs', in *Biotechnology for the Environment: Wastewater Treatment and Modeling, Waste Gas Handling. Focus on Biotechnology, vol 3C*, Springer, Dordrecht, 2003, pp. 101–186.

[97] M. Zeng, A. Soric, and N. Roche, 'Modeling partial nitrification and denitrification in a hybrid biofilm reactor: calibration by retention time distribution and respirometric tests', *Environ. Sci. Pollut. Res.*, vol. 22, no. 17, pp. 12849–12860, 2015.

[98] ASCE, *Measurement of Oxygen Transfer in Clean Water, Standard ASCE 2-91*. New York: American Society of Civil Engineers, 1993.

[99] H. Spanjers, P. Vanrolleghem, G. Olsson, and P. Dold, 'Respirometry in control of the activated sludge process', *Water Sci. Technol.*, vol. 34, no. 3–4, pp. 117–126, 1996.

[100] F. Garcia-Ochoa, E. Gomez, V. E. Santos, and J. C. Merchuk, 'Oxygen uptake rate in microbial processes: An overview', *Biochem. Eng. J.*, vol. 49, no. 3, pp. 289–307, 2010.

[101] T. Katipoglu-Yazan, E. Ubay Cokgor, and D. Orhon, 'Modeling sequential ammonia oxidation kinetics in enriched nitrifying microbial culture', *J. Chem. Technol. Biotechnol.*, vol. 90, no. 1, pp. 72–79, 2015.

[102] P. J. Roeleveld and M. C. M. Van Loosdrecht, 'Experience with guidelines for wastewater characterisation in The Netherlands', *Water Sci. Technol.*,

vol. 45, no. 6, pp. 77–87, 2002.

[103] M. N. Gatti, F. García-Usach, A. Seco, and J. Ferrer, 'Wastewater COD characterization: Analysis of respirometric and physical-chemical methods for determining biodegradable organic matter fractions', *J. Chem. Technol. Biotechnol.*, vol. 85, no. 4, pp. 536–544, 2010.

[104] C. Fall *et al.*, 'COD fractionation and biological treatability of mixed industrial wastewaters', *J. Environ. Manage.*, vol. 113, pp. 71–77, 2012.

[105] V. Aravinthan and M. A. Hoque, 'Development and calibration of bio-kinetic model for surfactant biodegradation with combined respirometric and titrimetric measurements', *Bioresour. Technol.*, vol. 102, no. 9, pp. 5504–5513, 2011.

[106] K. Gernaey, P. Vanrolleghem, and W. Verstraete, 'On-line estimation of Nitrosomonas kinetic parameters in activated sludge samples using titration in-sensor-experiments', *Water Res.*, vol. 32, no. 1, pp. 71–80, 1998.

[107] G. Ciudad, A. Werner, C. Bornhardt, C. Muñoz, and C. Antileo, 'Differential kinetics of ammonia- and nitrite-oxidizing bacteria: A simple kinetic study based on oxygen affinity and proton release during nitrification', *Process Biochem.*, vol. 41, no. 8, pp. 1764–1772, 2006.

[108] J. Kappeler and W. Gujer, 'Estimation of kinetic parameters of heterotrophic biomass under aerobic conditions and characterization of wastewater for activated sludge modelling', *Water Sci. Technol.*, vol. 25, no. 6, pp. 125–139, 1992.

[109] V. Torretta *et al.*, 'Assessment of biological kinetics in a conventional municipal WWTP by means of the oxygen uptake rate method', *Sustain.*, vol. 6, no. 4, pp. 1833–1847, 2014.

[110] M. Capodici, S. Fabio Corsino, F. Di Pippo, D. Di Trapani, and M. Torregrossa, 'An innovative respirometric method to assess the autotrophic active fraction: Application to an alternate oxic-anoxic MBR pilot plant', *Chem. Eng. J.*, vol. 300, pp. 367–375, 2016.

[111] G. Insel *et al.*, 'Unified basis for the respirometric evaluation of inhibition for activated sludge', *J. Environ. Sci. Heal. - Part A*, vol. 41, pp. 1763–1780, 2006.

[112] M. Tobajas, V. Verdugo, A. M. Polo, J. J. Rodriguez, and A. F. Mohedano, 'Assessment of toxicity and biodegradability on activated sludge of priority and emerging pollutants', *Environ. Technol.*, vol. 37, no. 6, pp. 713–721, 2016.

[113] M. Vargas, A. Guisasola, J. Lafuente, C. Casas, and J. A. Baeza, 'On-line titrimetric monitoring of anaerobic-anoxic EBPR processes', *Water Sci. Technol.*, vol. 57, no. 8, pp. 1149–1154, 2008.

[114] F. Coen, B. Vanderhaegen, I. Boonen, P. A. Vanrolleghem, and P. Van Meenen, 'Improved design and control of industrial and municipal nutrient removal plants using dynamic models', *Water Sci. Technol.*, vol. 35, no. 10, pp. 53–61, 1997.

[115] Z. Ning, G. G. Patry, and H. Spanjers, 'Identification and quantification of nitrogen nutrient deficiency in the activated sludge process using respirometry', *Water Res.*, vol. 34, no. 13, pp. 3345–3354, 2000.

[116] J. B. Copp and H. Spanjers, 'Simulation of respirometry-based detection and mitigation of activated sludge toxicity', *Control Eng. Pract.*, vol. 12, no. 3, pp. 305–313, 2004.

[117] Q. Yang, S. Gu, Y. Peng, S. Wang, and X. Liu, 'Progress in the development

of control strategies for the SBR process', *Clean - Soil, Air, Water*, vol. 38, no. 8, pp. 732–749, 2010.

[118] H. Spanjers, P. Vanrolleghem, K. Nguyen, H. Vanhooren, and G. G. Patry, 'Towards a simulation-benchmark for evaluating respirometry-based control strategies', *Water Sci. Technol.*, vol. 37, no. 12, pp. 219–226, 1998.

[119] I. Nopens *et al.*, 'Benchmark Simulation Model No 2: Finalisation of plant layout and default control strategy', *Water Sci. Technol.*, vol. 62, no. 9, pp. 1967–1974, 2010.

[120] L. Rieger *et al.*, *Guidelines for Using Activated Sludge Models*. London, UK, 2012.

[121] J. Im, D. Kim, and K. Gil, 'COD fraction analysis of anaerobic digester supernatant and piggery wastewater, using respirometric method', *Environ. Earth Sci.*, vol. 75, no. 1, pp. 1–6, 2016.

[122] M. Cramer, J. Tränckner, P. Schelhorn, and U. Kotzbauer, 'Degradation kinetics and COD fractioning of agricultural wastewaters from biogas plants applying biofilm respirometry', *Environ. Technol.*, vol. 1, 2019.

[123] P. A. Vanrolleghem, H. Spanjers, B. Petersen, P. Ginestet, and I. Takacs, 'Estimating (combinations of) Activated Sludge Model No. 1 parameters and components by respirometry', *Water Sci. Technol.*, vol. 39, no. 1, pp. 195–214, 1999.

[124] G. Munz, R. Gori, L. Cammilli, and C. Lubello, 'Characterization of tannery wastewater and biomass in a membrane bioreactor using respirometric analysis', *Bioresour. Technol. J.*, vol. 99, pp. 8612–8618, 2008.

[125] P. Ginestet, J. M. Audic, V. Urbain, and J. C. Block, 'Estimation of nitrifying bacterial activities by measuring oxygen uptake in the presence of the

metabolic inhibitors allylthiourea and azide', *Appl. Environ. Microbiol.*, vol. 64, no. 6, pp. 2266–2268, 1998.

[126] K. Chandran, Z. Hu, and B. F. Smets, 'A critical comparison of extant batch respirometric and substrate depletion assays for estimation of nitrification biokinetics', *Biotechnol. Bioeng.*, vol. 101, no. 1, pp. 62–72, 2008.

[127] L. M. Ruiz, J. I. Pérez, and M. Á. Gómez, 'Comparison of five wastewater COD fractionation methods for dynamic simulation of MBR systems', *J. Environ. Sci. Heal. - Part A Toxic/Hazardous Subst. Environ. Eng.*, vol. 49, no. 13, pp. 1553–1563, 2014.

[128] E. U. Cokgor, S. Ozdemir, O. Karahan, G. Insel, and D. Orhon, 'Critical appraisal of respirometric methods for metal inhibition on activated sludge', *J. Hazard. Mater.*, vol. 139, no. 2, pp. 332–339, 2006.

[129] G. R. Hernandez-Martinez, D. Ortiz-Alvarez, M. Perez-Roa, N. A. Urbina-Suarez, and F. Thalasso, 'Multiparameter analysis of activated sludge inhibition by nickel, cadmium, and cobalt', *J. Hazard. Mater.*, vol. 351, pp. 63–70, 2018.

[130] S. Basak, D. Güven, E. Cokgor, and D. Orhon, 'Respirometric evaluation and modeling of the impact of continuous benzo[a]anthracene feeding on activated sludge', *J Chem Technol Biotechno*, vol. 94, pp. 2621–2629, 2019.

[131] V. Kapoor, M. Elk, X. Li, C. A. Impellitteri, and J. W. Santo Domingo, 'Effects of Cr(III) and Cr(VI) on nitrification inhibition as determined by SOUR, function-specific gene expression and 16S rRNA sequence analysis of wastewater nitrifying enrichments', *Chemosphere*, vol. 147, pp. 361–367, 2016.

[132] B. S. Xing and R. C. Jin, 'Inhibitory effects of heavy metals and antibiotics

on nitrifying bacterial activities in mature partial nitritation', *Chemosphere*, vol. 200, pp. 437–445, 2018.

[133] A. M. J. Kliphuis, L. de Winter, C. Vejrazka, D. E. Martens, M. Janssen, and R. H. Wijffels, 'Photosynthetic Efficiency of Chlorella sorokiniana in a Turbulently Mixed Short Light-Path Photobioreactor', *Biotechnol. Prog.*, vol. 26, no. 3, pp. 687–696, 2010.

[134] C. Brindley, F. G. Acién, and J. M. Fernández-Sevilla, 'The oxygen evolution methodology affects photosynthetic rate measurements of microalgae in well-defined light regimes', *Biotechnol. Bioeng.*, vol. 106, no. 2, pp. 228–237, 2010.

[135] J. U. Grobbelaar *et al.*, 'Photosynthetic characteristics of five high light and low light exposed microalgae as measured with super(14)C-uptake and oxygen electrode techniques', *Mar. Microb. Food Webs.*, vol. 6, no. 1, pp. 3–19, 1992.

[136] R. J. Geider and B. A. Osborne, 'Respiration and Microalgal Growth : A Review of the Quantitative Relationship between Dark Respiration and Growth', *New Phytol.*, vol. 112, pp. 327–341, 1989.

[137] N. T. Eriksen, F. K. Riisgård, W. S. Gunther, and J. J. Lønsmann Iversen, 'On-line estimation of O2production, CO2uptake, and growth kinetics of microalgal cultures in a gas-tight photobioreactor', *J. Appl. Phycol.*, vol. 19, pp. 161–174, 2007.

[138] V. Mezzanotte, C. Colombo, E. Ficara, and A. Rozzi, 'Initial results on the use of pH-stat titration (AIDA method) for the measurement of algal photosynthesis', *Water SA*, vol. 30, no. 3, pp. 347–352, 2004.

[139] B. Decostere *et al.*, 'A combined respirometer-titrimeter for the

determination of microalgae kinetics: Experimental data collection and modelling', *Chem. Eng. J.*, vol. 222, pp. 85–93, 2013.

[140] S. Lefebvre, J. L. Mouget, P. Loret, P. Rosa, and G. Tremblin, 'Comparison between fluorimetry and oximetry techniques to measure photosynthesis in the diatom Skeletonema costatum cultivated under simulated seasonal conditions', *J. Photochem. Photobiol. B Biol.*, vol. 86, no. 2, pp. 131–139, 2007.

[141] E. Gnaiger and H. Forstner, *Polarographic Oxygen Sensors: Aquatic and Physiological Applications*. Springer-Verlag, 1983.

[142] A. Richmond and Q. Hu, *Handbook of microalgal culture: Applied Phycology and Biotechnology*. 2013.

[143] J. Cabello, A. Toledo-cervantes, L. Sánchez, S. Revah, and M. Morales, 'Effect of the temperature, pH and irradiance on the photosynthetic activity by Scenedesmus obtusiusculus under nitrogen replete and deplete conditions', *Bioresour. Technol.*, vol. 181, pp. 128–135, 2015.

[144] T. Tang, H. Fadaei, and Z. Hu, 'Rapid evaluation of algal and cyanobacterial activities through specific oxygen production rate measurement', *Ecol. Eng.*, vol. 73, pp. 439–445, 2014.

[145] G. Trentin, A. Bertucco, and E. Sforza, 'Mixotrophy in Synechocystis sp. for the treatment of wastewater with high nutrient content: effect of - CO2 and light', *Bioprocess Biosyst. Eng.*, pp. 1–9, 2019.

[146] E. Sforza, M. Pastore, E. Barbera, and A. Bertucco, 'Respirometry as a tool to quantify kinetic parameters of microalgal mixotrophic growth', *Bioprocess Biosyst. Eng.*, vol. 42, no. 5, pp. 839–851, 2019.

[147] C. Brindley, F. G. Acién Fernández, and J. M. Fernández-Sevilla, 'Analysis of light regime in continuous light distributions in photobioreactors',

Bioresour. Technol., vol. 102, pp. 3138–3148, 2011.

[148] C. Vejrazka, M. Janssen, G. Benvenuti, M. Streefland, and R. H. Wijffels, 'Photosynthetic efficiency and oxygen evolution of Chlamydomonas reinhardtii under continuous and flashing light', *Appl. Microbiol. Biotechnol.*, vol. 97, no. 4, pp. 1523–1532, 2013.

[149] A. Kazbar *et al.*, 'Effect of dissolved oxygen concentration on microalgal culture in photobioreactors', *Algal Res.*, vol. 39, no. January, p. 101432, 2019.

[150] T. de Mooij, Z. R. Nejad, L. van Buren, R. H. Wijffels, and M. Janssen, 'Effect of photoacclimation on microalgae mass culture productivity', *Algal Res.*, vol. 22, pp. 56–67, 2017.

[151] D. J. Suggett, H. L. MacIntyre, T. M. Kana, and R. J. Geider, 'Comparing electron transport with gas exchange: Parameterising exchange rates between alternative photosynthetic currencies for eukaryotic phytoplankton', *Aquat. Microb. Ecol.*, vol. 56, no. 2–3, pp. 147–162, 2009.

[152] S. Roberty, B. Bailleul, N. Berne, F. Franck, and P. Cardol, 'PSI Mehler reaction is the main alternative photosynthetic electron pathway in Symbiodinium sp., symbiotic dinoflagellates of cnidarians', *New Phytol.*, vol. 204, no. 1, pp. 81–91, 2014.

[153] A. M. J. Kliphuis, M. Janssen, E. J. van den End, D. E. Martens, and R. H. Wijffels, 'Light respiration in Chlorella sorokiniana', *J. Appl. Phycol.*, vol. 23, pp. 935–947, 2011.

[154] P. G. Falkowski, Z. Dubinsky, and K. Wyman, 'Growth-irradiance relationships in phytoplankton', *Limnol. Oceanogr.*, vol. 30, no. 2, pp. 311–321, 1985.

[155] F. García-Camacho, A. Sánchez-Mirón, E. Molina-Grima, F. Camacho-

Rubio, and J. C. Merchuck, 'A mechanistic model of photosynthesis in microalgae including photoacclimation dynamics', *J. Theor. Biol.*, vol. 304, pp. 1–15, 2012.

[156] P. G. Falkowski and T. G. Owens, 'Effects of light intensity on photosynthesis and dark respiration in six species of marine phytoplankton', *Mar. Biol.*, vol. 45, no. 4, pp. 289–295, 1978.

[157] J. Cabello, M. Morales, and S. Revah, 'Dynamic photosynthetic response of the microalga Scenedesmus obtusiusculus to light intensity perturbations', *Chem. Eng. J.*, vol. 252, pp. 104–111, 2014.

[158] D. de los Cobos-Vasconcelos, E. L. García-cruz, M. Franco-Morgado, and A. González-Sánchez, 'Short-term evaluation of the photosynthetic activity of an alkaliphilic microalgae consortium in a novel tubular closed photobioreactor', *J. Appl. Phycol.*, vol. 28, no. 2, pp. 795–802, 2015.

[159] J. Beardall *et al.*, 'Studies on enhanced post-illumination respiration in microalgae', *J. Plankton Res.*, vol. 16, no. 10, pp. 1401–1410, 1994.

[160] D. P. Häder and J. Schäfer, 'In-situ measurement of photosynthetic oxygen production in the water column', *Environ. Monit. Assess.*, vol. 32, pp. 259–268, 1994.

[161] B. Tamburic, M. Szabó, N. A. T. Tran, A. W. D. Larkum, D. J. Suggett, and P. J. Ralph, 'Action spectra of oxygen production and chlorophyll a fluorescence in the green microalga Nannochloropsis oculata', *Bioresour. Technol.*, vol. 169, pp. 320–327, 2014.

[162] V. M. Luimstra, J. M. Schuurmans, A. M. Verschoor, K. J. Hellingwerf, J. Huisman, and H. C. P. Matthijs, 'Blue light reduces photosynthetic efficiency of cyanobacteria through an imbalance between photosystems I

and II', *Photosynth. Res.*, vol. 138, no. 2, pp. 177–189, 2018.

[163] Y. C. Jeon, C. W. Cho, and Y. S. Yun, 'Oxygen evolution rate of photosynthetic microalga Haematococcus pluvialis depending on light intensity and quality', *Stud. Surf. Sci. Catal.*, vol. 159, pp. 157–160, 2006.

[164] C. W. Kim, M. Sung, K. Nam, M. Moon, J. Kwon, and J. Yang, 'Effect of monochromatic illumination on lipid accumulation of Nannochloropsis gaditana under continuous cultivation', *Biores. Technol.*, vol. 159, pp. 30–35, 2014.

[165] Y. S. Yun and J. M. Park, 'Kinetic modeling of the light-dependent photosynthetic activity of the green microalga Chlorella vulgaris', *Biotechnol. Bioeng.*, vol. 83, no. 3, pp. 303–311, 2003.

[166] N. Du *et al.*, 'Simultaneous quantum yield measurements of carbon uptake and oxygen evolution in microalgal cultures', *PLoS One*, vol. 13, no. 6, pp. 1–21, 2018.

[167] R. L. Shuler and W. A. Affens, 'Effect of Light Intensity and Thickness of Culture Solution on Oxygen Production by Algae', *Appl. Microbiol.*, vol. 19, no. 1, pp. 76–86, 1970.

[168] K. H. Park, D. I. Kim, and C. G. Lee, 'Effect of flashing light on oxygen production rates in high-density algal cultures', *J. Microbiol. Biotechnol.*, vol. 10, no. 6, pp. 817–822, 2000.

[169] M. Barceló-villalobos, P. Fernández-del Olmo, J. L. Guzmán, J. M. Fernández-sevilla, and F. C. Acién Fernández, 'Evaluation of photosynthetic light integration by microalgae in a pilot-scale raceway reactor', *Bioresour. Technol.*, vol. 280, pp. 404–411, 2019.

[170] J. U. Grobbelaar, 'The influence of light/dark cycles in mixed algal cultures

on their productivity', *Bioresour. Technol.*, vol. 38, pp. 189–194, 1991.

[171] B. Decostere, A. M. Alvarado, E. A. Sanchez, D. Rousseau, I. Nopens, and S. W. Van Hulle, 'Kinetic exploratoin of the microalgal growth rate of species residing in a waste stabilization pond', *1st Int. Conf. Bioenergy Clim. Chang. Towar. a Sustain. Dev.*, 2016.

[172] Yuvraj and P. Padmanabhan, 'Technical insight on the requirements for CO2-saturated growth of microalgae in photobioreactors', *3 Biotech*, vol. 7, no. 2, pp. 1–7, 2017.

[173] Y. Qiao, J. Rong, H. Chen, C. He, and Q. Wang, 'Non-Invasive Rapid Harvest Time Determination of Oil-Producing Microalgae Cultivations for Biodiesel Production by Using Chlorophyll Fluorescence', *Front. Energy Res.*, vol. 3, pp. 1–10, 2015.

[174] S. Wang, Y. Pan, C. Liu, L. Chuang, and C. N. Chen, 'Characterization of a green microalga UTEX 2219-4 : Effects of photosynthesis and osmotic stress on oil body formation', *Bot. Stud.*, vol. 52, pp. 305–312, 2011.

[175] D. Zhang, F. Yan, Z. Sun, Q. Zhang, S. Xue, and W. Cong, 'On-line modeling intracellular carbon and energy metabolism of Nannochloropsis sp . in nitrogen-repletion and nitrogen-limitation cultures', *Bioresour. Technol.*, vol. 164, pp. 86–92, 2014.

[176] H. Hu and Q. Zhou, 'Regulation of inorganic carbon acquisition by nitrogen and phosphorus levels in the Nannochloropsis sp.', *World J. Microbiol. Biotechnol.*, vol. 26, no. 5, pp. 957–961, 2010.

[177] M. M. El-Sheek and A. A. Rady, 'Effect of Phosphorus Starvation on Growth, Photo- synthesis and Some Metabolic Processes in the Uni-cellular Green Alga Chlorella kessleri', *Phyton (B. Aires).*, vol. 35, pp. 139–

151, 1995.

[178] M. E. Theodorou, I. R. Elrifi, D. H. Turpin, and W. C. Plaxton, 'Effects of Phosphorus Limitation on Respiratory Metabolism in the Green Alga Selenastrum minutum', *Plant Physiol.*, no. 95, pp. 1089–1095, 1991.

[179] I. R. Davison, 'Environmental effects on algal photosynthesis: temperature', *J. Phycol.*, vol. 27, pp. 2–8, 1991.

[180] A. C. Mongra and H. O. Agrawal, 'Effect of light and temperature on photosynthetic oxygen evolution in Mastigocladus laminosus', *Int.J.Curr.Microbiol.App.Sci*, vol. 3, no. 3, pp. 56–65, 2014.

[181] T. A. Costache, F. G. Acién Fernández, M. M. Morales, J. M. Fernández-Sevilla, I. Stamatin, and E. Molina, 'Comprehensive model of microalgae photosynthesis rate as a function of culture conditions in photobioreactors', *Appl. Microbiol. Biotechnol.*, vol. 97, pp. 7627–7637, 2013.

[182] B. Decostere, S. W. Van Hulle, M. Duyck, T. Maere, H. Vervaeren, and I. Nopens, 'The use of a combined respirometric-titrimetric setup to assess the effect of environmental conditions on micro-algal growth rate', *J. Chem. Technol. Biotechnol.*, vol. 91, no. 1, pp. 248–256, 2016.

[183] O. Bernard and B. Rémond, 'Validation of a simple model accounting for light and temperature effect on microalgal growth', *Bioresour. Technol.*, vol. 123, pp. 520–527, 2012.

[184] D. Manhaeghe, S. Michels, D. P. L. Rousseau, and S. W. H. Van Hulle, 'A semi-mechanistic model describing the influence of light and temperature on the respiration and photosynthetic growth of Chlorella vulgaris', *Bioresour. Technol.*, vol. 274, no. November 2018, pp. 361–370, 2019.

[185] L. Rosso, J. R. Lobry, and J. P. Flandrois, 'An unexpected correlation

between cardinal temperatures of microbial growth highlighted by a new model', *J. Theor. Biol.*, vol. 162, no. 4, pp. 447–463, 1993.

[186] F. Le Borgne and J. Pruvost, 'Investigation and modeling of biomass decay rate in the dark and its potential influence on net productivity of solar photobioreactors for microalga Chlamydomonas reinhardtii and cyanobacterium Arthrospira platensis', *Bioresour. Technol.*, vol. 138, pp. 271–276, 2013.

[187] M. Barceló-Villalobos *et al.*, 'Variations of culture parameters in a pilot-scale thin-layer reactor and their influence on the performance of Scenedesmus almeriensis culture', *Bioresour. Technol. Reports*, vol. 6, no. February, pp. 190–197, 2019.

[188] A. Wieland and M. Kühl, 'Regulation of photosynthesis and oxygen consumption in a hypersaline cyanobacterial mat (Camargue, France) by irradiance, temperature and salinity', *FEMS Microbiol. Ecol.*, vol. 55, pp. 195–210, 2006.

[189] Q. Béchet, P. Chambonnière, A. Shilton, G. Guizard, and B. Guieysse, 'Algal productivity modeling: A step toward accurate assessments of full-scale algal cultivation', *Biotechnol. Bioeng.*, vol. 112, no. 5, pp. 987–996, 2015.

[190] Q. Béchet, M. Laviale, N. Arsapin, H. Bonnefond, and O. Bernard, 'Biotechnology for Biofuels Modeling the impact of high temperatures on microalgal viability and photosynthetic activity', *Biotechnol. Biofuels*, pp. 1–11, 2017.

[191] C. Posten, 'Design principles of photo-bioreactors for cultivation of microalgae', *Eng. Life Sci.*, vol. 9, no. 3, pp. 165–177, 2009.

[192] F. Camacho Rubio, F. G. Acién Fernandez, J. A. Sànchez Pérez, F. Garcìa

Camacho, and E. Molina Grima, 'Prediction of dissolved oxygen and carbon dioxide concentration profiles in tubular photobioreactors for microalgal culture', *Biotechnol. Bioeng.*, vol. 62, no. 1, pp. 71–86, 1999.

[193] J. L. Mendoza *et al.*, 'Oxygen transfer and evolution in microalgal culture in open raceways', *Bioresour. Technol.*, vol. 137, pp. 188–195, 2013.

[194] P. Sudhir and S. D. S. Murthy, 'Effects of salt stress on basic processes of photosynthesis', *Photosynthetica*, vol. 42, no. 4, pp. 481–486, 2004.

[195] O. Lefebvre and R. Moletta, 'Treatment of organic pollution in industrial saline wastewater: A literature review', *Water Res.*, vol. 40, no. 20, pp. 3671–3682, 2006.

[196] A. J. Martínez-Roldán, H. V. Perales-Vela, R. O. Cañizares-Villanueva, and G. Torzillo, 'Physiological response of Nannochloropsis sp. to saline stress in laboratory batch cultures', *J. Appl. Phycol.*, vol. 26, no. 1, pp. 115–121, 2014.

[197] A. Vonshak, L. Chanawongse, B. Bunnag, and M. Tanticharoen, 'Physiological characterization of spirulina platensis isolate Response to light and salinity', *Plant Physiol.*, vol. 14, pp. 161–166, 1995.

[198] C. Lu and A. Vonshak, 'Effects of salinity stress on photosystem II function in cyanobacterial Spirulina platensis cells', *Physiol. Plant.*, vol. 114, no. 3, pp. 405–413, 2002.

[199] A. J. Alyabyev *et al.*, 'The effect of changes in salinity on the energy yielding processes of Chlorella vulgaris and Dunaliella maritima cells', *Thermochim. Acta*, vol. 458, no. 1–2, pp. 65–70, 2007.

[200] A. Abeliovich and Y. Azov, 'Toxicity of ammonia to algae in sewage oxidation ponds', *Appl. Environ. Microbiol.*, vol. 31, no. 6, pp. 801–806, 1976.

[201] J. Gutierrez, T. A. Kwan, J. B. Zimmerman, and J. Peccia, 'Ammonia inhibition in oleaginous microalgae', *Algal Res.*, vol. 19, pp. 123–127, 2016.

[202] H. Zúñiga, C. Vergara, A. Donoso-Bravo, and D. Jeison, 'E ff ect of Delays on the Response of Microalgae When Exposed to Dynamic Environmental Conditions', *Processes*, vol. 8, no. 87, pp. 1–11, 2020.

[203] J. González-Camejo *et al.*, 'Short and long-term experiments on the effect of sulphide on microalgae cultivation in tertiary sewage treatment', *Bioresour. Technol.*, vol. 244, no. June, pp. 15–22, 2017.

[204] H. Andemichael and J. W. Lee, 'Toxicological study of biofuel ethanol with blue green alga Spirulina platensis', *Algal Res.*, vol. 18, pp. 110–115, 2016.

[205] L. Campanella, F. Cubadda, M. P. Sammartino, and A. Saoncella, 'An algal biosensor for the monitoring of water toxicity in estuarine environments', *Water Res.*, vol. 35, no. 1, pp. 69–76, 2001.

[206] T. Debenest, J. Silvestre, M. Coste, and E. Pinelli, 'Effects of Pesticides on Freshwater Diatoms', in *Reviews of Environmental Contamination and Toxicology (Continuation of Residue Reviews)*, New York, NY: Springer, 2010, pp. 87–104.

[207] J. Gonzalez-Camejo *et al.*, 'Nitrite inhibition of microalgae induced by the competition between microalgae and nitrifying bacteria', *Water Res.*, vol. 172, no. 172, p. 115499, 2020.

[208] K. Gao and D. Zou, 'Photosynthetic bicarbonate utilization by a terrestrial cyanobacterium, Nostoc flagelliforme (Cyanophyceae)', *J. Phycol.*, vol. 37, no. 5, pp. 768–771, 2001.

[209] M. Drábková, W. Admiraal, and B. Maršálek, 'Combined exposure to hydrogen peroxide and light-selective effects on cyanobacteria, green

algae, and diatoms', *Environ. Sci. Technol.*, vol. 41, no. 1, pp. 309–314, 2007.

[210] B. Liu, X. Nie, W. Liu, P. Snoeijs, C. Guan, and M. T. K. Tsui, 'Toxic effects of erythromycin, ciprofloxacin and sulfamethoxazole on photosynthetic apparatus in Selenastrum capricornutum', *Ecotoxicol. Environ. Saf.*, vol. 74, pp. 1027–1035, 2011.

[211] M. Drath, N. Kloft, A. Batschauer, K. Marin, J. Novak, and K. Forchhammer, 'Ammonia triggers photodamage of photosystem II in the cyanobacterium Synechocystis sp. strain PCC 6803', *Plant Physiol.*, vol. 147, no. 1, pp. 206–215, 2008.

[212] G. Markou, D. Vandamme, and K. Muylaert, 'Microalgal and cyanobacterial cultivation: the supply of nutrients', *Water Res.*, vol. 65, pp. 186–202, 2014.

[213] S. Belkin and S. Boussiba, 'High internal pH conveys ammonia resistance in spirulina platensis', *Bioresour. Technol.*, vol. 38, no. 2–3, pp. 167–169, 1991.

[214] G. Markou, D. Vandamme, and K. Muylaert, 'Ammonia inhibition on Arthrospira platensis in relation to the initial biomass density and pH', *Bioresour. Technol.*, vol. 166, pp. 259–265, 2014.

[215] A. Abeliovich and Y. Azov, 'Toxicity of Ammonia to Algae in Sewage Oxidation Ponds', *Appl. Environ. Microbiol.*, vol. 31, no. 6, pp. 801–806, 1976.

[216] T. Källqvist and A. Svenson, 'Assessment of ammonia toxicity in tests with the microalga, Nephroselmis pyriformis, Chlorophyta', *Water Res.*, vol. 37, pp. 477–484, 2003.

[217] M. Goto *et al.*, 'High ammonia tolerance on growth rate of marine microalga Chlorella vulgaris White', *J. Environ. Biol.*, vol. 39, no. September, pp. 843–848, 2018.

[218] G. Dai, C. P. Deblois, S. Liu, P. Juneau, and B. Qiu, 'Differential sensitivity of five cyanobacterial strains to ammonium toxicity and its inhibitory mechanism on the photosynthesis of rice-field cyanobacterium Ge-Xian-Mi (Nostoc)', *Aquat. Toxicol.*, vol. 89, no. 2, pp. 113–121, 2008.

[219] C. Segura, C. Vergara, M. Seeger, A. Donoso-Bravo, and D. Jeison, 'When constants are no longer constant: The case of inhibition in bioprocesses', *Biochem. Eng. J.*, vol. 123, pp. 24–28, 2017.

[220] J. Wang, W. Zhou, H. Chen, J. Zhan, C. He, and Q. Wang, 'Ammonium Nitrogen Tolerant Chlorella Strain Screening and Its Damaging Effects on Photosynthesis', *Front. Microbiol.*, vol. 9, p. 3250, 2019.

[221] C.-W. Cho *et al.*, 'Microalgal photosynthetic activity measurement system for rapid toxicity assessment', *Ecotoxicology*, vol. 17, no. 6, pp. 455–463, 2008.

[222] ISO, 'Fresh water algal growth inhibition test with Scenedesmus subspicatus and Selenastrum capricornutum (ISO Standard 869:1989)', 1989.

[223] K. Hancke, T. B. Hancke, L. M. Olsen, G. Johnsen, and R. N. Glud, 'Temperature effects on microalgal photosynthesis-light responses measured by O2 production, pulsa-amplitude-modulated fluorescencec, and 14C assimilation', *J. Phycol.*, vol. 514, pp. 501–514, 2008.

[224] N. R. Baker, 'Chlorophyll Fluorescence: A Probe of Photosynthesis In Vivo', *Annu. Rev. Plant Biol.*, vol. 59, pp. 89–113, 2008.

[225] H. Qiao and G. Wang, 'Effect of carbon source on growth and lipid accumulation in Chlorella sorokiniana GXNN01', *Chinese J. Oceanol. Limnol.*, vol. 27, no. 4, pp. 762–768, 2009.

[226] C. A. Oakley, B. M. Hopkinson, and G. W. Schmidt, 'A modular system for the measurement of CO2 and O2 gas flux and photosynthetic electron transport in microalgae', *Limnol. Oceanogr. Methods*, vol. 10, pp. 968–977, 2012.

[227] M. Gilbert, C. Wilhelm, and M. Richter, 'Bio-optical modelling of oxygen evolution using in vivo fluorescence: Comparison of measured and calculated photosynthesis/irradiance (P-I) curves in four representative phytoplankton species', *J. Plant Physiol.*, vol. 157, pp. 307–314, 2000.

[228] E. P. Morris and J. C. Kromkamp, 'Influence of temperature on the relationship between oxygen- and fluorescence-based estimates of photosynthetic parameters in a marine benthic diatom (Cylindrotheca closterium)', *Eur. J. Phycol.*, vol. 38, no. 2, pp. 133–142, 2003.

[229] H. El Ouarghi, B. E. Boumansour, O. Dufayt, B. El Hamouri, and J. L. Vasel, 'Hydrodynamics and oxygen balance in a high-rate algal pond', *Water Sci. Technol.*, vol. 42, no. 10, pp. 349–356, 2000.

[230] L. Ho *et al.*, 'A closer look on spatiotemporal variations of dissolved oxygen in waste stabilization ponds using mixed models', *Water (Switzerland)*, vol. 10, no. 2, 2018.

[231] R. A. Evans, H. J. Fallowfield, and N. J. Cromar, 'Characterisation of oxygen dynamics within a high-rate algal pond system used to treat abattoir wastewater', *Water Sci. Technol.*, vol. 48, no. 2, pp. 61–68, 2003.

[232] Z. Arbib, I. de Godos Crespo, E. L. Corona, and F. Rogalla, 'Understanding the biological activity of high rate algae ponds through the calculation of oxygen balances', *Appl. Microbiol. Biotechnol.*, vol. 101, no. 12, pp. 5189–5198, 2017.

[233] N. G. A. I. Karya, N. P. van der Steen, and P. N. L. Lens, 'Photo-oxygenation to support nitrification in an algal-bacterial consortium treating artificial wastewater', *Bioresour. Technol.*, vol. 134, pp. 244–250, 2013.

[234] J. Ye, J. Liang, L. Wang, and G. Markou, 'The mechanism of enhanced wastewater nitrogen removal by photo-sequencing batch reactors based on comprehensive analysis of system dynamics within a cycle', *Bioresour. Technol.*, vol. 260, no. March, pp. 256–263, 2018.

[235] A. Pizzera *et al.*, 'Digestate treatment with algae-bacteria consortia : A field pilot-scale experimentation in a sub-optimal climate area', *Bioresour. Technol.*, vol. 274, pp. 232–243, 2019.

[236] J. U. Grobbelaar, C. J. Soeder, J. Groenweg, E. Stengel, and P. Hartig, 'Rates of biogenic oxygen production in mass cultures of microalgae, absorption of atmospheric oxygen and oxygen availability for wastewater treatment', *Water Res.*, vol. 22, no. 11, pp. 1459–1464, 1988.

[237] W. Huang *et al.*, 'Effect of algae growth on aerobic granulation and nutrients removal from synthetic wastewater by using sequencing batch reactors', *Bioresour. Technol.*, vol. 179, pp. 187–192, 2015.

[238] D. L. Sutherland, V. Montemezzani, C. Howard-Williams, M. H. Turnbull, P. A. Broady, and R. J. Craggs, 'Modifying the high rate algal pond light environment and its effects on light absorption andphotosynthesis', *Water Res.*, vol. 70, no. March, pp. 86–96, 2015.

[239] M. Pastore, S. Santaeufemia, A. Bertucco, and E. Sforza, 'Light intensity affects the mixotrophic carbon exploitation in chlorella protothecoides: Consequences on microalgae-bacteria based wastewater treatment', *Water Sci. Technol.*, vol. 78, no. 8, pp. 1762–1771, 2018.

[240] A. Rada-Ariza, 'Photo-Activated Sludge: A Novel Algal-Bacterial Biotreatment for Nitrogen Removal from Wastewater', Ph.D. Thesis, IHE-Delft Institute for Water Education, 2018.

[241] C. Vergara, R. Muñoz, J. L. Campos, M. Seeger, and D. Jeison, 'Influence of light intensity on bacterial nitrifying activity in algal-bacterial photobioreactors and its implications for microalgae-based wastewater treatment', *Int. Biodeterior. Biodegrad.*, vol. 114, pp. 116–121, 2016.

[242] S. Rossi, M. Bellucci, F. Marazzi, V. Mezzanotte, and E. Ficara, 'Activity assessment of microalgal-bacterial consortia based on respirometric tests', *Water Sci. Technol.*, vol. 78, no. 1, pp. 207–215, 2018.

[243] T. Berner *et al.*, 'The measurement of primary productivity in a high-rate oxidation pond (HROP)', *J. Plankton Res.*, vol. 8, no. 4, pp. 659–672, 1986.

[244] R. Blanc and U. Leshem, 'Utilizing algal oxygen production for advanced wastewater treatment in a Moving Bed Biofilm Reactor (MBBR) – the Biologically Aerated Reactor (BAR®)', *Proc. Water Environ. Fed.*, vol. 2013, no. 10, pp. 5425–5435, 2014.

[245] G. Vargas, A. Donoso-Bravo, C. Vergara, and G. Ruiz-Filippi, 'Assessment of microalgae and nitrifiers activity in a consortium in a continuous operation and the effect of oxygen depletion', *Electron. J. Biotechnol.*, vol. 23, pp. 63–68, 2016.

[246] M. Wang, H. Yang, S. J. Ergas, and P. van der Steen, 'A novel shortcut nitrogen removal process using an algal-bacterial consortium in a photo-sequencing batch reactor (PSBR)', *Water Res.*, vol. 87, pp. 38–48, 2015.

[247] O. Choi, A. Das, C. P. Yu, and Z. Hu, 'Nitrifying bacterial growth inhibition in the presence of algae and cyanobacteria', *Biotechnol. Bioeng.*, vol. 107, no.

6, pp. 1004–1011, 2010.

[248] M. Xu, M. Bernards, and Z. Hu, 'Algae-facilitated chemical phosphorus removal during high-density Chlorella emersonii cultivation in a membrane bioreactor', *Bioresour. Technol.*, vol. 153, pp. 383–387, 2014.

[249] F. Meng *et al.*, 'Effects of light intensity on oxygen distribution, lipid production and biological community of algal-bacterial granules in photo-sequencing batch reactors', *Bioresour. Technol.*, vol. 272, pp. 473–481, 2018.

[250] D. Kang, K. Kim, Y. Jang, H. Moon, D. Ju, and D. Jahng, 'Nutrient removal and community structure of wastewater-borne algal-bacterial consortia grown in raw wastewater with various wavelengths of light', *Int. Biodeterior. Biodegrad.*, vol. 126, no. September 2017, pp. 10–20, 2018.

[251] D. Kang, K. T. Kim, T. Heo, G. Kwon, and C. Lim, 'Inhibition of Photosynthetic Activity in Wastewater-Borne Microalgal – Bacterial Consortia under Various Light Conditions', *Sustainability*, vol. 11, pp. 1–13, 2019.

[252] D. Bilanovic, M. Holland, J. Starosvetsky, and R. Armon, 'Co-cultivation of microalgae and nitrifiers for higher biomass production and better carbon capture', *Bioresour. Technol.*, vol. 220, pp. 282–288, 2016.

[253] N. J. Cromar and H. J. Fallowfield, 'Use of image analysis to determine algal and bacterial biomass in a high rate algal pond following Percoll ® fractionation', *Water Sci. Technol.*, vol. 48, no. 2, pp. 53–60, 2003.

[254] L. Pell, S. Löhn, G. Weinberger, K. Kuchta, and D. Hanelt, 'Mild disintegration methods of microalgae–bacteria flocs from wastewater treatment', *J. Appl. Phycol.*, vol. 29, no. 2, pp. 843–851, 2017.

[255] I. Krustok, M. Odlare, J. Truu, and E. Nehrenheim, 'Inhibition of

nitrification in municipal wastewater-treating photobioreactors: Effect on algal growth and nutrient uptake', *Bioresour. Technol.*, vol. 202, pp. 238–243, 2016.

[256] C. C. Tang, W. Zuo, Y. Tian, N. Sun, Z. W. Wang, and J. Zhang, 'Effect of aeration rate on performance and stability of algal-bacterial symbiosis system to treat domestic wastewater in sequencing batch reactors', *Bioresour. Technol.*, vol. 222, pp. 156–164, 2016.

[257] K. Tatari, A. Gülay, B. Thamdrup, H. J. Albrechtsen, and B. F. Smets, 'Challenges in using allylthiourea and chlorate as specific nitrification inhibitors', *Chemosphere*, vol. 182, pp. 301–305, 2017.

[258] S. Rossi, F. Casagli, M. Mantovani, V. Mezzanotte, and E. Ficara, 'Selection of photosynthesis and respiration models to assess the effect of environmental conditions on mixed microalgae consortia grown on wastewater', *Bioresour. Technol.*, vol. 305, p. 122995, 2020.

[259] S. Rossi *et al.*, 'Free ammonia inhibition in microalgae and cyanobacteria grown in wastewaters: photo-respirometric evaluation and modelling', *Bioresour. Technol.*, vol. 305, p. 123046, 2020.

[260] B. S. Grama, S. N. Agathos, and C. S. Jeffryes, 'Balancing Photosynthesis and Respiration Increases Microalgal Biomass Productivity during Photoheterotrophy on Glycerol', *ACS Sustain. Chem. Eng.*, vol. 4, no. 3, pp. 1611–1618, 2016.

[261] P. Schwerna, H. Hübner, and R. Buchholz, 'Quantification of oxygen production and respiration rates in mixotrophic cultivation of microalgae in nonstirred photobioreactors', *Eng. Life Sci.*, vol. 17, no. 2, pp. 140–144, 2017.

[262] B. D. Shoener *et al.*, 'Microalgae and cyanobacteria modeling in water resource recovery facilities: A critical review', *Water Res. X*, vol. 2, pp. 1–18, 2019.

[263] P. Van Der Steen, K. Rahsilawati, A. M. Rada-Ariza, C. M. Lopez-Vazquez, and P. N. L. Lens, 'A new photo-activated sludge system for nitrification by an algal-bacterial consortium in a photo-bioreactor with biomass recycle', *Water Sci. Technol.*, vol. 72, no. 3, pp. 443–450, 2015.

[264] E. Barbera, A. Grandi, L. Borella, A. Bertucco, and E. Sforza, 'Continuous cultivation as a method to assess the maximum specific growth rate of photosynthetic organisms', *Front. Bioeng. Biotechnol.*, vol. 7, no. OCT, pp. 1–12, 2019.

[265] J. Zambrano, I. Krustok, E. Nehrenheim, and B. Carlsson, 'A simple model for algae-bacteria interaction in photo-bioreactors', *Algal Res.*, vol. 19, pp. 155–161, 2016.

[266] N. C. Boelee, H. Temmink, M. Janssen, C. J. N. Buisman, and R. H. Wijffels, 'Balancing the organic load and light supply in symbiotic microalgal-bacterial biofilm reactors treating synthetic municipal wastewater', *Ecol. Eng.*, vol. 64, pp. 213–221, 2014.

[267] S. N. Merbt, S. Bernal, L. Proia, E. Martí, and E. O. Casamayor, 'Photoinhibition on natural ammonia oxidizers biofilm populations and implications for nitrogen uptake in stream biofilms', *Limnol. Oceanogr.*, vol. 62, no. 1, pp. 364–375, 2017.

[268] A. Babaei, M. R. Mehrnia, J. Shayegan, and M. H. Sarrafzadeh, 'Comparison of different trophic cultivations in microalgal membrane bioreactor containing N-riched wastewater for simultaneous nutrient

removal and biomass production', *Process Biochem.*, vol. 51, no. 10, pp. 1568–1575, 2016.

[269] M. Mantovani, F. Marazzi, R. Fornaroli, M. Bellucci, E. Ficara, and V. Mezzanotte, 'Outdoor pilot-scale raceway as a microalgae-bacteria sidestream treatment in a WWTP', *Sci. Total Environ.*, vol. 710, p. 135583, 2019.

[270] D. Scaglione *et al.*, 'Autotrophic nitrogen removal by a two-step SBR process applied to mixed agro-digestate', *Bioresour. Technol.*, vol. 176, pp. 98–105, 2015.

[271] J. García *et al.*, 'Nutrient removal from agricultural run-off in demonstrative full scale tubular photobioreactors for microalgae growth', *Ecol. Eng.*, vol. 120, no. July, pp. 513–521, 2018.

[272] D. M. Arias, 'Production of carbohydrates and Polyhudroxybutyrate by Cyanobacteria grown in wastewater', Ph.D. Thesis, Univeristat Politècnica de Catalunya·Barcelona Tech, 2018.

[273] R. Díez-Montero, E. Uggetti, M. J. García-Galán, and J. García, 'Start-up of a demonstrative scale microalgae-based system for wastewater treatment and production of biopolymers', in *2nd IWA Conference on Algal Technologies for Wastewater Treatment and Resource Recovery - IWAlgae2019*, 2019.

[274] V. Andreotti, 'Microalgae in aquaculture wastewater: a new forecasting method of production in a marine system', Ph.D. Thesis, Universitat Politècnica de Catalunya, 2019.

[275] APHA, *Standard Methods for the Examination of Water and Wastewater*. American Public Health Association, American Water Works Association,

Water Environment Federation, Washington, USA, 2017.

[276] R. I. Amann, B. J. Binder, R. J. Olson, S. W. Chisholm, R. Devereux, and D. A. Stahl, 'Combination of 16S rRNA-targeted oligonucleotide probes with flow cytometry for analyzing mixed microbial populations', *Appl. Environ. Microbiol.*, vol. 56, no. 6, pp. 1919–1925, 1990.

[277] M. Bellucci and T. P. Curtis, 'Ammonia-oxidizing bacteria in wastewater', in *Methods in Enzymology*, 1st ed., vol. 496, Elsevier Inc., 2011, pp. 269–286.

[278] S. Kayombo, T. S. A. Mbwette, A. W. Mayo, J. H. Y. Katima, and S. E. Jorgensen, 'Diurnal cycles of variation of physical-chemical parameters in waste stabilization ponds', *Ecol. Eng.*, vol. 18, no. 3, pp. 287–291, 2002.

[279] H. Ali, T. A. Cheema, and C. W. Park, 'Effect of Paddle-Wheel Pulsating Velocity on the Hydrodynamic Performance of High-Rate Algal Ponds', *J. Energy Eng.*, vol. 141, no. 4, pp. 1–12, 2015.

[280] L. T. Arashiro, N. Montero, I. Ferrer, F. G. Acién, C. Gómez, and M. Garfí, 'Life cycle assessment of high rate algal ponds for wastewater treatment and resource recovery', *Sci. Total Environ.*, vol. 622–623, pp. 1118–1130, 2018.

[281] J. González-camejo, S. Aparicio, M. V Ruano, L. Borrás, R. Barat, and J. Ferrer, 'Effect of ambient temperature variations on an indigenous microalgae-nitrifying bacteria culture dominated by Chlorella', *Bioresour. Technol.*, vol. 290, p. 121788, 2019.

[282] R. K. Hynes and R. Knowles, 'Inhibition of Chemoautotrophic Nitrification by Sodium Chlorate and Sodium Chlorite: a Reexamination', *Appl. Environ. Microbiol.*, vol. 45, no. 4, pp. 1178–1182, 1983.

[283] R. Sander, 'Compilation of Henry's law constants (version 4.0) for water as

solvent', *Atmos. Chem. Phys.*, vol. 15, pp. 4399–4981, 2015.

[284] Q. Béchet, A. Shilton, and B. Guieysse, 'Modeling the effects of light and temperature on algae growth : State of the art and critical assessment for productivity prediction during outdoor cultivation', *Biotechnol. Adv.*, vol. 31, pp. 1648–1663, 2013.

[285] B. D. Shoener *et al.*, 'Microalgae and cyanobacteria modeling in water resource recovery facilities : A critical review', *Water Res. X J.*, vol. 2, pp. 1–18, 2019.

[286] I. Angelidaki, L. Ellegaard, and B. K. Ahring, 'A Mathematical Model for Dynamic Simulation of Anaerobic Digestion of Complex Substrates: Focusing on Ammonia Inhibition', *Biotechnol. Bioeng.*, vol. 42, pp. 159–166, 1993.

[287] H. Prinz, 'Hill coefficients , dose – response curves and allosteric mechanisms', *J. Chem. Biol.*, vol. 3, pp. 37–44, 2010.

[288] J. H. Steele, 'Environmental control of photosynthesis in the sea', *Limnol. Oceanogr.*, vol. 7, no. 2, pp. 137–150, 1962.

[289] H. Y. Lee, L. E. Erickson, and S. S. Yang, 'Kinetics and Bioenergetics of Light-Limited Photoautotrophic Growth of Spirulina platensis', *Biotechnol. Bioeng.*, vol. 29, pp. 832–843, 1987.

[290] D. A. Ratkowsky, R. K. Lowry, T. A. Mcmeekin, A. N. Stokes, and R. E. Chandler, 'Model for Bacterial Culture Growth Rate Throughout the Entire Biokinetic Temperature Range', *J. Bacteriol.*, vol. 154, no. 3, pp. 1222–1226, 1983.

[291] G. F. Blanchard, J.-M. Guarini, P. Richard, P. Gros, and F. Mornet, 'Quantifying the short-term temperature effect on light-saturated

photosynthesis of intertidal microphytobenthos', *Mar. Ecol. Prog. Ser.*, vol. 134, pp. 309–313, 1996.

[292] D. J. Batstone *et al.*, 'Anaerobic Digestion Model No. 1', IWA Publishing, London, UK, 2002.

[293] G. Y. Di Veroli *et al.*, 'An automated fitting procedure and software for dose-response curves with multiphasic features', *Nat. Sci. reports*, pp. 1–11, 2015.

[294] R Core Team, 'R: A Language and Environment for Statistical Computing', Vienna, Austria, 2017.

[295] F. Marazzi, E. Ficara, R. Fornaroli, and V. Mezzanotte, 'Factors Affecting the Growth of Microalgae on Blackwater from Biosolid Dewatering', *Water, Air, Soil Pollut.*, vol. 228:68, 2017.

[296] A. Rozzi, E. Ficara, and A. Rocco, 'Dissolved Oxygen-Stat Titration Respirometry: Principle of Operation and Validation', *J. Environ. Eng.*, vol. 129, no. 7, pp. 602–609, 2003.

[297] G. Ricco, M. C. Tomei, R. Ramadori, and G. Laera, 'Toxicity assessment of common xenobiotic compounds on municipal activated sludge: Comparison between respirometry and Microtox®', *Water Res.*, vol. 38, no. 8, pp. 2103–2110, 2004.

[298] M. J. Griffiths, C. Garcin, R. P. Van Hille, and S. T. L. Harrison, 'Interference by pigment in the estimation of microalgal biomass concentration by optical density', *J. Microbiol. Methods*, vol. 85, pp. 119–123, 2011.

[299] A. Ruiz-Martinez, J. Serralta, A. Seco, and J. Ferrer, 'Behavior of mixed Chlorophyceae cultures under prolonged dark exposure. Respiration rate modeling', *Ecol. Eng.*, vol. 91, pp. 265–269, 2016.

[300] F. Casagli, G. Zuccaro, A. Pizzera, J. P. Steyer, and E. Ficara, 'A comprehensive model to optimize microalgae-bacteria wastewater treatment in raceway ponds', in *2nd IWA Conference on Algal Technologies for Wastewater Treatment and Resource Recovery - IWAlgae2019*, 2019, no. July, pp. 255–256.

[301] E. P. Y. Tang and W. F. Vincent, 'Strategies of thermal adaptation by high-latitude cyanobacteria', *New Phytol.*, vol. 142, pp. 315–323, 1999.

[302] H. Wang *et al.*, 'Coordinated response of photosynthesis, carbon assimilation, and triacylglycerol accumulation to nitrogen starvation in the marine microalgae Isochrysis zhangjiangensis (Haptophyta)', *Bioresour. Technol.*, vol. 177, pp. 282–288, 2015.

[303] S. Umamaheswari and J. Shanthakumar, 'Efficacy of microalgae for industrial wastewater treatment : a review on operating conditions , treatment efficiency and biomass productivity', *Rev. Environ. Sci. Bio/Technology*, vol. 15, no. 2, pp. 265–284, 2016.

[304] Q. Béchet, P. Moussion, and O. Bernard, 'Calibration of a productivity model for the microalgae Dunaliella salina accounting for light and temperature', *Algal Res.*, vol. 21, pp. 156–160, 2017.

[305] E. Bitaubè Perez, I. Caro Pina, and L. Perez Rodrıguez, 'Kinetic model for growth of Phaeodactylum tricornutum in intensive culture photobioreactor', *Biochem. Eng. J.*, vol. 40, pp. 520–525, 2008.

[306] M. Gilbert, C. Wilhelm, and M. Richter, 'Bio-optical modelling of oxygen evolution using in vivo fluorescence: Comparison of measured and calculated photosynthesis/irradiance (P-I) curves in four representative phytoplankton species', *J. Plant Physiol.*, vol. 157, no. 3, pp. 307–314, 2000.

[307] B. Kozłowska-Szerenos, I. Bialuk, and S. Maleszewski, 'Enhancement of photosynthetic O2 evolution in Chlorella vulgaris under high light and increased CO2 concentration as a sign of acclimation to phosphate deficiency', *Plant Physiology and Biochemistry*, vol. 42, no. 5. pp. 403–409, 2004.

[308] J. F. Sánchez, J. M. Fernández-Sevilla, F. G. Acién, M. C. Cerón, J. Pérez-Parra, and E. Molina-Grima, 'Biomass and lutein productivity of Scenedesmus almeriensis: Influence of irradiance, dilution rate and temperature', *Appl. Microbiol. Biotechnol.*, vol. 79, no. 5, pp. 719–729, 2008.

[309] R. D. Robarts and T. Zohary, 'Temperature effects on photosynthetic capacity, respiration, and growth rates of bloom-forming cyanobacteria', *New Zeal. J. Mar. Freshw. Res.*, vol. 21, no. 3, pp. 391–399, 1987.

[310] P. Claquin, I. Probert, S. Lefebvre, and B. Veron, 'Effects of temperature on photosynthetic parameters and TEP production in eight species of marine microalgae', *Aquat. Microb. Ecol.*, vol. 51, no. 1, pp. 1–11, 2008.

[311] O. Bernard and B. Rémond, 'Validation of a simple model accounting for light and temperature effect on microalgal growth', *Bioresour. Technol.*, vol. 123, pp. 520–527, 2012.

[312] A. W. Mayo, 'Effects of temperature and pH on the kinetic growth of unialga Chiarella vulgaris cultures containing bacteria', *Water Environ. Res.*, vol. 69, no. 1, pp. 64–72, 1997.

[313] K. Ying, D. J. Gilmour, and W. B. Zimmerman, 'Effects of CO2 and pH on growth of the microalga Dunaliella salina', *J. Microb. Biochem. Technol.*, vol. 6, no. 3, pp. 167–173, 2014.

[314] J. E. Burris, 'Effects of oxygen and inorganic carbon concentrations on the

photosynthetic quotients of marine algae', *Mar. Biol.*, vol. 65, no. 3, pp. 215–219, 1981.

[315] A. A. Cortés Téllez, S. Sánchez-Fortún Rodríguez, A. D'ors de Blas, L. C. García, M. G. Garnica-Romo, and M. C. Bartolomé Camacho, 'Evolution in the photosynthetic oxygen rate of a Cd-resistant strain of Dictyosphaerium chlorelloides by changes in light intensity and temperature', *Chemosphere*, vol. 239, p. 124672, 2020.

[316] D.-J. Kim, D.-I. Lee, and J. Keller, 'Effect of temperature and free ammonia on nitrification and nitrite accumulation in landfill leachate and analysis of its nitrifying bacterial community by FISH', *Bioresour. Technol.*, vol. 97, pp. 459–468, 2006.

[317] V. M. Vadivelu, J. Keller, and Z. Yuan, 'Free ammonia and free nitrous acid inhibition on the anabolic and catabolic processes of Nitrosomonas and Nitrobacter', *Water Sci. Technol. Technol.*, vol. 56, no. 7, pp. 89–97, 2007.

[318] I. Jubany Güell, 'Operation, modeling and automatic control of complete and partial nitrification of highly concentrated ammonium wastewater', Ph.D. thesis, Universitat Autònoma de Barcelona, 2007.

[319] S. Park and W. Bae, 'Modeling kinetics of ammonium oxidation and nitrite oxidation under simultaneous inhibition by free ammonia and free nitrous acid', *Process Biochem.*, vol. 44, pp. 631–640, 2009.

[320] L. Giannuzzi, 'Cyanobacteria Growth Kinetics', in *Algae*, Y. K. Wong, Ed. IntechOpen, 2019, pp. 1–17.